NUFFIELD DEPARTMENT OF OPHTHALMOLOGY



The Influence Of Selected Flavonoids On The Survival Of Retinal Cells Subjected To Different Types Of Oxidative Stress

Thesis submitted for the degree of Doctor of Philosophy

Tengku Ain Fathlun Bt Tengku Kamalden

GREEN TEMPLETON COLLEGE

TRINITY TERM 2012

Supervisor: Professor Neville Osborne

THESIS ABSTRACT

The general aim of the thesis was to deduce whether selected naturally occurring flavonoids (genistein, epicatechin gallate (EC), epigallocatechin gallate (EGCG), baicalin) attenuate various secondary insults that may cause death of ganglion cells in primary open angle glaucoma (POAG).

An ischemic insult to the rat retina significantly causes the inner retina to degenerate indexed by changes of various antigens, proteins and mRNAs located to amacrine and ganglion cells. These changes are blunted in animals treated with genistein as has been shown for ECGC.

Studies conducted on cells (RGC-5 cells) in culture showed that hydrogen peroxide, L-buthionine sulfoximine (BSO)/glutamate and serum deprivation (mimicking oxidative stress), rotenone, sodium azide (affecting mitochondria function in specific ways) and light (where the mitochondria are generally affected) all generated reactive oxygen species and caused death of RGC-5 cells. EGCG was able to attenuate cell death caused by hydrogen peroxide, sodium azide and rotenone. Only EC was able to attenuate BSO/glutamate-induced cell death, in addition to cell death caused by hydrogen peroxide and rotenone. Genistein had no positive effect on cell death in experiments carried out on RGC-5 cells.

Exposure of RGC-5 cells to flavonoids showed that EC and EGCG increased the mRNA expression of endogenous antioxidants such as HO-1 (heme oxygenase 1) and Nrf-2 (nuclear erythroid factor-2-related factor 2). Light insult, rotenone and sodium azide activate the p38 (protein kinase 38) pathway, while only light and rotenone activate the JNK (c-Jun amino-terminal kinase) pathway. Serum deprivation affects mitochondrial apoptotic proteins causing an increase in the ratio of Bax/Bcl2 (Bax: Bcl-2-associated X protein; Bcl-2: B-cell lymphoma 2). An insult of light to RGC-5 cells, unlike that induced by sodium azide, is inhibited by necrostatin-1 and causes an activation of AIF (apoptosis-inducing factor) with alpha-fodrin being unaffected.

These studies suggest that ganglion cell death caused by insults as may occur in POAG involves various cellular signaling pathways. The selected flavonoids have diverse actions in increasing cellular defense mechanisms, and in negating the effects of ischemia and specific types of oxidative stress. The results argue for the possible use of flavonoids in the treatment of POAG to slow down ganglion cell death.

DEDICATIONS

To both my parents,

For being my pillars of strength, for giving me the motivation to carry on, and for the continuing support and unconditional love. No words can describe my gratitude; I dedicate all my successes past, present and future, to the both of you.

And in the memory of my beloved brother, Feisal,

For whom I dedicate this thesis especially. My constant presence next to you in your time of need was the most painful sacrifice I ever had to make in the pursuit of this degree. I will always cherish your love and support, and will never stop missing and loving you.

To both my siblings, Izam and Fadilah,

For your love and encouragement, and for taking pride in all my achievements.

ACKNOWLEDGEMENTS

It gives me great honour to thank and duly acknowledge those who made this thesis possible. Firstly I would like to thank the my sponsors, the University of Malaya, Kuala Lumpur, and the Ministry of Higher Educations (MOHE) of Malaysia, for providing me the opportunity and scholarship to undertake this study at the University of Oxford. I am deeply indebted to my supervisor, Professor Neville Osborne, for his supervision, patience and continuing guidance throughout the duration of my DPhil studies. His support and advice has been imperative for the completion of my studies.

I wish to thank Professor Anthony Bron, for his kind encouragement and warm company during some wonderful dinners. His generosity and financial support for travel grants has benefited me on several occasions. I would also like to extend my deep gratitude to Drs Dan Ji, Rebecca Fawcett, and Rukhsana Safa whose companionships and friendships made my experience in Oxford memorable.

I thank Mrs Carol Holder for her help and assistance in administration details and Mr Nigel Swietalski for his technical assistance and willingness to help at every possible occasion. I would also like to thank Dr Stephanie Halford for her kind concern, and encouragement in the completion of my studies, and Professors Russell Foster and Robert MacLaren for their kind understanding and support especially during the very difficult times when I lost my brother. I wish all the other members of the Nuffield Laboratory of Ophthalmology for their friendship and assistance

Finally, I would like to express my gratitude to my wonderful colleagues and friends at the Department of Ophthalmology, University of Malaya, Kuala Lumpur, for the continuous support, encouragement and motivation in many ways over the many years I was away. The research outlined in the thesis below would not have been made possible if not for the encouragement and support from people too numerous to mention here, but whose role in my success will always be greatly appreciated.

DECLARATION

Wherever contributions are involved, every effort is made to indicate this clearly with due acknowledgements. Specific help with experimental work was provided by the following people:

- Professor Neville Osborne for his help and guidance in the editing and correcting of this thesis
- Dr Dan Ji and Dr Rebecca Fawcett for the early work of this study and data derived from *in vivo* studies concerning genistein
- Dr Dan Ji for the joint experimental work concerning sodium azide and light.
- Mr Nigel Swieltaski for his assistance in lipid peroxidation experiments.
- Dr Jung Sang Hoon for his assistance and discussion concerning work with baicalin.

With these exceptions, I declare the work described in this thesis as the result of my own work and effort and has not been submitted anywhere for any award.

Tengku Ain Fathlun binti Tengku Kamalden
July 2012

PRESENTATIONS AND PUBLICATIONS RELEVANT TO THE THESIS

Poster presentations

1. **Kamalden TA**, AJ Bron, Osborne NN. *RGC-5 cell death caused by serum deprivation and rotenone occur by different processes and only the latter is blunted by green tea flavonoids.* The Association for Research in Vision and Ophthalmology (ARVO); May 2011, Ft Lauderdale, Florida
2. **Kamalden TA**, Osborne NN. RGC-5 Cell Death Caused by Rotenone and Light is Dissimilar. Asia-ARVO meeting; Jan 2011, Singapore
3. **Kamalden TA,** Bron AJ, Osborne NN. *Rotenone is similar but not identical to light-induced apoptosis in RGC-5 cells and is attenuated by two green tea flavonoids.* The Association for Research in Vision and Ophthalmology (ARVO); May 2010, Ft Lauderdale, Florida
4. **Kamalden TA,** Bron AJ, Osborne NN. *Rotenone is similar but not identical to light-induced apoptosis in RGC-5 cells and is attenuated by two green tea flavonoids.* The 1st Young Researcher Vision Camp; June 2010, Leibertingen, Germany.
5. **Tengku-Kamalden TA**, Osborne NN. *Retinal ganglion cells in culture induced to die by insults of hydrogen peroxide, rotenone and glutamate/buthionine sulfoxamine are differentially protected by the flavonoids, epicatechin gallate, epigallocatehin gallate and genistein.* European Association for Vision and Eye Research Meeting,; Sep 2009, Portoroz, Slovenia.

Publications

1. **Kamalden TA**, Ji D, Osborne NN. *Rotenone-induced death of RGC- 5 cells is caspase independent, involves the JNK and p38 pathways and is attenuated by specific green tea flavonoids.* Neurochem Res 2012;37(5):1091-101
2. **Kamalden TA**, Ji D, Fawcett RJ, Osborne NN. *Genistein blunts the negative effect of ischaemia to the retina caused by an elevation of intraocular pressure.* Ophthalmic Res, 2011: 45(2); 65-72
3. Ji D, **Kamalden TA**, del Olmo-Aguado, Osborne NN. *Light and Sodium azide-induced death of RGC-5 cells in culture occurs via different mechanisms.* Apoptosis, Apr 2011: 16(4); 425-437
4. Osborne NN, **Kamalden TA**, Majid AS, del Olmo-Aguado S, Manso AG, Ji D. *Light effects on mitochondrial photosensitizers in relation to retinal degeneration.* Neurochem Res, Dc 2010:35(12); 2027-34
5. Jung SH, Kang KD, Ji D, Fawcett RJ, Safa R, **Kamalden TA**, Osborne NN. *The flavonoid baicalin counteracts ischemic and oxidative insults to retinal cells and lipid peroxidation to brain membranes.* Neurochem Int, Dec 2008: 53(6-8); 325-37

ABBREVIATIONS

Ac-DEVD-pNA.....Acetyl-Asp-Glu-Val-Asp p-nitroanilide
Aβ.....Amyloid β protein
ADP.....Adenosine diphosphate
AEC.....3-amino-9-ethylcarbazole
AIF.....Apoptosis inducing factor
ALS.....Amyotrophic lateral sclerosis
AMPA.....2-amino-3-(5-methyl-3-oxo-1,2- oxazol-4-yl)propanoic acid
ANOVA..... Analysis of variance
AP-1.....Activator protein 1
Apaf-1.....Apoptosis activating factor 1
Ape-1.....Apurinic endonuclease-1
APB.....2-amino-4-phosphonobutyrate
AQP4.....Aquaporin 4 protein
ARVO.....Association for Research in Vision and Ophthalmology
ATF-2.....Activating transcription factor 2
ATP.....Adenosine triphosphate
Bak.....Bcl-2 homologous antagonist/killer
Bax.....Bcl-2-associated X protein
Bcl-2.....B-cell lymphoma-2
BDNF.....Brain-derived neurotrophic factor
bdUTP.....biotinyl-dUTP
bFGF-2.....Basic fibroblast growth factor 2
Bid.....BH3 interacting domain death agonist
BSA.....Bovine serum albumin
BSO.....L-buthionine sulfoximine
Ca^{2+}.....Calcium
ChAT.....Choline acetyltransferase
c-FLIP.....cellular FLICE-inhibitory proteins
CNS.....Central nervous system
CNTF.....Ciliary neurotrophic factor
CO_2.....Carbon Dioxide
CRALBP.....Cellular retinaldehyde-binding protein
Cu^{2+}.....Copper
Cyt. *C*.....Cytochrome *c*
dATP.....Deoxyadenosine triphosphate
dCTP.....Deoxycytidine triphosphate
dGTP.....Deoxyguanosine triphosphate
dTTP.....Deoxythymidine triphosphate
dUTP.....Deoxyuridine triphosphate
dNTPs.....Deoxynucleotide triphosphate
DD.....Death domain
DEPC.....Diethylpyrocarbonate
DHE.....2', 7'-dihydroethidium
DISC.....Death-inducible signaling complex
DNA.....Deoxyribonucleic acid
DNase.....Deoxyribonuclease
DMSO.....Dimethyl sulfoxide

DR……Death receptor
DTT……Dithiothreitol
E1A……Adenovirus early region 1A
EC……Epicatechin gallate
EDTA……..Ethylene diamine tetraacetic acid
EGTA……..Ethylene glycol tetraacetic acid
EGCG……..Epigallocatechin gallate
EGF……Epidermal growth factor
Elk-1……E twenty-six (ETS)-like transcription factor 1
Endo G……....Endonuclease G
eNOS……..Endothelial nitric oxide synthase
ELM……External limiting membrane
ERα……Estrogen receptor α-subtype
ERβ……Estrogen receptor β-subtype
ERG……Electroretinogram
ERK……Extracellular signal-regulated kinase
FAD……Flavin adenosine dinucleotide
FADD……..Fas-associated Death Domain complex
FADD……..Fas-associated death domain
FADH2……....Flavin adenine dinucleotide (hydroquinone form)
FDA……....Fluorescein diacetate
Fe^{2+}……..Iron
FGF……Fibroblast growth factor
FITC……Fluorescein isothiocyanate
FLICE……FADD-like ICE
FBS……Fetal bovine serum
GABA……Gamma-amino-butyric acid
GAPDH……..Glyceraldehyde phosphate dehydrogenase
GCL……Ganglion cell layer
GFAP……..Glial fibrillary acidic protein
Gpx……..Glutathione peroxidase
GSH……Glutathione (reduced)
GSSG……..Glutathione disulfide
H^+……Hydrogen
H_2O_2……... Hydrogen peroxide
HCl……..Hydrochloric acid
HDAC……Histone deacetylase
HEPES……N-2-hydroxyl piperazine-N'-2-elthane sulfonic acid
HO-1……Heme oxygenase 1
HPC……Hereditary prostate cancer 1
HRP……Horseradish peroxidase
HST……High saline Tris buffer
IAPs……Inhibitor of apoptosis proteins
ICE……..Interleukin-1 coverting enzyme
IEB……..Immunoelectroblotting
IL6……...Interleukin 6
ILβ……...Interleukin β
ILM……Inner limiting membrane
IMM……Inner mitochondrial membrane
iNOS……Inducible nitric oxide synthase

INL……..Inner nuclear layer
IPL……..Inner plexiform layer
IOP……..Intraocular pressure
JNK…….c-Jun amino-terminal kinase
K^+……Potassium
LDL…….Low-density lipoprotein
LHON…….Leber's Hereditary Optic Neuropathy
MAPK…….Mitogen-associated protein kinase pathway
MDA……Malondialdehyde
Mg……Magnesium
MIP1α……....Macrophage inflammatory protein 1α
MIP2……Macrophage inflammatory protein 2
MnSOD……Manganese superoxide dismutase
MOMP……....Mitochondrial outer membrane permeabilization
MPTP……..1-methyl-4-phenyl-1,2,3,6-tetrahydropyridine
mRNA…….Messenger ribonucleic acid
mtDNA……Mitochondrial deoxyribonucleic acid
MTT……....3, 4, 5-dimethylthiazol-2-yl)-2, 5-diphenyl tetrazolium Bromide
Na^+……..Sodium
NMDA……....N-methyl-D-aspartate
NAD……....Nicotinamide adenosine dinucleotide
NADH…….Nicotinamide adenosine dinucleotide (reduced)
NADP……..Nicotinamide adenosine dinucleotide phosphate
NADPH……..Nicotinamide adenosine dinucleotide phosphate(reduced)
NF-κβ……..Nuclear factor kappa-light-chain-enhancer of activated B cells
NFL…….Nerve fibre layer
NF-L……Neurofilament light form
NGF……....Nerve Growth Factor
nNOS……..Neuronal nitric oxide synthase
NO……..Nitric oxide
NOS……Nitric oxide synthase
Nrf-2……Nuclear factor erythroid-2-related factor 2
NT3…….Neurotrophin 3
NU1025……8-hydroxy-2-methyl-quinazolin-4-[3H] one
OD……Optical density
OFL…….Optic fibre layer
OH……Hydroxyl group
6-OHDA……..6-hydroxydopamine
ONH……....Optic nerve head
ONL……....Outer nuclear layer
OPL…….Outer plexiform layer
p38……..Protein kinase 38 (from MAPK family)
PARP……..Poly (ADP-ribose) polymerase
PBS…….Phosphate buffered saline
PCD…….Programmed cell death
PDGF-B……..Platelet-derived growth factor-B
PEDF……Pigment Epithelium-derived Growth Factor

PHAP……..Putative HLA-DR-associated protein
PI…….Propidium iodide
PIDD……p53-induced protein with a death domain
PI3K……Phosphotidylinositol 3-kinase
PKC…….Protein kinase C
PKCα……..Protein kinase Cα
PLA_2……$Phospholipase\ A_2$
PLCγ……Phospholipase Cγ
PMSF……..Phenylmethylsulfonyl fluoride
PN1…….Postnatal day 1
pNA…….p-nitroanilide
POAG……..Primary open angle glaucoma
PS……Phosphotidylserine
PTK…….Protein tyrosine kinase
PUFA……..Polyunsaturated fatty acid
K^+……Potassium
PAGE……..Polyacrylamide gel electrophoresis
PR……Photoreceptor
RCS…….Royal College Surgeons
RGC……....Retinal ganglion cell
RGC-5…….Retinal ganglion cell 5 cell transformed cell line
RIP1……Receptor-Interacting Protein 1
RIP3……Receptor-Interacting Protein 3
RK……..Rhodopsin kinase
RNA……Ribonucleic acid
ROS…….Reactive oxygen species
RPE…….Retinal pigment epithelium
rRNA……..Ribosomal ribonucleic acid
SAPK……..Stress-activated protein kinase
sConA…….Succinyl concavanalin A
SD……Serum deprivation
SDS…….Sodium dodecyl sulphate
SEM……Standard error of the mean
Smac……Second mitochondrial activator of caspases
SNP…….Sodium nitroprusside
SOD……Superoxide dismutase
STAT……..Signal transducer and activator of transcription
TdT…….Terminal deoxynucleotidyl transferase
tBID……Truncated Bid protein
tRNA……..Transcriptional ribonucleic acid
TBA …….. Thiobarbituric acid
TBARS ……..Thiobarbituric acid reactive species
TBE…….Tris-borate-ethylene-diamino-tetra-acetic acid
TBS…….Tris-buffer saline
TBS-T…….Tris-buffer saline containing 0.1% Tween-20
TEMED……..N,N,N',N'-tetramethylethylenediamine
TGF-β…….Transforming growth factor β
Thy-1……..Thymocyte differentiation antigen 1
TNF-α…….Tumour necrosis factor-alpha
TRAIL…….Tumour necrosis factor-related apoptosis-inducing

ligand
TSA…….Trichostatin A
TUNEL……TdT-dUTP-linked nick end labelling
UV……...Ultraviolet
VB ……..Vitreous body
VDAC1……Voltage-dependent anion channel 1
VEGF……..Vascular Endothelial Growth Factor
WHO……World Health Organization
WST-1…….4-[3-(-iodophenyl)-2-(4-nitrophenyl)-2H-5-tetzolio]-1,3-benzene disulfonate
XIAP……X-linked inhibitor of apoptosis protein
Z-VAD-fmk……....Benzoylcarbonyl-Val-Ala-Asp-fluoromethyl ketone

Table of contents

CHAPTER 1: General introduction....1

1.1 Introduction....2

1.2 Basic anatomy of the retina....3
1.2.1 Histology and cell type....3
1.2.1.1. Neuronal retinal cell subtypes....4
1.2.1.2 Glial cells....12

1.3 Modes of cell death....17
1.3.1 Apoptosis....17
1.3.2 Necrosis....22
1.3.3 Necroptosis....22

1.4 MAPK kinase signaling pathway....25
1.4.1 ERK pathway....25
1.4.2 SAPK/JNK signaling pathway....27
1.4.3 p38 signaling pathway....29

1.5 Glaucoma....29
1.5.1 A brief overview of glaucoma....29
1.5.2 Pathogenesis of ganglion cell death in POAG....30
1.5.2.1 Retinal ischaemia....33
1.5.2.2 Neurotrophin deprivation....34
1.5.2.3 Oxidative stress....34
1.5.2.4 Mitochondrial dysfunction....35
1.5.2.5 Light as a possible risk factor for glaucoma....36

1.6 Experimental approaches in trying to understand more about ganglion cell death....38
1.6.1 Mixed retinal cell cultures....39
1.6.2 Retinal explants....39
1.6.3 Purified ganglion cells....39
1.6.4 RGC-5 cell line....40

1.7 Flavonoids....43
1.7.1 Brief review of tea catechins....44
1.7.1.1 Pharmacokinetics and elimination of green tea catechins....46
1.7.1.2 Epigallocatechin gallate (EGCG) actions....48
1.7.1.3 Epicatechin gallate (EC)....52
1.7.2 Genistein....54
1.7.2.1 Pharmacokinetics and elimination....55
1.7.2.2 Neuroprotective effects....57
1.7.2.3 Antioxidant effects....60
1.7.2.4 Genistein and the retina....61

CHAPTER 2: Materials and methods....62

2.1 Materials....63
2.1.1 General reagents....63
2.1.2 Anaesthetics....63
2.1.3 Immunochemicals....63
2.1.4 DNA Labelling Reagents....64

2.1.5 Retinal Ganglion Cell Line (RGC-5) **64**
2.1.6 Cell Culture Reagents **66**
2.1.7 PCR reagents **66**
2.1.8 qPCR reagents **67**

2.2 Methods **67**
2.2.1 Lipid peroxidation **67**
2.2.2 RGC-5 Cell Cultures **68**
2.2.3 Preparation of Cytoplasmic, Mitochondrial and Nuclear Extracts **69**
2.2.4 Cell Viability Assays **70**
2.2.4.1 Basic Principles of MTT Assay 70
2.2.4.2 Methodology of MTT Assay 71
2.2.4.3 WST-1 Assay 72
2.2.5 Assessment of reactive oxygen species (ROS) production (DHE staining) **72**
2.2.6 Assessment of apoptosis using APOPercentage™ Assay **73**
2.2.7 Assessment of cell viability and death by simultaneous staining with fluorescein diacetate (FDA) and propidium iodide (PI) **73**
2.2.8 Terminal-Deoxynucleotidyl Transferase (TdT)-Mediated dUTP-Biotin Nick End Labeling (TUNEL) **74**
2.2.8.1 Basic Principles of TUNEL staining 74
2.2.8.2 Methodology of TUNEL Staining 76
2.2.9 Immunohistochemistry and Immunocytochemistry **77**
2.2.9.1 Basic Principles of Immunohistochemistry and Immunocytochemistry 77
2.2.9.2 Methodology of Immunohistochemistry and Immunocytochemistry 77
2.2.10 Caspase-3 colourimetric assay **78**
2.2.11 Light treatment regime **79**
2.2.12 Induction of retinal ischemia **81**
2.2.12.1 Genistein *in vivo* study 81
2.2.13 Polymerase chain reaction (PCR) **82**
2.2.13.1 Basic principles of PCR 82
2.2.13.2 Methodology of PCR in optic nerves and retina 84
2.2.13.3 Real-Time quantitative PCR (qPCR) 89
2.2.14 Electrophoresis / SDS-PAGE **92**
2.2.14.1 Basic principle of eletrophoresis/ SDS-PAGE 92
2.2.14.2 Methodologies of electrophoresis/ SDS-PAGE 92
2.2.15 Immunoelectroblotting (IEB or Western Blotting) **94**
2.2.15.1 Basic principle of immunoelectroblotting (IEB or Western Blotting) 94
2.2.15.2 Methodology of immunoelectroblotting (IBE or Western Blotting) 94

2.3 Statistical Analysis **97**

CHAPTER 3: Genistein blunts the negative effect of ishcaemia to the retina caused by an elevation of intraocular pressure **98**

3.1 Introduction **99**
3.1.1 Aim **99**
3.1.2 Brief overview **99**
3.1.3 Summary of results **100**

3.2 Experimental design **101**

3.3 Results **102**
3.3.1 Immunohistochemistry **102**
3.3.2 Western blot data **104**
3.3.3 PCR data **110**

3.4 Discussion 117

CHAPTER 4: Influence of selected flavonoids on the survival of RGC-5 cells subjected to different types of oxidative stress.....121

4.1 Introduction 122
4.1.1 Aim 122
4.1.2 Brief overview 122
4.1.3 Summary of results 126

4.2 Results 127
4.2.1 Lipid peroxidation studies 127
4.2.2 RGC-5 cells 131
4.2.3 Flavonoids dose response 133
4.2.4 Hydrogen peroxide-induced toxicity 134
4.2.3.1 MTT assay 134
4.2.3.2 WST-1 assay 136
4.2.3.2 Reactive oxygen species (ROS) production 137
4.2.3.3 Cell death by apoptosis 139
4.2.4 Glutamate/BSO-induced toxicity 144
4.2.4.1 MTT assay 144
4.2.4.2 WST-1 assay 147
4.2.4.3 Apoptotic membrane alteration with the APOPercentage™ assay 148
4.2.5 Serum deprivation-induced toxicity 151
4.2.5.1 MTT assay 151
4.2.5.2 Western blot analysis 154
4.2.5.3 qPCR analysis 156
4.2.6 Effects of flavonoids alone on RGC-5 cells 160

4.3 Discussion 164

CHAPTER 5: Rotenone-induced death of cultured RGC-5 cells is caspase independent, involves the JNK and p38 pathways and is attenuated by specific green tea flavonoids.....171

5.1 Introduction 172
5.1.1 Aim 172
5.1.2 Brief overview 172
5.1.3 Summary of results 174

5.2 Results 175
5.2.1 Assessment of cell viability 175
5.2.2 Assessment of caspase-3 activity 183
5.2.3 Assessment of reactive oxygen species (ROS) production 184
5.2.4 Assessment of apoptosis by APOPercentage™ and TUNEL staining 186
5.2.5 Role of MAPK kinase pathway in rotenone-induced RGC-5 cell death 192

5.3 Discussion 199

CHAPTER 6: Light- and sodium azide-induced cell death of RGC-5 cells in culture occurs via different mechanisms and is attenuated by epigallocatehin gallate.....202

6.1 Introduction 203

6.1.1 Aim **203**
6.1.2 Brief overview **203**
6.1.3 Summary of results **206**

6.2 Results **207**
6.2.1 Cell viability **207**
6.3.2 Production of reactive oxygen species (ROS) **218**
6.3.3 Dead/live cell assay with propidium iodide (PI) **219**
6.3.4 Apoptosis by APOPercentage™ and TUNEL methods **221**
6.3.5 Western blot analysis **224**
6.3.6 Immunocytochemistry **230**

6.4 Discussion **233**

CHAPTER 7: General discussion **238**

7.1 General discussion **239**

CHAPTER 8: References **248**

References **249**

List of figures

Chapter 1

1.1. Haematoxylin and eosin staining of a cross section of a human retina. 3
1.2. Schematic diagrams of rod (left) and cone (right) photoreceptors. 6
1.3. A schematic diagram illustrating the retinal cone ON/OFF pathway. 8
1.4. A schematic view of the rod pathway in mammalian retina. 9
1.5. A Drawing of a Müller cell. 13
1.6. Stellate-shaped dye-filled astrocytes of a rat hippocampus 15
1.7. Molecular detection of apoptosis in cells by TUNEL labelling. 19
1.8. Scheme of the extrinsic and intrinsic pathways. 21
1.9. Schematic overview for possible modes of neuronal death. 24
1.10. Mitogen-activated protein kinase (MAPK) signaling pathways. 26
1.11. An overview of the JNK pathway 28
1.12. Hypothetical cascade of events to account for differential ganglion cell death as occur in glaucoma. 32
1.13. The electron transport chain contains four complexes for ATP production. 37
1.14. The basic chemical structure of epicatechin gallate (EC) and epigallocatechin gallate (EGCG) 46
1.15. A comparison of chemical structures of genistein with 17β-estradiol. 55
1.16. Diagram depicting the metabolism of isoflavones. 57

Chapter 2

2.1 MTT assay in RGC-5 cells 71
2.2. TUNEL localization of DNA fragmentation in apoptosis 75
2.3. The spectral irradiance profile of the fluorescent light source used 80
2.4. Three basic steps in PCR. 83
2.5. Amplification of target DNAs 84
2.6. Detection of protein on a gel by western blotting. 96

Chapter 3

3.1. Immunohistochemistry staining of rat retinal sections for ChAT and GFAP 103
3.2. NF-L retinal protein expression following ischaemia/reperfusion 105
3.3. PARP retinal protein expression following ischaemia/reperfusion 106
3.4. GFAP retinal protein expression following ischaemia/reperfusion 107

3.5. NF-L protein expression in optic nerves following ischaemia/reperfusion.....108
3.6. Tubulin protein expression in optic nerves following ischaemia/reperfusion.....109
3.7. NF-L retinal mRNA levels following ischaemia/reperfusion.....111
3.8. Thy-1 retinal mRNA levels following ischaemia/reperfusion. 112
3.9. Caspase-3 retinal mRNA levels following ischaemia/reperfusion.....113
3.10. Caspase-8 retinal mRNA levels following ischaemia/reperfusion. 114
3.11. GFAP retinal mRNA levels following ischaemia/reperfusion. 115
3.12 PARP retinal mRNA levels following ischaemia/reperfusion. 116

Chapter 4

4.1. Sodium nitroprusside (SNP)-induced stimulation of lipid peroxidation in rat brain homogenates.....127
4.2. EGCG inhibits the effect of SNP-induced lipid peroxidation 128
4.3 EC in inhibits the effect of SNP-induced lipid peroxidation 129
4.4 EC in inhibits the effect of SNP-induced lipid peroxidation 130
4.5 Unstained microscopic view of RGC-5 cells in culture.....131
4.6A BDNF staining of RGC-5 cells 132
4.6B NF-L staining of RGC-5 cells 132
4.7 Dose response curve of EC, EGCG and genistein 133
4.8A Cell viability of RGC-5 cells exposed to increasing concentrations of H_2O_2 135
4.8B Cell viability of RGC-5 cells exposed to H_2O_2 400μM and co-incubated with EGCG 50μM, EC 50μM and genistein 10μM.....135
4.9 Mitochondrial dehydrogenase activity of RGC-5 cells exposed to H_2O_2 400μM and co-incubated with EGCG 50μM, EC 50μM and genistein 10μM 136
4.10A-E DHE staining of ROS in RGC-5 cells exposed to H_2O_2 400mM and co-incubated with EGCG 50μM, EC 50μM and genistein 10μM 138
4.11A-E Apoptosis detected by the APOP*ercentage*™ assay in RGC-5 cells exposed to H_2O_2 400μM and co-incubated with EGCG 50μM, EC 50μM and genistein 10μM.....140
4.12 Quantitative analysis of phosphotidylserine staining in RGC-5 cells exposed to H_2O_2 400μM.....141
4.13A-F TUNEL staining of RGC-5 cells exposed to DNAse treatment, H_2O_2 400μM and co-incubated with EGCG 50μM, EC 50μM and genistein 10μM 142
4.14 Quantitative analysis of TUNEL-positive RGC-5 cells exposed to H_2O_2 400μM.....143
4.15 Cell viability of RGC-5 cells exposed to increasing concentrations of glutamate with and without co-incubation with BSO 1mM 145

4.16 Cell viability of RGC-5 cells exposed to glutamate 1mM and BSO 1mM and co-incubated with EGCG 50μM, EC 50μM and genistein 10μM.....146
4.17 Mitochondrial dehydrogenase activity of RGC-5 cells exposed to glutamate 1mM and BSO 1mM and co-incubated with EGCG 50μM, EC 50μM and genistein 10μM.....147
4.18A-E Apoptosis detected by the APOP*ercentage*™ assay in RGC-5 cells exposed to glutamate 1mM and BSO 1mM and co-incubated with EGCG 50μM, EC 50μM and genistein 10μM 149
4.19 Quantitative analysis of phosphotidylserine staining in RGC-5 cells exposed to glutamate toxicity.....150
4.20 Cell viability of RGC-5 cells exposed to increasing duration of exposure to serum deprivation conditions 151
4.21A Effects of serum deprivation on RGC05 cells in culture after 48 hours incubation 152
4.21B DHE staining for ROS in RGC-5 cells exposed to serum deprivation conditions for 48 hours.....152
4.22 Cell viability of RGC-5 cells exposed to serum deprivation for 48 hours and co-incubated with EGCG (10μM and 50μM), EC (10μM and 50μM) and genistein 10μM ..153
4.23A P-c-Jun and P-p38 protein expression in RGC-5 cells following exposure to serum deprivation conditions from western blotting 155
4.23B Bcl2, Bax and actin protein expression in RGC-5 cells following exposure to serum deprivation conditions from western blotting.....155
4.24A Melt curve for B_2M gene 157
4.24B Staining of the generated B_2M gene products on agarose gel 157
4.25A Melt curve for Bax gene 158
4.25B Staining of the generated Bax gene products on agarose gel 158
4.26 Fold change in Bcl-2, Bax and Bax/Bcl-2 genes expression in RGC-5 cells following exposure to serum deprivation conditions.....160
4.27 Staining of the generated Nrf-2, HO-1 and Bcl-2 gene products after incubation with genistein 10μM, EC 50μM and EGCG 50μM.....161
4.28 Fold change in Nrf-2, HO-1 and Bcl-2 genes expression in RGC-5 cells after incubation with genistein 10μM, EC 50μM and EGCG 50μM.....163

Chapter 5

5.1 Cell viability of RGC-5 cells exposed to increasing concentrations of rotenone 175

5.2 Cell viability of RGC-5 cells exposed to rotenone 10μM and co-incubated with EGCG (10μM, 50μM, 75μM and 100μM) and trolox 2mM.....176

5.3 Cell viability of RGC-5 cells exposed to rotenone 10μM and co-incubated with EC (10μM, 50μM, 75μM and 100μM) and EGCG 50μM.....177

5.4 Cell viability of RGC-5 cells exposed to rotenone 10μM and co-incubated with baicalin (1μM, 10μM and 25μM), genistein (1μM, 10μM and 25μM) and EGCG 50μM 178

5.5 Cell viability of RGC-5 cells exposed to rotenone 10μM and co-incubated with SP600125 (50μM, 100μM and 200μM) and EC 50μM 179

5.6 Cell viability of RGC-5 cells exposed to rotenone 10μM and co-incubated with z-VAD-fmk (50μM, 100μM and 200μM) and EC 50μM 180

5.7 Cell viability of RGC-5 cells exposed to rotenone 10μM and co-incubated with NU1025 (50μM, 100μM and 200μM) and EC 50μM 181

5.8 Cell viability of RGC-5 cells exposed to rotenone 10μM and co-incubated with Necrostatin-1 (50μM, 100μM and 200μM) and EC 50μM 182

5.9 Caspase-3 activity of RGC-5 cells exposed to staurosporine 500nM and rotenone 10μM.....183

5.10A-F DHE staining of ROS in RGC-5 cells exposed to rotenone 10μM and co-incubated with EGCG 50μM, EC 50μM, baicalin 10μM and genistein 10μM 185

5.11A-F Apoptosis detected by the APOP*ercentage*™ assay in RGC-5 cells exposed to rotenone 10μM and co-incubated with EGCG 50μM, EC 50μM, baicalin 10μM and genistein 10μM 187

5.12 Quantitative analysis of phosphotidylserine staining in RGC-5 cells exposed to rotenone 10μM.....188

5.13A-F TUNEL staining of ROS in RGC-5 cells exposed to rotenone 10μM and co-incubated with EGCG 50μM, EC 50μM, baicalin 10μM and genistein 10μM 190

5.14 Quantitative analysis of TUNEL-positive RGC-5 cells exposed to rotenone 10μM 191

5.15A-D P-p38 counterstaining with DAPI of RGC-5 cells exposed to rotenone 10μM 193

5.16A-B P-p38 protein expression in RGC-5 cells after exposure to rotenone 10μM from western blotting 194

5.17A-D P-c-Jun counterstaining with DAPI of RGC-5 cells exposed to rotenone 10μM 196
5.18 P-JNK, P-c-Jun and P-p38 proteins expression in the cytoplasm, mitochondria and nuclei of RGC-5 cells after exposure to rotenone 10μM from western blotting 197
5.19 AIF protein expression in RGC-5 cells after exposure to rotenone 10μM from western blotting 198

Chapter 6

6.1 Cell viability of RGC-5 cells exposed to increasing duration of light 1000lux 207
6.2 Cell viability of RGC-5 cells exposed to increasing concentrations of sodium azide 208
6.3 Cell viability of RGC-5 cells exposed to light 1000lux for 48 hours and co-incubated with EGCG 10μM, 20μM and 50μM 209
6.4 Cell viability of RGC-5 cells exposed to sodium azide 5mM and co-incubated with EGCG 10μM, 50μM and 80μM 210
6.5 Mitochondrial dehydrogenase activity of RGC-5 cells exposed to light 1000lux for 48 hours and co-incubated with EGCG 10μM, 20μM and 50μM 211
6.6 Mitochondrial dehydrogenase activity of RGC-5 cells exposed to sodium azide 5mM and co-incubated with EGCG 10μM, 50μM and 80μM 212
6.7 Cell viability of RGC-5 cells exposed to light 1000lux for 48 hours and co-incubated with z-VAD-fmk 25μM and 50μM 213
6.8 Cell viability of RGC-5 cells exposed to sodium azide 5mM and co-incubated with z-VAD-fmk 25μM and 50μM 214
6.9 Caspase-3 activity of RGC-5 cells exposed to sodium azide 25mM and staurosporine 500nM for 24 hours, and dark and light conditions for 96 hours 215
6.10 Cell viability of RGC-5 cells exposed to light 1000lux for 48 hours and co-incubated with Necrostatin-1 25μM and 50μM 216
6.11 Cell viability of RGC-5 cells exposed to sodium azide 5mM and co-incubated with Necrostatin-1 25μM and 50μM 217
6.12A-C DHE staining for ROS in RGC-5 cells exposed to sodium azide 5mM, and co-incubated with EGCG 80μM 218
6.12 D-F DHE staining for ROS in RGC-5 cells exposed to dark and light (1000lux) conditions for 48 hours, and co-incubated with EGCG 20μM 218
6.13A-C FDA/PI live-death staining in RGC-5 cells exposed to sodium azide 5mM, and co-incubated with EGCG 80μM 220

6.13D-F FDA/PI live-death staining in RGC-5 cells exposed to dark and light (1000lux) conditions for 48 hours, and co-incubated with EGCG 20μM 220
6.14A-C Apoptosis detected by the APOP*ercentage*™ assay in RGC-5 cells exposed to sodium azide 5mM, and co-incubated with EGCG 80μM 222
6.14D-F Apoptosis detected by the APOP*ercentage*™ assay in RGC-5 cells exposed to dark and light (1000lux) conditions for 48 hours, and co-incubated with EGCG 20μM 222
6.15A-C TUNEL staining in RGC-5 cells exposed to sodium azide 5mM, and co-incubated with EGCG 80μM 223
6.15D-F TUNEL staining in RGC-5 cells exposed to dark and light (1000lux) conditions for 48 hours, and co-incubated with EGC.....223
6.16 Alpha-fodrin protein expression in RGC-5 cells exposed to sodium azide 5mM and light 1000lux from western blotting 224
6.17 Quantitative analysis of alpha fodrin protein levels in relation to actin in RGC-5 cells exposed to sodium azide 5mM and light 1000lux from western blotting 225
6.18 AIF protein expression in RGC-5 cells exposed to sodium azide 5mM and light 1000lux from western blotting 226
6.19 Bcl-2 protein expression in RGC-5 cells exposed to sodium azide 5mM and light 1000lux from western blotting and densitometry analysis 227
6.20 HO-1 protein expression in RGC-5 cells exposed to sodium azide 5mM and light 1000lux from western blotting and densitometry analysis 228
6.21 P-JNK and P-c-Jun protein expression in RGC-5 cells exposed to sodium azide 5mM and light 1000lux from western blotting 229
6.22 P-p38 counterstaining with DAPI in RGC-5 cells exposed to sodium azide 5mM and light 1000lux 231
6.23 P-c-Jun counterstaining with DAPI in RGC-5 cells exposed to sodium azide 5mM and light 1000lux 232

List of tables

Chapter 1

1.1. Summary of selected functions of Müller cells. 14

Chapter 2

2.1. List of dilution ratio for primary and secondary antibodies..... 65
2.2. Primer sequence and annealing temperatures for conventional PCR..... 88
2.3. Primer sequences and annealing temperatures for qPCR. 91

Chapter 4

4.1. Melting temperatures (T_m) and the sizes measured in basepairs (bp) for each primer used in qpCR analysis. 159

Chapter 7

7.1. Summary of neuroprotective effects of flavonoids against various oxidative stress 241
7.2. Summary of cytokines and pathway activated by various oxidative stress 245

CHAPTER 1

GENERAL INTRODUCTION

1.1 Introduction

Optic neuropathies, like glaucoma (primary open angle glaucoma or POAG), are diseases affecting the retinal ganglion cells and have a myriad of causes. According to the World Health Organization, approximately 36 million people worldwide are registered blind because of glaucoma. Glaucoma results in irreversible loss of sight and is a leading cause for blindness followed by age-related macular degeneration (Resnikoff *et al* 2004). Mitochondrial dysfunction caused by a variety of factors is postulated to be a cause for both the initiation and progression of glaucoma (Osborne 2010). In contrast, optic neuropathies such as Leber's hereditary optic neuropathy (LHON) are genetic diseases that affect their mitochondria (Carelli *et al* 1997, Carelli *et al* 1999). Glaucoma (POAG) is a treatable chronic disease, with strategies primarily aimed at delaying the rate of progression. One treatment strategy for POAG is neuroprotection. This concept implies that appropriate pharmacological agents can be delivered to the retina in sufficient amounts to slow-down any of the processes that are the cause for the gradual death of retinal ganglion cells and loss of vision. One group of compounds that have been highlighted for possible use in this context are naturally occurring substances that have known beneficial properties in man and are tolerated when taken orally. Flavonoids constitute such a large group of naturally occurring compounds. Flavonoids are present in plants of various types and individual members have a number of described beneficial health properties. They can also be ingested in fairly large quantities without being toxic. A purpose of the described studies was therefore to determine whether specific flavonoids have characteristics that allow them to blunt the effects of defined insults to cells in culture as postulated to occur in POAG.

1.2 Basic anatomy of the retina

1.2.1 Histology and cell type

The retina is a thin stratified layer of neural tissue that captures light signals and is converted to visual information which is then relayed to the visual cortex of the brain for further processing and analysis. The retina consists of neuronal cells (photoreceptor cells, horizontal cells, bipolar cells, amacrine cells, interplexiform cells, and ganglion cells) and glial cells (Müller cells, astrocytes, microglial) as shown in figure 1.1 below.

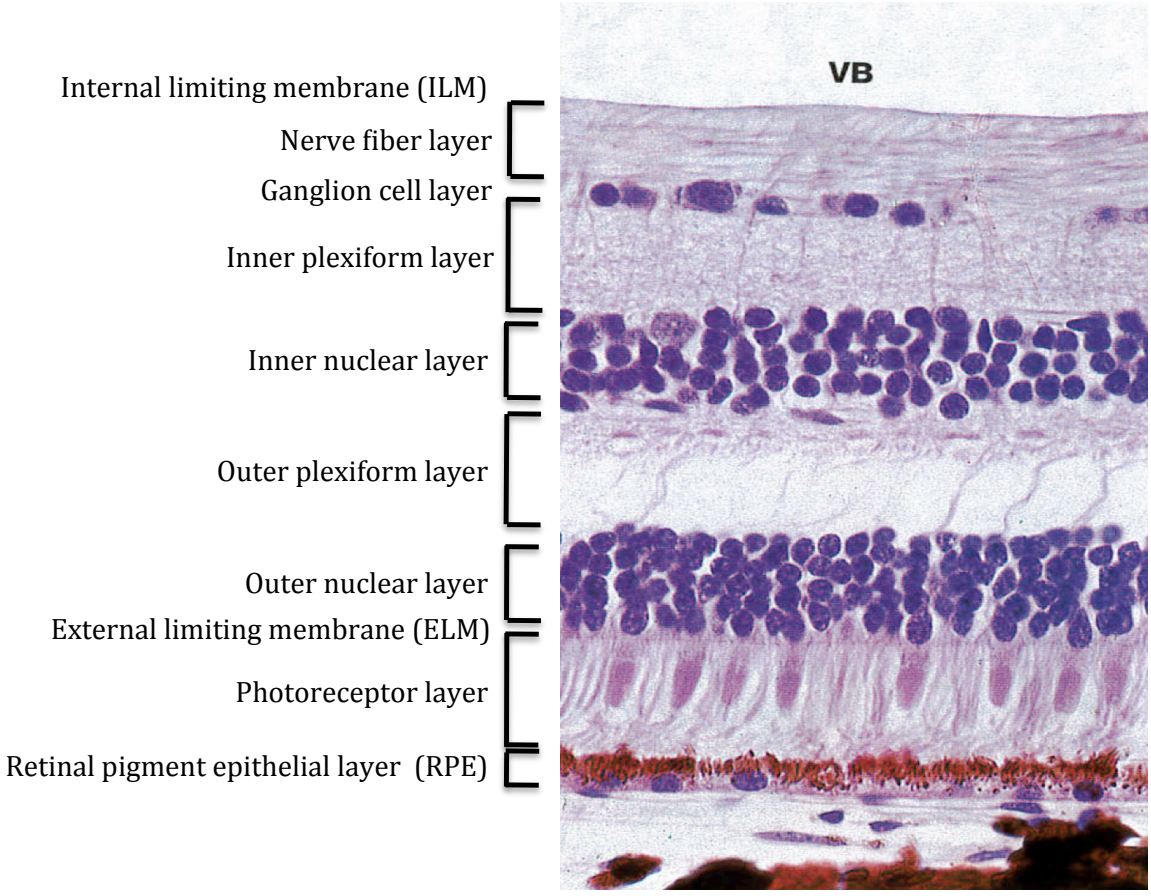


Figure 1.1. Haematoxylin and eosin staining of a cross section of a human retina.[1] (VB: vitreous body)

[1] Diagram taken from Wheater's Functional Histology: A text and colour atlas, 5th edition, 2007, pp 405.

1.2.1.1. Neuronal retinal cell subtypes

Photoreceptors

Mammalian visual system relies upon light detection by two photoreceptor-types, the rods and cones. Cones mediate photopic vision, which is rich in colour and marked by high temporal spatial resolution. Rods, on the other hand, are responsible for scotopic vision, which lack colour information. There are between 4 to 6 million cones in the human retina, which are concentrated in the central retina. Rods number between 78 to 110 million and are found throughout the retina with the exception of the fovea centralis (Osterberg 1935, Curcio *et al* 1990).

Both rod and cone photoreceptors consists of two morphologically distinct regions, which extend from the cell bodies: the outer and inner segments, as shown in figure 1.2. The outer segment is oriented towards the retinal pigment epithelium and is surrounded by the interphotoreceptor matrix. This part of photoreceptors function to convert light into electrical impulses by a process known as phototransduction (Shichida & Matsuyama 2009). These impulses are propagated through the neural retina and along the optic nerve to reach the visual cortex in the brain. The rod outer segment is cylindrical in shape and contains stacks of disc membranes, which are surrounded by a plasma membrane. In comparison, the plasma membrane in a cone outer segment invaginates repeatedly to form a tightly stacked lamellae structure. The rod and cone outer segments contain different visual pigments which are responsible for scotopic vision by rods, and colour vision by cones. The visual pigment in rods is known as rhodopsin. The human cones are divided into three spectral classes according to their visual pigments which are sensitive to short- (424 nm), middle- (530nm) and long-wavelengths (560nm) (Bowmaker & Dartnall 1980, Schnapf *et al*

1987). Outer segments are constantly renewed with discs added and shed (Young 1967, Young & Bok 1969, Bok 1985).

The outer segment is connected to the inner segment by a thin cytoplasmic isthmus containing a modified cilium (Bron *et al* 1997). Histologically, there are two regions identified in the inner segment: an eosinophilic ellipsoid and basophilic myoid (Bron *et al* 1997). The myoid region contains protein machinery and the ellipsoid region contains elongated mitochondria (Sjostrand 1953, De Robertis 1956).

The photoreceptor synaptic terminals are located in the outer plexiform layer of the retina. The synaptic terminal is called spherule in rods and pedicle in cones. Both spherule and pedicle are specialized for intercellular signaling and form synapses with bipolar cells.

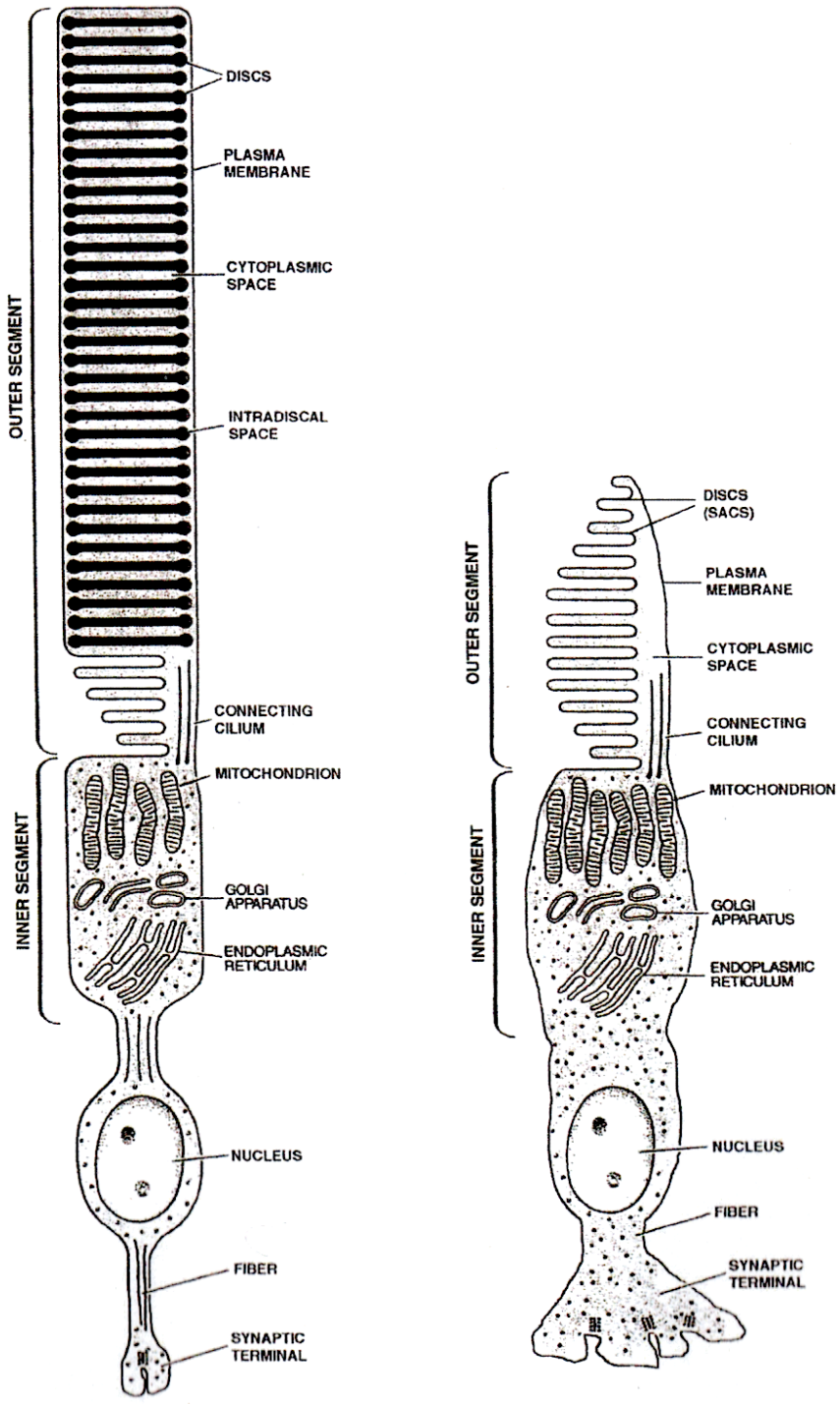


Figure 1.2. Schematic diagrams of rod (left) and cone (right) photoreceptors. The photoreceptors are oriented with the outer segment towards the sclera and the synaptic terminal toward the vitreous.[2]

[2]Taken from Albert & Jakobiec: Principles and Practice of Ophthalmology, 2nd edition, volume 3, pp1625.

Horizontal cells

Horizontal cells have long processes that arborize exclusively in the outer plexiform layer. There are two types of horizontal cells in the mammalian retina, which are characterized by their contact with photoreceptor cells. The HII subtype makes contact only with cones, whereas the HI subtype contacts axons of both rod and cone cells. Horizontal cells use GABA as their neurotransmitter, and provide inhibitory feedback to photoreceptor cells or inhibitory feed-forward contact with bipolar cells.

Bipolar cells

Bipolar cells are responsible for transmitting signals from photoreceptors to ganglion cells and/or amacrine cells. Bipolar cells are second order neurons and form synapses between photoreceptors and ganglion cells. Some bipolar cells are postsynaptic to rods while others to cones and some receive mixed rod-cone input. Some cone bipolar cells selectively innervate only red, green or blue cones, while others are non-selective (Scholes 1975, Ishida *et al* 1980). Two types of hyperpolarizing and depolarizing bipolar cells have been described as the ON and OFF-types (Werblin & Dowling 1969, Kaneko 1970). These bipolar cells have opposing response to light stimulus although initiated by the same neurotransmitter (glutamate) released from all photoreceptors. The ON-type cells are hyperpolarised while the OFF-type cells are depolarized by glutamate (Nelson & Connaughton 2005).

The ON and OFF bipolar cells initiate two functionally independent pathways and relayed separately to different brain loci. As shown in figure 1.3, the axon terminal arborizations of OFF-type bipolar cell lie in sublamina a in the inner plexiform layer, where they synapse with OFF-type ganglion cells. The ON-type bipolar cells synapse with the ON-type ganglion cells in sublamina b (Famiglietti & Kolb 1976, Nelson *et al* 1978).

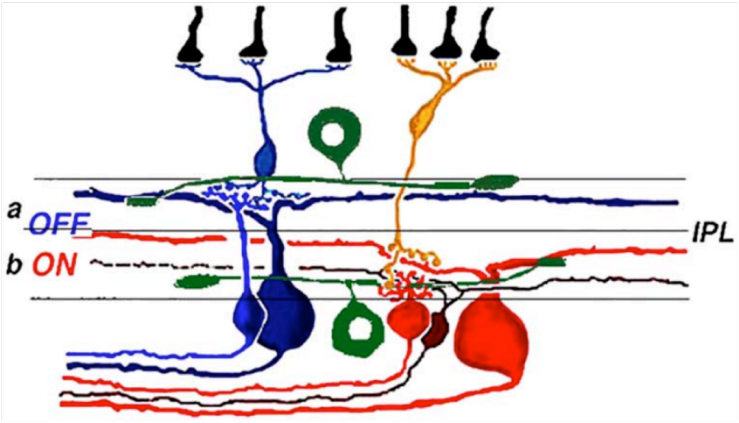


Figure 1.3. A schematic diagram illustrating the retinal cone ON/OFF pathway. Three cell types are shown above that contribute to these pathways: cone bipolar cells (blue and yellow), amacrine cells (green) and retinal ganglion cells (blue and red). Cells in blue are involved in the OFF pathway, while those in red are involved in the ON pathway.[3]

Unlike cone bipolar cells, only a single morphological type of rod bipolar cell is recognized in mammalian retinas (Kolb 1970, Famiglietti & Kolb 1975). Rod bipolar cells do not have direct contact with ganglion cells, instead they transfers signals to ganglion cells through AII amacrine cells as shown in figure 1.4 (Kolb & Famiglietti 1974, Nelson 1982). Rods hyperpolarize in light and cause depolarization of rod bipolar cells through inhibitory glutamate (2-amino-4 phosphonobutyrate, APB) synapse. The rod bipolar cells in turn depolarize the AII amacrine cells through excitatory synapses, probably also using glutamate as the neurotransmitter. Light-evoked depolarization from AII amacrine cells are relayed to cone ON-bipolar cells through excitatory gap junctions in sublamina b, which in turn excites the ON-centre ganglion cells through excitatory glutamate synapse. At the same time, the AII amacrine cells inhibit the OFF-centre ganglion cells through inhibitory glycine synapses (Kolb & Famiglietti 1974, Famiglietti & Kolb 1975, Müller *et al* 1988, Daw *et al* 1990, Strettoi *et al* 1990, Vaney *et al* 1991).

[3] Chalupa LM and Günham E. Development of On and Off retinal pathways and retinogeniculate projections. Prog Ret Eye Res, 2004 (23)31-51

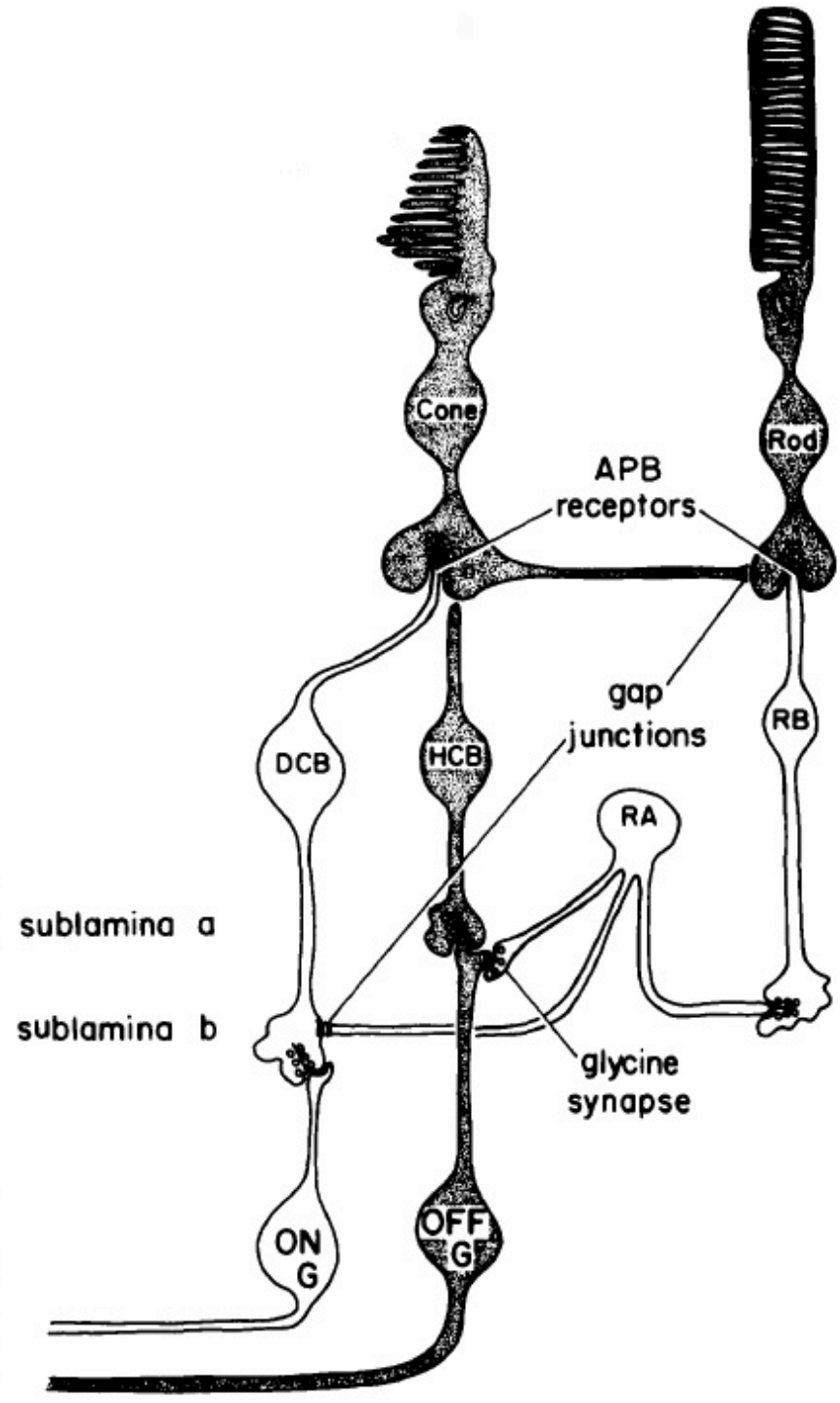


Figure 1.4. A schematic view of the rod pathway in mammalian retina. Cells that depolarize in light are shown in white, whereas cells that hyperpolarize in light are shaded. Abbreviations: DCB: depolarizing cone bipolar cell; HCB: hyperpolarizing cone bipolar cell; ON G: ON-centre ganglion cell; OFF G: OFF-centre ganglion cell; RA: AII amacrine cell; RB: rod bipolar cells.[4]

[4] Diagram taken from Daw et al. Rod pathways in mammalian retinae. Trends in Neuroscience, 1990 (269) 381-391.

Ganglion cells

Ganglion cells are third order retinal neurons. Their perikarya lie outside the inner plexiform layer close to the vitreous. They are responsible for relaying all visual information to the visual occipital cortex in the brain, and subthalamic structures serving non-visual processes such as pupillary reflexes and circadian functions. There are about 1.2 million ganglion cells present in the human retina which converge and exit the eye as the optic nerve (Sigelman & Ozanics 1982). Ganglion cells are large, with diameters ranging from 10 to 30μm. Mammals have a variety of ganglion cell types (Perry 1982, Wässle 1982). Midget ganglion cells are the most numerous type of ganglion cells, and are also called P ganglion cells as their axons project to the parvocellular portion of the lateral geniculate nucleus (Shapley & Perry 1986, Kaplan *et al* 1990, Rodieck & Watanabe 1993). In the human fovea, midget cells account for 90 to 95% of all ganglion cells. Their density decreases to about 45% in the retina periphery (Dacey 1993). They are thought to be responsible for acuity and colour vision (Dacey 1993, Goodchild *et al* 1996).

The second, larger group of ganglion cells are called parasol cells, and are also known as M ganglion cells as their axons extend to the magnocellular portion of the lateral geniculate nucleus (Rodieck & Watanabe 1993). These cells are recognized by their larger cell bodies, extensive dendritic tree and thick axons (Silveira & Perry 1991). They make up only 5% of all ganglion cells in the human fovea, and 20% of ganglion cells in the periphery. These cells probably transmit information about moving or changing objects (Dacey 1994). Another type of ganglion cell is the small bistratified ganglion cell which represents 1% of the total ganglion cells in the central retina and 6 to 10% in the periphery.

Amacrine cells

Amacrine cells modulate transfer of light signals from bipolar to ganglion cells. Most amacrine cell neurons are located in the inner part of the inner nuclear layer, but some can also be found in the ganglion cell layer (called displaced amacrine cells) or rarely in the inner plexiform layer (called intersitital amacrine cells). Each amacrine cell has a single process with extensive branches, which extend over a wide area in the inner plexiform layer. The vast majority of amacrine cells do not have axons (Dowling & Boycott 1966). Two types of amacrine cells have been identified based on the distribution of their processes in the inner plexiform layer: (1) diffuse and (2) stratified. The main process of the diffuse amacrine cells extend through the inner aspect of the inner plexiform layer, and are further divided into narrow-field and wide-field cells. The stratified amacrine cells are divided into unistratified (located in the outer half of the inner plexiform layer), multistratified (located in the central region of the inner plexiform layer) and diffuse or polystratified cells. Amacrine cells contain a variety of neuroactive substances (neurotransmitters glycine, GABA, acetylcholine and dopamine) as well as neuropeptides (somatostatin, substance P, neuropeptide Y, vasoactive intestinal peptide, cholecystokinin) (Bron *et al* 1997).

Interplexiform cells

Interplexiform cells send their processes to both the outer and inner plexiform layers. Sensory inputs to these cells occur in the inner plexiform layer, and most synapses are in the outer plexiform layer. They contain either dopamine or GABA neurotransmitters (Ryan & Hendrickson 1987), and carry feedback signals between the amacrine and bipolar cells.

1.2.1.2 Glial cells

Müller cells

Three types of glial cells exist in the mammalian retina: Müller cells, astrocytes and microglial cells. The Müller cell is the major glial cell type of the retina, carrying out many functions served by brain glial cells such as oligodendrocytes, astrocytes and ependymal cells. Müller cells were first described as radial fibers with thread-like structures that transverse across the full thickness of the vertebrate retina in 1851 (Müller 1851). Kölliker (Kölliker 1854) subsequently named analogous cells in the human retinas as 'radial fibers of Müller' (Pedler 1963). Müller cells extend inwardly to terminate in the inner limiting membrane in an expansion called *endfoot,* and outwardly to end in the photoreceptor layer as shown in figure 1.5A. Müller cells envelop neuronal cell bodies and processes as well as blood vessels in the retina through many horizontal processes (as shown in figures 1.5A and 1.5B) providing structural, nutritional and metabolic support.

Müller cells are reponsible in maintaining water homeostasis and pH (Newman 1994), stimulating glycogenolysis (Reichenbach *et al* 1993) and removal of excess extracellular K^+ which is released to the vitreous humor and termed K^+ siphoning (Newman *et al* 1984, Karwoski *et al* 1989, Oakley *et al* 1992, Kofuji *et al* 2000). Apart from providing support for the immature retina during development (Willbold *et al* 1997), Müller cells may also play a role in synthesizing vitreal collagens (Ponsioen *et al* 2008). Other functions of the Müller cells are described in Table 1.1.

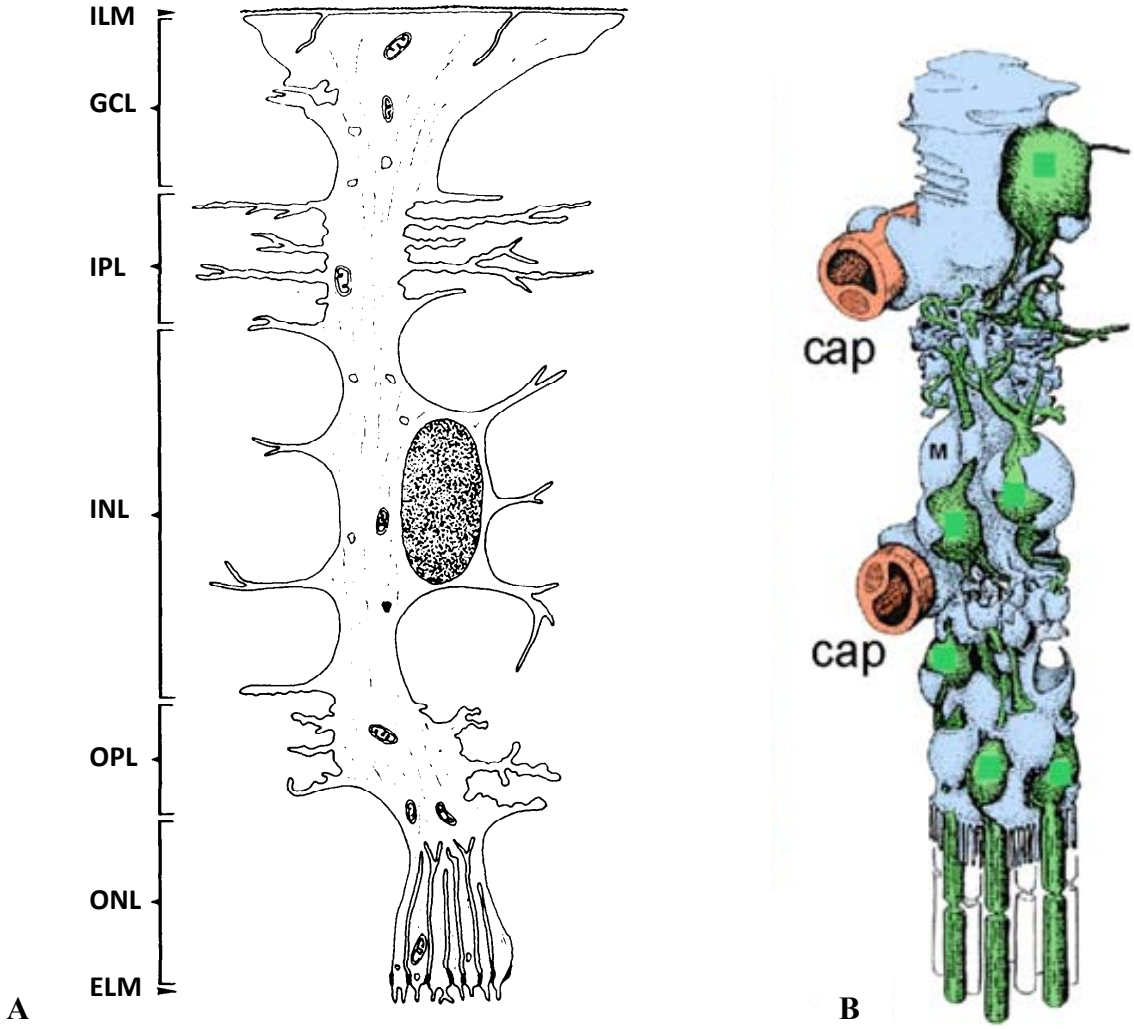


Figure 1.5. (A) Drawing of a Müller cell showing its radial configuration which spans the entire depth of the neural retina giving out multiple lateral processes in each layer of the retina. (ELM: external limiting membrane; ONL: outer nuclear layer; OPL: outer plexiform layer; INL: inner nuclear layer; IPPL: inner plexiform layer; GCL: ganglion cell layer; ILM: inner limiting membrane).[5] (B) An artist's view of a human Müller cell (blue) enveloping various types of retinal neurons (green) and establishing contacts to retinal blood vessels (red).[6]

[5] Diagram taken from Miller RF, Dowling JE: Intracellular responses of the Müller cells of mudpuppy retina: Their relation to b-wave of the electroretinogram. J Neurophysiol 33:323-34, 1970.

[6] Modified from Reichenbach A. et al: What do retinal Müller (glial) cells do for their neuronal 'small siblings'? J Chem Neuroanat 6:201-213, 1993.

Physiological process	**Müller cell function**	**Glia-specific protein/peptide**
Metabolic support and nutrition of neurons	• Delivery of lactate/pyruvate	• Lactate dehydrogenase
	• Storing of glycogen and glycogenolysis	• Glycogen phosphorylase
K^+ and water homeostasis	• CO2-buffering	• Carbonyl anhydrase
	• Removal of external K^+ ions (spatial buffering)	• Kir4.1 channel
	• Dehydration of inner retina	• AQP4 water channel
Protection against oxidative stress	• Scavenging free radicals	• Glutathion
Contribution to neuronal signaling	• Transmitter uptake	• Glutamate transporter
		• GABA transporter
	• Transmitter recylcling	• Glutamine synthetase
Recycling of photopigments	• Transport and conversion of bleached photopigments	• CRALBP
Release of neuroactive substances	Storage and release of • D-serine • Glutamine • ATP	
Release of vasoactive substances	Synthesis and release of • VEGF • PEDF • TGF-β	
Retinal development	• Scaffold for orientation (immature radial glia cells)	

Table 1.1. Summary of selected functions of Müller cells.[7]

[7] Table taken from Bringman A. et al Müller cells in the healthy and diseased retina. Prog Ret Eye Res 25: 397-424, 2006.

Astrocytes

Apart from Müller cells, astrocytes are the only other type of macroglia cells found in the retina. Astrocytes are so named based on their star-like appearance with numerous processes as shown in figure 1.6. Unlike the Müller cells, astrocytes are not homogenously distributed throughout the retina. Astrocytes are predominantly found in the nerve fiber layer and their density is correlated with the nerve fiber layer thickness (Bussow 1980, Schnitzer 1988). As a macroglia, astrocytes are thought be a special glia for the axons of the ganglion cells, providing nutritional and metabolic support. In the brain, astrocytes are shown to influence tight junctions which form the blood-brain barrier (Reese & Karnovsky 1967, Janzer & Raff 1987), and Janzer and Raff had showed that astrocytes are capable of inducing blood-brain barrier properties in non-neural endothelial cells (Janzer & Raff 1987). The co-distribution of astrocytes with the retinal blood vessels (Schnitzer 1988) may suggest that astrocytes play a role in maintaining blood-retinal barrier (Constable & Lawrenson 2009, Kim *et al* 2009).

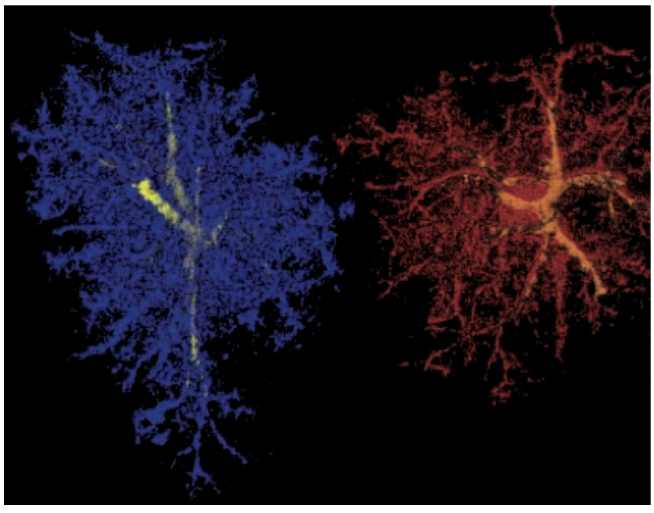


Figure 1.6. Stellate-shaped dye-filled astrocytes of a rat hippocampus showing numerous branching processes.[8]

[8] Diagram taken from Kimelberg HK. Function of mature mammalian astrocytes: A current view (Review). The Neuroscientist, 16(1): 79-106, 2010.

Microglia

Microglia cells are small glial cells that are derived from mesodermal invasion of the retina at the time of vascularization during embryogenesis (Sigelman & Ozanics 1982). They have been described as a separate cell group from astrocytes and oligodendrocytes by Rio Hortega based on the silver carbonate staining method of animal brains (del Rio Hortega & Penfield 1927). These cells can be found anywhere between the nerve fiber layer to the outer plexiform layer and are the only glial cells present in Henle's layer. Microglia cells are immunocompetent cells with phagocytic capacity during physiological and pathological conditions (Perry & Gordon 1988, Block *et al* 2007). In response to stimuli associated with injury, infection, aging and neurodegenerative diseases, microglia are activated and secret both neuroprotective substances such as brain-derived nerve factor (BDNF), nerve growth factor (NGF), neurotrophin 3 (NT3) (Giulian *et al* 1994, Elkabes *et al* 1996, Miwa *et al* 1997) and neurotoxic cytokines such as tumour necrosis factor alpha (TNFα), interleukin 6 (IL6), macrophage inflammatory proteins, (MIP1α, and MIP2) and nitric oxide (Prinz *et al* 1999, Lee *et al* 2000, Wu *et al* 2009). Activation of microglia has been shown to occur in animal models of optic nerve crush injury and chronic glaucoma (Wu *et al* 2009, Bosco *et al* 2011).

1.3 Modes of cell death

Cell death occurs regularly under physiologic as well as pathologic conditions. In physiologic terms, cell death may be defined as the irreversible breakdown of the energy-dependent functions of the cell. In pathologic terms, cell death refers to a series of morphological changes that occur following irreversible cell injury. The morphological process in dead cells occurs as a result of enzymatic degradation and protein breakdown. Traditionally, two types of cell death are described based on their cellular features, necrosis and apoptosis, or programmed cell death. The first morphological classification of cell death was proposed by Schweichel and Merker (Schweichel & Merker 1973) who described three types of cell deaths based on changes seen in rat embryos exposed to specific toxicants, as type I (associated with heterophagy), type II, (associated with autophagy) and type III (occurring without digestion). Today these cell modes are referred to as apoptosis, autophagy and necrosis, respectively. In contrast to apoptosis and necrosis, autophagy is involved in cell recycling and renewal process in maintaining cellular homeostasis rather than cell death (He & Klionsky 2009, Ravikumar *et al* 2010).

1.3.1 Apoptosis

The term apoptosis was introduced by Kerr in 1972 to indicate a particular form of death in which cells commit suicide by chopping themselves into membrane-bounded apoptotic bodies (Kerr *et al* 1972). Apoptosis is a Greek word describing 'falling leaves', and as its name suggests, apoptosis occur at different rates not unlike leaves falling off trees, leaf by leaf, as opposed to sudden massive cell death as would occur as a result of myocardial infarction. The hallmarks of apoptosis are listed below:

1) cytoplasmic and nuclear condensation with formation of apoptotic bodies which contain intact organelles and large nuclear fragments. These apoptotic

bodies are phagocytosed by neighbouring macrophages or other phagocytic cells

2) inflammation is absent in surrounding tissues
3) energy is required for RNA and protein synthesis, therefore apoptosis is an active process
4) membrane alteration and loss of plasma membrane integrity
5) chromatin condensation and DNA cleavage by Ca^{2+}-dependent non-lysosomal endonuclease resulting in small undigested DNA fragments in multiples of 180 base pairs (Wyllie 1980). These fragments represent DNA that was wrapped around the histone core and protected from degradation by the endogenous endonuclease. The fragments can be visualized by agarose gel electrophoresis as DNA 'ladder', or by a histochemical method which labels the ends of fragmented DNA, as shown in figure 1.7 (Gavrieli *et al* 1992). This method is referred to as TUNEL which is an abbreviation for *T*erminal tranferase d*U*TP *N*ick *E*nd *L*abelling.

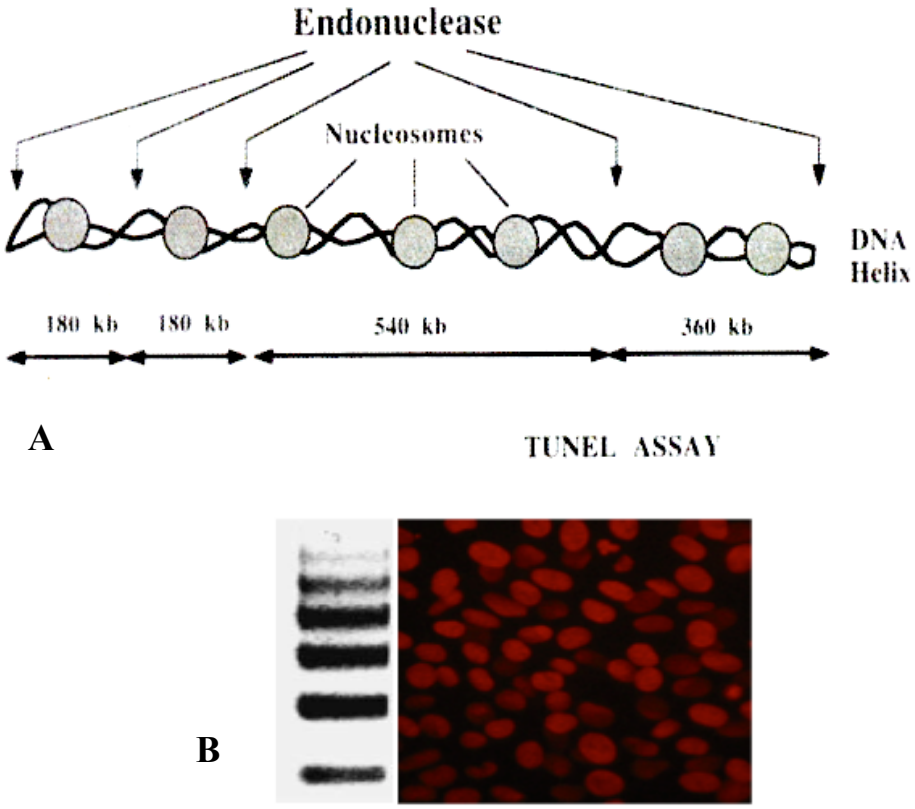


Figure 1.7. Molecular detection of apoptosis in cells. (A) DNA is cleaved by a specific endonuclease at internucleosome sites, into smaller fragments in the multiples of 180 base pairs[9]. These fragments form a 'DNA ladder' which can be visualized on agarose gel electrophoresis as shown on the right in (B)[10]. Apoptosis can be detected histologically by TUNEL staining assay by labelling the ends of fragmented DNA (nick) with deoxyribonucleotidyl transferase (TDT) and a biotinyl-dUTP substrate (bdUTP) or other tagged nucleotide. The bound biotins are then visualized by streptavidin-horseradish peroxidase (HRP) and diaminobenzidine, or by fluorescence staining such as Cy-3, as shown in the left in (B). In this case, RGC-5 cells were exposed to DNAse and subjected to TUNEL staining. The cleaved DNA stained with red Cy-3 fluorescence.

[9] Diagram taken from Papermaster DS. Death at an Early Age: Inves Ophth Vis Sci 36(6):977-983, 1995.
[10] Diagram taken from Wyllie AH et al. Chromatin cleavage in apoptosis: association with condensed chromatin morphology and dependence on macromolecular synthesis. J Patho 142:67-77, 1984.

One of the early hallmark of apoptosis is membrane alteration, in which phosphotidylserine (PS) loses its symmetrical distribution across the lipid bilayer and 'flips' from the inner to the outer membrane towards the cell surface (Martin *et al* 1995). Subsequently, PS may serve as a trigger for recognition by macrophages to initiate phagocytosis (Schroit *et al* 1985, Fadok *et al* 1992). Phosphotidylserine staining by assays such as APOP*ercentage*™ is another method of detecting early apoptosis changes.

Apoptosis can occur by the extrinsic (death receptor, DR) or the intrinsic (mitochondrial) pathways (Krammer 2000). The extrinsic pathway is initiated upon stimulation of members of the DR family, which are characterized by a cytoplasmic region called Death Domain (DD) (Tartaglia *et al* 1993, Weber & Vincenz 2001). Simulation of a DR by the corresponding death ligand leads to formation of the death-inducing signaling complex (DISC) (Kischkel *et al* 1995). The DISC consists of oligomerised receptors, Fas-Associated Death Domain molecule (FADD), procaspase-8 (FADD-like ICE [interleukin-1 converting enzyme], or FLICE) and the c-FLIP (cellular FLICE-inhibitory proteins) (Krammer *et al* 2007). DISC formation will activate procaspase 8/10 and subsequently initiate the apoptotic cascade, as shown in figure 1.8. Activation of caspase-3, caspase-7 and caspase-9 in the cytosol can be blocked by X-linked inhibitor of apoptosis protein, XIAP.

The intrinsic pathway may be triggered by factors such as irradiation (UV or gamma) and trophic factor withdrawal. Upon activation, a complex chain of events will eventually lead to mitochondrial outer membrane permeabilization (MOMP) and subsequent release of cytochrome *c* from the mitochondria (Green & Kroemer 2004). Cytochrome *c* induces apoptosome formation with the activation of procaspase-9,

which leads to further activation of downstream effector proteins such as caspases-3, 6 and 7, and eventually apoptosis (figure 1.8).

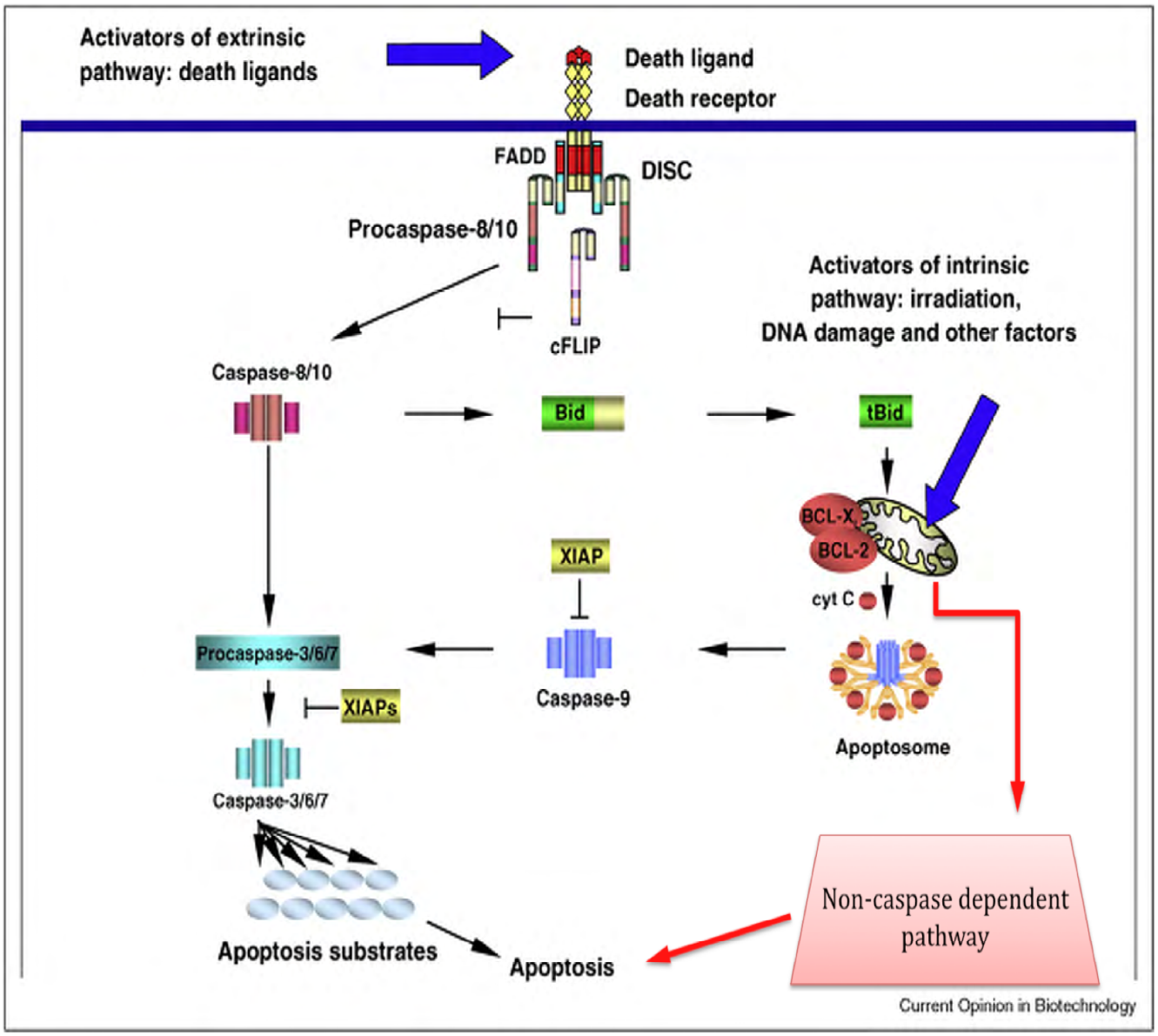


Figure 1.8. Scheme of the extrinsic and intrinsic pathways. Abbreviations: Fas-Associated Death Domain molecule (FADD), procaspase-8 (FADD-like ICE [interleukin-1 converting enzyme], or FLICE), c-FLIP (cellular FLICE-inhibitory proteins), X-linked inhibitory of apoptosis protein (XIAP), truncated Bid (tBid)[11]

[11] Adapted from Lavrik IN. Systems biology of apoptosis in signaling networks. Curr Opin Biotech (21): 551-555, 2010.

1.3.2 Necrosis

Necrosis is typically a non-physiological, unregulated pathological form of cell death characterized by disintegration of cellular membrane resulting in release of intracellular components into the intercellular space, causing an inflammatory response in the surrounding tissues. Necrosis has been described as being morphologically distinct from apoptosis. The hallmarks of necrosis are listed below (Majno & Joris 1995, Papermaster & Windle 1995, Kitanaka & Kuchino 1999):

1) swelling of cytoplasm and organelles, leading to dissolution and rupture of plasma membrane
2) large clusters of cells die simultaneously and provoke surrounding inflammatory response
3) passive process, not requiring energy for protein synthesis
4) enzymatic digestion of cells
5) denaturation of proteins
6) gene expression is not a prerequisite

1.3.3 Necroptosis

Until recently, the main modes of cell death have been described under different categories as apoptosis or necrosis based on their morphological features. However, recent evidence has emerged demonstrating overlapping pathways of induction and morphological characteristics between the three. The term describing this new mode of cell death has been coined 'necroptosis' by Degterev who demonstrated that death-domain receptors (DRs), which activate the classical apoptotic pathway, are able to trigger a common alternative non-apoptotic cell death pathway (Degterev *et al* 2005). They showed that by stimulating cellular tumour necrosis factor-α (TNFα) receptors, necrotic-like changes occur which involve organelle swelling, rapid mitochondrial

dysfunction, plasma membrane permeabilization and lack of nuclear fragmentation. Another observation reported is the activation of autophagy by necroptotic signaling where double membrane-enclosed vesicles indicative of autophagy, were observed by electron microscopy. Interestingly, similar overlapping features of apoptosis and necrosis were described by Formigli (Formigli *et al* 2000) in cells exposed to chemical hypoxia to block the mitochondrial respiratory chain complexes and termed aponecrosis. The initiation of necroptosis requires the kinase activity of receptor-interacting protein 1 (RIP1) and RIP 3 (Holler *et al* 2000). Inhibition of necroptosis by use of necrostatin-1 which specifically inhibits RIP1 kinase, significantly reduces infarct volume caused by ischemic brain injury (Degterev *et al* 2005). This implicates necroptosis in ischaemia and suggests RIP1 as a potential treatment target where ischaemic-reperfusion damage occurs as in stroke and possibly also in glaucoma.

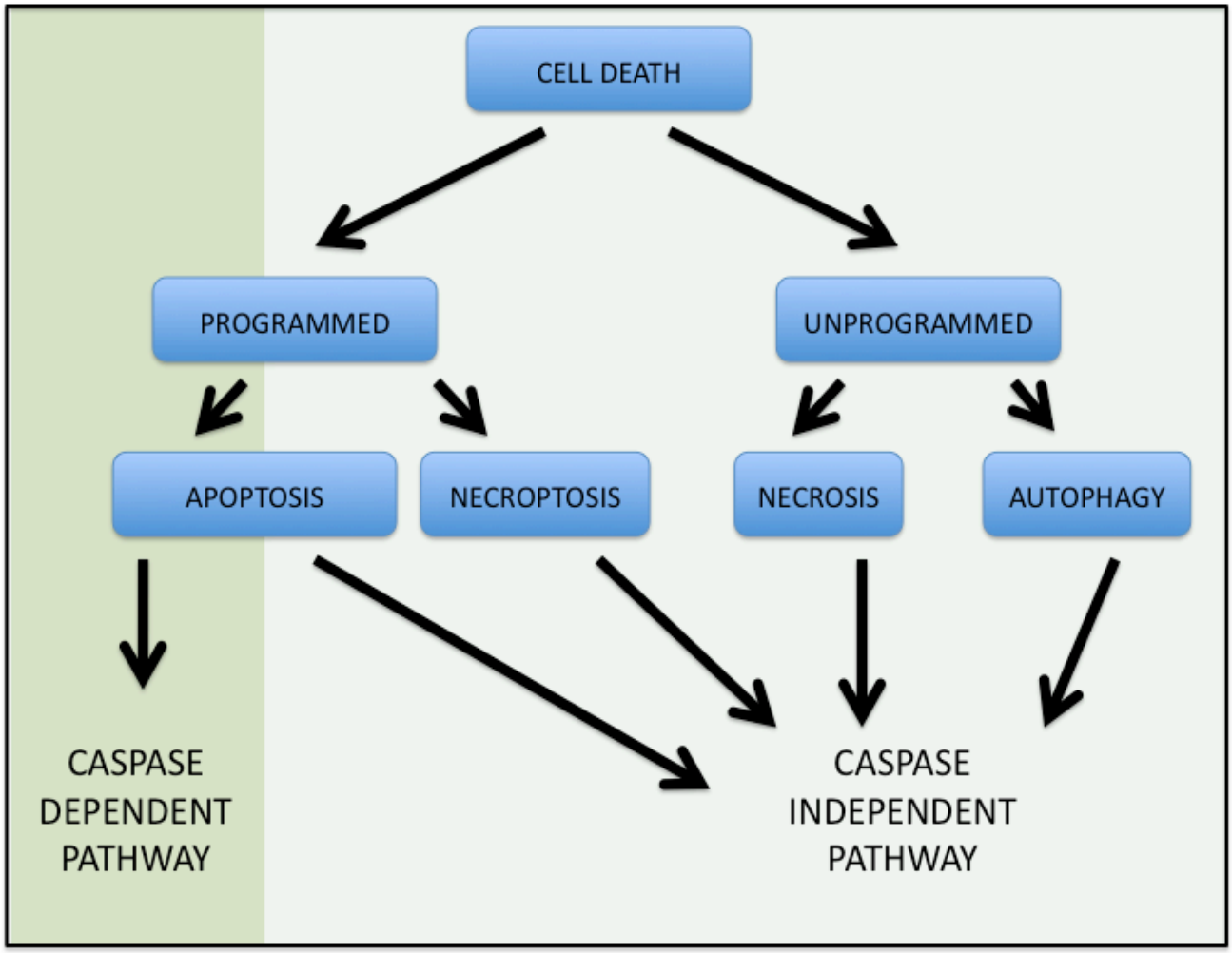


Figure 1.9. Schematic overview for possible modes of neuronal death. (Original drawing).

1.4 MAPK kinase signaling pathway

There are many intracellular signaling pathways involved in cellular death and survival process which include the mitogen-activated protein kinases pathway (MAPKs), Akt pathway, caspase cascade, STAT3 signaling pathway, to name a few. The MAPKs are evolutionarily conserved serine/threonine kinases that take part in transduction of external stimuli from cell surfaces to the nucleus (Johnson & Lapadat 2002). These kinases are activated by phosphorylation and they in turn phosphorylate the next downstream proteins to exert their effects. The MAPKs form a highly integrated network and involves cross talk among themselves and other pathways. They control a wide array of physiological processes including cell differentiation, cell proliferation and cell death. Three MAPK families have been identified in vertebrates: the extracellular-regulating kinase (ERK) or p42/44 MAPK, the c-jun amino-terminal kinase (JNK) or stress-activated protein kinase (SAPK), and the p38 MAPK (Kyriakis & Avruch 2001), as shown in figure 1.10. The ERK pathway utilizes two ERK isoforms, ERK1 and ERK 2, also known as p42/44 MAP kinases, which phosphorylate members of the AP-1 and ELK-1 family of transcriptional factors (Davis 1995). The JNK signaling pathway consists of three isoforms, JNK-1, JNK-2 and JNK-3. The p38 MAPK pathway consists of four isoforms activated by inflammatory cytokines and environmental stresses (Hershenson *et al* 1997).

1.4.1 ERK pathway

The ERK cascade is stimulated by a large variety of extracellular signals, and, as a consequence, regulates many distinct cellular processes. For example, the selective activation of the ERK MAP kinase pathway prevents apoptosis and suppresses JNK and p38 MAP kinase activities, suggesting an important role for ERK MAP kinase neuronal cell survival (Xia *et al* 1995). Although ERKs generally are thought to

regulate cell growth and cell differentiation, this is not always the case. Depending on cell type and nature of injury, ERK has been implicated in apoptosis (Wang *et al* 2000, Kim *et al* 2003).

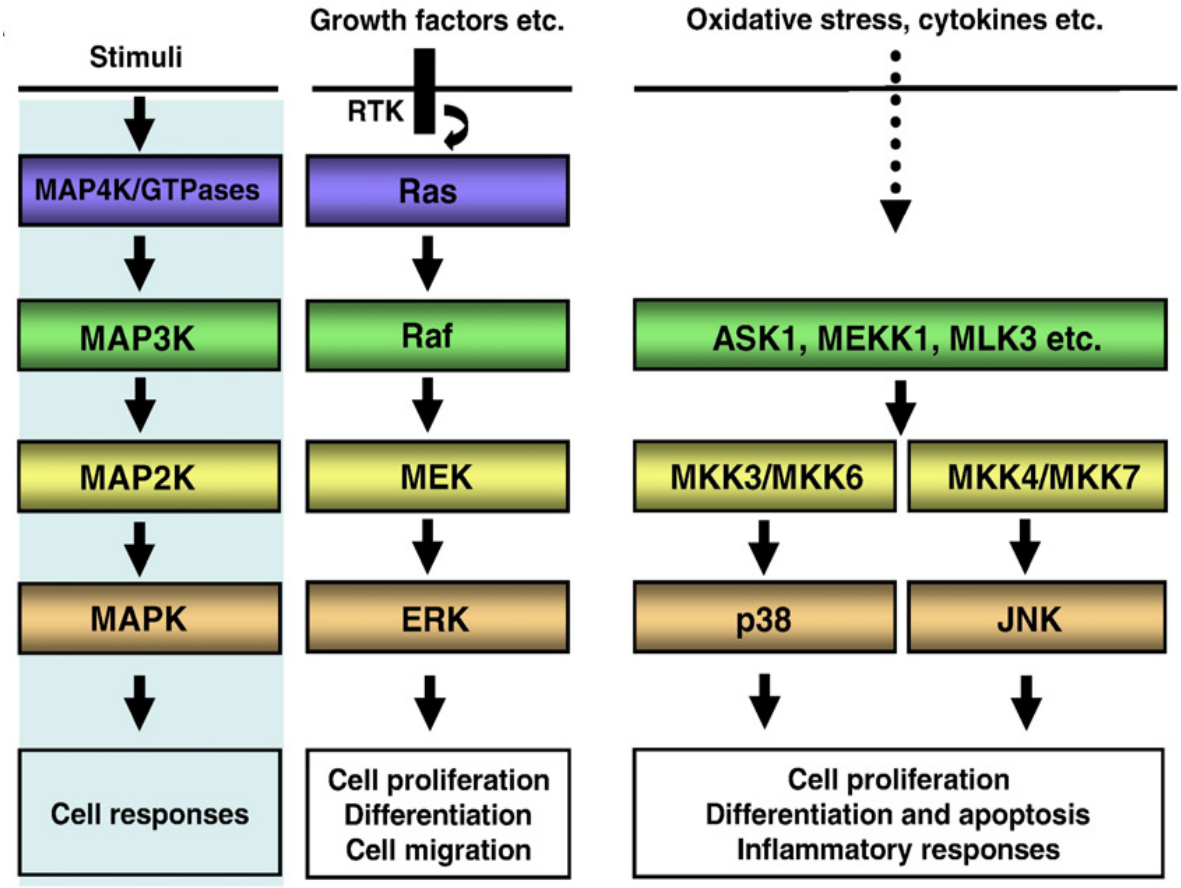


Figure 1.10. Mitogen-activated protein kinase (MAPK) signaling pathways. MAPK signaling pathways mediate intracellular signaling initiated by extracellular or intracellular stimuli. MAP3Ks, which are activated by MAP4Ks or GTPases, mediate phosphorylation and activation of MAP2Ks, which in turn phsophorylate and activate MAPKs. Activated MAPKs phosphorylate various substrate proteins including transcription factors, resulting in regulation of a variety of cellular activities including cell proliferation, differentiation, migration, inflammatory responses, and death. The mammalian MAPK family includes ERK, p38 and JNK. In the ERK signaling pathway, ERK1/2 is activated by MEK1/2, which is activated by Raf. Raf is activated by the Ras GTPase, whose activation is induced by receptor tyrosine kinases (RTKs) such as the epidermal growth factor (EGF) receptor. The p38 and JNK pathways consist of a MAP3K such as ASK1, MEKK1 or MLK3 as well as MAP2K such as MKK3 or MKK6 for the p38 pathway or MKK4 or MKK7 for the JNK pathway.[12]

[12] Figure adapted from Kim EK & Choi EJ. Pathological roles of MAPK signaling pathways in human diseases. Biochim Biophysica Act, 1802: 396-405, 2010.

1.4.2 SAPK/JNK signaling pathway

JNKs were originally identified as stress-activated protein kinases (SAPK) in the livers of cycloheximide-challenged rats (Kyriakis & Avruch 1990). Their subsequent purification, cloning, and termed as JNKs, emphasized their ability to phosphorylate and activate the transcription factor c-Jun (Pulverer *et al* 1991, Derijard *et al* 1994, Minden *et al* 1994). JNK is ubiquitously expressed and is activated by various types of stressors that include UV irradiation, ischaemia/reperfusion, heat shock and inflammation. The JNK stress signaling pathway is involved in numerous cellular processes including cell proliferation, differentiation, transformation, apoptosis, migration and cytoskeletal integrity (Nishina *et al* 2004). JNK1 and JNK2 are widely expressed in many tissues within the body, but JNK3 are mainly expressed in the brain, heart and testis (Gupta *et al* 1996, Yang *et al* 1997). Depending on their tissue location, the different isoforms act on nuclear substrates such as c-Jun and non-nuclear substrates such as Bad and Bim in the mitochondria, as shown in figure 1.11.

A paradigm for JNK-regulated gene expression is the phosphorylation of transcription factors leading to increased transcriptional activities. In consequence of its activation, JNK can phosphorylate nuclear substrates including c-Jun, ATF-2, Elk-1 as well as non-nuclear targets such as the mitochondrial proteins Bcl-2 family (Lei & Davis 2003). The c-Jun transcription factor has a short half-life, and phosphorylation of c-Jun by activated JNK increases its half-life and causes the accumulation of c-Jun protein. The first report on JNK-induced apoptosis demonstrated that the JNK signaling pathway is required for neuronal apoptosis (Xia *et al* 1995). Later studies demonstrated that JNK activation in neuronal apoptosis is not caspase-dependent (Park *et al* 1996) and that inhibitors of the JNK pathway block apoptosis (Xia *et al* 1995, Guan *et al* 2006). Induction of c-Jun expression is observed in neurons

following ischaemia/reperfusion (Okuno *et al* 2004, Schenkel 2004), NMDA-induced toxicity (Munemasa *et al* 2006) or insults to retinal ganglion cells as in a rat glaucoma model or following optic nerve injury (Levkovitch-Verbin *et al* 2005, Kwong & Caprioli 2006, Levkovitch-Verbin *et al* 2007). The use of JNK inhibitors has been shown to protect neurons against apoptosis in ischemic models of the brain (Borsello *et al* 2003, Guan *et al* 2006). These data together implicate the JNK signaling pathway in neuronal apoptosis.

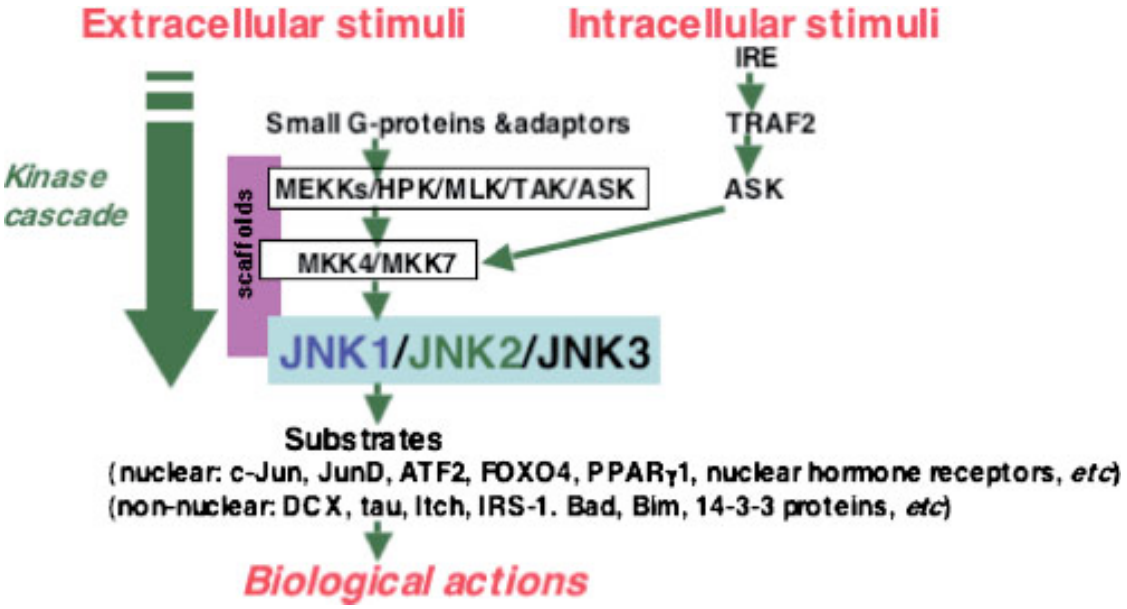


Figure 1.11. An overview of the JNK pathway. Extracellular stimuli (stress, cytokines and growth factors) and intracellular stimuli (endoplasmic reticulum stress) result in activation of the JNK pathway. This includes activation of protein kinase cascade involving JNK-interacting protein (JIP) family. As shown above, there are three JNK isoforms that exert their biological actions through their substrates.[13]

[13] Diagram taken from Bogoyevitch MA. The isoform-specific functions of the c-Jun N-terminal Kinases (JNKs): differences revealed by gene targeting. Bioessays 28:923-934, 2006.

1.4.3 p38 signaling pathway

The p38 signaling pathway, like JNK, is also activated in stressed conditions and have been implicated in neurodegenerative conditions such as Alzheimer's disease (Ando *et al* 2011) and amyotrophic lateral sclerosis (ALS) (Bendotti *et al* 2005). In the retina, the p38 pathway has been shown to be activated in retinal ganglion cells apoptosis after optic nerve axotomy and inhibition of the p38 pathway increased the ganglion cell survival (Kikuchi *et al* 2000).

1.5 Glaucoma

1.5.1 A brief overview of glaucoma

Glaucoma is a chronic, progressive neurodegenerative disease caused by a loss of ganglion cells and their axons along the optic nerve resulting in characteristic optic nerve head atrophy and visual field defects. The World Health Organization in 2010 estimated that, the number of people with visual impairment is 285 million, and that glaucoma is the third cause for this visual impairment. Glaucoma is second to cataract for numbers of people registered blind worldwide (WHO 2010). The number of people with glaucoma is expected to increase and Quigley and Roman (Quigley & Broman 2006) predicted that 80 million people worldwide would suffer from either open or close angle glaucoma by 2020.

Glaucoma comes in a variety of presentations: primary or secondary, open or closed angle, adult or juvenile onset, developmental or congenital, with or without elevated intraocular pressures. All forms of glaucoma lead to ganglion cell damage, although the path to ganglion cell death differs in risk factors and the progression of disease (Quigley 1999). Some forms of glaucoma have been proposed to be related to systemic disease, such as pigmentary glaucoma (Atalar *et al* 2006, Schlotzer-

Schrehardt & Naumann 2006, Citirik *et al* 2007). To date, there is no cure for glaucoma. Treatment is at best focused at delaying the progression of disease which is the aim of a possible neuroprotection strategy.

1.5.2 Pathogenesis of ganglion cell death in POAG

An understanding of how ganglion cells die in POAG is vital in developing treatment strategies aimed at preventing and delaying this process. POAG affects mainly retinal ganglion cells and their axons, sparing other neurons including the retinal photoreceptors (Quigley & Green 1979, Quigley *et al* 1981, Kendell *et al* 1995, Wygnanski *et al* 1995). The primary site of injury in glaucoma occurs in the optic nerve head and is probably caused by various interdependent factors (Flammer *et al* 2002, Flammer & Mozaffarieh 2007). The insults at the optic nerve head will lead to mechanical and/or ischaemic damage to the cellular structures around the optic nerve head that include ganglion cell axons, astrocytes, microglia and the lamina cribosa (Hernandez & Pena 1997, Osborne *et al* 2001, Boland & Quigley 2007). Once injury has occurred at the optic nerve head, the ganglion cells are thought to exist in a compromised energetic state. In this state, the ganglion cells are able to function normally, but are more susceptible to secondary insults (Osborne 2009). Secondary insults may occur as a result of accumulation of various chemicals from activated glial cells in the extracellular space (Osborne *et al* 2001, Osborne *et al* 2006a). Examples of such chemicals include glutamate, TNFα, interleukins and nitric oxide which are known to be released from activated microglia and astrocytes in cell culture experiments (Prinz *et al* 1999, Lee *et al* 2000, Wu *et al* 2009). It has been proposed that such substances would eventually have differential effects on individual ganglion cells depending on their receptor profile and density for different receptor types

shown in figure 1.12. This would result in retinal ganglion cell death being triggered at different time points over many years (Osborne 2009).

Several major risk factors for the development of glaucoma have been identified. These include elevated intraocular pressure (Ekstrom 2010, Topouzis *et al* 2011), reduced ocular perfusion at the optic nerve head (Flammer *et al* 2002, He *et al* 2011), genetic predisposition (Fan *et al* 2006, Chakrabarti *et al* 2010, Fernandez-Martinez *et al* 2011), ethnic groups (Fansi *et al* 2009, Stein *et al* 2011) and anterior segment anatomy (Nongpiur *et al* 2011, Wittstrom *et al* 2011). These factors provide a variety of stimuli which contribute to the pathogenesis of retinal ganglion cell death in glaucoma. Some of the stimuli proposed for causing ganglion cell death include (1) ischaemia (Hayreh 1969, Hayreh *et al* 1970, Flammer *et al* 2002) (2) neurotrophin factor deprivation (Mansour-Robaey *et al* 1994) (3) oxidative stress (Majsterek *et al* 2011, McElnea *et al* 2011) (4) glutamate excitotoxicity (Dreyer *et al* 1996) and (5) mitochondrial dysfunction (Ju *et al* 2008, Osborne 2010, Izzotti *et al* 2011, McElnea *et al* 2011).

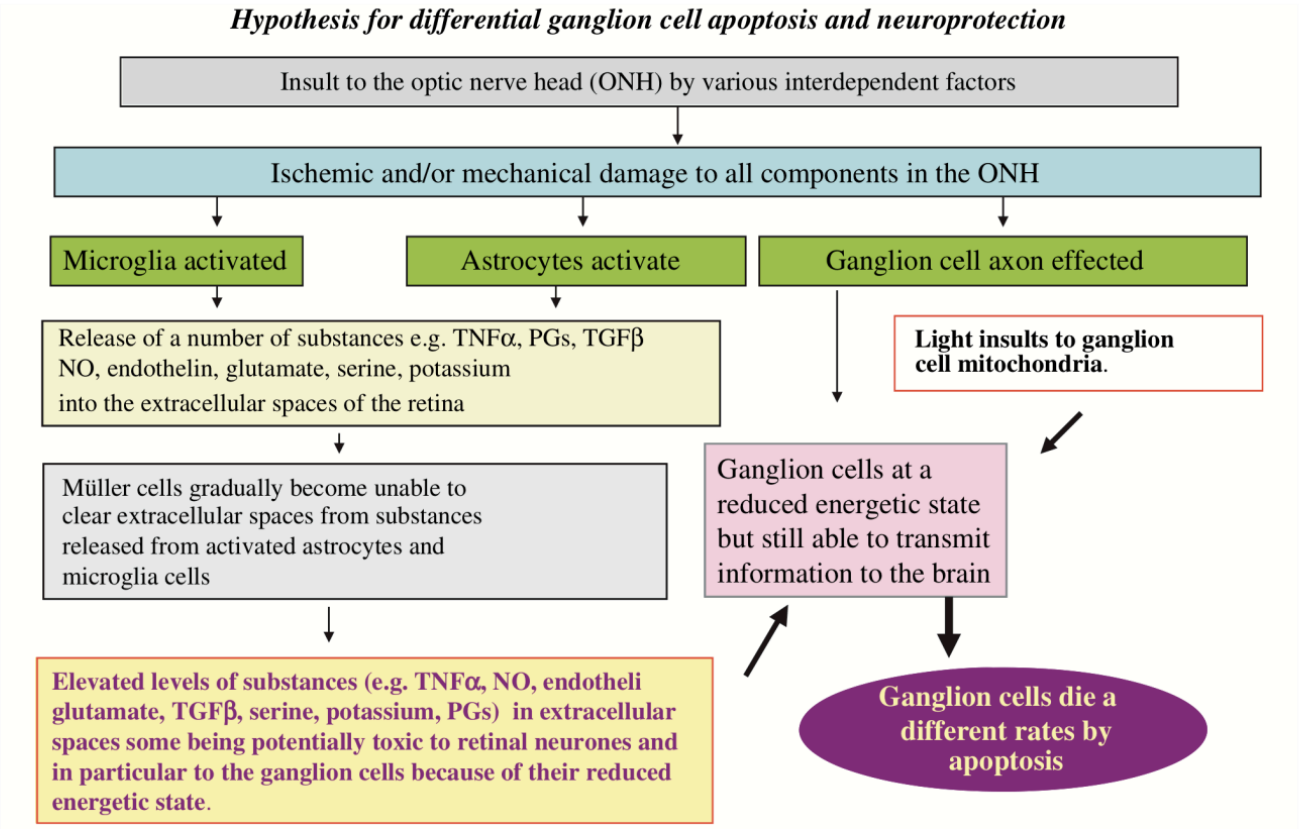


Figure 1.12. Hypothetical cascade of events to account for differential ganglion cell death as occur in glaucoma. It is proposed that the initial insults in glaucoma takes place in the optic nerve head, resulting in mechanical and/or ischaemic damage. Insults to ganglion cell axons result in the cells existing at a reduced energetic state. In this state, ganglion cells still function normally but are more vulnerable than before. An insult to the optic nerve head will also result in glial cells (microglia and astrocytes) being activated, causing them to release different chemicals into the extracellular space. Initially, these chemicals will be removed by the retinal Müller cells but this process will become inefficient with time. A gradual increase of these chemicals in the extracellular space will occur over time. Some of these chemicals will be potentially toxic (e.g. glutamate) or protective [e.g. transforming growth factor-β (TGF-β)] to neurons containing the appropriate receptors. Ganglion cells are likely to be particularly affected in the retina because they exist at a reduced energetic state. As a result, ganglion cells will be triggered to die by apoptosis at varying time depending on their receptor profile and density for different receptor types.[14]

[14] Osborne NN. Recent clinical findings with memantine should not mean that the idea of neuroprotection in glaucoma is abandoned. Act Ophthal 2009:87:450-454

1.5.2.1 Retinal ischaemia

Ischaemia refers to an interruption of blood flow to tissues which results in reduced nutrients and oxygen supply and appropriate removal of waste products and thus compromising energy production and causing oxidative stress (Siesjo & Katsura 1992, Nagahiro *et al* 1998). Such a situation is likely to occur in ischaemic optic neuropathy where the blood supply is interrupted for one reason or another. When a cell is deprived of glucose or oxygen, there will be a fall in cellular adenosine triphosphate (ATP) production. As a result, there will be failure of cellular homeostasis maintenance such as membrane pumps and channels, intracellular signaling pathways and maintenance of organelles and membrane integrity (Osborne *et al* 2004).

The initial outcome of compromised ATP production is the failure of plasma membrane-based, ATP-driven sodium-potassium pump (Siesjo & Katsura 1992, Nagahiro *et al* 1998). This will lead to a slow elevation of membrane potential, and increase the likelihood of depolarization and release of the voltage-dependent Mg^{2+} block on the NMDA-type glutamate receptor channel (Henneberry 1989). This leads to membrane instability and opening of multiple ligand- and voltage-gated ion channels. This results in influx of sodium, calcium and chloride ions leading to a loss of control for many cellular regulatory systems and an activation of enzymes that may contribute to cell death or degradation, e.g. lipases, nitric oxide (NO) synthases, kinases, endonucleases, protesases, phosphotases and caspases (Nagahiro *et al* 1998). The net result of the energy production failure is, therefore, an irreversible commitment to death via a series of self-reinforcing events.

1.5.2.2 Neurotrophin deprivation

The neurotrophin deprivation hypothesis is essentially an adaptation of the traditional mechanical theory: raised IOP and/or defects in the extracellular matrix cause compression and displacement of the lamina cribrosa. The resultant damage to the ganglion nerve axons in the optic nerve leads to blockage of retrograde delivery of neurotrophic survival factors to the cell bodies and the initiation of RGC apoptosis (Chidlow *et al* 2007).

The neurotrophin family includes brain derived neurotrophic factor (BDNF), nerve growth factor (NGF), fibroblast growth factor (FGF), ciliary neurotrophic factor and neurotrophin 3, 4/5 and 6. It was shown that retrograde axonal transport of radioactive BDNF was inhibited in rats with acutely elevated intraocular pressure (Pease *et al* 2000, Quigley *et al* 2000). In chronic ocular hypertension models, it is reported that there is a gradual depletion of BDNF and neurotrophin-4/5 in the proximal optic nerve and superior region of the inner retina (Johnson *et al* 2000).

1.5.2.3 Oxidative stress

Reactive oxygen species (ROS) refers to partially reduced metabolites of molecular oxygen which possess higher reactivity. The generation of ROS occur through a variety of cellular processes such as by-products of normal aerobic metabolism, or as a consequence of cellular damage. ROS are involved in numerous cellular signaling pathways and are produced at homeostatic levels in healthy cells. Controlled ROS production is an essential part of signal transduction pathways serving important regulatory functions. However, when present at high concentrations, ROS may cause damaging effects to mitochondrial and cellular proteins, lipids and nucleic acids. Cells possess intrinsic protective mechanisms to overcome the damaging effects of excess ROS in the form of antioxidant enzymes such as superoxide dismutase,

glutathione peroxidase and catalase. When ROS generation exceeds the cellular antioxidant capacity, the cell is said to be in a state of "oxidative stress" where it is susceptible to injury and damage. Oxidative stress has been implicated in the aging process (Wei *et al* 2001, Romano *et al* 2010) as well as in a number of human diseases including cardiovascular (Sugamura & Keaney 2011) and neurodegenerative diseases such as Parkinson's and Huntington's diseases (Li *et al* 2010, Watfa *et al* 2011).

Good evidence exists to support the notion that oxidative stress plays a role in POAG. For example, an increased level of lipid peroxidation products (Birich *et al* 1986) and lower level of glutathione (Gherghel *et al* 2005) occur in the serum of POAG patients. Additionally, an increase in the antioxidant enzymes, superoxide dismutase and glutathione peroxidase occurs in the aqueous humor of glaucoma patients (Ferreira *et al* 2004, Ghanem *et al* 2010). Moreover, McElnea (McElnea *et al* 2011) recently found that ROS was elevated in lamina cribrosa cells of glaucomatous human donor eyes.

1.5.2.4 Mitochondrial dysfunction

In neurons, energy is generated in the form of adenosine tripohosphate (ATP) by oxidative phosphorylation which occurs in the mitochondrial respiratory chain or electron transport chain. The mitochondrial respiratory chain consists of four complexes which shuttle electrons from one complex to the other and synthesizing ATP from adenosine diphosphate (ADP) in the process (figure 1.13).

Unlike other neuronal axons, RGCs have both myelinated and unmyelinated portions. Myelination of nerve fibers allows efficient energy consumption by saltatory conduction of nerve impulses between nodes of Ranvier (Waxman 1978). Unmyelinated nerve fibers have much slower conduction velocities and require far

greater energy to conduct nerve impulses through the axons (Carelli *et al* 2004). Bristow and colleagues showed asymmetric mitochondrial distribution in the RGC axons which is related to the energy and functional requirements of the axons (Bristow *et al* 2002). Single unmyelinated RGC axons are described as having varicosities rich in mitochondria (Wang *et al* 2003) and this supports the notion that RGCs are especially rich in mitochondria to meet its high energy demand. Therefore any conditions that affect the mitochondrial function such as ischaemia as a result of high IOP or altered ocular perfusion pressure as would occur in glaucoma, would compromise its energy production and render the RGC susceptible to damage. Furthermore, deficient mitochondrial metabolism would lead to a net increase of ROS production that can create havoc in the cell.

1.5.2.5 Light as a possible risk factor for glaucoma

The human retina is exposed to the visible electromagnetic spectrum between 400 and 760nm (Marshall 1985). Light, in particular blue light is absorbed by retinal photopigments such as lipofuscin (Boulton *et al* 1990) and melanin (Margrain *et al* 2004) located in photoreceptors and RPE to cause a generation of ROS and ultimately photoreceptor degeneration in certain situations (Organisciak & Vaughan 2010). More recently, a subset of retinal ganglion cells was found to contain the photosensitive pigment melanopsin (Foster & Hankins 2002, Dacey *et al* 2005). Mitochondria also contain photosensitive pigments, but unlike the mitochondria of photoreceptors which are protected from light by the macular pigments (Krinsky *et al* 2003), these organelles in the RGC axons are not. The suggestion has been made that in glaucoma subjects, RGCs exist in bioenergetically compromised states and that the interaction between light and RGC mitochondrial photosensitive pigments results in RGC death to be stimulated (Osborne *et al* 2006b). This hypothesis is supported by

studies on cell cultures where it has been shown that white light (400-760 nm, 1000lux) causes a stimulation of ROS in isolated mitochondria and only kill cells in culture that have functional mitochondria (Osborne *et al* 2006b, Osborne *et al* 2008).

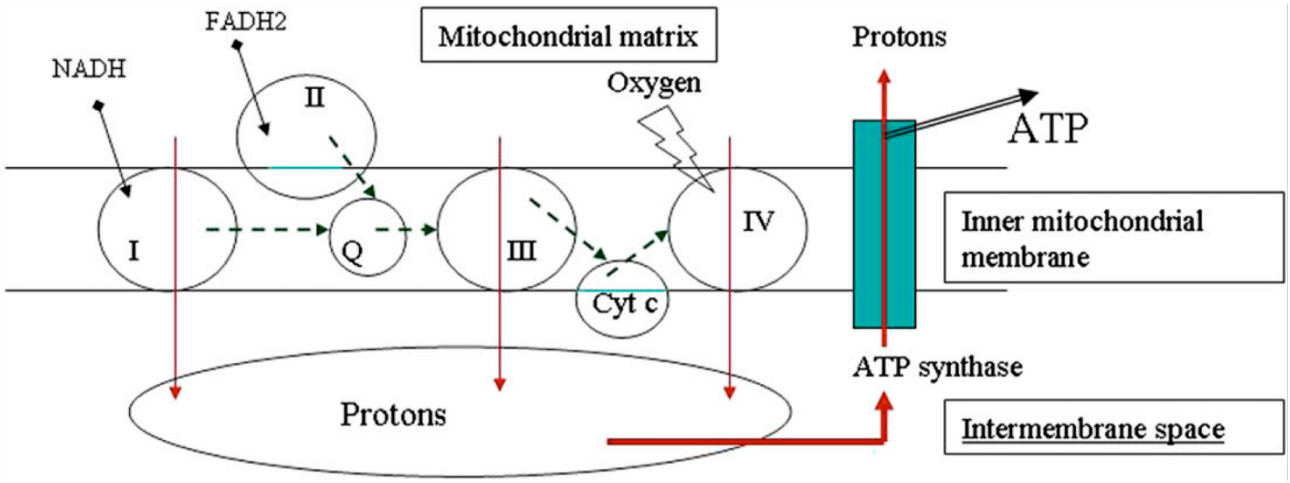


Figure 1.13. The electron transport chain contains four complexes for ATP production. This process requires substrates NADH and FADH2 to donate electrons (black arows) to the electron transport chain at complexes I and II and transfer them along a chain of other carriers (ubiquinone or Q, complex III, cytochrome c or cyt c and complex IV or cytochrome c oxidase) also situated in the inner mitochondrial membrane. At complexes I, III and IV the electrons are used to translocate protons from the mitochondrial matrix to the intermembrane space (red thin arrows). This process generates a proton-electrochemical gradient across the inner mitochondrial membrane, which is known as the proton-motive force. The proton-motive force (red thick arrow) is used to drive gradient-dissipated activities, including the generation of ATP by ATP synthase, which is the main pathway for the return of protons to the matrix.[15]

[15]adapted from Osborne, NN. Mitochondria: Their role in ganglion cell death and survival in primaryopen angle glaucoma. Exp Eye Res 90(6): 750-757, 2010.

1.6 Experimental approaches in trying to understand more about ganglion cell death

A variety of animal models to simulate retinal ganglion cell damage as in glaucoma have been employed by a number of groups. These include animal (mainly rat and mouse) models that involved delivery of ischaemia to the retina followed by reperfusion (Jehle *et al* 2008, Sakamoto *et al* 2009), optic nerve crush (Xie *et al* 2010), axotomy or transection of the optic nerve (Levkovitch-Verbin *et al* 2001, Kashimoto *et al* 2008, Peng *et al* 2010) and damage to the trabecular meshwork directly (Levkovitch-Verbin *et al* 2002, Sappington *et al* 2010) or indirectly by e.g. episcleral vessel destruction (Danias *et al* 2006, Hernandez *et al* 2008). In addition studies have been conducted on mutant mice such as DBA/2J type, that have characteristics resembling that of glaucoma (John 2005, Lindsey & Weinreb 2005).

Cell and tissue cultures have also been used extensively as they provide a means for not only delivering a defined insult to the cells but also establishing the manner by which neuroprotective compounds work. Cell culture procedures allow for the possibility to (1) determine the efficacy and potency of a defined drug, (2) allow for the direct access of a substance to a cell without it having to cross the blood-retinal barrier, (3) control of the cellular microenvironment, and (4) has good experimental repeatability (Chidlow *et al* 2007). However, it is clear that the relevance of any studies conducted on cell cultures in relation to glaucoma has limitations and cannot be compared to studies on animal models where the complex interaction of the blood-retinal barrier, the different retinal cell types and the unique micro- and macro-environments remain intact.

Cell culture systems that allow for studies that are of relevance to retinal ganglion cells include (1) mixed primary retinal cultures (2) cultures of purified RGCs (3)

retinal explants and (4) cultures of specific cell lines, like RGC-5 cells (Goodyear & Levin 2008).

1.6.1 Mixed retinal cell cultures

Isolated retinas from neonatal or adult rats or mice are enzymatically dissociated and the cells maintained in culture where serum and trophic factors are present. Here the diversity of retinal cells are more-or-less maintained, without the physiological interaction between the different cell-types. The disadvantages of this type of cell culture are (1) the physical stress the cells undergo as a result of enzymatic dissociation and (2) the typically short survival period (Goodyear & Levin 2008).

1.6.2 Retinal explants

Retinal explants are prepared by culturing small dissected pieces of whole retina (Smalheiser *et al* 1981). The traumatic effects of enzymatic dissociation are avoided, and the anatomic architecture of the retina is maintained. This type of culture allows for the characteristics and interactions between the different cell-types in the retina to be retained. As with studies on primary retinal cultures, removal of the retina results in ganglion cell function being compromised because of the cutting of the optic nerve.

1.6.3 Purified ganglion cells

Similar to mixed retinal cultures, purified ganglion cell cultures are first enzymatically dissociated from the retina and then isolated through immunoselection. The purification process involved a panning technique described by Barres and colleagues where RGCs are separated by using primary antibodies to the ganglion cell surface marker, Thy-1 (Barres et al 1988). The two-step panning technique described was able to produce a high purity of retinal ganglion cells (99.5%). However, this process had a relatively low yield and was only able to isolate 50% of the total RGC population, which may be explained in part by the loss of RGCs through a vigorous

rinsing process (Barres et al 1988). Furthermore, it remains unclear as to how long these cells were able to survive in culture.

Takahashi and co-workers described another method for isolating rat RGCs which could survive more than one month in culture (Takahashi *et al* 1991). In this method, dissociated retinas from 5 to 7 day-old Sprague-Dawley rats were cultured on a monolayer of glial cells derived from cerebral cortex of neonatal rats, which acted as a substrate for neuronal attachment and survival. Electrophysiological recordings characteristic of viable RGCs were detected at up to 31 days in culture (Takahashi et al 1991). Neverthelesss, this method provides a low yield of RGCs and is time-consuming, requiring more than two weeks to complete the whole process.

In humans, RGCs from adult human donor eyes can be cultured *in vitro* and form neurites when supplemented with basic fibroblast growth factor (bFGF) (Hu & Ritch 1997). However, this culture method has a low yield and is not purified as they also contain a mixture of astrocytes and Müller cells.

1.6.4 RGC-5 cell line

Although pure retinal ganglion cells can be successfully isolated in culture, the low yield of cells makes them difficult to employ for use in multiple assays. Moreover, the purity and life span of these cells vary each time they are isolated from the retina, hence the lack of reliable experimental repeatability. The need for large cell populations of retinal ganglion cells for *in vitro* experiments, has lead to the development of a transformed cell line (RGC-5 cells) that express certain retinal ganglion cell properties. Krishnamoorthy and co-workers generated RGC-5 cells by permanently transforming a mixed population of retinal cells (including ganglion cells) from 1 day old rats with the virus Ψ2 E1A (Krishnamoorthy *et al* 2001). However, later analysis of mitochondrial and nuclear DNA from RGC-5 cells showed

that the cell clones used by Krishnamoorthy et al (2001) were derived from the mouse (*Mus musculus*) and not from rat (*Rattus norvegicus*) (Van Bergen *et al* 2009).

RGC-5 cells have a doubling rate of 24 hours in culture and grow as a monolayer exhibiting axonal-like processes which intercalate with one another. RGC-5 cells express the retinal ganglion cell markers Thy-1 and Brn-3C (Krishnamoorthy *et al* 2001), and not GFAP (Müller cells and astrocytes), calretinin and syntaxin or HPC-1 (amacrine cells), PKCα (ON-bipolar cells) and 8A1 and calbindin (horizontal cell marker) (Krishnamoorthy *et al* 2001, Wood *et al* 2010). The expression of Thy-1 by RGC-5 cells has been confirmed by analysis of mRNA and protein as well as by immunocytochemistry (Krishnamoorthy *et al* 2001, Frassetto *et al* 2006, Agarwal *et al* 2007, Ganapathy *et al* 2010, Nieto *et al* 2010). Thy-1 is a cell surface glycoprotein and has the highest concentration in the brain and thymus of rats (Barclay & Hyden 1978). In the eye, Thy-1 is predominantly found on retinal ganglion cell axons, soma and dendrites, as well as the optic nerve (Beale & Osborne 1982, Barnstable & Drager 1984, Leifer *et al* 1984). Thy-1 staining is not exclusively located to retinal ganglion cells being present in a sub-population of horizontal cells (Barres *et al* 1988, Takahashi *et al* 1991). Nevertheless, most of the retinal Thy-1 immunoreactivity is associated with RGCs and remains the most commonly used marker for these cells of the retina (Beale & Osborne 1982, Barnstable & Drager 1984, Leifer *et al* 1984, Guenther *et al* 1994, Krishnamoorthy *et al* 2001, Frassetto *et al* 2006, Agarwal *et al* 2007, Van Bergen *et al* 2009, Ganapathy *et al* 2010, Nieto *et al* 2010, Wood *et al* 2010). While certain reports could not demonstrate Thy-1 protein expression in RGC-5 cells (Van Bergen *et al* 2009, Wood *et al* 2010), most other studies reported the contrary (Ju *et al* 2005, Frassetto *et al* 2006, Agarwal *et al* 2007, McKernan *et al* 2007, Maher & Hanneken 2008, Ganapathy *et al* 2010, Nieto *et al* 2010).

Significantly, passages of RGC-5 cells at later stages have a much reduced staining for Thy-1 immunoreactivity (Nieto *et al* 2010) which may explain why certain studies could not demonstrate its presence

Although RGC-5 cells express some retinal ganglion cell characteristics (Krishnamoorthy *et al* 2001, Agarwal *et al* 2007), they differ from true retinal ganglion cell in many ways, one being their electrophysiological properties. RGCs isolated from rat retina have resting membrane potentials that are more negative than -45mV, exhibit large Na^+, Ca^{2+} and K^+ currents and display action potentials in response to depolarization (Lipton & Tauck 1987, Ishida 1995, Wang *et al* 1997, Schmid & Guenther 1998, Guenther *et al* 1999). In contrast, undifferentiated RGC-5 cells are quite unexcitable, with no action potentials or voltage-dependent inward Na^+ or Ca^{2+} currents. Furthermore, their resting membrane potentials are between -35 and 0mV (Moorhouse *et al* 2004). These observations suggest that undifferentiated RGC-5 cells may not possess the range of ionic channels present in actual retinal RGCs. Other differences associated with RGC-5 cells include their ability to proliferate, their different morphology to a normal post-mitotic retinal ganglion cell, and their resemblance to glial cells more than retinal ganglion cells in culture (Goodyear & Levin 2008).

Several authors have described procedures to differentiate RGC-5 cells in culture into cells that more resemble true retinal ganglion cells (Krishnamoorthy *et al* 2001, Frassetto *et al* 2006, Lieven *et al* 2007, Schwechter *et al* 2007, Wood *et al* 2010). These methods involve incubating RGC-5 cells for a defined period of time with a variety of substances such as nonagglutinating lectin succinyl concanavalin A (sConA), the protein kinase inhibitor staurosporine and histone deacetylase (HDAC) inhibitors such as trichostatin A (TSA) and sodium butyrate. The main difference

following RGC-5 differentiation is the development of long thin processes which resemble neurite formation and their inability to proliferate (Frassetto *et al* 2006, Lieven *et al* 2007, Schwechter *et al* 2007). Thus at best RGC-5 cells resemble true ganglion cells by expressing common proteins but they are not neurons as they proliferate and electrophysiologically have distinctive properties. These cells were nevertheless used extensively in this thesis to gain knowledge that might be applicable for how true ganglion cells behave in certain situations.

1.7 Flavonoids

Flavonoids are a large group of polyphenols found in plant-based foods such as vegetables, fruits, tea and wine (Ross & Kasum 2002, Arts & Hollman 2005). There are about 5000 types of flavonoids, which are subdivided into flavonols, flavonones, flavones, isoflavonoids, flavans-3-ols, and anthocyanidins (Neuhouser 2004). Isoflavones are isomers of flavonoids, and are found most often in legumes, including soybeans, black beans, chick beans and green beans.

Most flavonoids are ROS scavengers and antioxidants (Bors *et al* 1994, Pannala *et al* 1997, Heijnen *et al* 2001) which is related to their ability to form stable radicals, a property shared by aromatic compounds containing 0-dihydroxyl groups or closed hydroxyl and carbonyl groups (Husain 1987). Individual flavonoids have been documented to exert various modes of actions to allow them to reduce inflammatory (Garcia-Lafuente *et al* 2009) and cardiovascular (Rimbach *et al* 2008) diseases and also act as chemotherapeutic agents (Delmulle *et al* 2006, Amin & Buratovich 2007, Garcia-Lafuente *et al* 2009, Imai *et al* 2009). Some flavonoids also reduce osteoclastic activity to increase bone mineral density (Kim *et al* 2008, Mardon *et al* 2008, Ju *et al* 2009). Certain flavonoids exhibit neuroprotective properties in

experimental studies related to neurodegenerative diseases such as Parkinson's (Baluchnejadmojarad *et al* 2009, Reznichenko *et al* 2010) and Alzheimer's (Wang *et al* 2010, Shih *et al* 2011) diseases and glaucoma (Falsini *et al* 2009).

1.7.1 Brief review of tea catechins

Tea is the second most consumed fluid in the world, next to water (Katiyar & Mukhtar 1996). It is estimated that 2.5 million metric tons of dried tea leaves are manufactured annually (Chen *et al* 1997) The tea plant, *Camellia sinensis* originates from South China and was thought to be introduced to Japan in ancient times by the Zen priest, Eisai. Three types of tea can be produced from different manufacturing processes of *Camellia sinensis*: green tea, black tea and oolong tea. Black tea is most commonly consumed (78% of total tea consumption), followed by green tea (20%) and oolong tea (<2%) (Mukhtar & Ahmad 2000). Varying manufacturing processes produces the different types of tea. Green tea is produced by a steaming process of pan-fried freshly harvested leaves. This process inactivates many enzymes, thereby preventing fermentation and producing a dry, stable product. Black tea and oolong tea are produced by allowing fresh tea leaves to wither and dry, followed by crushing the leaves to initiate fermentation process. The fermentation process in oolong tea is shortened compared to black tea (Mukhtar & Ahmad 2000).

Green tea contains a rich source of flavonoids commonly known as catechins, which falls under the flavanol family of flavonoids. The major catechins in green tea are (-)-epicatehin, (-)-epicatechin-3-gallate (EC), (-)-epigallocatehin and (-)-epigallocatehin-3-gallate (EGCG) are present in especially high amounts (Mukhtar & Ahmad 2000). These polyphenolic compounds accounts for 30-40% of the extractable solid products of green tea leaves. The composition of the dry weight of green tea is as follows (unit

calculated in % of dry weight): EGCG 7-13%, EC 3-6%, epigallocatechin 3-6% and epicatechin 1-3% (Graham 1992).

The chemical structure of catechin is made up of 3 carbon rings, as shown in figure 1.14. The gallocatechin group (e.g. EGCG) has 3 hydroxyl groups in the B-ring and the catechins gallate group (e.g. EC) is esterified to gallic acid at the 3-OH group in C-ring. The number of hydroxyl groups in catechins structure as well as the insertion of a third hydroxyl group in the B-ring as in EC, enhances the antioxidant activity. The antioxidant potentials of green tea catechins are as follows (in descending order): epicatechin gallate (EC) ≈ epigallocatechin gallate (EGCG) > epigallocatechin > gallic acid > epicatechin (Rice-Evans *et al* 1996).

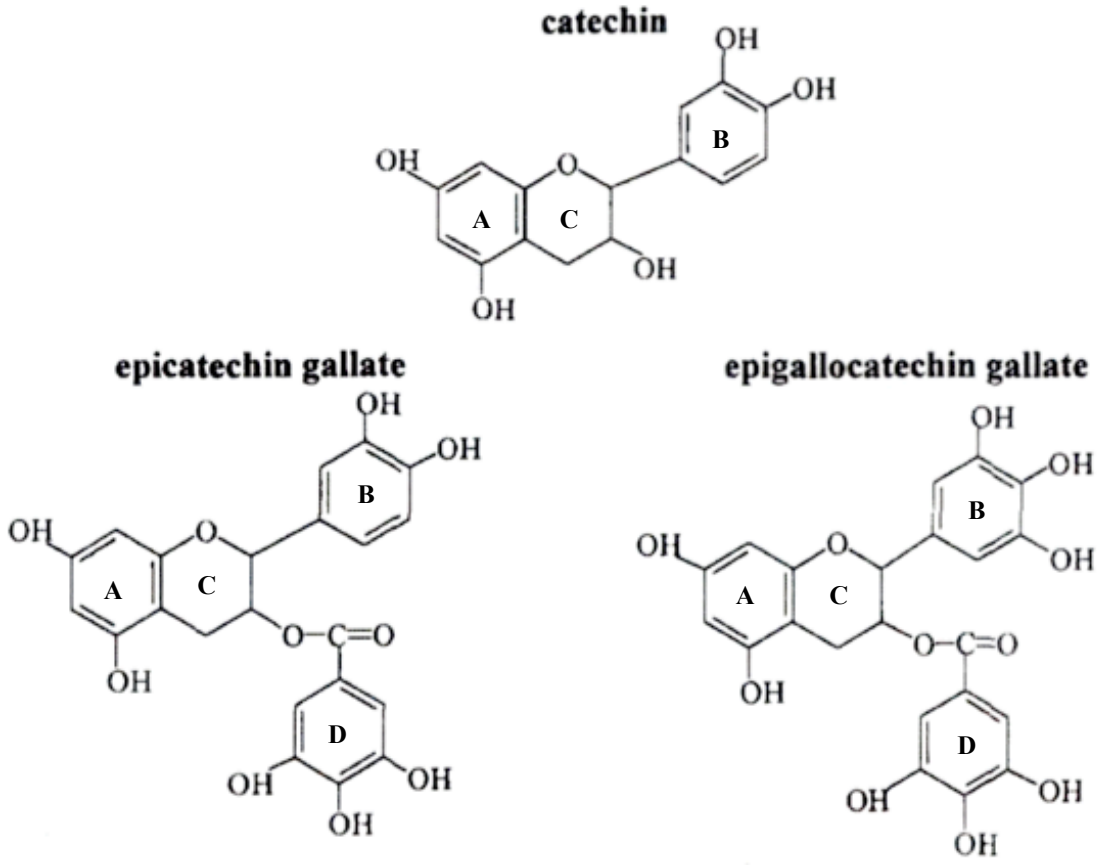


Figure 1.14. The basic chemical structure of catechins, epicatechin gallate (EC) and epigallocatechin gallate (EGCG). EGCG has 3 hydroxyl groups in the B-ring, and both EGCG and EC are esterified to gallic acid (D-ring) at the 3-OH group in C-ring.[16]

1.7.1.1 Pharmacokinetics and elimination of green tea

Tea can be consumed in large quantities and toxicity studies demonstrate a wide safety margin for consumption. Long-term administration of EGCG (up to 200mg/kg body weight for 13 weeks) to rats has no toxic effects (Isbrucker *et al* 2006). In a study to assess the effect of green tea catechins on fetal development in rats, no fetal malformations were observed when gravid female rats were fed with gastric gavage

[16] Diagram taken from Rice-Evans CA et al. Structure-antioxidant activity relationships of flavonoids and phenolic acids. Free Rad Biol Med 20(7): 933-956, 1999.

of green tea catechins up to 2000mg/kg/day during 6-17 gestational days (Morita *et al* 2009).

Like most polyphenols, tea catechins are not subjected to phase I metabolism as the polyphenolic structures make them unfavourable substrates for cytochrome P450 enzyme in the liver (Lambert & Yang 2003, Lambert *et al* 2007). Instead, these compounds can directly undergo phase II metabolism, predominantly methylation, glucuronidation and sulfation, which represent the major metabolic pathways for tea catechins (Lambert & Yang 2003, Lu *et al* 2003).

Green tea catechins are soluble in water and widely distributed in the body. Studies using radioactive-labelled, single dosing of 200μl 0.05% EGCG given directly through gastric tube showed good distribution of EGCG in the brain, lung, heart, liver, kidney and other tissues after 24 hours (Suganuma *et al* 1998). Pharmacokinetic studies in humans and mice showed the low bioavailability of green tea catechins (Suganuma *et al* 1998, Lee *et al* 2002). In humans, the half-life of EGCG range from 2-3.4 hours, with a mean peak plasma concentration of 0.17μM after 1.6-2.1 hours following ingestion of an equivalent of 2 cups of tea (~200mg of pure EGCG) (Chow *et al* 2001, Lee *et al* 2002). Both EGCG and EC were present in trace amounts in the urine, compared to the other two green tea catechins, EGC and epicatechin, which were found in high concentrations (Lee *et al* 2002). EGCG appears to be preferentially excreted through bile to the colon, as suggested by the high concentration of EGCG in the intestines following intravenous injection of green tea catechins in rats (Chen *et al* 1997, Lee *et al* 2002)

Green tea polyphenols have been studied extensively and found to exhibit multifunctional properties. They act as antioxidant (Nakagawa & Yokozawa 2002, Nakagawa *et al* 2002, Yokozawa *et al* 2002, Raza & John 2007), anticancer (Chung *et*

al 2001, Uesato *et al* 2001), antiparasitic (Paveto *et al* 2004, Mukai *et al* 2008), antimalarial (Sannella *et al* 2007), antiviral (Song *et al* 2005), antibacterial (Gibbons *et al* 2004) and as lipid lowering (Koo & Noh 2007) agents.

1.7.1.2 Epigallocatechin gallate (EGCG) actions

EGCG is the most abundant catechin in green tea, comprising of 7-13% of total dry weight of green tea leaves. EGCG has multifunctional properties including antioxidant (Nakagawa & Yokozawa 2002, Raza & John 2007), anti-tumorigenesis (Shimizu *et al* 2005, Urusova *et al* 2011), anti-inflammatory (Tedeschi *et al* 2002, Gokulakrisnan *et al* 2011), anti-viral (Song *et al* 2005), anti-bacterial (Yamamoto *et al* 2004) and anti-thrombotic (Kang *et al* 1999) properties. Moreover, EGCG has vasodilator (Lorenz *et al* 2004), anti-angiogenic (Rodriguez *et al* 2006) and neuroprotective (Reznichenko *et al* 2005, Koh *et al* 2006, Hou *et al* 2008) influences.

1.7.1.2.1 Neuroprotective actions of EGCG

Good evidence exists from *in vitro* and *in vivo* studies to show the neuroprotective properties of EGCG. EGCG reduces the formation of amyloid plaques in a mouse model of Alzheimer's disease (Rezai-Zadeh *et al* 2005) and decreases glutamate excitotoxicity in a mouse model of amyotrophic lateral sclerosis (Koh *et al* 2006, Xu *et al* 2006). The neuroprotection effects of EGCG have also been demonstrated in several animal models of cerebral ischaemia. Intraperitoneal EGCG reduces brain oedema and infarct volume after unilateral cerebral ischaemia in rats (Choi *et al* 2004) and gerbils (Lee *et al* 2004a). At a molecular level, EGCG reduces the expression of ischaemia-induced nitric oxide synthase (NOS) isoforms and subsequently nitric oxide formation, as well as NADPH diaphorase activity (Nagai *et al* 2002, Suzuki *et al* 2004, Wei *et al* 2004). Nitric oxide is an important free radical generated following cerebral ischaemia and is synthesized by nitric oxide synthase (NOS) enzymes, and

exists as three isoforms. Two NOS isoforms are generally present in neurons (nNOS) and endothelial cells (eNOS). The third isoform, termed inducible NOS (iNOS), occurs in many cell-types and can be activated by a variety of stimuli to cause various effects that might be part of an immune response. Activation of eNOS in vascular smooth muscle leads to increased vasodilation, for example, in cerebral blood flow, while activation of iNOS and nNOS is often associated with cell death process. EGCG is reported to reduce the activity and level of nNOS and iNOS following ischaemia/reperfusion injury to the retina (Suzuki *et al* 2004, Peng *et al* 2008).

The inhibition of calcium influx may be another mechanism by which EGCG prevents neuronal damage. In a study using rat hippocampal neurons, EGCG was shown to attenuate the increase in intracellular calcium in AMPA-induced toxicity (Bae *et al* 2002). Levites et al (2002) demonstrated that EGCG modulate cell survival/death genes based on cDNA array-based studies and caused down-regulation of the pro-apoptotic genes, Bax, Bad, caspase-6, caspase-1 and tumour necrosis factor-related apoptosis-inducing ligand (TRAIL) (Levites *et al* 2002).

A number of intracellular signaling pathways have been described to play central functions in neuronal protection against a variety of extracellular insults. These include MAPK (Levites *et al* 2002), phosphotidylinositol-3-kinase-AKT (Kaplan & Miller 2000) and protein kinase C (PKC) (Maher 2001) pathways. The extracellular signal-regulated kinases or ERK1/2 is one of the MAPK family members. The involvement of ERK1/2 signaling in neuronal survival is demonstrated by the decrease of its activity in SH-SY5Y neuroblastoma cells treated with 6-hydroxydopamine (6-OHDA) (Levites *et al* 2002) and glutamate-induced primary cortical neurons toxicity (Singer *et al* 1999). EGCG also blunts the reduction of

ERK1/2 phosphorylation induced by 6-OHDA in human neuroblastoma cells (Levites *et al* 2002).

A PKC signaling pathway has been linked to preservation of cell survival. Its loss of function, especially induced by oxidative stress, corresponds to the severity of the damage (Durkin *et al* 1997, Maher 2001). PKC is a family of serine/threonine kinases consisting of 11 isoforms, which are divided into three subclasses: conventional (α, β_I, β_{II}, γ), novel (δ, ε, θ, η, μ) and atypical (ι/λ, ζ). The rapid decline of neuronal PKC activity is a common outcome for severe brain damage, such as occurs after ischaemia (Cardell & Wieloch 1993, Busto *et al* 1994). The induction of PKC activity by EGCG in neurons is thought to be necessary for neuroprotection against several neurotoxins. EGCG attenuates amyloid beta toxicity (Levites *et al* 2003), serum withdrawal (Mandel *et al* 2003) and 6-OHDA induced cell death (Levites et al 2003) and were accompanied by a rapid phosphorylation of PKC. This was validated by the finding that pretreatment with a general PKC inhibitor abolished the protection induced by EGCG against 6-OHDA toxicity in human neuroblastoma cells, SH-SY5Y (Levites *et al* 2002).

Many *in vitro* (Nakagawa & Yokozawa 2002, Raza & John 2007) and *in vivo* (Buttemeyer *et al* 2003) studies have shown EGCG to be an effective antioxidant. The antioxidant ability might be explained, in part, by its chemical structure of EGCG. The tri-hydroxyl groups in the B-ring, and the presence of the tri-hydroxyl structure in the D ring (gallate) (see figure 1.15) increases the antioxidant capacity of EGCG (Rice-Evans *et al* 1996, Wiseman *et al* 1997, Nakagawa *et al* 2002). The principle site of antioxidant reactions appears to occur in the B-ring (Valcic *et al* 2000). EGCG has been shown to scavenge free radicals attributed to the tri-hydroxyl group in its B-ring (Nanjo *et al* 1996, Sang *et al* 2007). EGCG can scavenge both superoxide and

hydroxyl radicals (Yoo *et al* 2009), nitric oxide (Crispo *et al* 2010), peroxyl radicals (Kondo *et al* 1999, Valcic *et al* 2000) and peroxynitrite which prevents tyrosine nitration (Pannala *et al* 1997). The tri-hydroxyl structures associated with EGCG are also thought to be responsible in chelating metal such as copper (II) and iron (III) to form inactive complexes, thereby preventing free radical formation (Kashima 1999, Hashimoto *et al* 2000).

Apart from direct antioxidant effects, EGCG also stimulates certain endogenous antioxidant enzymes such as glutathione, superoxide dismutase and catalase and reduces the formation of malondialdehyde, (MDA), a product of lipid peroxidation formed during oxidative stress (Yin *et al* 2008, Wei & Meng 2010).

1.7.1.2.3 Evidence for EGCG attenuating retinal cell death

It is generally thought that oxidative stress plays a part in the pathogenesis of glaucoma (Izzotti *et al* 2006, Tezel 2006), initiated by ischaemia to the optic nerve head components (Osborne *et al* 1999) because of a reduced optic nerve head blood supply (Flammer & Orgul 1998). In RGC-5 cell cultures, EGCG reduces ROS generation and significantly attenuates cell death induced by an exogenous source of oxidative stress (hydrogen peroxide) (Zhang *et al* 2007). EGCG, when co-injected with a potent oxidant, sodium nitroprusside (SNP), into the vitreous humor of adult rats, blunted the damaging effects of SNP on retinal photoreceptors, as well as reduced the number of TUNEL-positive cells in the outer nuclear layer of the retina (Zhang & Osborne 2006). In rats, ischaemia/reperfusion injury affects the function of the outer retina as evident by diminished a- and b-waves on the electroretinogram (ERG), increases the mRNA expression of pro-apoptotic proteins such as caspase-3 and caspase-8 and damages the ganglion cells as shown by thinning of Thy-1 staining in the inner plexiform layer as well as reduction of neurofilament and tubulin proteins

in the optic nerves. These effects were significantly attenuated by EGCG when given either intraperitoneally (Zhang *et al* 2007) or orally (Zhang *et al* 2008). EGCG was also shown to blunt the effects of light-induced photoreceptor degeneration when given orally in rats (Costa *et al* 2008).

1.7.1.3 Epicatechin gallate (EC)

Epicatechin gallate (EC) is the second major catechin in green tea, making up 3-6% of total dry weight (Graham 1992). EC is also present in plants such as grapes (Mitjans *et al* 2004) and buckwheat (Danila *et al* 2007). Like EGCG, EC is associated with various beneficial effects being an anti-oxidant (Huang *et al* 2007, Raza & John 2007) and also having anti-bacterial (Gibbons *et al* 2004), anti-atherosclerotic (Kawai *et al* 2008), anti-cancer (Kurbitz *et al* 2011, Vyas *et al* 2011), anti-inflammatory (Kurbitz *et al* 2011), cholesterol-lowering (Matsuda *et al* 1986), anti-allergic (Ohmori *et al* 1995, Fujimura *et al* 2008) and wound healing (Kapoor *et al* 2004) properties.

1.7.1.3.1 Neuroprotective effects

EC is known to protect rat hippocampal cells from Aβ toxicity (Bastianetto *et al* 2006) and phaeochromocytoma PC12 cells from lead- and hydroxydopamine-induced toxicity (Nie *et al* 2002, Chen *et al* 2003b). Moreover, cognitive deficits in rats caused by infusion of amyloid beta peptide into their cerebral ventricles, is reduced by long-term oral administration of EC. EC also causes a reduction of ROS generation in the hippocampus, by acting as a ferrous (III) chelator (Haque *et al* 2008). In rat hippocampal primary cell cultures, both EGCG and EC inhibit apoptosis induced by $A\beta_{25-35}$ and decrease ROS production. These effects were not observed with epicatechin and epigallocatechin which lack the gallic acid in C-ring, suggesting that this galloyl moiety contributed to the neuroprotective effects of EC and EGCG

(Bastianetto *et al* 2006). Apart from its role as a free radical scavenger, EC also increases superoxide dismutase and catalase (Li *et al* 2007).

The antioxidant effects of EC are not the sole mechanism to explain the neuroprotective action of the substance. EC is comparable to EGCG at attenuating the negative effects of lead on PC12 cells by blunting the increase of intracellular $Ca2^{+}$ concentration and preserving changes in the mitochondrial membrane potential (Chen *et al* 2003b). Intracellular neuronal $Ca2^{+}$ concentration is also increased in glutamate excitotoxicity (Dolga *et al* 2011, Zhang *et al* 2011), which has been suggested to be involved in the pathogenesis of glaucoma (Dreyer *et al* 1996). Yet a further possible mechanism of neuroprotection by EC is by it stimulating astrocytes to increase glutamate uptake, which reduces the damaging effects of excess glutamate (Abib *et al* 2008). EC also plays a role in cell survival/death signaling pathways by reducing the activation of p38 and JNK proteins, which are involved in neuronal cell death (Huang *et al* 2007, Kamruzzaman *et al* 2010).

1.7.1.3.2 Antioxidant capacity

Like EGCG, EC has strong antioxidant properties which is attributed by di-hydroxyl groups in B-ring, and the presence of the tri-hydroxyl structure in the D ring (gallate) as shown in figure 1.15 (Rice-Evans *et al* 1996, Wiseman *et al* 1997, Nakagawa *et al* 2002). The presence of di-hydroxyl structure in the B-ring confers higher stability to the radical form and participates in electron delocalization, and the 3- and 5-OH groups in A and C-rings provide radical scavenging potential (Bors *et al* 1990, Sichel *et al* 1991). EC has direct scavenging activity against free radicals such as nitric oxide (NO) and superoxide (Nakagawa & Yokozawa 2002), as well as peroxynitrite (Salah *et al* 1995, Pannala *et al* 1997). Peroxynitrite is a highly toxic, oxidizing and nitrating

species that can be produced *in vivo* through the interaction of superoxide and nitric oxide.

1.7.2 Genistein

Genistein (4,5,7-trihydroxyisoflavone) is a major soybean isoflavone also found in other phytoestrogen-rich plants such as *Pueraria mirifica* (Cherdshewasart & Sriwatcharakul 2007) and *Trifolium pratense L.* or red clover (Occhiuto *et al* 2008). The main source of dietary genistein is in soybean-based foods such as tofu, miso, and fermented soybean products e.g. tempeh (Fukutake *et al* 1996). Other isoflavones such as daidzein and glycetein exist at lower levels in soyfood. Genistein is a phytoestrogen present in plants and has estrogenic actions. Genistein is often referred to as a 'weak estrogen' and much interest in genistein stems from its beneficial effects related to a range of estrogen-related actions, such as breast cancer, osteoporosis, postmenopausal symptons and hypercholesterolemia (Setchell 1998, Messina & Loprinzi 2001, Vitolins *et al* 2001, Setchell & Lydeking-Olsen 2003, Vitolins 2003).

Isoflavones, similar to 17β-estradiol, contain an aromatic ring with a hydroxyl group (figure 1.15), so having an affinity for the estrogen receptor subtypes, ERα and ERβ. Genistein is known to have the greatest affinity for estrogen receptors when compared with other isofavones that include daidzein and biochanin A (Kuiper *et al* 1998).

Genistein possess a myriad of other positive actions, having anti-oxidant (Guo *et al* 2002, Wei *et al* 2002), anti-cancer (Banerjee *et al* 2008), anti-angiogenesis (Kruse *et al* 1997, Majji *et al* 1999), anti-atherosclerotic (Gottstein *et al* 2003), anti-allergy (Tsang & Fred Wong 2000), and anti-inflammatory (Ye *et al* 2004, Valsecchi *et al* 2008) actions as well as being a neuroprotectant (Ho *et al* 2003, Li & Zhang 2003, Kajta *et al* 2007). Genistein is also an inhibitor of protein tyrosine kinase (PTK), which may attenuate cancer cells from proliferating by acting on the PTK mediated

signaling pathway (Akiyama *et al* 1987, Hunter 1987, Ullrich & Schlessinger 1990). Genistein also inhibits topoisomerase I and II (Okura *et al* 1988), 5α-reductase (Evans *et al* 1995), protein histidine kinase (Huang *et al* 1992) and NF-κB and Akt signaling pathways (Li & Sarkar 2002), all of which may contribute to the anti-proliferative or pro-apoptotic actions of genistein.

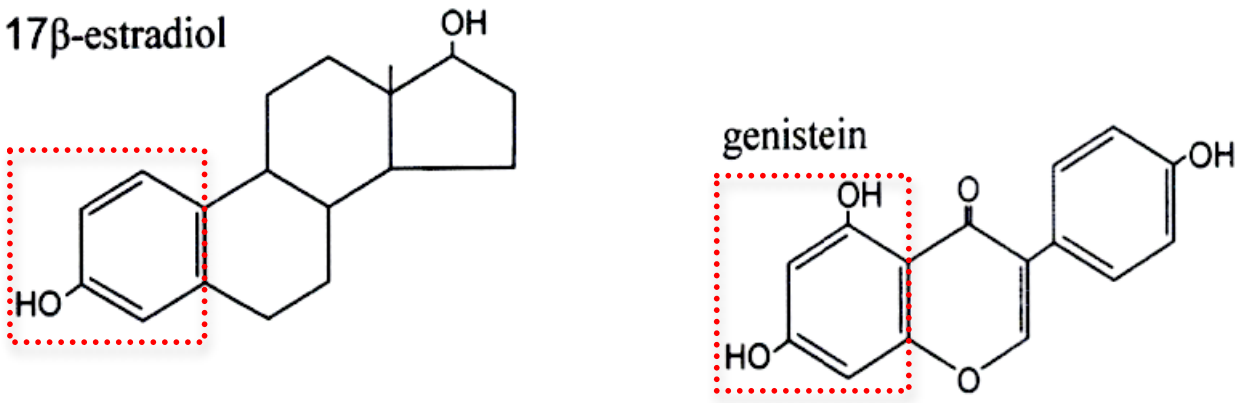


Figure 1.15. A comparison of chemical structures of genistein with endogenous circulating estrogen, 17β-estradiol. The aromatic ring (shown in red dashed box) is necessary for binding to estrogen receptors.[17]

1.7.2.1 Pharmacokinetics and elimination

Isoflavones exists in four isomeric forms: aglycones, and three glycoside conjugate, namely the β-, acetyl-, malonyl- and glucoside-conjugates (Wang & Murphy 1994b, Xu *et al* 2000). In whole soybeans and unfermented soy products, 97-98% of the isoflavones are present as their esterified conjugates (Wang & Murphy 1994a). The conjugates undergo hydrolysis to form free aglycones which are then rapidly absorbed via passive diffusion across the intestinal brush border (Scalbert & Williamson 2000). This process is called deglycosylation, and is catalyzed by colon microflora as well as

[17] Diagram taken from Szkudelska, K & Nogowski, L. Genistein-A dietary compound inducing hormonal and metabolic changes. J Steroid Biochem Mol Biol 105: 27-45, 2007.

the enzyme lactase phlorizin hydrolase (LPH) located at the enterocyte brush border (Day *et al* 2000).

The bioavailability of genistein is low as shown in figure 1.16. A pharmacokinetic study involving 6 women who were each fed with 50mg of purified genistein, showed that the mean maximum plasma concentration of genistein after an hour was only 1.26 ± 0.27μM , with overall absorption being 5 μg/ml . After the initial absorption, isoflavones undergo extensive first pass metabolism, which explains their low bioavailability (Chen *et al* 2003a). The isoflavones undergo enterohepatic circulation and are conjugated in the liver (Winter & Bokkenheuser 1987). In the circulation, most isoflavones are in the conjugated form, and aglycones represent only a small fraction of the total plasma isoflavones (Shelnutt *et al* 2002). The conjugates are then transported via the systemic circulation to tissues, from where they will eventually be excreted via the kidneys, or secreted in the bile and returned to the intestine (Xu *et al* 1995). After deconjugation by intestinal bacteria, isoflavone aglycones can be reabsorbed, returned to the liver for reconjugation, and either undergo further enterohepatic circulation or renal excretion (Winter & Bokkenheuser 1987).

Maximal plasma concentrations of isoflavones occur after 5-8 hour (Xu *et al* 1995, King & Bursill 1998, Setchell *et al* 2003a, Setchell *et al* 2003b). The plasma half-life of genistein is about 8-11 hours after intake of soy foods (Shelnutt *et al* 2002). Genistein is distributed widely in the tissues and have been shown to accumulate in breast tissue and milk (Maubach *et al* 2003), and to cross the blood-brain barrier and placenta (Adlercreutz *et al* 1999, Setchell & Cassidy 1999). Genistein is excreted in the urine, typically highest 7-8 hours post-meal (Lu *et al* 1995).

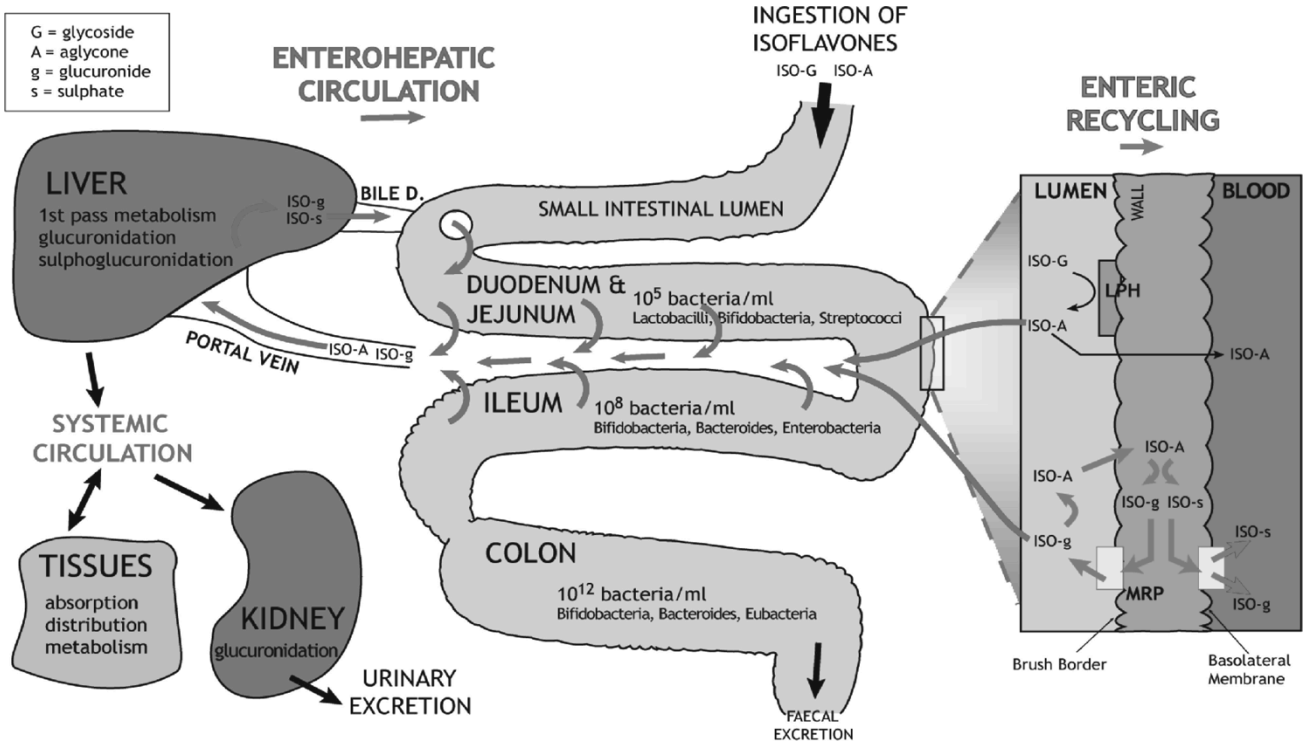


Figure 1.16. Diagram depicting the metabolism of isoflavones. Isoflavones are ingested in the form of glycosides or aglycones (ISO G: isoflavone in glycoside form; ISO A: isoflavone in aglycone form). Hydrolysis and initial absorption occur in duodenum and jejunum, and isoflavones are absorbed as aglycones. They undergo first pass metabolism in the liver, and are conjugated before released into the circulation and distributed in tissues. Some of the conjugated isoflavones are secreted in bile and returned to the intestine for faecal excretion, but most are excreted in the urine. In rats, it has been shown that the multi-drug resistance-related protein (MRP) in the intestinal wall conjugates and the small intestine secretes glucuronidated isoflavones into the intestinal lumen (Liu & Hu 2002).[18]

1.7.2.2 Neuroprotective effects

A variety of studies suggest that genistein can function as a neuroprotective agent. Lee et al showed that long-term oral administration of soy isoflavones for 16 weeks protect cholinergic neurons and reduce age-related cognitive decline in male rats (Lee *et al* 2004b). In addition, repeated intra-peritoneal injection of genistein reduced the

[18] Diagram taken from Larkin, T et al. The key importance of soy isoflavone bioavailability to understanding health benefits. Crit Rev Food Sci Nutr, 48:538-553, 2008.

infarct area to the mouse brain caused by experimental stroke , and also delayed the onset of disease symptoms and mortality in a murine model of familial amyotrophic lateral sclerosis (Trieu & Uckun 1999). Genistein also significantly reduced neuronal cell death in rat hippocampus caused by kainic acid (Azcoitia *et al* 2006) and the effects of global cerebral ischaemia following ligation of both carotid arteries (Liang *et al* 2008). Several *in vitro* studies showed that genistein reduced neuronal damage caused by thapsigargin-, β-amyloid- and glutamate-induced toxicity, as well as iron-induced lipid peroxidation (Linford & Dorsa 2002, Zhao *et al* 2002, Ho *et al* 2003, Bang *et al* 2004, Kajta *et al* 2007, Yu *et al* 2009).

There are several possible mechanisms that may account for the neuroprotective action of genistein one being that it mimics estrogen by binding to estorogen receptors. For example, Donzelli et al (2010) demonstrated that changes in the EEG and degree of neuronal damage caused by an ischemic insult to the cerebellum in gerbils were attenuated by administration of genistein 5 minutes after reperfusion, and that these effects were prevented by co-injection with an estrogen receptor antagonist (Donzelli *et al* 2010). The positive effect of genistein on the survival of motorneuron cells (VSC4.1) (McDowell *et al* 2011) and primary rat cortical cells (Schreihofer & Redmond 2009) in culture are also known to be inhibited by the estrogen receptor antagonist, ICI182,780.

Ischaemia/reperfusion injury to the brain is known to result in enhanced tyrosine kinase activity (Pei *et al* 2000) which is involved in several cell signaling pathways such as phosphatidylinositol 3-kinase (PI3K) and MAPK (Hayashi *et al* 1996), as well as signal transducer and activator of transcription-3, or STAT3 (Li & Zhang 2003). Genistein being a specific inhibitor of tyrosine kinase (Akiyama *et al* 1987), blocks phosphorylation of MAP kinase and as a consequence has been found to prevent

delayed neuronal death in the CA1 region of the hippocampus following ischaemia/reperfusion injury to gerbils (Kindy 1993). Furthemore, in primary rat cortical cultures, glutamate- and thapsigargin-induced cell death are attenuated by genistein, which can be blunted by PI3K or MAPK inhibitors (Schreihofer & Redmond 2009). It has also been shown that genistein inhibits tyrosine phosphorylation of STAT3 and prevents an increase in phosphorylated-STAT3 in the rat brain following ischemia/reperfusion (Li & Zhang 2003). In the central nervous system, STAT3 is continuously expressed in neurons (Stromberg *et al* 2000), and can be activated by a variety of pathologic stimuli such as oxidative stress (Carballo *et al* 1999) and ischaemia (Justicia *et al* 2000).

Ischaemia/reperfusion injury to the cerebellum results in an increase in excitatory neurotransmitters such as glutamate and aspartate, which may contribute to neuronal damage (Phillis *et al* 1996). The mechanism of the neurotransmitter release involves tyrosine phosphorylation and significantly genistein reduces ischaemia-induced neurotransmitter release (Phillis *et al* 1996).

Genistein's endogenous anti-oxidant characteristic contributes to its neuroprotective action. For example, orally administered genistein significantly reduces the infarct size in the rat cerebellum following ischaemia and this is accompanied by a decrease in superoxide level and NAD(P)H oxidase activity (Ma *et al* 2010). Moreover, genistein completely restored glutathione (GSH) basal levels and blunts the increase in ROS following glutamate-induced toxicity to cells (Caccamo *et al* 2005).

Microglial cells are activated by various pathologic stimuli as part of the immune response, and release cytotoxic factors including nitric oxide, hydrogen peroxide, superoxide radical and other cytokines. In the pathogenesis of POAG, activated microglial cells are thought to release cytotoxic chemicals such as glutamate and

TNFα following the initial injury at the optic nerve head (Osborne *et al* 2001, Osborne *et al* 2006a). Marotta et al (2006) showed that oral administration for two weeks of a phytoestrogen compound that contained genistein, significantly reduced the release of pro-inflammatory cytokines such as TNFα, ILβ- and IL-6 from microglia.

1.7.2.3 Antioxidant effects

The beneficial intake of genistein and other isoflavones in certain types of carcinoma, is thought to be associated with their capacity to function as antioxidants (Barnes *et al* 2000). For instance, genistein is known to inhibit low-density lipoprotein (LDL) oxidation (Hwang *et al* 2000, Cassidy *et al* 2003) which otherwise can promote atherosclerosis (Berliner & Heinecke 1996). In addition the antioxidant properties of genistein and other isoflavones are related to the hydroxyl group at the 4' position in the B-ring (Wei *et al* 1995, Ruiz-Larrea *et al* 1997). Genistein scavenges free radicals (e.g. hydrogen peroxide) and inhibit free radical formation (e.g. superoxide anion) (Wei *et al* 1993, Wei *et al* 1996). However, these processes are not the primary reason for the known antioxidant properties of genistein. In mice, dietary genistein increase the endogenous antioxidant enzymes catalase, superoxide and glutathione-S-transferase (Cai & Wei 1996). The low bioavailability of genistein suggests that the phenolic structure of genistein is not entirely responsible for its antioxidant properties. The binding of genistein to ERβ is thought to contribute to its antioxidant activity. Borrás and colleagues showed that genistein (0.5μM) decreased the basal level of peroxide production in MCF-7 cells (human mammary gland tumor cell line), and this effect was largely inhibited by the estrogen antagonist, tamoxifen (Borras *et al* 2006). In the same study, genistein was also shown to increase the mRNA level of the antioxidant enzyme manganese superoxide dismutase (MnSOD), by mimicking the

actions of 17β-estradiol through the activation of ERK 1/2 and NFκB signaling pathways (Borras *et al* 2006).

1.7.2.4 Genistein and the retina

Genistein reduces retinal degeneration following ischaemia/reperfusion injury in a rat model (Hayashi *et al* 1997), inhibit retinal vascular leakage in diabetic rats (Nakajima *et al* 2001), inhibit choroidal neovascularization in rats (Kwak *et al* 2000) and stimulates the regeneration of choriocapillaries in rabbits (Majji *et al* 1999). These effects of genistein are thought to be linked to the inhibition of the protein tyrosine kinase. Hayashi and colleagues showed that tyrosine kinase signaling pathway is activated following ischaemia/reperfusion injury caused by optic nerve compression in rats (Hayashi *et al* 1996). Immunoblotting studies showed increases in protein tyrosine phosphorylation of phospholipase Cγ (PLCγ), SHC and MAPK, as well as increases in angiogenic growth factors such as vascular endothelial growth factor (VEGF), basic fibroblast growth factor (bFGF) and platelet-derived growth factor-B chain (PDGF-B). These proteins not only reflect mitogenesis but neuronal degeneration (Hayashi *et al* 1996). In a subsequent study, 3.4 mg of genistein administered intraperitoneally was shown to attenuate retinal degeneration caused by ischaemia/reperfusion injury, and was associated with the inhibition of tyrosine phosphorylation (Hayashi *et al* 1997).

The increase of VEGF following retinal ischaemia has been linked to the neovascularization in the retina (Okamoto *et al* 1997, Tobe *et al* 1998, Kwak *et al* 2000) as well as increase in vascular permeability in diabetic retina (Murata *et al* 1995, Mathews *et al* 1997). Genistein also attenuates choroidal neovascularization induced by VEGF when given by intravitreal injection in rabbits (Kwak *et al* 2000) or orally in mice (Majji *et al* 1999).

CHAPTER 2

MATERIALS AND METHODS

2.1 Materials

2.1.1 General reagents

2', 7'-dihydroethidium (DHE) was from Boehringer Mannheim Biochemica (Lewes, UK). TdT-dUTP-linked nick end labelling (TUNEL) system was from Promega Corp. (Madison, WI). APOPercentage^{TM} Apoptosis Assay kits were from Biocolor Ltd. (Newtownabbey, Northern Ireland). MTT (3, 4, 5-dimethylthiazol-2-yl)-2, 5-diphenyl tetrazolium bromide) were from Roche Diagnostics (Indianapolis, IN, USA) Unless otherwise mentioned, all chemicals were obtained from Sigma Chemical Co. (Gillingham, Dorset, UK) and were of the best quality available.

2.1.2 Anaesthetics

Hypnorm was purchased from Janssen Pharmaceutica (Grove, UK) and diazepam from CP Pharmaceuticals Ltd. (Wrexham, UK). Xylazine (Rompun; Bayer AG, Kiel, Germany) and ketamine (Ketalar; Parke-Davis, Pontypool, UK) were used to sedate rats.

2.1.3 Immunochemicals

The primary rabbit antibody to GFAP was from Dako Scientific Ltd, Denmark. The primary mouse antibody to neurofilament was purchased from Chemicon, Temesula, USA. The primary rabbit antibody to heme oxygenase-1 was purchased from Stressgen, Asssaydesigns, MI, USA. The primary rabbit antibodies to Bad was purchased from Cell Signalling Technology. The primary rabbit antibody to VDAC1 was purchased from Calbiochem. The primary mouse antibody to alpha-fodrin (α-fodrin) was purchased from Enzo Life Sciences (UK). Primary rat monoclonal antibodies against actin, and tubulin were purchased from Chemicon, Chandlers Ford, UK. Primary mouse antibody NF-L was from Chemicon (Chandlers Ford, UK).

Primary mouse monoclonal antibody to caspase-3 and poly (ADP-ribose) polymerase (PARP) were purchased from Becton-Dickinson, Cowley, Oxford. All other primary antibodies were purchased from Santa Cruz Biotechnology, Inc (USA).

The secondary antibodies anti-mouse IgG with fluorescein isothiacyanate (FITC) conjugate, anti-rabbit IgG with FITC conjugate, anti-mouse IgG peroxidase, anti-rabbit IgG peroxidise and anti-goat IgG peroxidase were purchased from Sigma-Aldrich, Poole, UK. The secondary anti- rabbit and anti-mouse biotinylated antibodies (VECTASTAIN ABC IgG kits) were purchased from Vector Laboratories (Peterborough, UK). The concentrations of the antibody used for immunostaining studies are detailed in Table 2.1.

2.1.4 DNA Labelling Reagents

Deoxyribonuclease 1 (DNase 1) and biotin-16-2'-deoxyuridine-5'-triphosphate (biotin-16-dUTP) were purchased from Boehringer Mannheim (Lewes, UK). Terminal deoxynucleotidyl transferase (TdT) was obtained from Promega (Southampton, UK) and avidin-biotin complex kits were purchased from Vector Laboratories.

2.1.5 Retinal Ganglion Cell Line (RGC-5)

A transformed retinal ganglion cell line, RGC-5 (Krishnamoorthy *et al* 2001) was a kind gift from Dr. Neeraj Agarwal (Department of Pathology and Anatomy, UNT Health Science Center, Fort Worth, Texas, USA).

Antibodies	Immunohistochemistry	Immunocytochemistry	Western blot
Actin	-	-	1:2000
Alpha-fodrin	-	-	1:1000
AIF	-	-	1:1000
Bad	-	-	1:500
BDNF	-	1:500	1:1000
Caspase-3	-	-	1:500
Caspase-8	-	-	1:500
ChAT	1:100	-	-
GFAP	1:1000	-	1:5000
HO-1	-	-	1:500
Lamin A/C	-	-	1:500
NFL	-	1:500	1:1000
P-c-Jun	-	1:200	1:500
P-JNK	-	1:200	1:500
P-p38	-	1:200	1:500
PARP	-	-	1:1000
Tubulin	-	-	1:1000
Thy-1	-	-	1:1000
VDAC	-	-	1:500
Anti-mouse	1:1000	1:1000	1:1000
Anti-rabbit	1:1000	1:1000	1:1000
Anti-goat	1:1000	1:1000	1:1000

Table 2.1. List of dilution ratio for primary and secondary antibodies used.

2.1.6 Cell Culture Reagents

Foetal bovine serum (FBS: E.C. approved), fungazone (amphotericin B), geneticin, gentamycin, glutamine and 0.25% [w/v] trypsin solution were from Invitrogen (Paisley, UK). 25 cm^2 and 75 cm^2 tissue culture flasks, polypropylene (centrifuge) tubes, as well as 6-, 24- and CellPlus charged-coat 96-well plates, were purchased from Fahrenheit and Sarstedt (Leicester, UK).

2.1.7 PCR reagents

Tri-Reagent (a mixture of guanidine thiocyanate and phenol in a mono-phase solution), chloroform, isopropanol and oligo-dithymidylate$_{30}$ (Oligo[dT]$_{30}$) were purchased from Sigma-Aldrich, Poole, UK. Mononey murine leukaemia virus (M-MLV) reverse transcriptase, reverse transcriptase buffer (50mM Tris [hydroxymethyl] ammonomethane-hydrochloric acid [Tris-HCl], 7.5mM KCl, 3mM $MgCl_2$, 10mM dithiothreitol), ribonucleic acid qualified-1 ribonuclease-free deoxyribonuclease (RQ1 RNase-free DNase), RNase inhibitor (RNasin) and deoxynucleotide triphosphates (dNTPs: deoxyadenosine triphosphate [dATP], deoxythymidine triphosphate [dTTP], deoxycytidine triphosphate [dCTP] and deoxyguanosine triphosphate [dGTP]) were from Promega UK Ltd. (Southampton, UK). Amplitaq Gold^{TM} (Taq; in glycerol/stored at -20°C) with GeneAmp (10x; 10mM Tris-HCl stored at -20°C at a pH of 8.3, plus 50 mM KCl), polymerase chain reaction buffer and $MgCl_2$ (25mM) were purchased from Perkin-Elmer Warrington, UK. PCR oligonucleotide primers were obtained from Invitrogen Life Technologies (Paisley, UK). Mitochondrial isolation kit was purchased form BioChain Institute, Inc, CA.

2.1.8 qPCR reagents

Trizol, chloroform, molecular biology grade water and oligo-dithymidylate$_{28}$ (Oligo[dT]$_{28}$ were purchased from Sigma Aldrich, Poole, UK. Superscript III First Strand Synthesis System for PCR was purchased from Invitrogen. For RNA extraction, RNAeasy Mini Kit and RNAse-Free DNAse set were purchased from Qiagen Ltd, UK. Deoxynucleotide triphosphates (dNTPs: deoxyadenosine triphosphate [dATP], deoxythymidine triphosphate [dTTP], deoxycytidine triphosphate [dCTP] and deoxyguanosine triphosphate [dGTP]) were purchased from Promega UK Ltd. (Southampton, UK). Quantitative PCR (qPCR) was measured using StepOnePlus™ Real-Time PCR System (Applied Biosystems^{TM}).

2.2 Methods

2.2.1 Lipid peroxidation

Lipid peroxidation was performed on rat brain homogenates as described by Zhang and Osborne (Zhang & Osborne 2006). Following decapitation the cerebral tissue (cerebral cortex) from adult Wistar rats was dissected and homogenised in 10 volumes of ice-cold 0.9% saline (pH 7.0) using a motor-driven polytetrafluoroethylene-glass homogeniser. The homogenate was centrifuged at 1000xg for 10 minutes at 4°C and the resulting low-speed supernatant was used for the lipid peroxidation experiments. The rate of membrane lipid peroxidation was determined from the amount of formed thiobarbituric acid reactive species (TBARS). Aliquots of supernatant (0.5ml) were pre-incubated at 37°C for 5 minutes with 0.3ml of 0.9% saline (pH 7.0) containing various concentration of the drug tested or vehicle. Lipid peroxidation was initiated by the addition of 0.2ml of 20μM SNP of buffer. After 30 minutes of incubation at 37°C, the test tubes were placed on ice to stop the

lipid peroxidation reaction. TBARS were determined as described by Ohkawa and colleagues (Ohkawa *et al* 1979), with some modifications, by measuring coloured products resulting from the reaction of thiobarbituric acid thought to be particularly malondialdehyde (a compound formed during lipid peroxidation). Briefly, the colour reaction was developed by the sequential addition of 0.2 ml 8.1% w/v sodium dodecyl sulfate (SDS), 1.5 ml 20% v/v acetic acid (pH 3.5) and 1.5 ml 0.8% w/v thiobarbituric acid. This mixture was incubated for 30 minutes in a boiling water bath. After allowing to cool, 2 ml of n-butanol:pyridine (15:1 v/v) was added and the reaction mixture was then centrifuged at 4000xg for 10 minutes. Absorbance of the organic layer (at the top of the tube) was measured at 532 nm wavelength and the amount of TBARS determined using a standard curve of the malondialdehyde derivative 1,1,3,3-tetraethoxypropane (1-30 nmol). Protein concentration in whole brain homogenate supernatant was determined with a bicinchoninic acid protein assay kit (Sigma) using bovine serum albumin as standard.

2.2.2 RGC-5 Cell Cultures

These cells have been previously characterised as expressing certain neuronal characteristics in culture (Krishnamoorthy *et al* 2001). Cells were cultured in RGC-5 culture medium, which consisted of 25mM glucose, 100IU/ml penicillin/streptomycin, 2mM glutamine, 5mg/ml active geneticin and 10% (v/v) heat inactivated foetal calf serum (FCS) in a humidified incubator with 5% CO_2 at 37^{o}C. Doubling time of these cells was approximately 20 hours under these conditions and they were generally passaged at a ratio of 1:8 to give a cell density of approximately 4-5 x 10^4 cells/ml. Cells were either passaged into sterile 75 cm^2 tissue flasks or plated onto sterile 6-, 24- or 96-well plates. For viability assays, cells were plated onto

96-well plates. For assessment of reactive oxygen species with DHE and TUNEL analysis, cells were grown on sterilised borosilicate glass coverslips in 24-well plates. For immunoblotting analysis, cells were plated onto 6-well plates.

Cells were grown to confluence in 75 cm^2 culture flasks. Sterile PBS (10 ml) was added to the flasks and then poured off. Subsequently, 5 ml of 0.25% trypsin solution (Gibco, Invitrogen, Paisley, UK) was added to the flasks, swirled and then placed in an incubator for 10 minutes. 5 ml of RGC-5 culture medium was added to the flasks and swirled. The cells were then scraped from the flasks using sterile cell scrapers and the contents poured into a 10 ml test tube. Following centrifugation (5 minutes at 100 x g), the supernatant was decanted from the test tube and the pellet resuspended in "RGC-5 culture medium" either for passaging into flasks or for plating, as already described.

2.2.3 Preparation of Cytoplasmic, Mitochondrial and Nuclear Extracts

Cytoplasmic, crude mitochondrial and nuclear extracts were obtained from subcellular fractionation process according to the Mitochondria Isolation Kit (BioChain Institute Inc, CA) protocol. Briefly, RGC-5 cells were scraped using a rubber cell scraper from 6-well plates and suspended in homogenisation buffer. Cells were collected by centrifuging at 600g for 5 minutes at 4°C. Cells were washed with cold PBS and centrifuged again at 600g for 5 minutes at 4°C. The supernatant was discarded, and the pellet was resuspended in 1x Mitochondrial Isolation Buffer and transferred to Dounce tissue grinder. Cell suspension was homogenized on ice until more than 80% of cells were lysed. Cell lysis was confirmed by visualizing the lysates under epifluorescence microscope. Cell homogenate was transferred to eppendorf tube and centrifuged at 600g for 10 minutes at 4°C. The supernatant was transferred to a fresh tube, and the pellet was resuspended and collected as crude nuclear fraction.

The supernatant was centrifuged at 12,000g for 15 minutes at 4°C. The pellet was collected as crude mitochondrial fraction and resuspended in mitochondrial storage buffer. The supernatant was collected and stored as cytoplasmic fraction. All samples were stored at -80°C until used for protein analysis and western blotting. Prior to electrophoresis in western blotting, all samples were processed for protein quantification and standardization using a bicinchoninic acid protein assay (Sigma-Aldrich). Proteinase inhibitors and sample buffers were added to each sample before protein analysis. Equal amounts of proteins were separated by electrophoresis using Western blot and transferred to nitrocellulose membrane before probing with appropriate antibodies.

2.2.4 Cell Viability Assays

2.2.4.1 Basic Principles of MTT Assay

Cell viability was assessed with a MTT reduction assay modified from that of Mosmann (Mosmann 1983). MTT can be used to quantify cell survival/viability. The MTT assay is based on the ability of mitochondrial dehydrogenase enzyme from viable and metabolically active cells to cleave the tetrazolium rings of the pale yellow MTT and form dark blue, insoluble formazan crystals by accepting electrons from cellular reducing equivalents such as NADH, NADPH or succinate in living cells (Lobner 2000, Takahashi *et al* 2002). The number of healthy cells is directly proportional to the level of the formazan product. An observed decrease in MTT reduction generally reflects a decrease in the ability of any given cell or group of cells to reduce the dye at all, rather than a summed response of all cells present (ie. a 50% reduction of MTT reduction represented a complete loss of viability of 50% of cells, rather than a reduction in metabolic activity to 50% of all cells). MTT is reduced into a blue coloured formazan crytals which accumulate in the cytoplasm (as shown in

figure 2.1) and dissolve in dimethyl sulfoxide (DMSO). The intensity of the solubilized blue formazan product is quantified by colourimetry, using Multiskan microplate reader using a 570 nm filter.

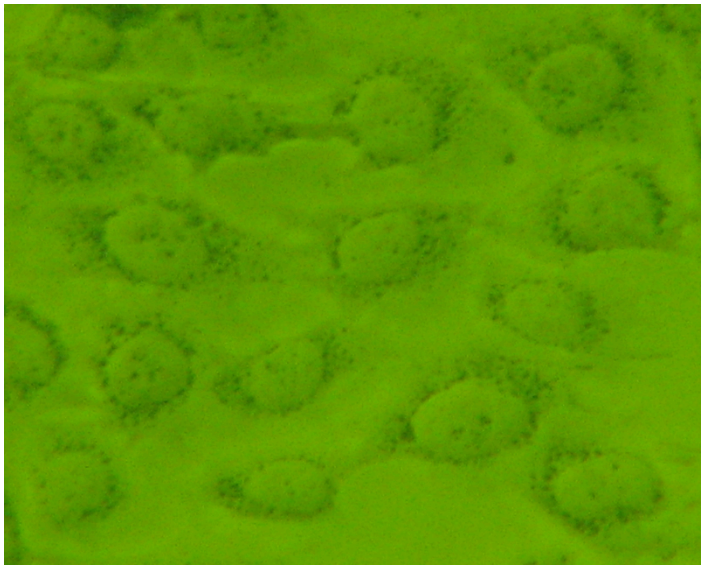


Figure 2.1. MTT assay in RGC-5 cells. Formazan crystals are seen as small dark blue spots which accumulates in the cytoplasm, as seen under epifluoresence microscope with a green filter. These crystals are dissolved in DMSO to form a purple solution, and measured using 570nm wavelength.

2.2.4.2 Methodology of MTT Assay

10 μl of a 5mg/ml MTT solution were added to each well of the 96-well plates containing cells or mitochondria at a final well concentration of 0.5mg/ml for one hour at 37^{o}C. After that, the medium from each well was removed and the reduced MTT (blue formazan product) attached to each well was solubilized by adding 100ml of dimethyl sulfoxide (DMSO). After agitation of plates for 15 minutes, the optical density of the solubilized formazan product in each well was measured using an Multiskan microplate reader (Titertek Plus MS212; ICN Flow, Thame, UK) with a 570nm test wavelength and a 690nm reference wavelength.

2.2.4.3 WST-1 Assay

WST-1 (4-[3-(4-iodophenyl)-2-(4-nitrophenyl)-2H-5-tetrazolio]-1, 3-benzene disulfonate) is a tetrazolium dye containing an electron-coupling agent that is cleaved by mitochondrial dehydrogenases to a formazan dye with an absorbance at 490nm (Toimela & Tahti 2004). 10 μl of the WST-1 solution were added to each well of the 96-well plates containing cells or mitochondria at a final well concentration of 0.5mg/ml for one hour at 37^{o}C. After this time, without removing the WST-1 medium the optical density of the solubilised formazan product in each well was measured using an automatic microplate reader (Titertek Plus MS212; ICN Flow, Thame, UK) with a 490nm test wavelength and a 690nm reference wavelength. The WST-1 assay is used to analyse the mitochondrial dehydrogenase activity of the cells or mitochondria. This activity is directly related to mitochondrial energy production – a fall in activity implies a reduced production.

2.2.5 Assessment of reactive oxygen species (ROS) production (DHE staining)

Cells were assessed for the production of ROS using the dye DHE as described by Carter et al (Carter *et al* 1994). The dye 2', 7'-dihydroethidium (DHE) in its reduced non-fluorescent form can cross plasma membranes of living cells (King *et al* 2004). Within the cell, it is then oxidised by ROS to ethidium bromide, which binds to DNA to yield a red fluorescence product (excitation 475nm/emission 610nm) that is proportional to the intracellular superoxide anion level. In order to visualise ROS, cells on coverslips in 24-well plates were stained with DHE at a final concentration of 10μg/ml for 30 minutes at 37^{o}C. After 30 minutes of incubation, cells were fixed in 4% paraformaldehyde for 15 minutes, washed in PBS for 5 minutes, mounted onto

glass slides using a drop of 1% glycerol and visualised by light microscopy, using a Zeiss microscope with epifluorescence microscope.

2.2.6 Assessment of apoptosis using APOPercentage™ Assay

The APOP*ercentage*™ Apoptosis Assay (Biocolor Ltd., Belfast, N. Ireland) was used to quantify apoptosis. The assay uses a dye that stains red the apoptotic cells undergoing the membrane "flip-flop" event when phosphatidylserine is translocated to the outer leaflet. 100ml/well fresh culture medium containing 5ml APOP*ercentage*™ dye was added to each well followed by incubation for 30 minutes at 37°C. After removal of the culture medium, cells were gently washed twice with 200ml/well PBS and then immediately viewed by epifluorescence microscopy. Quantification of the number of apoptotic cells were achieved by counting the pink apoptosis positive cells in at least five different fields of view under a magnification of 250x.

2.2.7 Assessment of cell viability and death by simultaneous staining with fluorescein diacetate (FDA) and propidium iodide (PI)

RGC-5 cells were grown overnight on cover slips in 24-well plates. Approximately after 24 hours following plating, cells were treated with defined substances or vehicle for 24 hours or exposed to light treatment (1000 lux, 400-600nm) for 96 hours. Following treatment, 5μM FDA were added into the wells for 2 minutes, followed by 3μM PI and left to incubate for 30 minutes at room temperature. Cells were then rinsed briefly with PBS and examined under fluorescence microscope (Jones & Senft 1985). Live cells show green fluorescence, while dead cells with stain with red fluorescence.

2.2.8 Terminal-Deoxynucleotidyl Transferase (TdT)-Mediated dUTP-Biotin Nick End Labeling (TUNEL)

2.2.8.1 Basic Principles of TUNEL staining

Apoptosis is characterized by chromatin condensation, intracellular fragmentation associated with membrane enclosed cellular fragments (apoptotic bodies) and internucleosomal DNA fragmentation (Kerr *et al* 1972, Wyllie *et al* 1984, Ellis *et al* 1991). Morphologically, apoptosis can also be characterized by cellular shrinkage, nuclear pyknosis and blebbing of the plasma membrane (Wyllie *et al* 1980, McConkey *et al* 1990, Kroemer *et al* 1995, Fink & Cookson 2005). Apoptotic endonucleases produce 3'-OH groups at the ends of DNA fragments to which TdT binds and catalyses the addition of biotin-labelled deoxynucleotides. Biotinylated nucleotides are detected using an avidin-biotin-peroxidase complex. Subsequently, diaminobenzidine is added to react with the labelled ends of the DNA fragments and generate an insoluble coloured substrate at the site of DNA fragmentation (see figure 2.2).

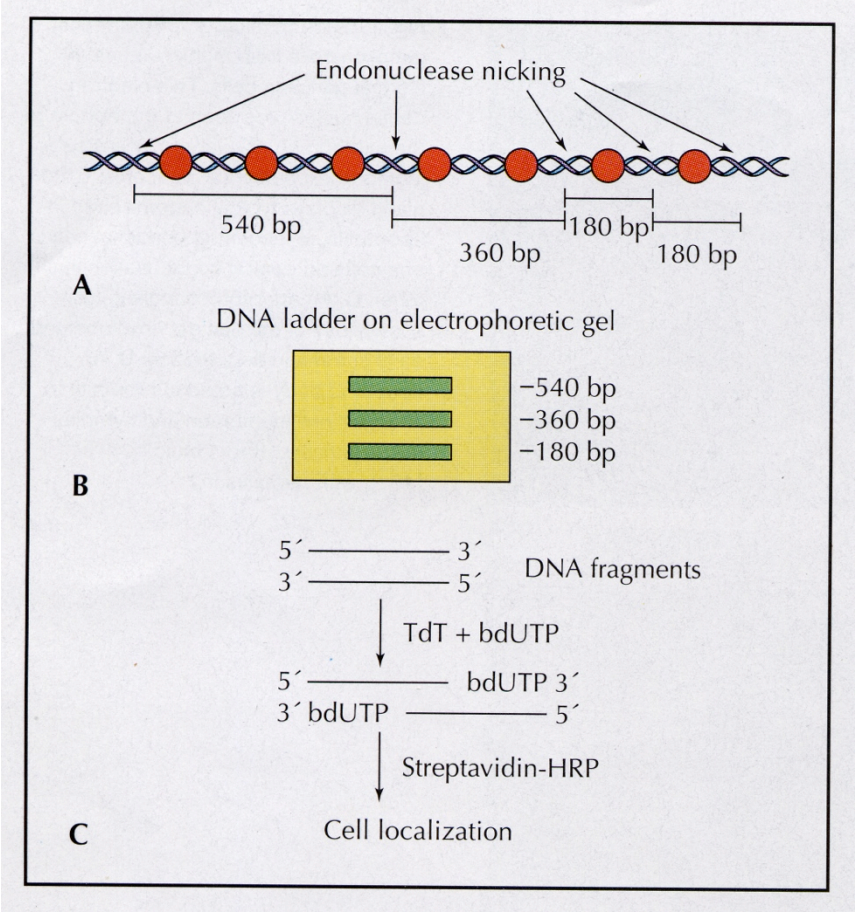


Figure 2.2. TUNEL localization of DNA frgamentation in apoptosis. A: endonucleases cleave DNA between DNA/histone complexes (circles), in multiples of 180 base pair units. B: electrophoretic gels show bands at multiples of 180 base pair untis (not performed in these studies). C: TdT adds biotinylated deoxyuridine (dUTP) to the 3' end of DNA strands. The bound biotins are localized immunohistochemically by an avidin-biotin-peroxidaes complex. [1]

[1] Diagram taken from McKinnon SJ. Glaucoma, apoptosis and neuroprotection. *Curr Opin Ophthalmol* 1997,8:28-37

2.2.8.2 Methodology of TUNEL Staining

Cells on coverslips which had been fixed for 30 minutes with 4% paraformaldehyde in 0.1 M sodium phosphate buffer (pH 7.4) were washed initially in Tris buffer (10 mM Tris–HCl, pH 8.0) for 5 min and then exposed to 1% (v/v) H_2O_2 for 5 minutes to remove endogenous peroxidase activity. Following a further wash in Tris buffer (5 minutes), cells were incubated in Tris buffer (30mM Tris-HCl, ph 7.8) in the presence of pepsin (800U/ml) for 10 minutes at 37°C in order to expose the free DNA ends. Following a rinse with Tris buffer for 5 minutes, cells were pre-incubated in TdT buffer (30 mM Tris–HCl, pH 7.2, containing 140 mM sodium cacodylate and 1 mM cobalt chloride) for 10 minutes at 37°C. Subsequent to this, the transferase reaction was performed by incubating for 60 minutes at 37°C with TdT buffer containing 0.25 units/µl of TdT and 40 µM biotin-16-dUTP. In order to check for the validity of this assay, positive-control samples were obtained by the addition of DNase 1 (50 µl in 500 µl TdT buffer) for 10 minutes prior to the transferase reaction. The reaction was stopped by incubation in sodium citrate buffer (300 mM NaCl, 30 mM sodium citrate) for 2×15 min at room. Coverslips were then rinsed for 10 minutes in Tris-buffered saline (TBS:20mM Tris, 150mM NaCl, pH7.3) and for a further 10 minutes in TBS solution containing 1% bovine serum albumin, and finally for 40 minutes with Cy-3-conjugated streptavidin. The final washing step was in TBS buffer and the coverslips were then mounted in buffered glycerol containing phenylendiamine to reduce fluorescence fading.

2.2.9 Immunohistochemistry and Immunocytochemistry

2.2.9.1 Basic Principles of Immunohistochemistry and Immunocytochemistry

These techniques are based on the specific binding of an antibody to a defined antigen to allow the visualisation of the antibody-antigen complex. Detection of antigens in tissues is generally known as immunohistochemistry, while detection in cultured cells is termed immunocytochemistry.

Immunocytochemistry and immunohistochemistry consist of the following steps:

* A primary antibody is initially used to recognise a specific antigen.

* Antibody-antigen complex is bound to by a secondary, FITC conjugated antibody.

Alternatively, the secondary antibody can be conjugated to an enzyme, for example alkaline phosphatase or horseradish peroxidase, which amplifies the reaction.

* In the presence of substrate and chromogen, the enzyme forms a coloured deposit at the sites of antibody-antigen binding. The colour of the deposit depends on the chromogen used. In the case of FITC, the fluorochrome fluoresces and can be viewed under UV light.

2.2.9.2 Methodology of Immunohistochemistry and Immunocytochemistry

2.2.9.2.1 Immunohistochemistry

Retinas were immediately dissected following decapitation and fixed in 2% paraformaldehyde (0.1M phosphate buffer) for 30 minutes at room temperature. The fixed retinas were then cryopreserved for roughly 4 hours in 30% sucrose / 0.1 M sodium phosphate buffer (pH 7.4). Individual retinas were then frozen onto a microtome chuck using dry ice/isopentane slurry at -20°C after which 10μm frozen retinal sections were cut using a microtome. The sections were recovered onto

gelatin-coated glass slides. Subsequently, sections were thawed and incubated overnight at 4 °C with rabbit anti-GFAP polyclonal antibody (diluted 1:1000; DAKO, UK) or mouse anti-choline acetyltransferase monoclonal (ChAT; 1:100; Sigma, UK) antibody. Development was with appropriate secondary antibodies conjugated to fluorescein.

2.2.9.2.2 Immunocytochemistry

For immunocytochemistry, RGC-5 cells were grown on 13 mm borosilicate glass coverslips, which were coated with 10μg/ml poly-L-lysine in PBS. Coverslips containing cell cultures were fixed in 4% paraformaldehyde in 0.1 M sodium phosphate buffer (pH 7.4) for 30 minutes at room temperature. After rinsing with PBS plus Triton X-100 (0.1%, v/v; PBS-T) for 5-10 minutes, the fixed cultures were incubated at room temperature for 4 hours with the primary antibody (between 1:100 and 1:500)) followed by a further 5-10 minute wash in PBS-T. Coverslips containing cultures were then exposed to secondary antibodies labelled with FITC for 60 minutes followed by 5-10 minute wash in PBS-T. Coverslips were then mounted to glass slides using 1% glycerol. Fluorescent antigens were visualized using a Zeiss epifluorescence microscope.

2.2.10 Caspase-3 colourimetric assay

This assay is based on the hydrolysis of the peptide substrate acetyl-Asp-Glu-Val-Asp p-nitroanilide (Ac-DEVD-pNA) moiety (Nicholson *et al* 1995). Cells were treated in 6-well plates, and were rinsed twice with ice-cold PBS. The cells were then scraped from the plates using sterile cell scrapers and cell suspension was collected in a 10 ml test tube. Following centrifugation (5 minutes at 100 x g) the supernatant was decanted from the test tube and the pellet resuspended in 150μL of ice-cold PBS. Cell

lysates were then homogenised and protein concentration was determined using bicinchoninic acid protein assay kit (Sigma) using bovine serum albumin as standard. 100μL of cell lysates from each sample were pipetted into each well of a 96-well plate. 2μL of Ac-DEVD-pNA (2mM) was added into each well to a final concentration of 200μM, and the plate was incubated for 2 hours at 37C. P-Nitroaniline has a high absorbance at 405 nm. The concentration of the pNA released from the substrate is calculated from the absorbance values at 405 nm using Multiskan microplate reader.

2.2.11 Light treatment regime

A normal culture incubator was equipped with two 8-Watt strip-lights that could be adjusted to be 30-60 cm directly above a tray containing 6-, 24- or 96-well plates with established cells. The strip-light bulbs were completely covered with a filter (number 2C UV, Lee Filters, Andover, UK). This filter excluded light wavelengths below 400nm to mimic the situation that occurs for light impinging on the retina, *in situ*. The actual emission spectra generated from the used strip light consists of seven clear peaks (figure 2.3) with the light peak of around 370 nm being excluded by the 2C UV filter.

The intensity of light directed onto the cells was determined by the use of a digital lux meter (LX-101, Luton, UK). To exclude control wells or plates from any light, white paper covers were placed over the control wells or plates. In this way any slight increase in temperature caused by the light over a 1-2 day period equally affects cells in the dark and light. In order to test the effect of different lighting intensities, the distance between the culture plates and light source were adjusted so as to achieve the desired amount of lux. For serum-deprivation experiments, serum-free retinal cell culture medium or RGC-5 culture medium (with all other additives present as

outlined previously) was used for the appropriate amount of time. In some cases selected substances were included in the culture medium at defined concentrations, and generally renewed with fresh medium every 24 hours.

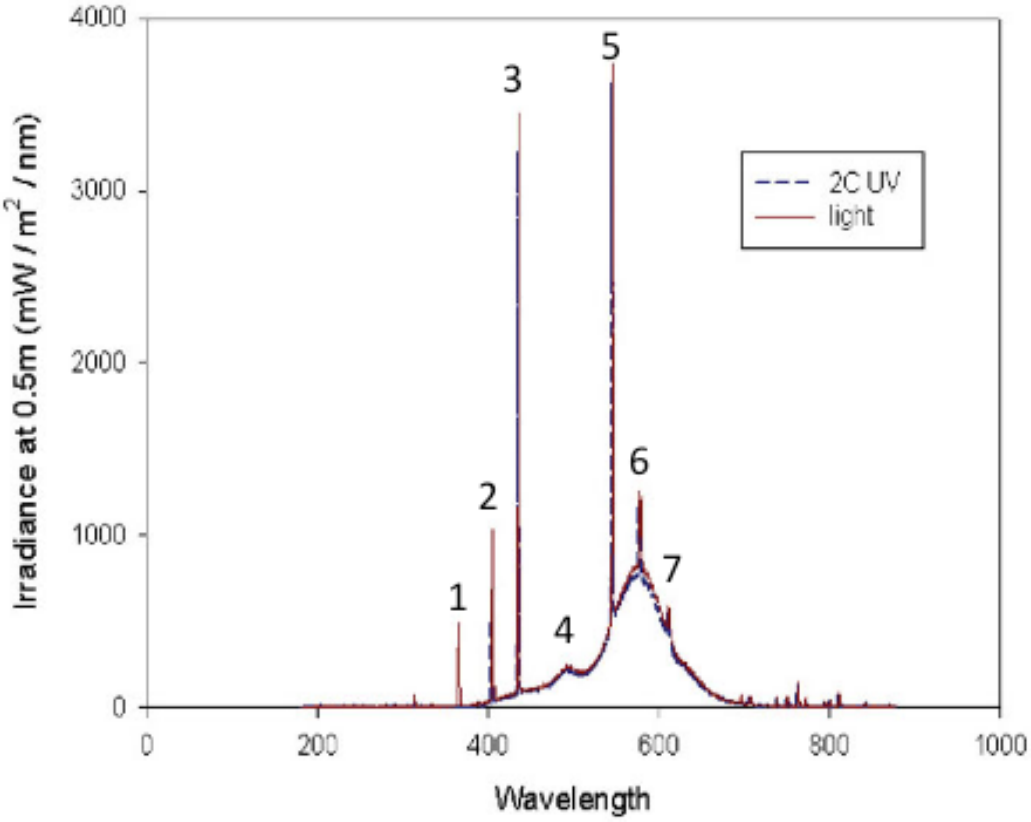


Figure 2.3. Graph showing the spectral irradiance profile of the fluorescent light source used. The filtration profile of the Lee 2C ultraviolet (UV) filter is shown in the left. Seven peaks of light (1-7) could be identified (shown in solid red line). The Lee 2C filter allows light with wavelengths above 400nm to pass (shown in blue dotted line) and excludes light peak 1.[2]

[2] Diagram taken from Wood et al. The influence of visible light exposure on cultured RGC-5 cells. Mol Vis, 14:334-344, 2008

2.2.12 Induction of retinal ischemia

The experiments were conducted in a blind, randomised design. Adult Wistar rats (200-250g) were numbered in a random manner and divided into two groups with equal numbers. The rats were anaesthetised by intramuscular injection of a combination of diazepam (CP Pharmaceuticals Ltd., Wrexham, UK; 2.5mg/kg) and Hypnorm (Janssen, Grove, UK; 0.3ml/kg). Ischaemia was induced by inserting a 30-gauge needle, connected to a sterile saline reservoir at a pre-determined height, into the anterior chamber of an eye to produce an intraocular pressure of 120 mmHg. Ischemia was confirmed by immediate whitening of the fundus and was induced for 50 minutes. The contralateral left eye remained untouched and served as control. Normal body temperature was maintained and monitored both during ischemia and in the recovery period before transfer to animal house conditions.

2.2.12.1 Genistein *in vivo* study

Two sets of syringes were labelled either A or B, one containing vehicle (25% DMSO and 75% water), and the other, genistein. Genistein (10 mg/kg) or vehicle was injected twice into the peritoneal cavity: the first bolus of intraperitoneal injection was given 1 hour before the induction of ischaemia, and the second bolus was administered immediately after ischaemia. Retina and optic nerve samples were harvested after 7 days of reperfusion.

2.2.13 Polymerase chain reaction (PCR)

2.2.13.1 Basic principles of PCR

The purpose of polymerase chain reaction (PCR) is to synthesize, *in vitro*, a large number of copies of a gene. There are three steps in each PCR cycle that are repeated for a set number of cycles. PCR is performed using an automated thermal cycler that can rapidly heat and cool the tubes containing the reaction mixture. There are three major steps in PCR, as shown in figure 2.4. The steps are as follows:

1) Denaturation at 94^{o}C: during denaturation, the double strand unwinds and is separated into two single strands of DNA. All enzymatic reactions stop at this high temperature. Subsequent rapid cooling of the reaction mix ensures the separated (denatured) strands do not re-anneal.
2) Hybridisation at 50-60^{o}C: the molecules are in perpetual motion and weak hydrogen bonds are constantly being formed and broken between different pieces of DNA. Stable bonds are formed between the base pairs on the oligonucleotide primers and complementary base pairs on the single stranded DNA templates. The large excess of the primers ensures that the two DNA strands of interest always bind to the primers rather than to each other.
3) Extension at 72^{o}C: DNA polymerase attaches to the small pieces of double-stranded DNA (template and primer) and adds dNTPs to the primer in a 5' to 3'direction. The primers flank the target for amplification and face inwards. DNA synthesis therefore proceeds across the region between the primers. 72^{o}C is the optimal working temperature for the heat-stable DNA polymerase. Primers that have bound to DNA strands at positions with no exact nucleotide base pair match are not extended because of weaker hydrogen bonding, which is unstable at higher temperatures.

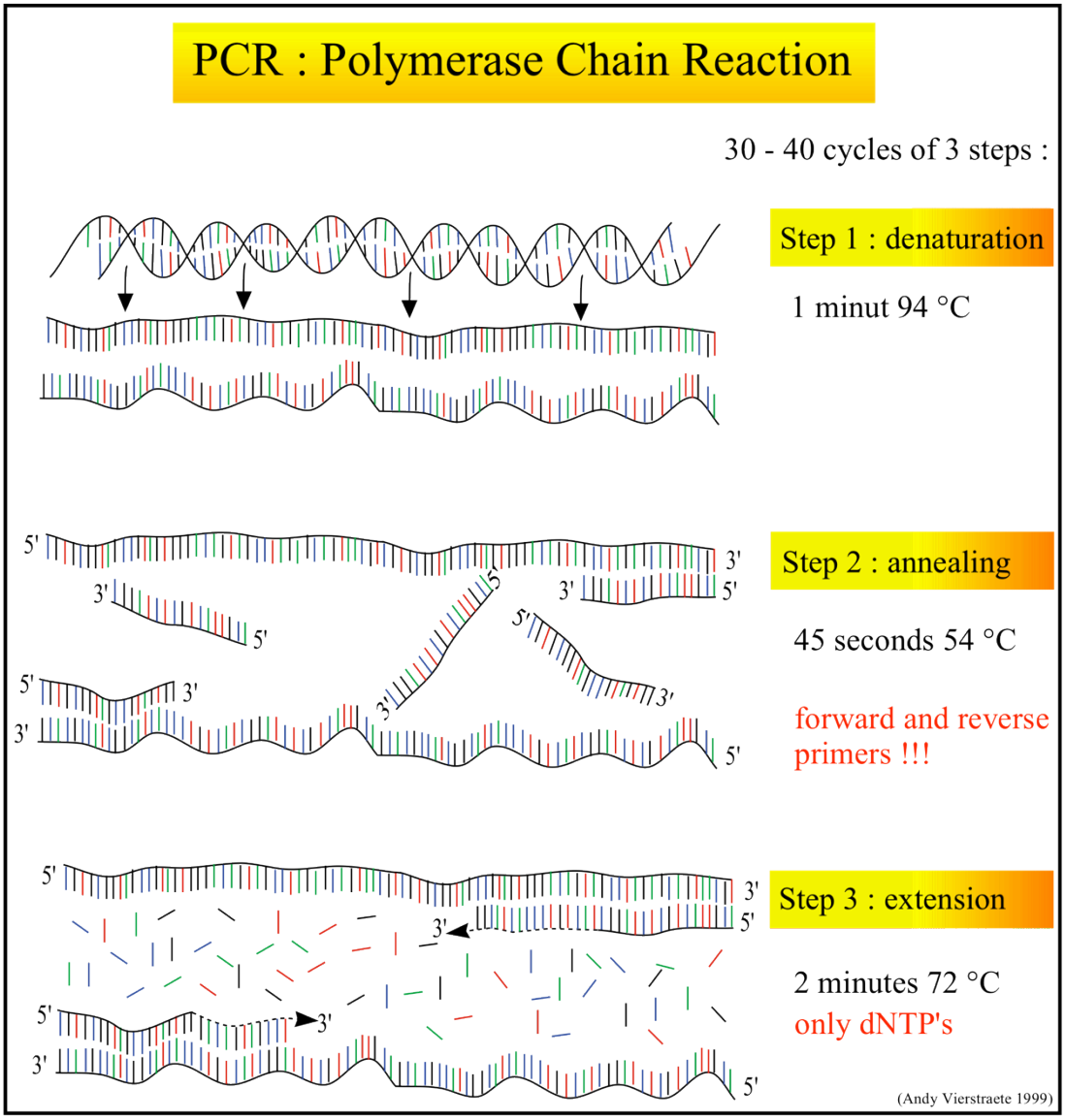


Figure 2.4. Each cycle of PCR consists of three major steps: denaturation, annealing and extension of primers.[3]

Each cycle is repeated many times and target DNAs are amplified exponentially, as shown in figure 2.5. The number of amplification cycles necessary to produce a band visible on a gel depends largely on the starting concentration of the target DNA. Both strands are copied during PCR such that there is an exponential increase in the number of copies of the gene. It is recommended that 40-50 cycles are needed to amplify 50 target molecules and 25-30 to amplify 3x 10^5 molecules to the same

[3] Diagram taken from http://users.ugent.be/~avierstr/pdf/PCR.pdf

concentration. This non-proportionality is due to a plateau effect, which is from the attenuation in the exponential rate of product accumulation in the late stages of the PCR, which may be caused by degradation of reactants (dNTPs, enzyme), reactant depletion (primers, dNTPs), end-product inhibition (pyrophosphate formation) and competition for reactions by non-specific products.

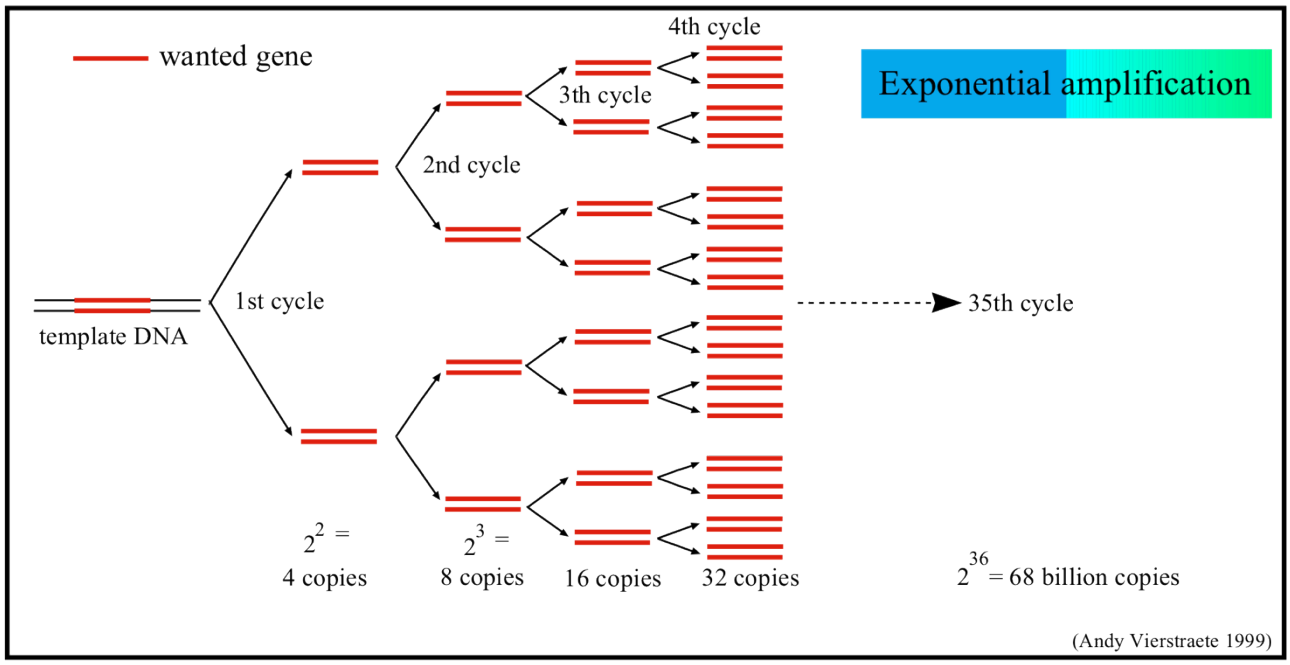


Figure 2.5. Each cycle of PCR will amplify target DNAs in an exponential manner.[4]

2.2.13.2 Methodology of PCR in optic nerves and retina

1) Preparation of tissue and RNA

Rats were killed and the globes were enucleated with forceps as described in previous studies (Nash & Osborne 1999, Chidlow *et al* 2005). The cornea was excised and the lens and vitreous removed. The sensory retina was then gently extracted from the eye cup and homogenized in 400µl of ice cold TriReagent™ with a sonicator (Burkard Scientific Ltd, Uxbridge, UK) for 13 seconds, and stored at -70°C until used. Once

[4] Diagram taken from http://users.ugent.be/~avierstr/pdf/PCR.pdf

thawed, the homogenates were vortexed and centrifuged at 14000 rpm for 10 minutes to remove insoluble materials. The supernatant was then transferred to a new tube. After 5 minutes at room temperature to ensure complete dissociation of nucleoprotein complex, 80µl of chloroform was added, the mixture was vortexed for 15-30 seconds and allowed to stand at room temperature for a further 10 minutes and then another 10 minutes at 4^{o}C (on ice) before centrifugation at 14000 rpm for 15 minutes at 4^{o}C. This produced separation of the sample into three phases: a top colourless aqueous phase containing RNA, an inter-phase containing DNA and a bottom organic phase containing protein. 150µl of the RNA-containing phase was carefully removed and transferred to a new 1.5ml tube. After 200ml of isopropanol was mixed with the RNA-containing phase, the samples were vortexed and then placed on ice for 60 minutes, to help precipitate the RNA, followed by centrifugation at 14000 rpm for 15 minutes. The supernatant was then decanted off and the RNA pellet washed with 1ml of 75% ethanol (to resolubilise various salts), vortexed and centrifuged at 14000 rpm for 5 minutes at 4^{o}C. After decanting the supernatant and removing excess liquid the pellet was allowed to dry at room temperature for at least 15 minutes before resuspending in 50µl of diethylpyrocarbonate (DEPC) treated water and the samples were placed in an ice bath.

The quality and quantity of RNA was determined using spectrophotometry, where 10µl of solution was added to 990µl of DEPC-treated water and the ratio of the optical density (OD) at 260 and 280nm wavelengths (OD_{260}/OD_{280}) was calculated. OD_{260} correlates with the amount of nucleic acid in the sample and the OD_{280} correlates with the protein content. Only samples with OD_{260}/OD_{280} ratios greater than 1.6 were considered appropriate for further analysis, and the volume of original

sample containing 2μg of RNA was determined using the following sequence of calculations:

1 OD_{260} unit = 40μg of total RNA/ml

OD_{260} (measured) x 40 = [RNA] in original sample (μg/ml)

[RNA] in diluted sample (μg/ml) x 100 = [RNA] in original sample (μg/ml)

[RNA] in original sample (μg/ml)/1000 = [RNA] in original sample (μg/μl)

Volume of sample containing 2μg RNA = 2/[RNA] in original sample (μg/μl)

The RNA sample was made up to a total volume of 7μl using DEPC-treated water.

2) DNase treatment

Residual DNA was digested by incubating at 37°C for 10 minutes 2μg of total RNA and the appropriate volume of DEPC-treated water with 0.5μl RNase (2U/μl), 1.5μl of DNase (0.05U/μl), 1.0μl reaction buffer (Sigma Chemical Co. Poole, UK) to give a total reaction mixture of 10μl. 1.0μl of stop solution (Sigma Chemical Co. Poole, UK) was then added to each tube and the mixture was incubated for 10 minutes at 70°C in order to denature the DNase.

3) Reverse transcription

The synthesis of the first-strand of cDNA was performed in a 17μl reaction mix at 42°C for 60 minutes. Each sample contained 11μl aliquote from the DNase-treated RNA sample, 0.6μl RNasin (24U), 1.0μl oligo$[dT]_{30}$ (5ng), which attaches to the poly-A-tail of the mRNA in order to form the cDNA product, 0.4μl dNTPs (0.6mM each dNTP) and 1μl reverse transcriptase (200U) and 3μl reverse transcriptase buffer pH 8.3 (Sigma Chemical Co. Poole, UK). Following this incubation 133μl of DEPC-treated water was added to each tube to give 150μl of the final cDNA product.

4) PCR amplification of cDNA

Individual cDNA (2µl of sample from the RT stage) were amplified in a reaction mixture containing 1µl GeneAmp PCR buffer, 1.6µl $MgCl_2$ (4mM), 0.8µl dNTPs (200µM each dNTP), 0.4µl of both the sense and antisense primers (4ng/µl each primer), 0.1µl of 1U AmpliTaq Gold^{TM} and 3.7µl of DEPC-treated water. PCR reactions were initiated by incubating tubes at 94^{o}C for 10 minutes (a pre-PCR thermal requirement to active the AmpliTaq Gold^{TM}). Subsequently, a suitable number of cycles were used in order to amplify the samples within the linear phase while avoiding saturation. Each cycle was comprised of denaturation at 94^{o}C for 12 seconds, hybridisation (annealing temperature) for 30 seconds, and extension at 72^{o}C for 30 seconds, using a Hybaid PCR Sprint thermal cycler (Ashford, Middlesex, UK). The reaction was completed by a final extension at 72^{o}C for 3 minutes. The appropriate number of cycles to be used for each set of primers had been previously determined in the laboratory. Moreover, all of the PCR products yielded single bands corresponding to the expected size in base pairs and had previously been sequenced to ensure their validity.

5) Visualisation and analysis of the PCR product using conventional method

PCR samples (10µl) plus loading buffer (2µl) were separated on a 1.2% agarose minigel. A fresh minigel was prepared each time by boiling 0.6g of agarose in 45ml DEPC-treated water and 5ml Tris-borate-ethylene-diamino-tetra-acetic acid (TBE) buffer. Ethidium bromide (5µl added to gel and running buffer) was used for DNA visualization under ultraviolet fluorescence. Digital images of the gel were taken and band densitometry performed using Labworks software (Ultra-Violet Products Ltd., Upland, CA).

The sequences and annealing temperatures of each primer used in conventional PCR are shown in table 2.2 below.

Primers	sequences	annealing temperature (°C)
Cyclophilin	TGGTCAACCCCACCGTGTTCTTCG	52
	GTCCAGCATTTGCCATGGACAAGA	
Bcl-2	TTGTGGCCTTCTTTGAGTTCG	52
	TACTGCTTTAGTGAACCTTTT	
GAPDH	CATCAAGAAGGTGGTGAAGCAGG	52
	CCACCACCCTGTTGCTGTAGCCAA	
Caspase-3	GTTAACACGAGTGAGGATGTG	52
	GTTAACACGAGTGAGGATGTG	
Caspase-8	ACTGGCTGCCCTCAAGTTCCTGTGC	60
	TCCCTCACCATTTCCTCTGGGCTGC	
Thy-1	CGCTTTATCAAGGTCCTTACTC	52
	GCGTTTTGAGATATTTGAAGGT	
NF-L	ATGCTCAGATCTCCGTGGAGATG	52
	GCTTCGCAGCTCATTCTCCAGTT	
GFAP	ATTCCGCGCCTCTCCCTGTCTC	55
	GCTTCATCCGCCTCCTGTCTGT	
PARP-1	CCTAAGGAGATTCGGTGAG	52
	GGCAAGCACAGTGTCAAA	

Table 2.2. Primer sequence and annealing temperatures for conventional PCR.[5]

[5] Abbreviations: NF-L = neurofilament light form, GAPDH = glyceraldehyde phosphate dehydrogenase; GFAP = glial fibrillary acidic factor; FGF-2 = basic fibroblast growth factor; CNTF = ciliary neurotrophic factor; PARP-1 = Poly (ADP-ribose) polymerase

2.2.13.3 Real-Time quantitative PCR (qPCR)

Similar to conventional PCR described in the previous section, quantitative PCR involves RNA extraction, cDNA synthesis using reverse transcriptase, and amplification of cDNA. The main difference is the quantification of cDNA by measuring the fluorescence intensity of fluorescent probes. The preparation of cDNA samples from RGC-5 cells was performed according to the Qiagen RNA extraction kit (Qiagen RNAeasy Mini Kit and Qiagen RNAse-Free DNAse set).

1. RNA extraction from RGC-5 cells

Briefly, RGC-5 cells were harvested from 6-well plates and collected by centrifuge at 600g. Cell pellets were rinsed with cold PBS once. The pellets were resuspended in 1ml of Trizol solution, mixed by vortexing and left at room temperature for 5 minutes. Then 200μl of chloroform,was added and the mixture was vortexed and left for 1 minute at room temperature before being centrifuged at 15,000g for 10 minutes to separate the liquid phases. The top liquid phase was transferred to a new tube (200μl) and added with 700μl of RLT buffer and 500μl pure ethanol. The mixture was vortexed, and centrifuged in a spin column for 15 seconds at 10,000 rpm. On-column DNAse treatment was performed, and the spin column is incubated for 15 minutes at room temperature. The sample is then rinsed with RW1 and RPE buffer before finally RNA sample was eluted using 40μl RNAse-free water. RNA was quantified using NanoDrop.

2. Reverse transcription and cDNA synthesis

For each reaction a 13μl reaction mixture was prepared consisting of 1μl OligodT (50μM), 1μl dNTP (10mM each) and 11μl RNA sample of equal RNA amount. The mixture was heated to 65°C and cooled on ice for 1 minute. A mastermix solution was used for each sample consisting of 4μl 5x First Strand buffer, 1μl 0.1M DTT, 1μl

RNAseOUT and 1μl Superscript III. The sample is mixed by pipetting and heated to 50°C for 60 minutes, before inactivated by heating to 70°C FOR 15 minutes. The cDNA samples were stored at -80C if not used immediately.

3. Measuring fluorescence

Each 1μl of sample was added with 10μl SybrGreen mastermix, 0.5μl Forward primer (10μM), 0.5μl Reverse primer 10μM) and 8μl molecular biology grade water into each well of a 96-well PCR plate. The plate was covered with a thin membrane and fluorescence was read using StepOnePlus™ Real-Time PCR System (Applied Biosystems^{TM}). For each primer, the melting temperature, T_m was determined, and the fluorescence was measured at 2.5°C lower than the T_m.

The sequences and annealing temperatures of the primers used in qPCR are shown in table 2.3.

Primers	sequences	T_M (°C)
Actin	TGTGATGGTGGGAATGGGTCAG	86.2
	TTTGATGTCACGCACGCACGATTTC	
GAPDH	CAACGGGAAGCCCATCA	79.4
	CGGCCTCACCCCATTTG	
B2M	TGCTGTCTCCATGTTTGATGTATCT	81.4
	TCTCTGCTCCCCACCTCTAAGT	
ARP	CGACCTGGAAGTCCAACTAC	78.5
	ATCTGCTGCATCTGCTTG	
Bcl-2	GATCATGCCGTCCTTAGAAAA	76.7
	CTGCTTTTTATTTCATGAGGTACATT	
BAX	ACCAAGAAGCTGAGCGAGTGTC	86.0
	ACAAAGATGGTCACGGTCTGCC	
HO-1	CAAGCCGCGAATGCTGAGTTCATG	84.0
	GCAAGGGATGATTTCCTGCCAG	
Nrf-2	TTCTTTCAGCAGCATCCTCTCCAC	82.2
	ACAGCCTTCAATAGTCCCGTCCAG	
JNK	GGAGCCGAGGGGTCTGACGAAG	81.0
	AAGTTGAGTCCGCCACCTGCAC	
cJun	GAGTGGGAAGGACGTGGAGC	88.3
	TCCATCGTTCTGGTCGCGCG	

Table 2.3. Primer sequences and annealing temperatures for qPCR.[6]

[6] Abbreviations: GAPDH = glyceraldehyde phosphate dehydrogenase; B2M = Beta-2-microglobulin; ARP = acidic ribosomal protein; HO-1 = heme oxygenase 1; NRF-2 = nuclear factor erythroid 2-related factor 2; JNK = c-Jun amino-terminal kinase

2.2.14 Electrophoresis / SDS-PAGE

2.2.14.1 Basic principle of eletrophoresis/ SDS-PAGE

Electrophoresis is the migration of charged molecules in solution in response to an electric field. The rate of this migration depends on the strength of the field, size and shape of the molecules, viscosity and the temperature of the medium in which the molecules are moving.

Typically, the samples are run in a support matrix such as agarose or polyacrylamide gel. The matrix inhibits convective mixing caused by heating and provides a visual record of the electrophoretic run. Both the agarose and polyacrylamide matrices, being porous gel, provide a means of separating molecules by size. A porous gel can act as a sieve by retarding or in certain cases completely obstructing the movement of large macromolecules, while allowing the movement of smaller molecules. Sodium dodecyl sulphate (SDS) is an anionic detergent, which denatures proteins by wrapping around the polypeptide backbone by binding to proteins in a mass ratio of 1.4:1. This thereby confers a negative charge to the polypeptide, which is directly proportional to its length. The denatured polypeptides become rods surrounded by a negatively charged cloud with equal charge densities per unit length. The denaturing process of SDS-PAGE separation allows migration of proteins not by intrinsic electrical charge but by molecular weight.

2.2.14.2 Methodologies of electrophoresis/ SDS-PAGE

1) Preparations of whole retina samples

After enucleation, retinas were dissected from other ocular tissues, and sonicated for 30 seconds in 100ml homogenization buffer/protease inhibitors solution (20 mM Tris HCl, pH 7.4, containing 2 mM EDTA, 0.5 mM EGTA, 1% SDS, 0.1 mM phenylmethylsulphonyl fluoride, 50 μg/ml aprotinin, 50 μg/ml leupeptin, and 50

μg/ml pepstatin A), using an ultrasonic tissue disrupter (Burkard Scientific Ltd., Uxbridge, UK). Subsequently, 100μl of sample buffer (62.5mM Tris-HCl, pH 7.4, containing 4% SDS, 10% glycerol, 10% β-mercaptoethanol and 0.002% bromophenol blue to colour the sample) was added and the samples were boiled for 3 minutes to allow denaturation of the proteins by the SDS.

Optic nerves (6-8mm long) were sonicated in 100μl homogenization buffer/protease inhibitors solution (20 mM Tris HCl, pH 7.4, containing 2 mM EDTA, 0.5 mM EGTA, 1% SDS, 0.1 mM phenylmethylsulphonyl fluoride, 50 μg/ml aprotinin, 50 μg/ml leupeptin, and 50 μg/ml pepstatin A) to which an equal volume of sample buffer (62.5 mM Tris/HCl, pH 7.4, containing 4% SDS or sodium dodecyl sulphate, 10% glycerol, 10% mercaptoethanol, and 0.002% bromophenol blue) was added and the samples were then boiled for 3 minutes to allow denaturation of the proteins by the SDS.

2) SDS/ Polyacrylamide gel electrophoresis

Electrophoresis of samples was performed using a LKB midget vertical gel slab system. Polyacrylamide (10%) separating gels (1.5mm thick) containing 0.1% [w/v] SDS in 1.5 Tris-HCl (pH 8.8) were polymerized with 0.1% [w/v] ammonium persulfate and 0.005% [v/v] N,N,N'N'-tetramethylethylenediamine (TEMED). As described by Laemmli (Laemmli 1970), samples (15ml) were loaded into a stacking gel (4% acrylamide, 0.1% SDS, 0.045% ammonium persulphate, 0.15% TEMED in 0.5M Tris-HCl, pH 6.8) above the separating gel. Proteins were separated with a current of 50mA for approximately 2 hours.

2.2.15 Immunoelectroblotting (IEB or Western Blotting)

2.2.15.1 Basic principle of immunoelectroblotting (IEB or Western Blotting)

Electroblotting is the method of transferring proteins transversely from gel to membrane as outlined by Towbin (Towbin *et al* 1979). The reason for transferring proteins to membrane from gel is to be able to reach them more easily with various probes that are typically large macromolecules, not amenable to diffusion in polyacrylamide. The most used type of probe of immobilised proteins is an antibody with specific affinity to a given antigen. Visualization of this antigen-antibody binding can be done using probes conjugated with anti-immunoglobins or those biotinylated antibodies (conjugated avidin). The immunoassay is done by incubating the membrane in a diluted antibody solution, followed by washing of the membrane, incubation with a diluted conjugated probe antibody or another detecting reagent, further washing and finally visualization using a colourimetric/ autoradiographic/ chemiluminescent technique. A summary of immunoelectroblotting is shown in figure 2.6.

2.2.15.2 Methodology of immunoelectroblotting (IBE or Western Blotting)

As described by Towbin et al (1979) proteins were blotted onto nitrocellulose paper from gels overnight at 80mA. The blots were washed for 5 minutes in Tris-buffer saline (TBS: 10mM Tris-HCl, 140mM NaCl, pH 7.4) and then for 5 minutes in TBS containing 0.1% Tween-20 (TBS-T). Primary antibodies for immunostaining were diluted in 2ml of TBS-T then incubated with the nitrocellulose blots for 3 hours at room temperature on a rollermixer. The dilutions for each antibody are detailed in Table 2.1. Unbound immunoglobulin and serum proteins were removed from the nitrocellulose with a 5 minute wash in TBS-T followed by a 5 minutes wash in high saline Tris buffer (HST: 10mM Tris-HCl, pH 7.4, containing 1 M NaCl and 0.5%

Tween-20) and a final 5 minutes wash in TBS-T. The nitrocellulose blots were then incubated for 90 minutes with the appropriate secondary antibodies conjugated to horseradish peroxidase (diluted in HST). Nitrocellulose blots were then washed in TBS-T for 15 minutes, then HST for 15 minutes, followed by a final wash in TBS-T for 15 minutes. The blots were developed with a 0.016% [w/v] solution of 3-amino-9-ethylcarbazole (AEC) in 50mM sodium acetate (pH 5.0) containing 0.05% [v/v] Tween-20 and 0.03% [v/v] H_2O_2. Colour reaction of the blots was stopped with 0.05% sodium azide solution. Digital images of the blots were captured and the band densitometry analysed using specialized software (Ultra-Violet Products Ltd., Cambridge UK).

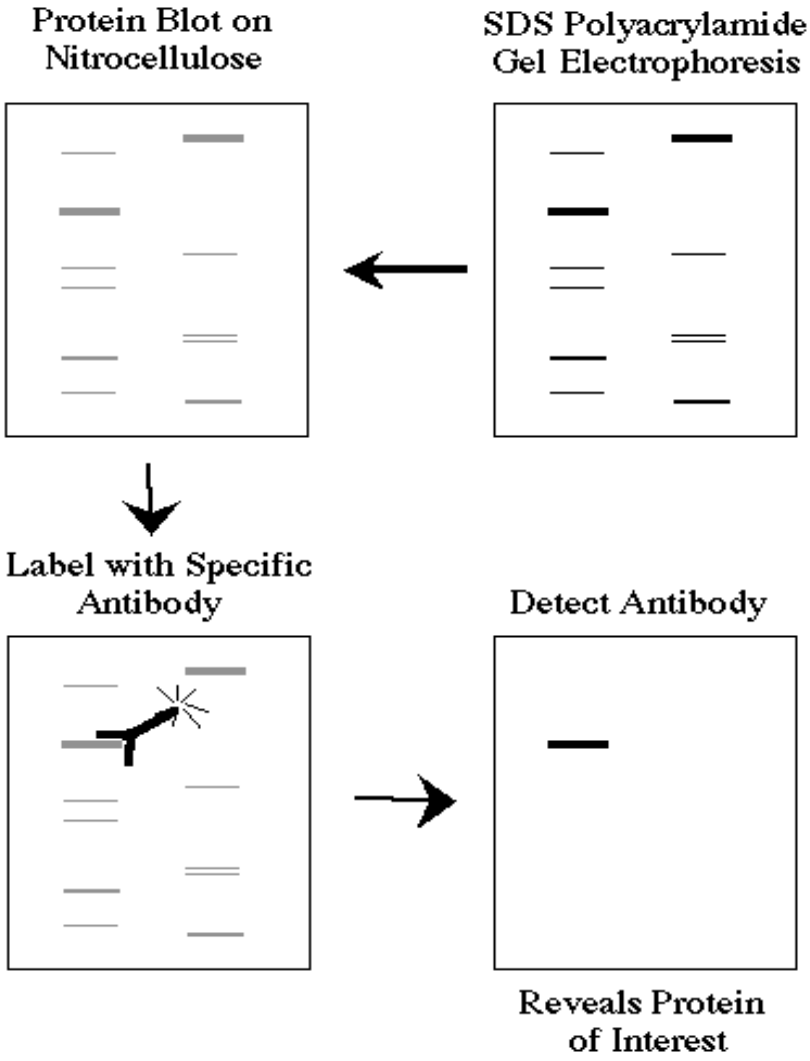


Figure 2.6. Detection of protein on a gel by western blotting.[7]

[7] Diagram taken from http://www.bio.davidson.edu/courses/genomics/method/Westernblot.html

2.3 Statistical Analysis

Student's independent t-test and one-way ANOVA were used to compare two or more independent means, respectively. All data are expressed as mean ± standard error of the mean (SEM) for the indicated number of experiments. Statistical significance was determined by Tukey HSD post-hoc tests after ANOVA using SPSS for Windows, version 16.0 (SPSS Inc, Chicago IL). Student's independent (unpaired) t-test was used to compare two independent means, such as the two left eyes of two different animals. Student's paired t-test was used to compare two correlated means, such as the left and the right eye of the same animal. For the Western Blotting data the densitometric reading of the protein of interest was measured using ImageJ software, and expressed as a percentage of the control gene product (actin), or to sample control. In all experiments a p-value of <0.05 was generally considered statistically significant.

CHAPTER 3

GENISTEIN BLUNTS THE NEGATIVE EFFECT OF ISCHAEMIA TO THE RETINA CAUSED BY AN ELEVATION OF INTRAOCULAR PRESSURE

3.1 Introduction

3.1.1 Aim

To deduce whether genistein blunts any of the effects of ischaemia to the retina.

3.1.2 Brief overview

Phytoestrogens are naturally occurring molecules in plants that can bind to oestrogen receptors and activate oestrogen receptor-mediated transcription in many cell-types (Molteni *et al* 1995, Wang *et al* 1996). Phytoestrogens are present in various dietary products, such as soya (Kurzer & Xu 1997, Zhang *et al* 2007), which contain abundant amounts of the isoflavone genistein (Zhang *et al* 2007). It is now clear that physiological doses of isoflavones can behave as phytoestrogens and mimic the well-known neuroprotective effects of oestrogens. Many examples exist which show oestrogens to have neuroprotective actions in the CNS (Arnold & Beyer 2009) but unfortunately oestrogen can also have potential deleterious side-effects which include increased risk of stroke and cancer (Wassertheil-Smoller *et al* 2003, Brass 2004). In contrast no good evidence exists to suggest that high soya diet has such detrimental side effects but instead data exists to show that it reduces stroke injury to female and male rats (Burguete *et al* 2006). Moreover, the soya isoflavone genistein blunts the damaging effects of ischaemia to the brain of mice (Trieu *et al* 1999) and rats (Liang *et al* 2008). In addition, *in vitro* studies demonstrate that genistein can protect primary neurones from glutamate toxicity (Zhao *et al* 2002, Liang *et al* 2008), thapsigargin-induced apoptosis (Linford & Dorsa 2002, Schreihofer & Redmond 2009) and β-amyloid toxicity (Yu *et al* 1998, Zeng *et al* 2004).

Ischaemia in its various guises is implicated to be a cause for retinal neurones dying in diseases such as glaucoma, diabetes, cardiac arrest and various retinal artery and

vein occlusions (Osborne *et al* 2004). It is now generally accepted that one possible way of treating such patients is to administer a substance that would reach the retina in sufficient quantities to blunt the rate of retinal neurones dying, a concept known as neuroprotection. Clearly a drug that can be taken orally on a daily basis, that has no detrimental side effects and that can reach the retina to act as a neuroprotectant in any of the aforementioned retinal diseases is the desired aim for the future. The non-toxic nature of genistein and its already described neuroprotective actions suggests that such a substance is therefore worthy of consideration for the treatment of retinal ischemic diseases.

3.1.3 Summary of results

The findings in these studies can be summarized as follows:

1) Ischaemia/reperfusion caused a significant reduction in choline acetyl-transferase (ChAT) and increase in glial fibrillary acidic protein (GFAP) immunoreactivities in the retina, and these effects are blunted by genistein.
2) Ischaemia/reperfusion caused a reduction in the mRNA levels of NF-L and Thy-1 while increasing caspase-3, caspase-8, PARP and GFAP levels in the retina. These effects are significantly attenuated by genistein with the exception of the increase in GFAP protein/mRNA and PARP mRNA levels.
3) Ischaemia/reperfusion caused a significant reduction of ganglion cell proteins in the optic nerve (NF-L and tubulin) and retina (NF-L), but these effects are attenuated by genistein.

3.2 Experimental design

The experiments were conducted in a blind, randomised design. Adult Wistar rats (200-250g) were numbered in a random manner and divided into two groups with equal numbers. The rats were firstly were anaesthetised by intramuscular injections of a combination of diazepam (2.5mg/kg) and Hypnorm (0.3ml/kg). Two sets of syringes were labelled either A or B, one containing vehicle (pure DMSO diluted in normal saline to a ratio of 1:3), and the other containing genistein solubilised in pure DMSO and diluted in normal saline (dilution ratio 1:3). Genistein (10 mg/kg) or vehicle was injected into the peritoneal cavity 1 hour before, and directly after induction of ischaemia. Ischaemia was delivered to the right eye by inserting a 30-gauge needle into the anterior chamber of the eye. The needle was connected to sterile saline reservoir placed at a pre-determined height to produce an intraocular pressure of 120mHg. Ischaemia was confirmed by the whitening of the fundus, and was maintained for 50 minutes. The contralateral left eye remained untouched and served as control. Throughout the whole process, normal body temperature was controlled and maintained. Immediately following ischaemia, another bolus of genistein (10mg/kg) or vehicle was injected into the peritoneal cavity. Retinas and optic nerves were harvested 7 days following reperfusion.

Retinal sections were fixed and stained for ChAT and GFAP immunoreactivities. Protein and mRNA samples extracted from the retina and optic nerves were analysed using electrophoresis and conventional PCR.

3.3 Results

3.3.1 Immunohistochemistry

Rat retinas subjected to 50 minutes of ischaemia followed by 7 days of reperfusion, were processed and stained for certain cell markers using immunohistochemistry. Changes in retinal ChAT and GFAP immunoreactivities caused by ischaemia/reperfusion were blunted by genistein treatment.

In control retinas ChAT was located to two tramlines of immunoreactivity in the inner plexiform layer and cell bodies (amacrine cells) on either side of the tram-lines (figure 3.1A) while GFAP-immunoreactivity was mostly associated with astrocytes and Müller cell end feet in the nerve fibre layer (figure 3.1D). Elevated intraocular pressure-induced ischaemia for 50min (120mm Hg) where vehicle was injected into the peritoneal cavity resulted in an almost complete loss of ChAT-immunoreactivity and a strong staining for GFAP immunoreactivity in Müller cells through out the retina (figures 3.1B and 3.1E) after 7 days. However, in retinas from eyes given ischaemia/reperfusion and where genistein was injected intraperitoneally, ChAT immunoreactivity was clearly partially preserved (figure 3.1C) and the amount of GFAP associated with Müller cells much reduced (figure 3.1F).

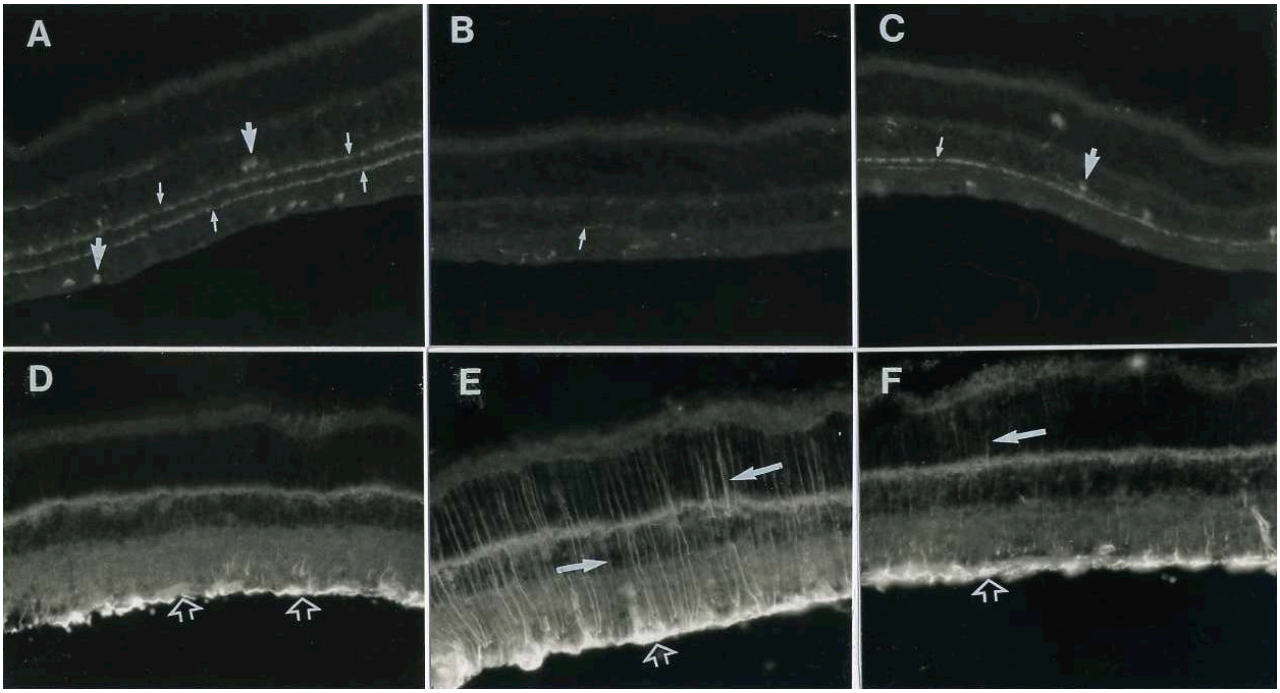


Figure 3.1. Retinal sections of similar eccentricities were compared for the localization of ChAT (figures 3.1A-C) and GFAP (figures 3.1D-F) in untouched retinas (figures 3.1A and D), retina given ischaemia from vehicle-treated rats (figures 3.1B and E) and retinas given ischaemia from genistein-treated rats (figures 3.1C and F). This figure summarises information obtained from the analysis of retinas from six rats where one eye in each case was given ischaemia and injected intraperitoneally either with vehicle or genistein. In control retinas ChAT immunoreactivity (figure 3.1A) appears as two lines in the inner plexiform layer (small arrows) and cell bodies on either side (arrow heads) while GFAP immunoreactivity (figure 3.1D) is primarily located to astrocytes and Müller cell end-feet (open arrows). Ischaemia/reperfusion causes almost a complete loss of ChAT immunoreactivity (figure 3.1B) while GFAP staining (figure 3.1E) is now clearly associated also with Müller cells spanning the whole of the retina (large arrows). Genistein clearly blunts the effect of ischaemia/reperfusion where staining for ChAT immunoreactivty is partially restored (figure 3.1C) and the intensity of GFAP immunoreactivity much reduced in the Müller cells (figure 3.1F).

3.3.2 Western blot data

Protein electrophoresis was carried out using Western blotting as described in section 2.2.11. In order to limit errors, the same nitrocellulose membrane was used to compare the level of actin with a defined protein. This was achieved by reference to pre-coloured molecular marker proteins which allowed for the membrane be cut into two pieces to allow for actin (42kDa) and any of a number of proteins [NF-L (70kDa), GFAP (53kDa), tubulin (50 kDa), caspase-3 (32 kDa) or PARP (116 kDa)] to be stained separately.

Ischaemia followed by seven days of reperfusion affected selected retinal and optic nerve proteins (figures 3.2-3.6). Ischaemia/reperfusion statistically decreased the protein level of NF-L but increased the level of PARP and GFAP proteins in the retina (figure 3.2-3.4). These effects of ischaemia /reperfusion on the protein levels of NF-L, PARP and GFAP are all altered when genistein instead of vehicle was injected into the peritoneal cavity one hour before and immediately after ischaemia but this was only significant for NF-L (figure 3.2). NF-L and tubulin proteins in the optic are also decreased by 53% and 42%, respectively after ischaemia/reperfusion (figures 3.5 and 3.6). The decrease in optic nerve NF-L and tubulin proteins caused by ischaemia/reperfusion are significantly nullified in rats treated with genistein (figures 3.5 and 3.6).

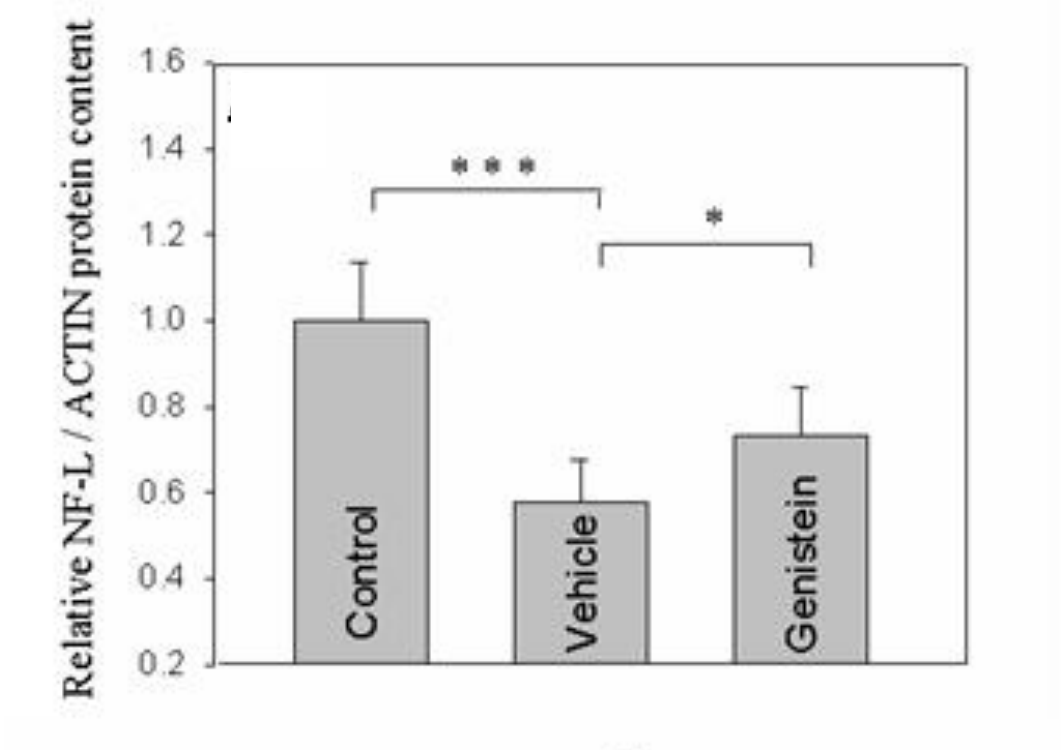


Figure 3.2. The retinal protein levels of NF-L (normalised to actin) in eyes following ischaemia/reperfusion with vehicle treatment (vehicle) or genistein was compared with the retinas of eyes which had not received any ischaemia (control). A significant (***$p<0.001$) reduction of NF-L level was found in retinas following ischaemia/reperfusion in rats receiving vehicle treatment. Treatment with genistein significantly (*$p<0.05$) blunted the changes seen in NF-L. Data are shown as means where error bars indicating ± SEM, where n=16, divided into 2 groups of 8 rats, each receiving either vehicle or genistein intraperitoneal injections.

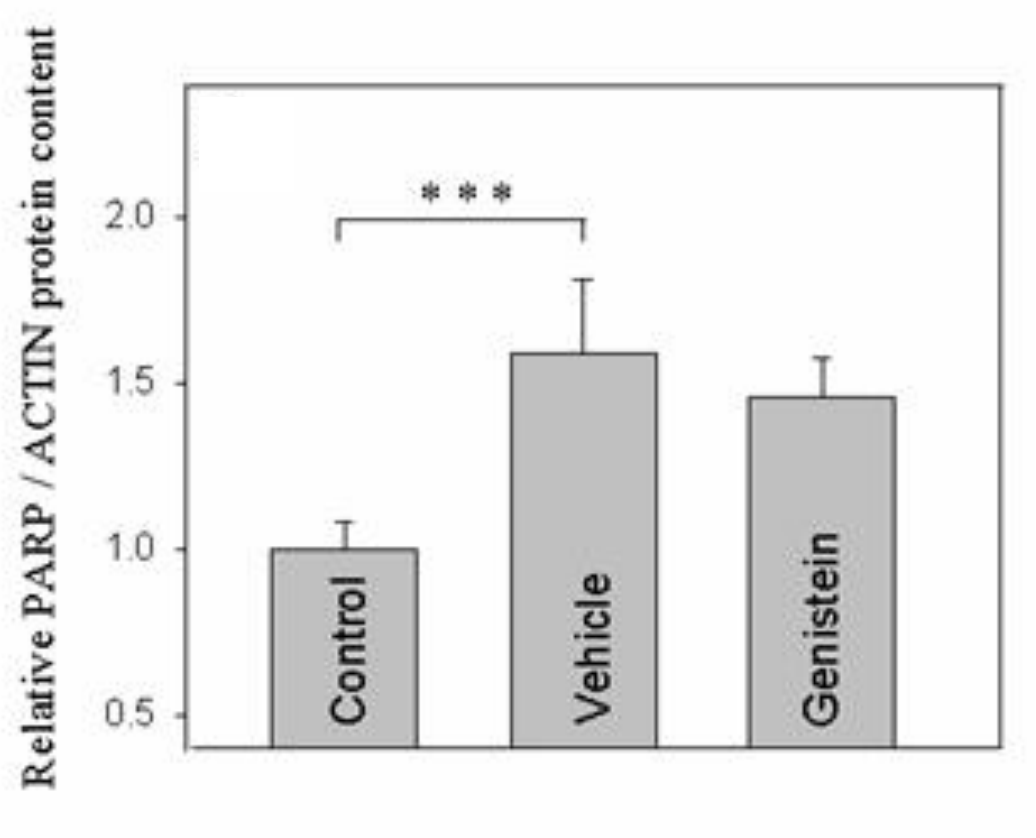


Figure 3.3. The retinal protein levels of PARP (normalised to actin) in eyes following ischaemia/reperfusion with vehicle treatment (vehicle) or genistein was compared with the retinas of eyes which had not received any ischaemia (control). A significant (***$p<0.001$) reduction of PARP level was found in retinas following ischaemia/reperfusion in rats receiving vehicle treatment. These changes were blunted in genistein-treated rats however the difference was not statistically significant. Data are shown as means where error bars indicating ± SEM where n=16, divided into 2 groups of 8 rats, each receiving either vehicle or genistein intraperitoneal injections.

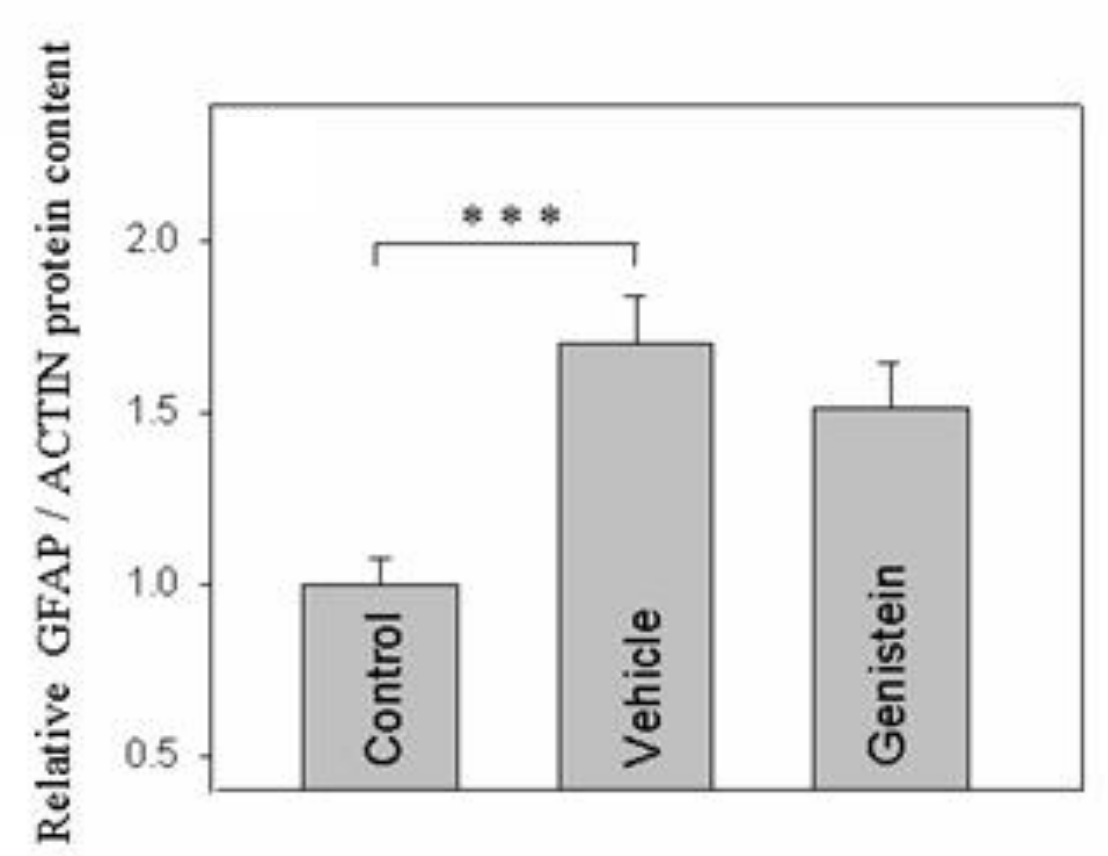


Figure 3.4. The retinal protein levels of GFAP (normalised to actin) in eyes following ischaemia/reperfusion with vehicle treatment (vehicle) or genistein was compared with the retinas of eyes which had not received any ischaemia (control). A significant (***$p<0.001$) increase of GFAP level was found in retinas following ischaemia/reperfusion in rats receiving vehicle treatment. These changes were blunted in genistein-treated rats however the difference was not statistically significant. Data are shown as means where error bars indicating ± SEM where n=16, divided into 2 groups of 8 rats, each receiving either vehicle or genistein intraperitoneal injections.

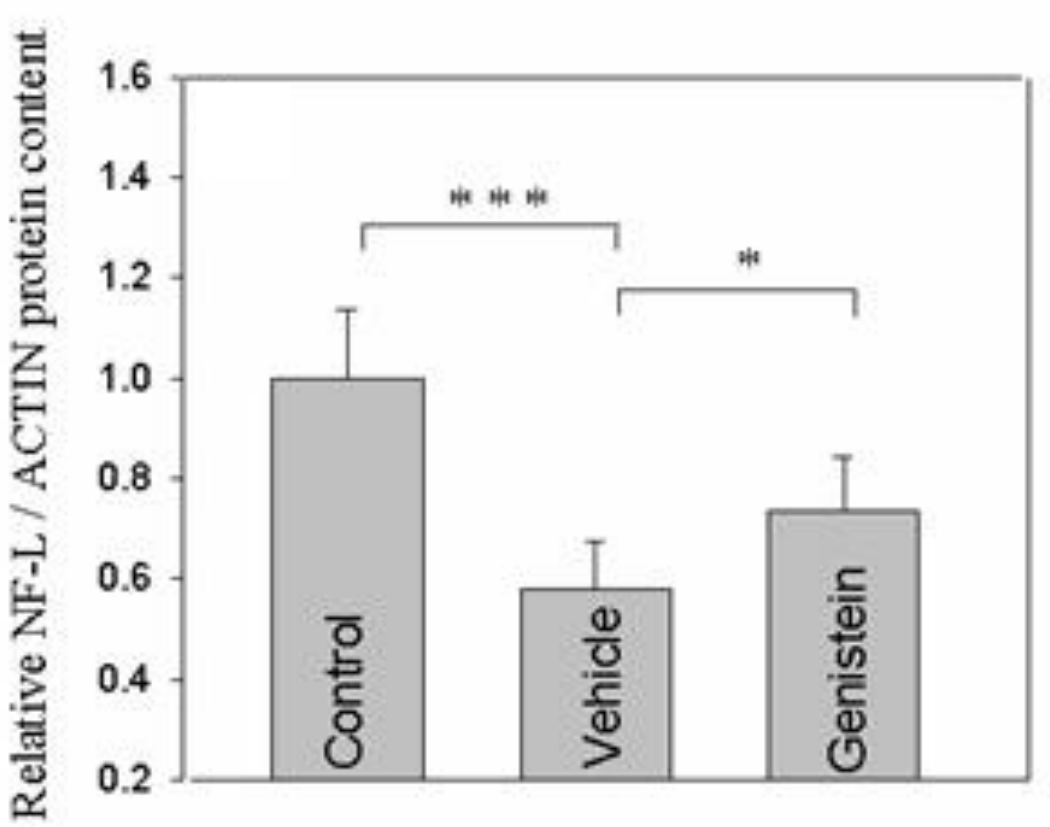


Figure 3.5. The optic nerve protein levels of NF-L (normalised to actin) in eyes following ischaemia/reperfusion with vehicle treatment (vehicle) or genistein was compared with the retinas of eyes which had not received any ischaemia (control). A significant (***$p<0.001$) reduction of NF-L level was found in retinas following ischaemia/reperfusion in rats receiving vehicle treatment. Treatment with genistein significantly (*$p<0.05$) blunted the changes seen in NF-L. Data are shown as means where error bars indicating ± SEM where n=16, divided into 2 groups of 8 rats, each receiving either vehicle or genistein intraperitoneal injections.

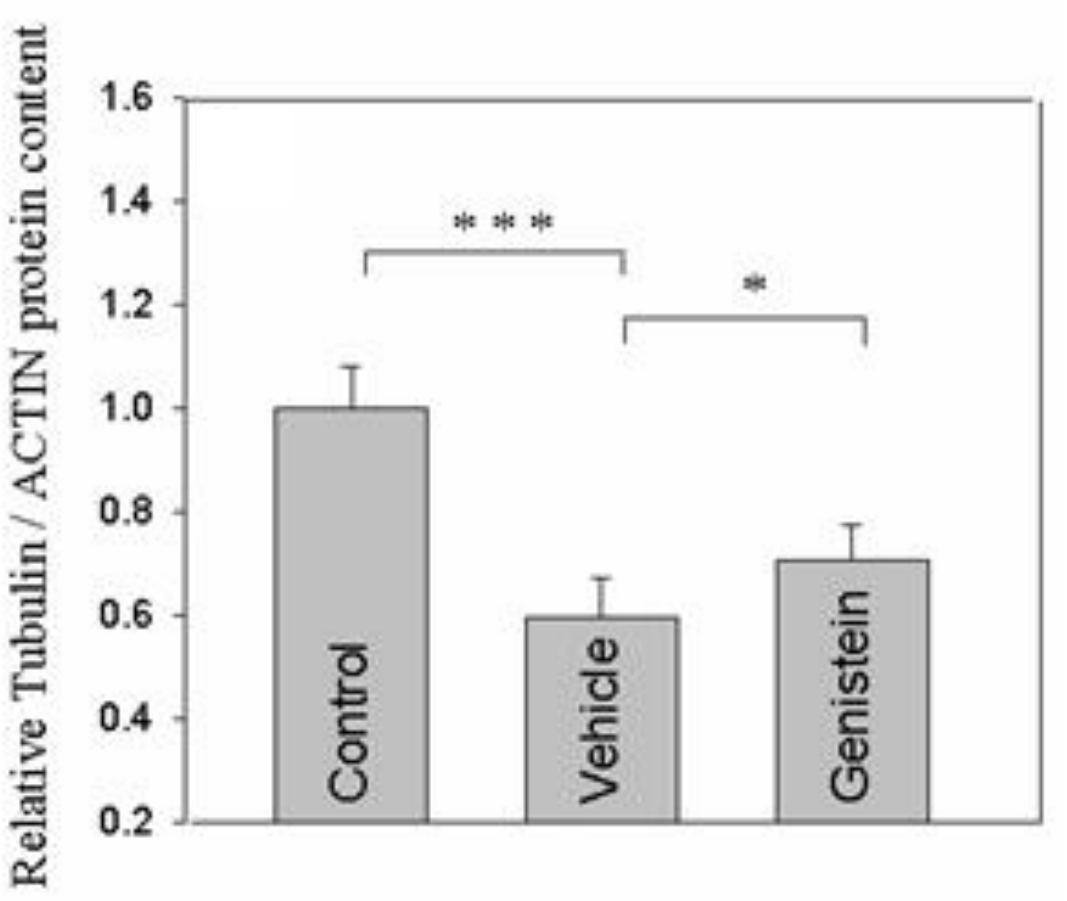


Figure 3.6. The optic nerve protein levels of tubulin (normalised to actin) in eyes following ischaemia/reperfusion with vehicle treatment (vehicle) or genistein was compared with the retinas of eyes which had not received any ischaemia (control). A significant (***$p<0.001$) reduction of tubulin level was found in retinas following ischaemia/reperfusion in rats receiving vehicle treatment. Treatment with genistein significantly (*$p<0.05$) blunted the changes seen in tubulin. Data are shown as means where error bars indicating ± SEM where n=16, divided into 2 groups of 8 rats, each receiving either vehicle or genistein intraperitoneal injections.

3.3.3 PCR data

Ischaemia/reperfusion also caused changes in the content of selected mRNAs. mRNA levels (normalized to cyclophilin) of NF-L and Thy-1, in vehicle-treated rat retinas were significantly reduced (figures 3.7 and 3.8). In contrast, the mRNA levels of caspase-3, caspase-8, PARP and GFAP were clearly elevated (figures 3.9-3.11). Importantly, when genistein rather than vehicle was injected intraperitoneally following ischaemia, the reductions of retinal mRNA NF-L, Thy-1 (figures 3.7 and 3.8) and increases of caspase-8 and caspase-3 (figures 3.9 and 3.10) were significantly blunted. Genistein treatment did not however affect the increased mRNA levels of GFAP and PARP mRNAs (figures 3.11 and 3.12).

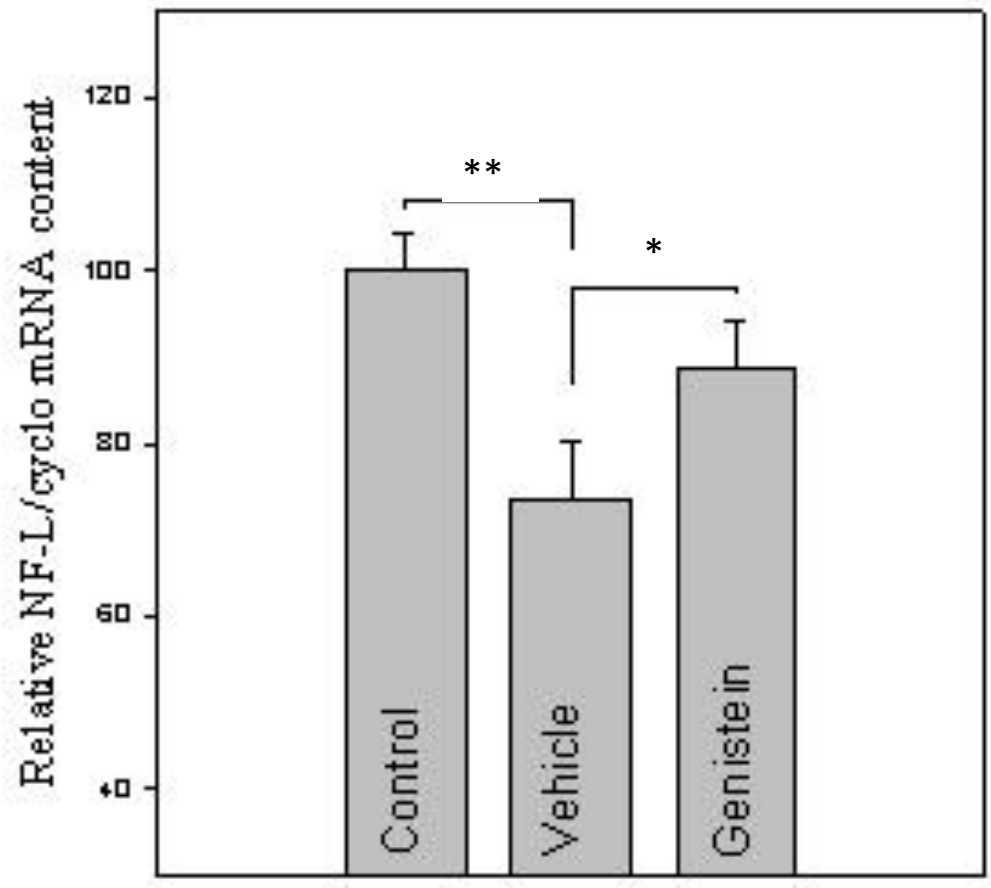


Figure 3.7. The retinal mRNA levels of NF-L (normalised to cyclophilin, cyclo) in eyes that were given following ischaemia/reperfusion with vehicle treatment (vehicle) or genistein was compared with the retinas of eyes which had not received any ischaemia (control). A significant (**$p<0.01$) reduction of NF-L level was found in retinas following ischaemia/reperfusion in rats receiving vehicle treatment. Treatment with genistein significantly (*$p<0.05$) blunted the changes seen in NF-L. Data are shown as means where error bars indicating ± SEM where n=16, divided into 2 groups of 8 rats, each receiving either vehicle or genistein intraperitoneal injections.

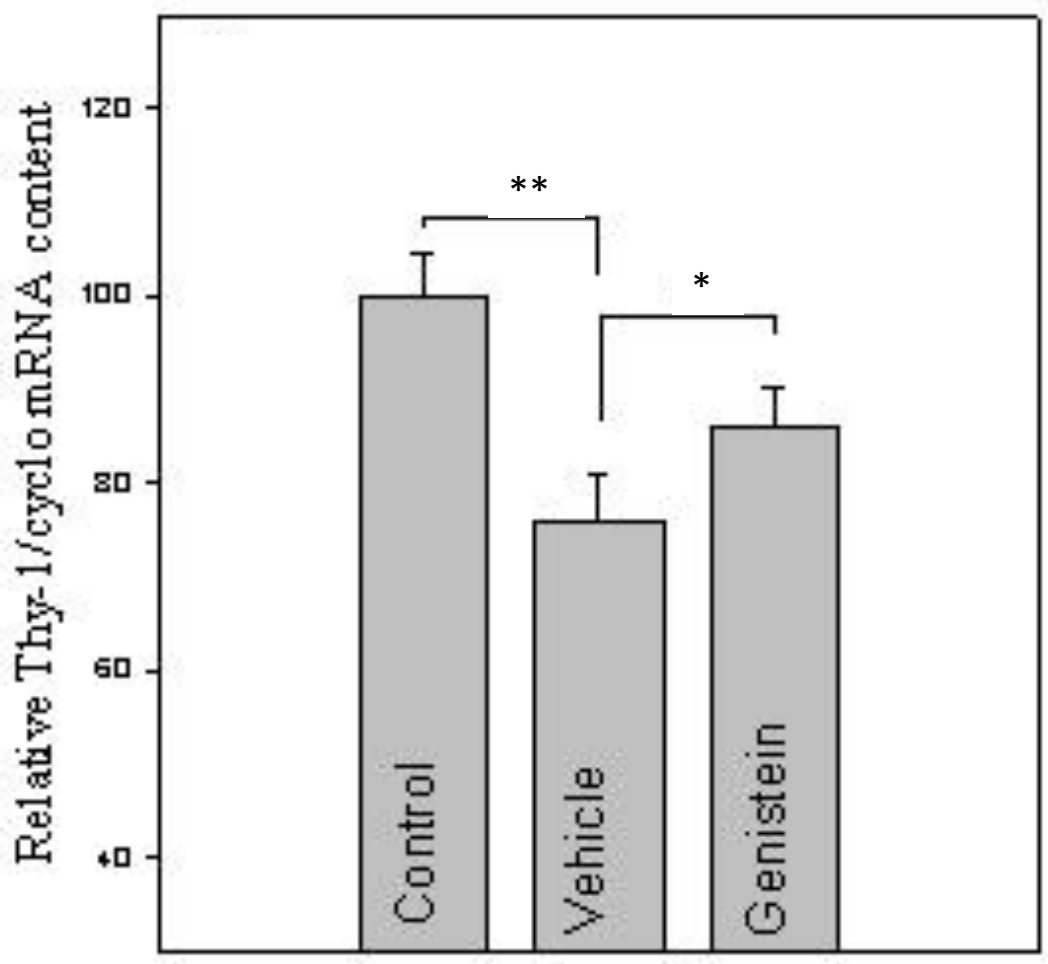


Figure 3.8. The retinal mRNA levels of Thy-1 (normalised to cyclophilin, cyclo) in eyes that were given following ischaemia/reperfusion with vehicle treatment (vehicle) or genistein was compared with the retinas of eyes which had not received any ischaemia (control). A significant (**$p<0.01$) reduction of Thy-1 level was found in retinas following ischaemia/reperfusion in rats receiving vehicle treatment. Treatment with genistein significantly (*$p<0.05$) blunted the changes seen in Thy-1. Data are shown as means where error bars indicating ± SEM where n=16, divided into 2 groups of 8 rats, each receiving either vehicle or genistein intraperitoneal injections.

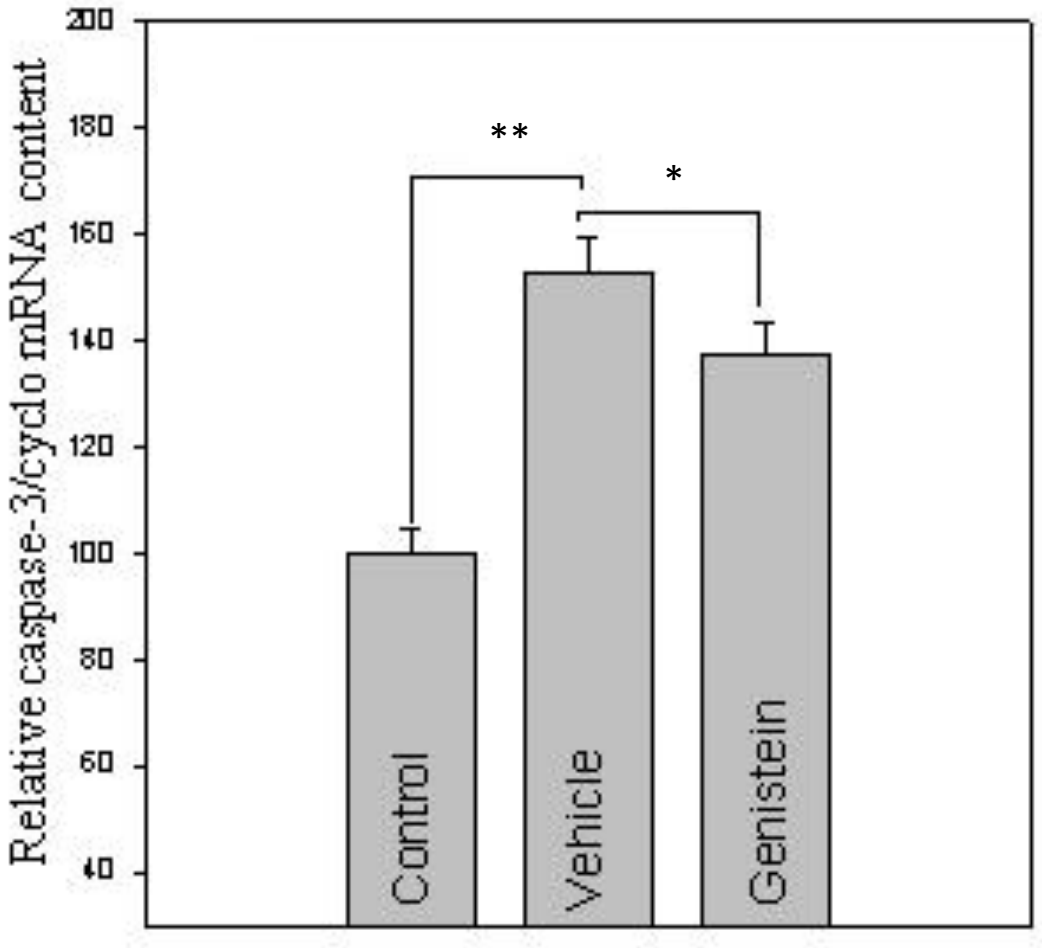


Figure 3.9. The retinal mRNA levels of caspase-3 (normalised to cyclophilin, cyclo) in eyes that were given following ischaemia/reperfusion with vehicle treatment (vehicle) or genistein was compared with the retinas of eyes which had not received any ischaemia (control). A significant (**$p<0.01$) increase of caspase-3 level was found in retinas following ischaemia/reperfusion in rats receiving vehicle treatment. Treatment with genistein significantly (*$p<0.05$) blunted the changes seen in caspase-3. Data are shown as means where error bars indicating ± SEM where n=16, divided into 2 groups of 8 rats, each receiving either vehicle or genistein intraperitoneal injections.

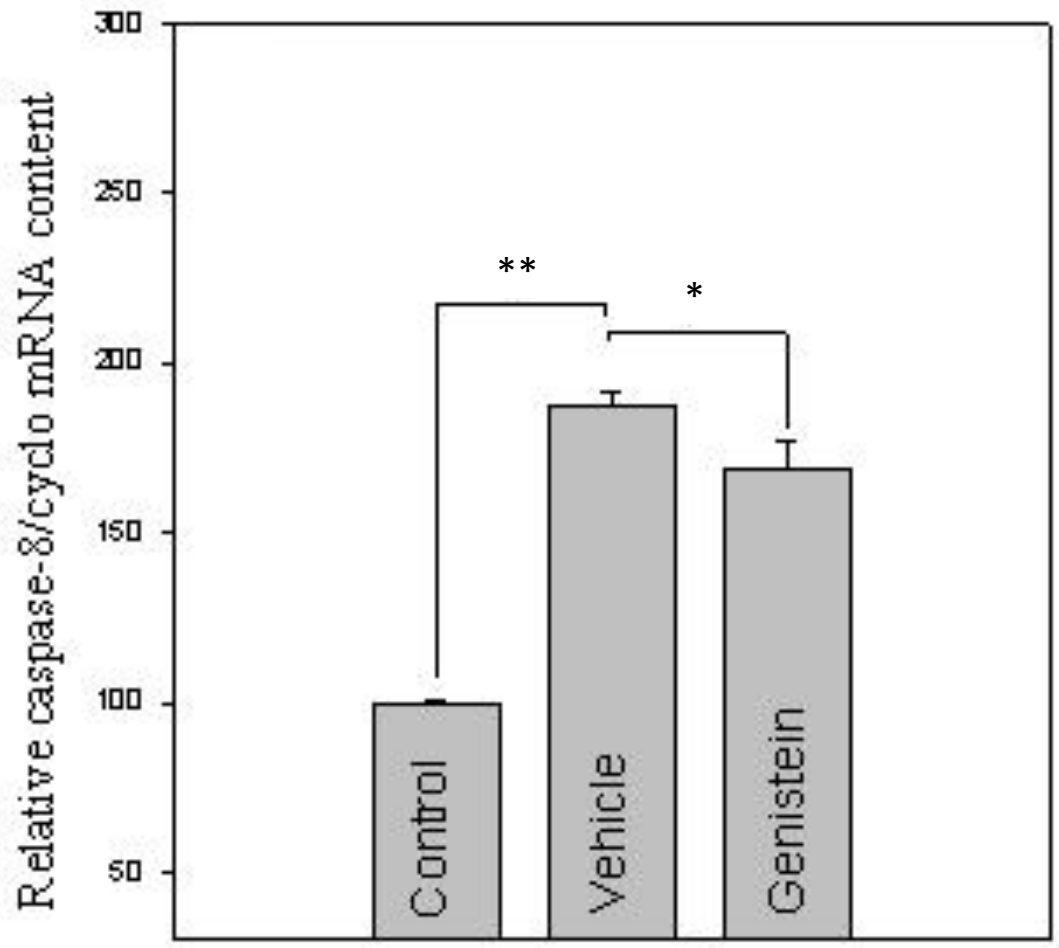


Figure 3.10. The retinal mRNA levels of caspase-8 (normalised to cyclophilin, cyclo) in eyes that were given following ischaemia/reperfusion with vehicle treatment (vehicle) or genistein was compared with the retinas of eyes which had not received any ischaemia (control). A significant (**$p<0.01$) increase of caspase-8 level was found in retinas following ischaemia/reperfusion in rats receiving vehicle treatment. Treatment with genistein significantly (*$p<0.05$) blunted the changes seen in caspase-8. Data are shown as means where error bars indicating ± SEM where n=16, divided into 2 groups of 8 rats, each receiving either vehicle or genistein intraperitoneal injections.

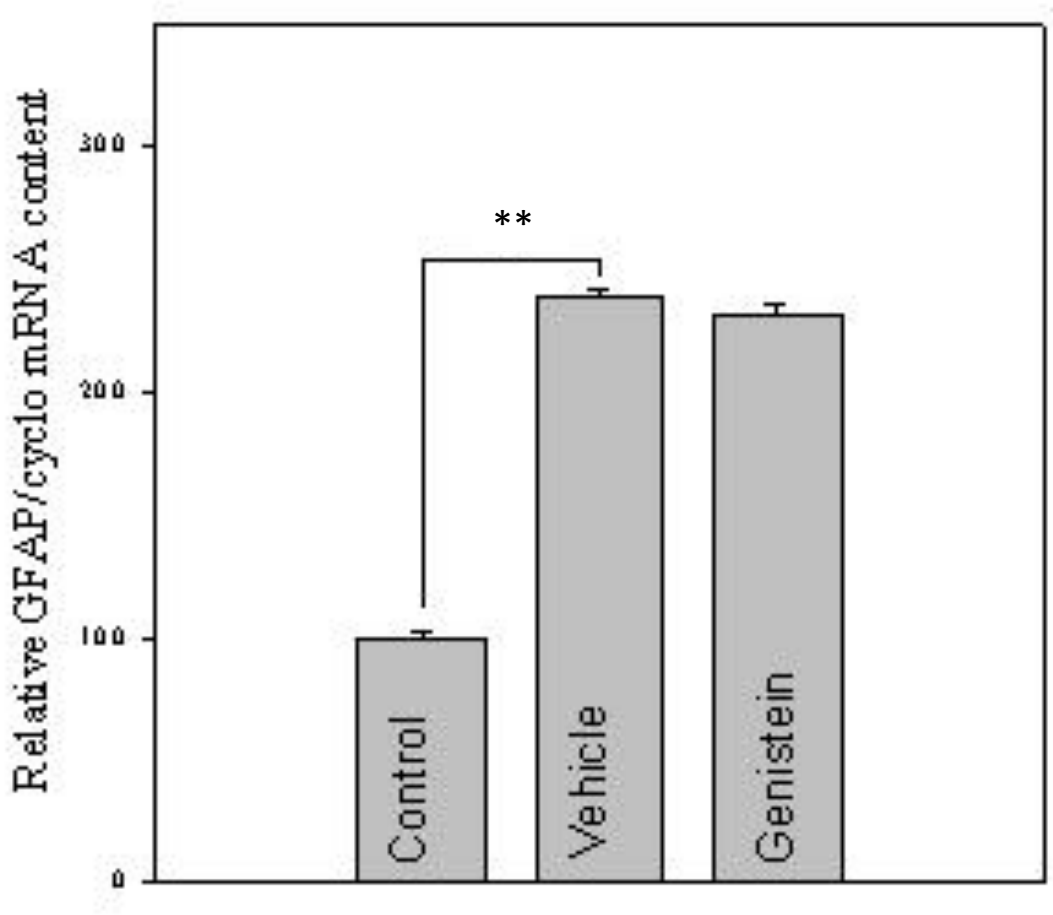


Figure 3.11. The retinal mRNA levels of GFAP (normalised to cyclophilin, cyclo) in eyes that were given following ischaemia/reperfusion with vehicle treatment (vehicle) or genistein was compared with the retinas of eyes which had not received any ischaemia (control). A significant (**$p<0.01$) increase of GFAP level was found in retinas following ischaemia/reperfusion in rats receiving vehicle treatment. These changes were not significantly blunted by treatment with genistein. Data are shown as means where error bars indicating ± SEM where n=16, divided into 2 groups of 8 rats, each receiving either vehicle or genistein intraperitoneal injections.

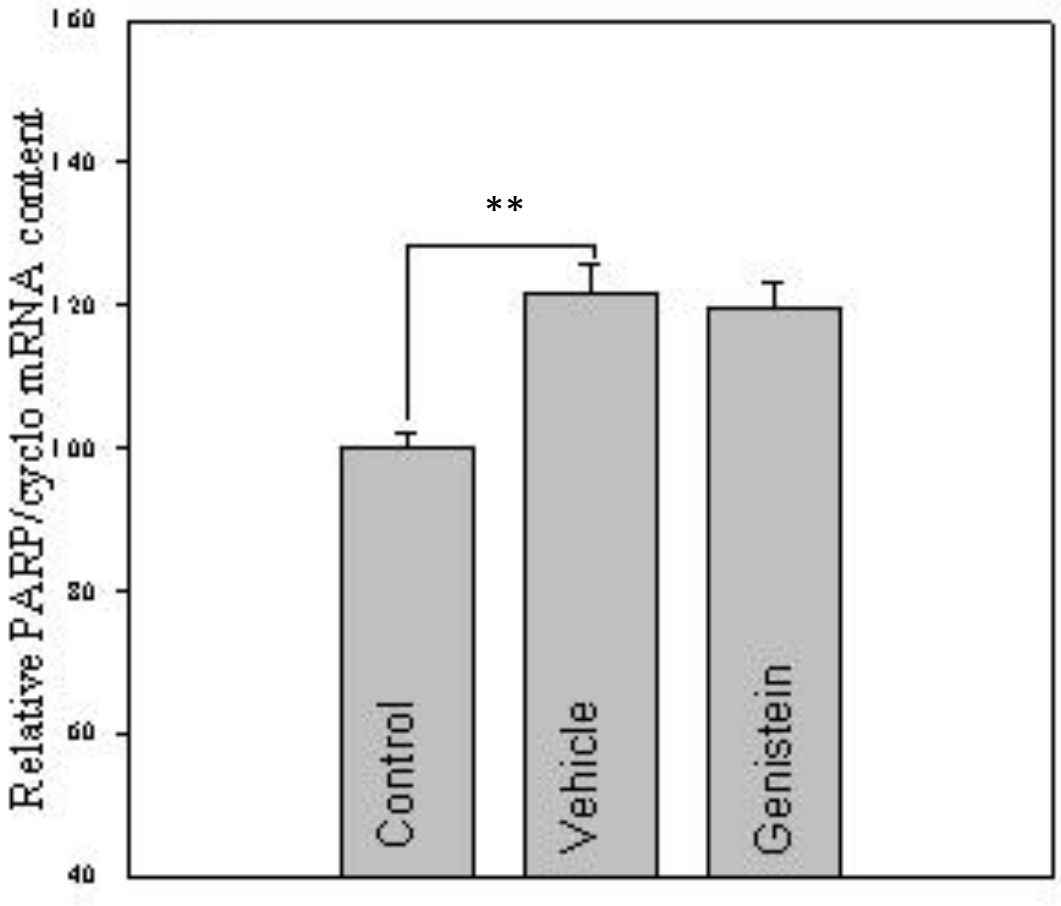


Figure 3.12. The retinal mRNA levels of PARP (normalised to cyclophilin, cyclo) in eyes that were given following ischaemia/reperfusion with vehicle treatment (vehicle) or genistein was compared with the retinas of eyes which had not received any ischaemia (control). A significant (**$p<0.01$) increase of PARP level was found in retinas following ischaemia/reperfusion in rats receiving vehicle treatment. These changes were not significantly blunted by treatment with genistein. Data are shown as means where error bars indicating ± SEM where n=16, divided into 2 groups of 8 rats, each receiving either vehicle or genistein intraperitoneal injections.

3.4 Discussion

The results of the present study show that intraperitoneal injection of genistein just before and after ischaemia counteracts this effect on the insult. These results are therefore consistent with the report by Hayashi et al (Hayashi *et al* 1997) where genistein was also injected intraperitoneally but the effects of ischaemia/reperfusion was based primarily on histological changes associated with the retina. Studies on brain tissues by Trieu et al (1999) and Liang et al (Liang *et al* 2008) have also shown that genistein is able to counteract ischemic insults. It is also known that a diet high in soya, where genistein is a major component, provides neuroprotection from focal cerebral ischaemia insult to rats (Schreihofer *et al* 2005, Burguete *et al* 2006). All these data therefore support the notion that oral administration of genistein not only reaches the retina but can also attenuate negative insults to the human retina induced by ischaemia.

The present study provides both immunohistochemical and molecular biological data to show that genistein blunts an insult of ischaemia/reperfusion to the retina *in situ.* In addition to the study by Hayashi et al (Hayashi *et al* 1997) where only histology was used to demonstrate neuroprotection. In the animal model used in the present study and also by Hayashi et al (Hayashi *et al* 1997), the inner retina is particularly affected by ischaemia/reperfusion (Osborne *et al* 2004). The resultant histological changes in the retina are difficult to quantify between retinas unless retinal sections of identical eccentricity are analysed. In practice it is impossible to compare sections of identical eccentricity in different retinas but by analysing a number of sections it is possible to obtain meaningful data as shown by Hayashi et al (Hayashi *et al* 1997). However, combining histology with other procedures provides a more reliable and quantitative method for demonstrating neuroprotection. For example, as shown in the present

study, following ischaemia an almost complete loss of ChAT (located to a subset of amacrine cells) and increase in GFAP (located primarily to Müller cells) immunoreactivities occurs in all retinal eccentricities and that this is clearly counteracted by treatment with genistein (see figure 3.1). It is well known that Müller cells are activated by ischaemia/reperfusion and that their GFAP content is significantly up-regulated (Bringmann *et al* 2006) as is shown in this study. However, the reduction of retinal GFAP protein and mRNA contents caused by treatment with genistein following ischaemia/reperfusion was insignificant. We suggest that increase in GFAP protein and mRNA caused by ischaemia/reperfusion was too great to be significantly reduced by genistein rather than genistein having no influence.

Evidence that the outer as well as the inner retina is affected by ischaemia/reperfusion is shown by immunohistochemical, Western blot and conventional PCR data. NF-L and Thy-1 are known to be located in the ganglion cells (Nash & Osborne 1999, Ruiz-Ederra *et al* 2004, Chidlow *et al* 2005), and are used to obtain information on ganglion cell death (Nash & Osborne 1999, Chidlow *et al* 2005). The degree of ganglion cell death after ischaemia/reperfusion was measured by relating the protein (NF-L) and mRNA (Thy-1 and NF-L) levels of ganglion cell specific markers with total retinal actin protein and cyclophilin mRNA levels, respectively. The results show that ischaemia/reperfusion causes a drastic effect on ganglion cells resulting in a large decrease in NF-L mRNA/protein, tubulin protein and Thy-1 mRNA levels. These effects are significantly blunted by intraperitoneal injection of genistein.

NF-L and tubulin proteins are present in ganglion cells and analysis of their levels in the optic nerve provides a measure of ganglion cell viability (Ji *et al* 2008, Zhang *et al* 2008). Ischaemia/reperfusion clearly reduces the levels of tubulin and NF-L proteins in the optic nerve, as well as NF-L in the retina, which are significantly blunted by

genistein. Thus ischaemia/reperfusion causes both a reduction in retinal mRNA/proteins and optic nerve proteins associated with ganglion cells and this is nullified by intraperitoneal injection of genistein.

Various studies have shown that an insult of ischaemia/reperfusion to the retina causes cells to die by apoptosis (Katai & Yoshimura 1999, Osborne *et al* 2004). Evidence for this to be the case in the present study is demonstrated by the observation that caspase-8 mRNA, caspase-3 mRNA and PARP mRNA/protein are up-regulated in the retina following ischaemia/reperfusion. In apoptosis, caspase-8, caspase-3 and PARP mRNAs are known to be up-regulated (Grutter 2000, Kroemer & Reed 2000, Dawson & Dawson 2004, Hong *et al* 2004). That genistein significantly attenuates the up-regulation of caspase-3 and caspase-8 mRNAs, caused by ischaemia/reperfusion provides further evidence for its neuroprotective action. However, it is difficult to explain why genistein did not significantly reduce the up-regulation of PARP mRNA/protein caused by ischaemia/reperfusion. One possible explanation is that ischaemia/reperfusion caused too great an elevation of PARP protein/mRNA, as in the case of GFAP, and that the positive influence of genistein was partial and not of statistical significance.

While the present study provides "proof of principle" that genistein attenuates the negative insults of ischaemia it is clearly necessary in future studies to show that daily oral intake of physiological levels of genistein functions in the same way. Moreover, it is desirable to understand the neuroprotective mode of action of genistein in the blunting of an ischemic insult to the retina. In the study by Hayashi et al (Hayashi *et al* 1997) it was shown that genistein inhibits tyrosine phosphorylation in the retina following ischaemia. This supports the view that one major action of genistein is to act as a tyrosine kinase inhibitor (Akiyama *et al* 1987) and that this mode of action

plays a role in the neuroprotective benefit of the substance. However, genistein is also known to be a full agonist of both oestrogen receptors, α and β, in a variety of cell culture receptor reported-gene and proliferation assays (Gutendorf & Westendorf 2001, Maggiolini *et al* 2001). Oestrogen has also been found to attenuate hydrogen peroxide-induced apoptosis to retinal cells in culture (Yu *et al* 2004). Thus one other possible mode of action for genistein attenuating retinal ischaemia is through the stimulation of oestrogen receptors. Another possibility is that the isoflavone characteristics of genistein result in it binding to an aryl hydrocarbon receptor to act as an agonist or antagonist (Moon *et al* 2006) to cause neuroprotection. It is known that genistein can stimulate an anti-apoptotic pathway in mouse neuronal cultures via interaction with an aryl hydrocarbon receptor (Kajta *et al* 2007). It remains, however, to be established whether the retina possesses aryl hydrocarbon receptors.

In conclusion, intraperitoneal injection of genistein protects neurones in the retina from transient ischaemia/reperfusion injury. However, further studies are required to elucidate the precise mode(s) of action by which this occurs and to establish whether physiological oral consumption of genistein is able to blunt ischemic insults to the retina as may occur in glaucoma.

CHAPTER 4

INFLUENCE OF SELECTED FLAVONOIDS ON THE SURVIVAL, OF RGC-5 CELLS SUBJECTED TO DIFFERENT TYPES OF OXIDATIVE STRESS

4.1 Introduction

4.1.1 Aim

The aim of the studies described in this chapter were: **A]** to investigate the influence of selected flavonoids on the survival of RGC-5 cells exposed to defined insults **B]** to identify the cell death mechanism caused by specific insults, and **C]** to determine any direct biochemical effects of the flavonoids on RGC-5 cells.

4.1.2 Brief overview

Flavonoids are comprised of a large group of polyphenolic substances which are present in a variety of plant-based foods such as tea, vegetables, fruits and legumes such as soybeans. There are about 5000 types of flavonoids, which are subdivided into flavonols, flavonones, flavones, isoflavonoids, flavans-3-ols and anthocyanidins (Neuhouser 2004). Flavonoids can be consumed in large amounts on a daily basis without any harmful effects, and have been associated with many beneficial health effects. These include anti-oxidant (Bors *et al* 1994, Heijnen *et al* 2001), neuroprotective (McDowell *et al* 2011, Hwang *et al* 2012), anti-inflammatory (Garcia-Lafuente *et al* 2009), cardioprotective (Rimbach *et al* 2008) and anti-cancer (Hsu & Liou 2011, Polier *et al* 2011) properties.

Green tea is an example of a flavonoid-rich food that may be consumed in large quantities without apparent harmful effects. The main tea flavonoids are commonly referred to as catechins and are (-)-epigallocatechin gallate (EGCG), (-)-epigallocatechin (EGC), (-)-epicatechin gallate (EC) and (-)-epicatechin (Ho *et al* 1992). The antioxidant potentials of green tea catechins in descending order, are as follows: EC≈EGCG > EGC > gallic acid > epicatechin (Rice-Evans *et al* 1996).

EGCG is the most abundant catechin in green tea, and have been found to have neuroprotective (Reznichenko *et al* 2005, Koh *et al* 2006, Hou *et al* 2008), antioxidant (Nakagawa & Yokozawa 2002, Raza & John 2007), anti-apoptosis (Cao *et al* 2012) and anti-cancer (Hsu & Liou 2011, Zhang *et al* 2012) influences. In addition, EGCG has been reported to increase retinal ganglion cell survival both *in vivo* (Zhang & Osborne 2006, Zhang *et al* 2007, Zhang *et al* 2008) and *in vitro* (Zhang *et al* 2007) using the RGC-5 cell line. Another green tea flavonoid, EC, has also been shown to play a role as a free radical scavenger and increases superoxide dismutase and catalase (Li *et al* 2007). Although EC has been shown to protect rat hippocampal cells from Aβ toxicity (Bastianetto *et al* 2006) and phaeochromocytoma PC12 cells from several defined insults (Nie *et al* 2002, Chen *et al* 2003), its neuroprotective effect on retinal ganglion cells have not been investigated. Therefore, one of the aims of this study was to analyze the influence of EC on RGC-5 cells when exposed to certain insults that might occur in glaucoma.

Much like EGCG, genistein has been demonstrated to possess neuroprotective attributes (Ho *et al* 2003, Li & Zhang 2003, Kajta *et al* 2007, McDowell *et al* 2011). In chapter 3, it is shown that genistein was able to protect rat retinal ganglion cells *in vivo* from cell death caused by ischaemia-reperfusion injury from elevated high intraocular pressures. In glaucoma a type of ischemia may also occur even when the intraocular pressure appears to be normal. . Currently the treatment of glaucoma is aimed at reducing intraocular pressures when it occurs, however it has been shown that the disease still progresses (Nakazawa *et al* 2012). This implies that other secondary contributory factors contribute in different ways in the pathogenesis of glaucoma. These include inappropriate neurotrophic factor support, oxidative stress,

inflammation and glutamate toxicity (Osborne *et al* 2001, Flammer *et al* 2002, Osborne *et al* 2006). Therefore, in this chapter, the effects of genistein on a transformed retinal ganglion cells (RGC-5 cells) (Krishnamoorthy *et al* 2001) exposed to secondary insults that may occur in glaucoma were explored.

Oxidative stress occurs when the production of reactive oxygen species (ROS) exceeds the rate of ROS removal by endogenous antioxidant enzyme activity (e.g. catalase, glutathione and superoxide dismutase). This results in ROS levels to increase over physiological values, which disrupts normal cellular homeostasis leading to cellular dysfunction and ultimately cell death. Examples of ROS are superoxide anion, hydrogen peroxide, hydroxyl radical, nitric oxide, peroxyl radical and singlet oxygen (Osborne *et al* 2008). Strong evidence suggests that oxidative stress has a major influence in the pathogenesis of glaucoma or glaucomatous optic neuropathy (Izzotti *et al* 2006, Tezel 2006, Sacca *et al* 2007, Osborne *et al* 2008). Glaucomatous human trabecular meshwork, which is the target tissue of glaucoma in the anterior chamber, was found to have higher levels of endogenous ROS (He *et al* 2008). Studies by Chang et al (2011), Gherghel et al (2005) and Yildirim et al (2005) reported a systemic increase in malondialdehyde (MDA) and a decrease in glutathione in the plasma of subjects with glaucoma (Ohkawa *et al* 1979, Gherghel *et al* 2005, Chang *et al* 2011). Malondialdehyde is a by-product of lipid peroxidation (Ohkawa *et al* 1979) and has been used as a biomarker of oxidative stress (Wisniewska-Knypl & Wronska-Nofer 1994, Nielsen *et al* 1997). This implies that in glaucoma, the increased levels of ROS by-products (such as MDA) are related to a reduction in endogenous anti-oxidant capacity (Gherghel *et al* 2005, Yildirim *et al* 2005).

Presently, the mainstay of glaucoma treatment is aimed at lowering intraocular pressure with medications or surgical procedures. However despite having normalised intraocular pressures, as high as 40% of patients with glaucoma continue to have progressive visual field loss (Werner & Drance 1977, Werner *et al* 1977, Cockburn 1983, Kidd & O'Connor 1985, Heijl 1989). Evidently, alternative pharmacological compounds are required for the treatment of glaucoma. Any substance that has neuroprotective effects that include it being an antioxidant, able to cross the blood-retinal barrier to reach the retina and can be taken regularly without significant adverse effects would appear to fulfil such a role. Certain flavonoids may well be suitable candidates for such role as a diversity of functions and health benefits have been ascribed to these substances, many appear to be non-toxic when taken long-term, and are able to reach the central nervous system (Hollman & Katan 1998, Ross & Kasum 2002, Manach & Donovan 2004).

The studies in this chapter were undertaken with this in mind. Selected flavonoids, namely EGCG, EC and genistein were tested to see whether they can protect retinal ganglion cells *in vitro*, from various insults which may cause ganglion cells to die in glaucoma. The use of a transformed retinal ganglion cell line (RGC-5 cells) allows direct access of the flavonoids to a cell without having to cross the blood-retinal barrier, control of cellular microenvironment and good experimental repeatability (Chidlow *et al* 2007). RGC-5 cells are transformed cells with certain retinal ganglion cell characteristics, have a short doubling time and provide large cell populations for repeated *in vitro* experiments (Krishnamoorthy *et al* 2001).

4.1.3 Summary of results

The results of this chapter are summarized below:

1. EGCG, EC and genistein have good antioxidant properties and are able to attenuate MDA production in lipid peroxidation.
2. EGCG and EC are similar in antioxidant potency, and genistein has much lower effect compared to EGCG and EC.
3. EGCG and EC have no detrimental effects on RGC-5 cells at concentrations as high as 75μM, however genistein have toxic effects on RGC-5 cells at lower concentrations (25μM).
4. Both EGCG and EC significantly protect RGC-5 cells from hydrogen peroxide-induced cell death at 50μM and 75μM concentrations, but this was not the case with genistein.
5. Only EC show protection of RGC-5 cells against glutamate/BSO-induced cell death, whereas EGCG and genistein did not have any effects.
6. EGCG, EC and genistein did not show any effects in increasing RGC-5 cells survival in serum deprivation conditions.
7. Serum deprivation caused an increase in Bax gene expression and Bax/Bcl-2 ratio in RGC-5 cells, suggesting a mitochondrial-related apoptotic pathway.
8. EGCG, EC and genistein increased HO-1 (heme oxygenase-1) gene expression, and both EC and genistein increase Nrf-2 (nuclear factor erythroid 2-related factor 2) and Bcl-2 (B-cell lymphoma-2) gene expression in RGC-5 cells.

4.2 Results

4.2.1 Lipid peroxidation studies

In these studies lipid peroxidation was induced by exposure of rat brain homogenates to SNP as described in section 2.2.1. Figure 4.1 shows that exposure of rat brain homogenate membranes to SNP causes a dose-dependent stimulation of thiobarbituric acid reactive species or TBARS (in terms of malondialdehyde/mg wet tissue) up to 25μM which then begins to saturate.

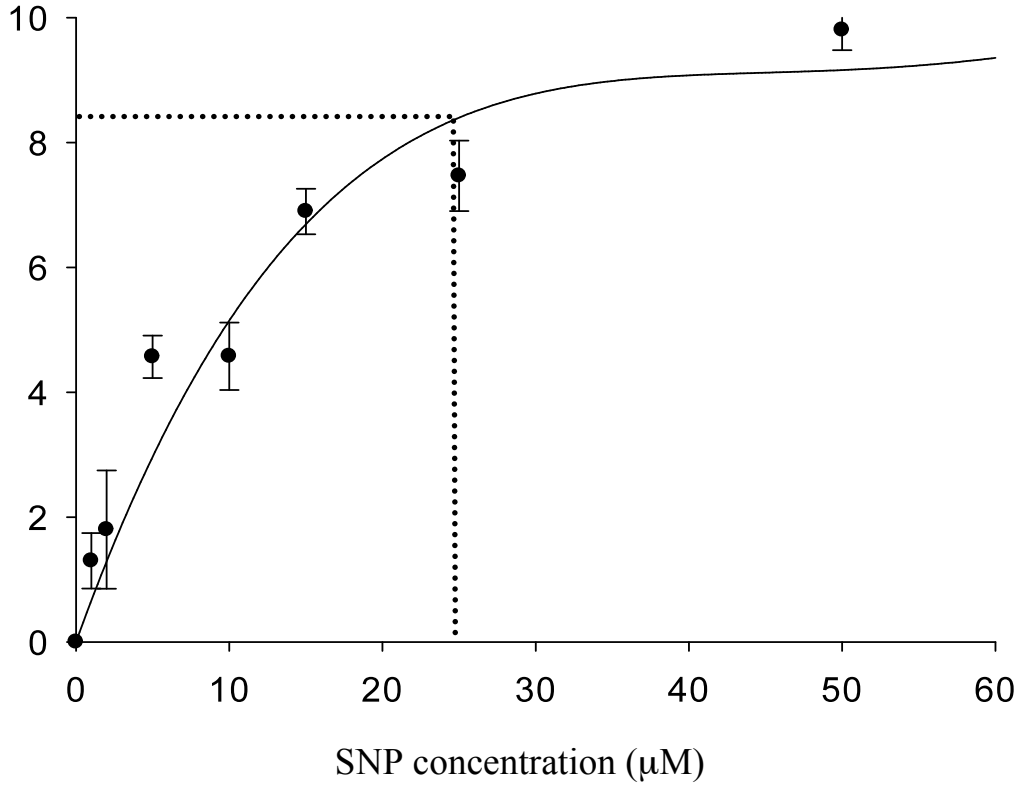


Figure 4.1. This figure shows sodium nitroprusside (SNP)-induced stimulation of lipid peroxidation in rat brain homogenates which is measured by the formation of malondialdehyde (MDA). Sodium nitroprusside (SNP) caused a submaximal stimulation of lipid peroxidation at a concentration of 25μM.

Lipid peroxidation induced by SNP in rat brain homogenates were inhibited by EGCG, EC and genistein in a more-or less dose-dependent manner as shown in figures 4.2, 4.3 and 4.4 respectively. EGCG and EC attenuate the maximum stimulation of TBARS formation induced with SNP 25μM in a concentration dependent manner giving IC_{50} values of 2.5 and 1.5μM, respectively.

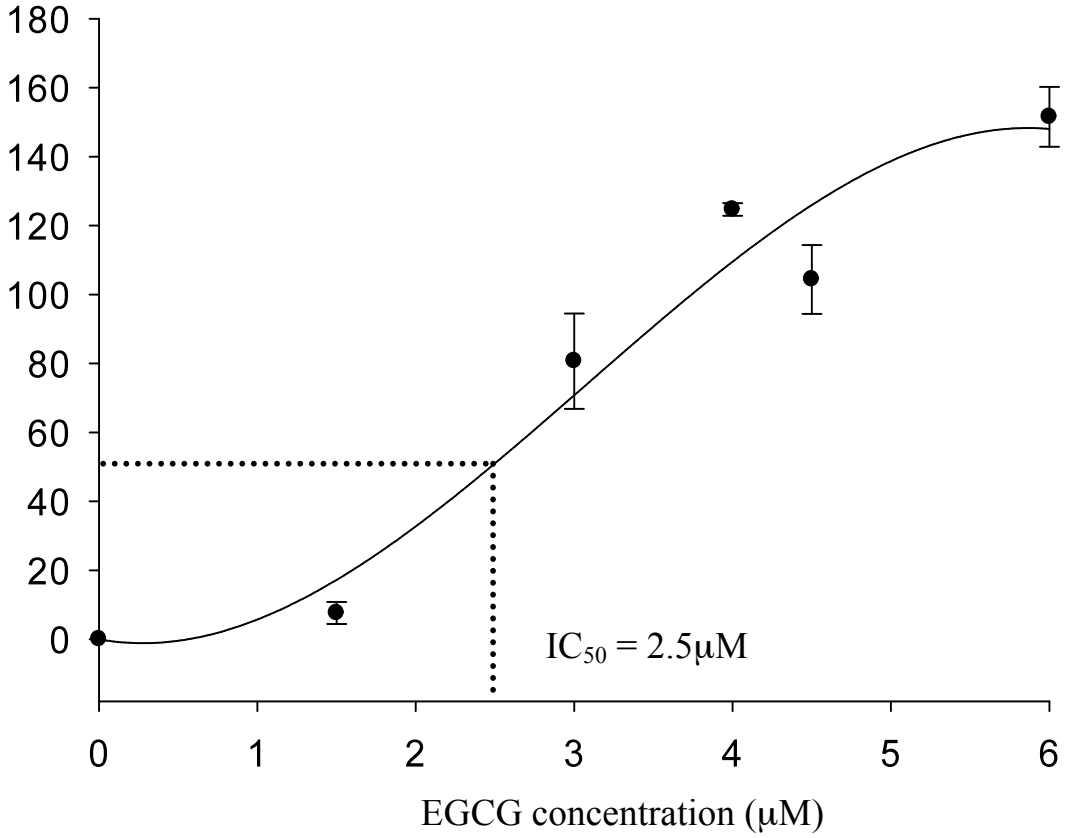


Figure 4.2. This figure shows the effect of EGCG in inhibiting the effect of SNP as an oxidant in stimulating lipid peroxidation in rat brain homogenates as measured by the formation of TBARS. In all experiments, 25μM SNP was used to stimulate TBARS formation. EGCG is effective at attenuating lipid peroxidation with an IC_{50} of 2.5μM. Values are expressed as percentage of inhibition of SNP and are the mean percentage ± SEM of 5 individual experiments.

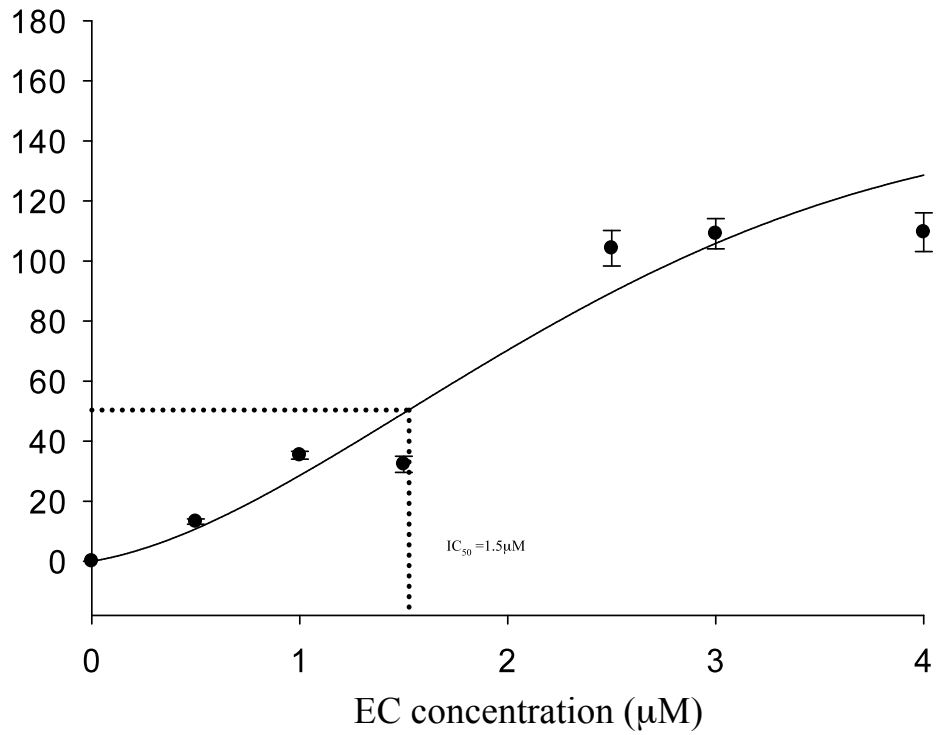


Figure 4.3. This figure shows the effect of EC in inhibiting the effect of SNP as an oxidant in stimulating lipid peroxidation in rat brain homogenates as measured by the formation of TBARS. In all experiments, 25μM SNP was used to stimulate TBARS formation. EGCG is effective at attenuating lipid peroxidation with an IC_{50} of 1.5μM. Values are expressed as percentage of inhibition of SNP and are the mean percentage ± SEM of 5 individual experiments.

In contrast to EGCG and EC, genistein is less potent in inhibiting SNP-induced lipid peroxidation. As shown in figure 4.4 below, the IC_{50} for genistein is 39μM, which is about 20 times higher compared to EGCG and EC.

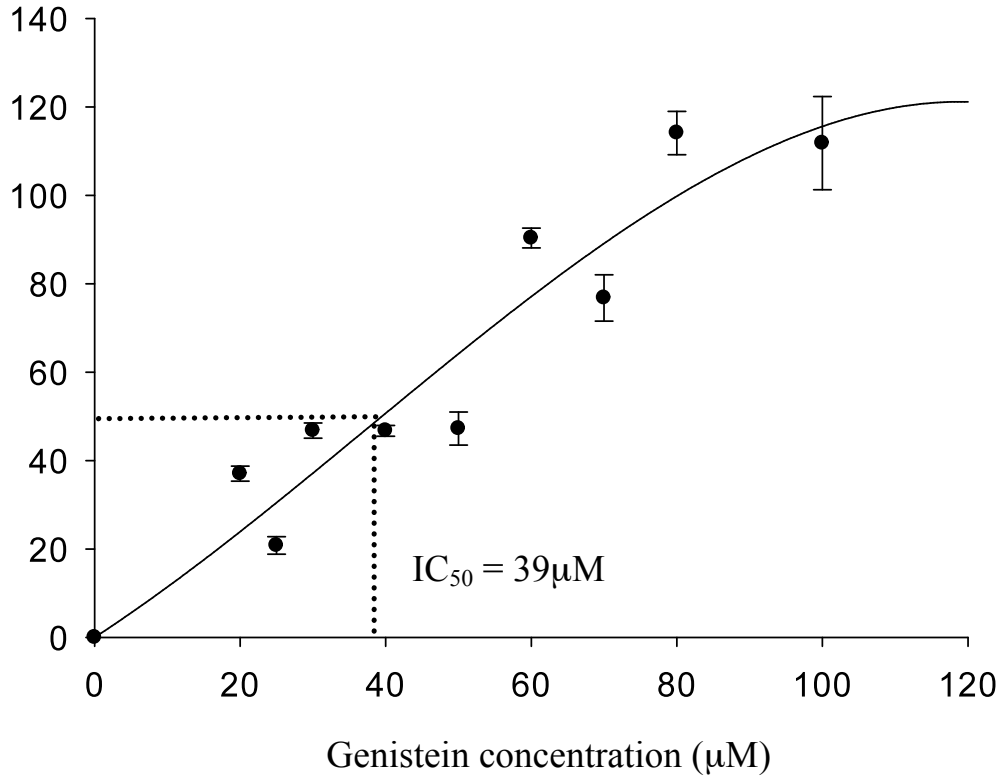


Figure 4.4. This figure shows the effect of genistein in inhibiting the effect of SNP as an oxidant in stimulating lipid peroxidation in rat brain homogenates as measured by the formation of TBARS. In all experiments, 25μM SNP was used to stimulate TBARS formation. Genistein is much less potent in inhibiting the TBARS formation induced by SNP with an IC_{50} of 39μM. Values are expressed as percentage of inhibition of SNP and are the mean percentage ± SEM of 5 individual experiments.

4.2.2 RGC-5 cells

RGC-5 cells were grown to confluence in 96-, or 6-well plates or on coverslips in 24-well plates. As shown in figure 4.5, a viable cell seedling has a typical appearance of being surrounded by a halo during plating. After 24 hours, the cells adhere to the bottom of the wells of culture plates with outgrowing processes. RGC-5 cells grow in a monolayer fashion, intercalating with neighbouring cells. Cells achieve about 80-90% confluence after 48 hours when plated at a density of 0.7x10-4 cells/µl. The volume plated on each well is 100µL/well in 96-well plates, 200µL/well in 24-well plates and 500µL/well in 6-well plates. After 72 hours, cells become overcrowded and start to die. For all experiments in this chapter, RGC-5 cells were treated after 24 hours of plating.

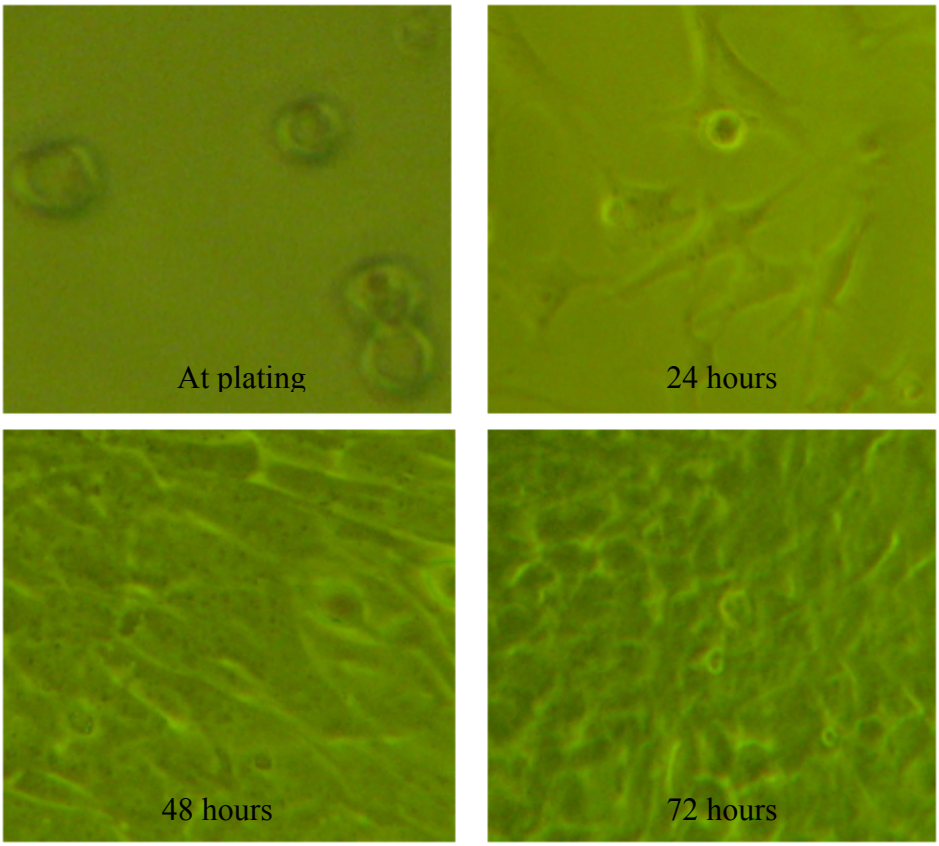


Figure 4.5. Unstained microscopic view of RGC-5 cells in culture. RGC-5 cells appear as seedlings with surrounding haloes when plated on Day 0. After 12 hours, about 30-40% confluence is achieved. After 72 hours, cells start to become overcrowded.

Semi-confluence stained cultures of RGC-5 cell are shown in figure 4.6. RGC-5 cells stained positive for brain-derived nerve factor (BDNF) and neurofilament-light (NF-L), which are markers of neuronal cells. NF-L is a specific marker for retinal ganglion cells *in situ* (Kong & Cho 1999, Chidlow & Osborne 2003).

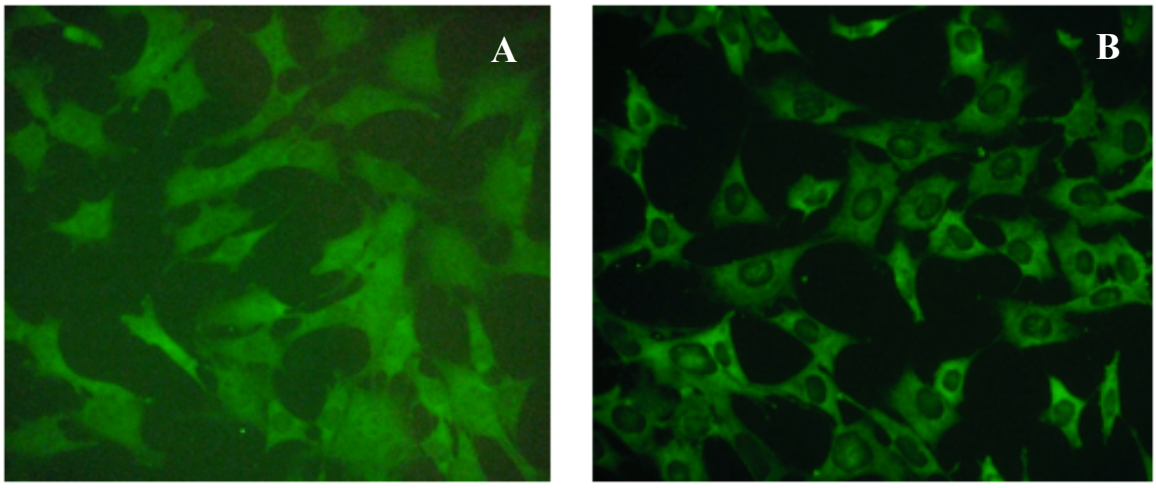


Figure 4.6. Immunocytostaining of RGC-5 cells. A: Brain-derived nerve factor (BDNF) which is a neuronal cell marker, and B: neurofilament-light chain (NFL-L), which is a marker for retinal ganglion cells.

4.2.3 Flavonoids dose response

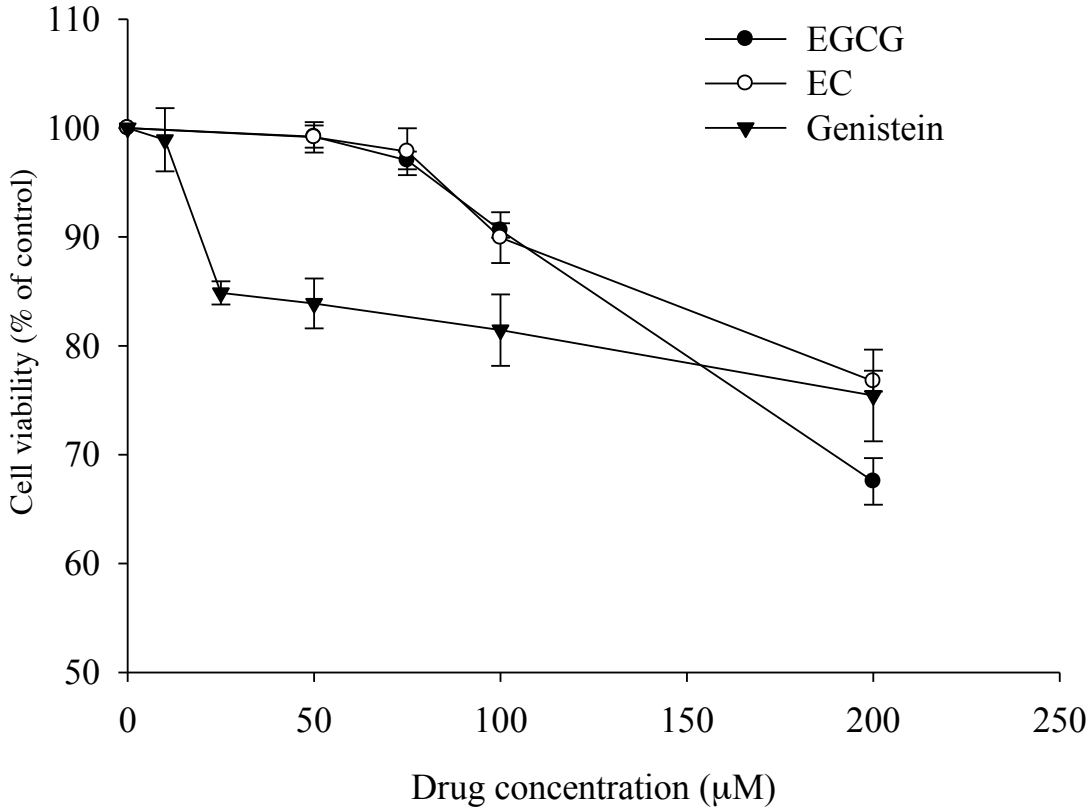


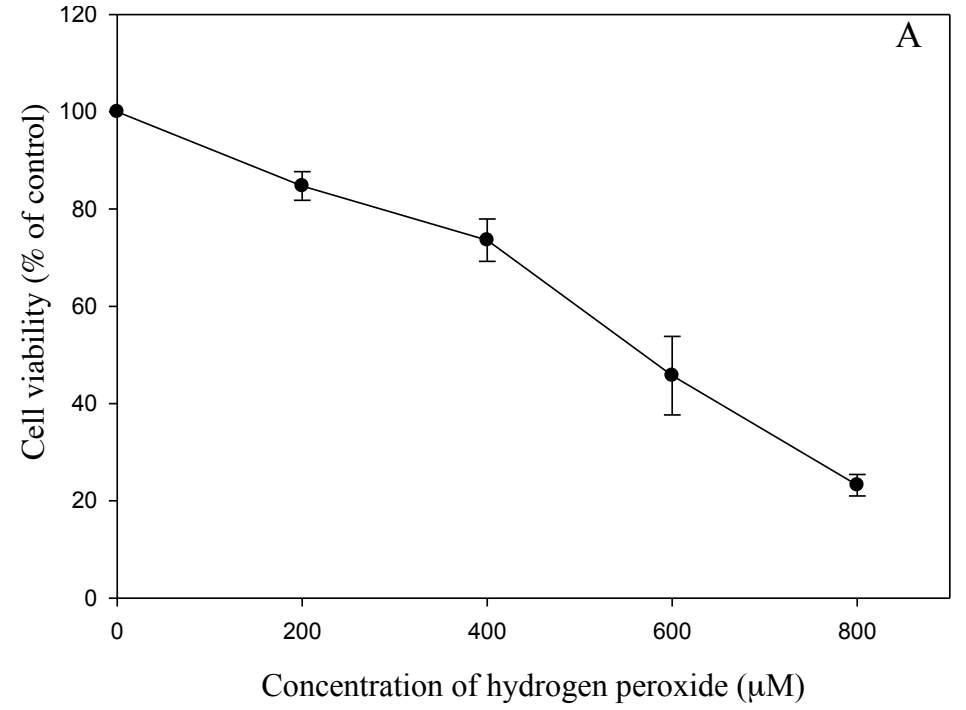
Figure 4.7. Dose response curve of EC, EGCG and genistein using MTT assay. Values are expressed as percentage of control and are the mean ± SEM of at least 5 individual experiments.

As shown in figure 4.7 above, EC and EGCG have similar dose response curves, causing RGC-5 cell toxicity at concentrations higher than 100μM. In contrast, genistein significantly reduce RGC-5 cell viability from a concentration of 25μM onwards. In subsequent experiments, the concentrations used for EC and EGCG were 50μM and 75μM, whereas a non-toxic concentration of 10μM was used for genistein.

4.2.4 Hydrogen peroxide-induced toxicity

4.2.3.1 MTT assay

The effects of increasing concentrations (200μM, 400μM, 600μM and 800μM) of hydrogen peroxide (H_2O_2) on RGC-5 cell viability as assessed by the MTT assay, are summarized in figure 4.8A below. In these studies, RGC-5 cells were plated on 96-well plates and exposed to increasing concentrations of H_2O_2 for 24 hours while the control cells were exposed to vehicle. Compared to vehicle-treated cells, H_2O_2 reduced RGC-5 cell viability in a dose-dependent manner, and a concentration of 400μM of H_2O_2 caused approximately 25% reduction in cell viability. This was the dose used in subsequent experiments with H_2O_2. Increasing the concentration of H_2O_2 caused a dose-dependent greater negative effect on cell viability. Pre-treatment of RGC-5 cells with EGCG 50μM and EC 50μM for 1 hour before exposure to H_2O_2 400μM reduced RGC-5 cell loss significantly. However, this effect was not seen with genistein (figure 4.8B).



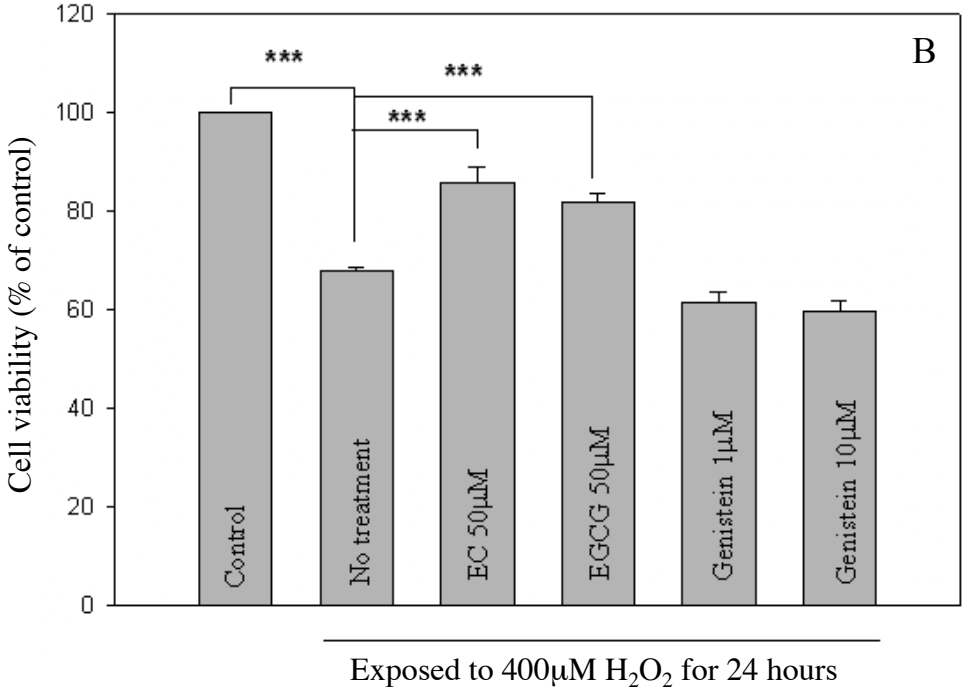


Figure 4.8 Figure A shows the effect of H_2O_2 on the viability of RGC-5 cells in culture as measured by the MTT assay. Viability of RGC-5 cells to H_2O_2 is concentration-dependent with 400μM H_2O_2 causing 25% reduction in cell viability. Figure B shows EC at 50μM significantly attenuates RGC-5 cell death caused by 400μM H_2O_2 in a concentration-dependent way but genistein at 1μM or 10μM has no positive effect in increasing RGC-5 cell viability. EGCG 50μM was used as a positive control in these studies. Values are expressed as percentage of control and are the mean ± SEM of at least 5 individual experiments. (***p<0.001)

4.2.3.2 WST-1 assay

In order to assess the effects of H_2O_2 on mitochondria, studies to assess the activity of mitochondrial dehydrogenase were carried out on RGC-5 cells by WST-1 assay. Figure 4.9 shows that H_2O_2 400μM caused a reduction of RGC-5 cells mitochondrial dehydrogenase activity over 24 hours. This effect was attenuated significantly by EC 50μM, but not by EGCG 50μM or genistein 10μM.

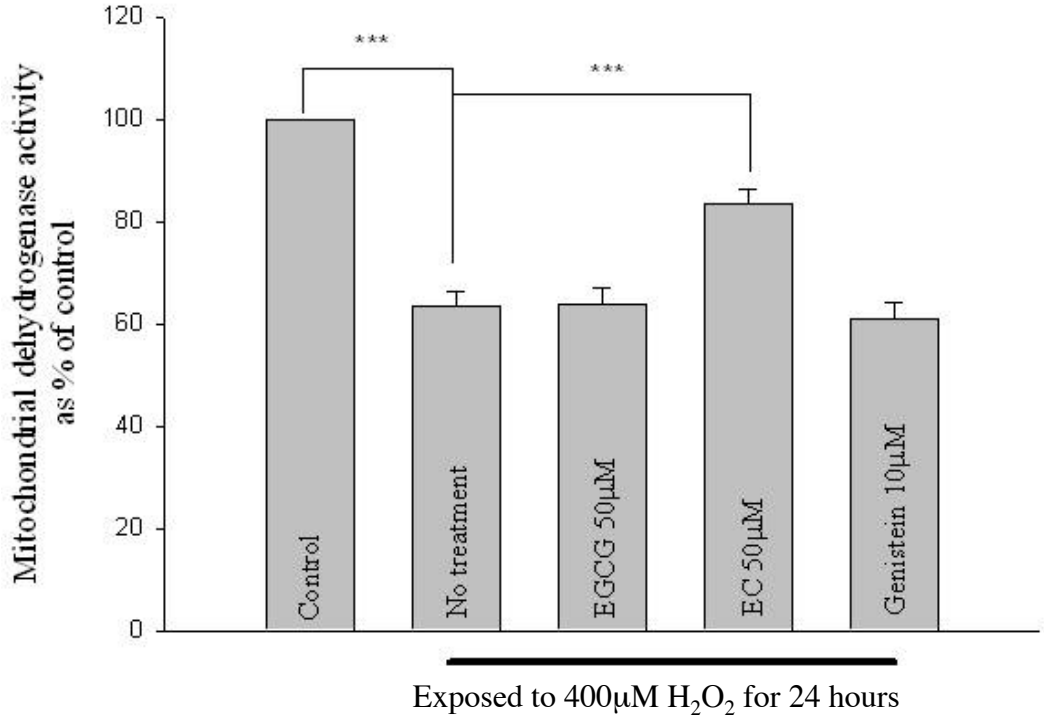


Figure 4.9. In these studies, RGC-5 cells grown in 96-well plates were exposed to 400μM H_2O_2 for 24 hours after pre-treatment with EGCG 50μM, EC 50μM and genistein 10μM. Only EC blunt the effects of H_2O_2 on mitochondrial dehydrogenase activity in RGC-5 cells. Values are expressed as percentage of control and are the mean ± SEM of at least 5 individual experiments. (***p<0.001)

4.2.3.2 Reactive oxygen species (ROS) production

RGC-5 cells were assessed for the production of reactive oxygen species (ROS) using the dye 2',7'-dihydroethidium (DHE) according to Carter et al (Carter *et al* 1994). DHE is a reduced from of ethidium bromide, which is non-fluorescent and can passively cross the membrane of live cells (King *et al* 2004). DHE can be oxidized in the cell by superoxide anions or hydrogen peroxide to ethidium bromide, which binds to DNA and, when excited, emits a red-yellow fluorescent product that is proportional to the intracellular superoxide anion/H_2O_2 level. After treatment in 24-well plates with selected flavonoids, RGC-5 cells grown on cover slips were stained with DHE (10mg/ml) by incubating for 30 minutes at 37°C in culture medium in a humidified chamber and then fixed with 4% paraformaldehyde for 20 minutes. The results of ROS staining using DHE are shown in figure 4.10. The ROS fluorescence is clearly enhanced when RGC-5 cells are exposed to 400μM H_2O_2 for 24 hours (figure 4.10B).

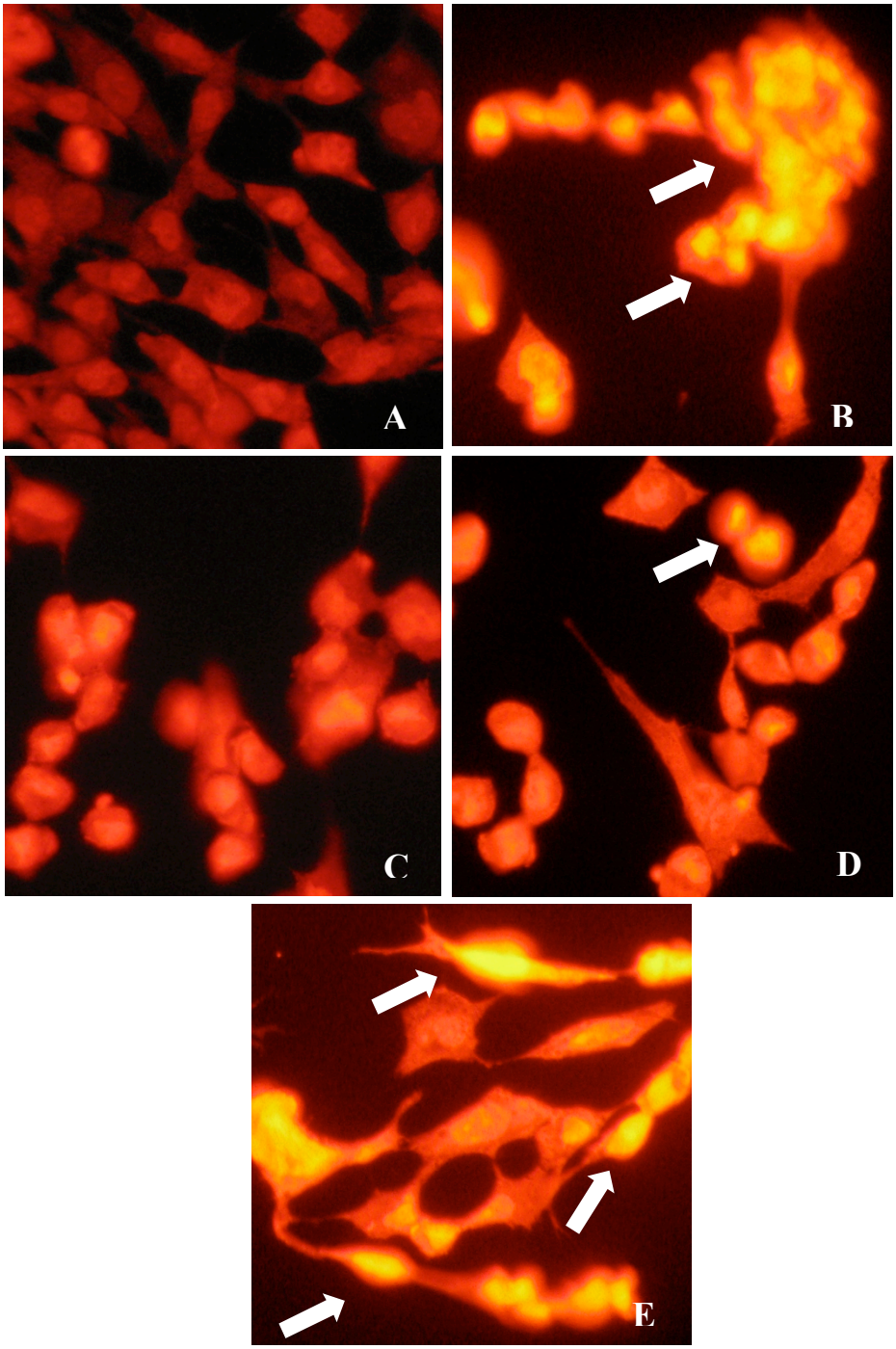


Figure 4.10. DHE staining for ROS in RGC-5 cells. In cells treated with 400μM H_2O_2 (B), DHE produces fluorescent staining (white arrows), indicating ROS formation, which is absent in control cells (A). ROS formation is clearly reduced when RGC-5 cells were pre-treated with EC 50μM (C) and EGCG 50μM (D) for 1 hour prior to exposure to H_2O_2. However, ROS formation is not blunted by genistein 10μM (E). These findings were repeated and confirmed to occur in at least three separate experiments.

4.2.3.3 Cell death by apoptosis

Extensive signs of apoptotic RGC-5 cells induced by H_2O_2 400μM were demonstrated by the APOPercentage^{TM} assay (figure 4.11B) compared with control cultures (figure 4.11A). EC 50μM and EGCG 50μM almost completely blunted apoptosis induced by H_2O_2. However, genistein 10μM has no effect in attenuating apoptosis in RGC-5 cells. Figure 4.12 shows the cell quantification of apoptotic RGC-5 cells staining positive for phosphotidylserine using the APOPercentage^{TM} staining kit, where cells are counted from at least 3 different random field of view.

Further evidence showing that H_2O_2 induced RGC-5 cell death by apoptosis was obtained by TUNEL labelling for DNA breakdown, is attenuated by EC 50μM and EGCG 50μM, as shown in figure 4.13. The corresponding quantitative analysis of cells counted from at least 3 different random field of view, is shown in figure 4.14.

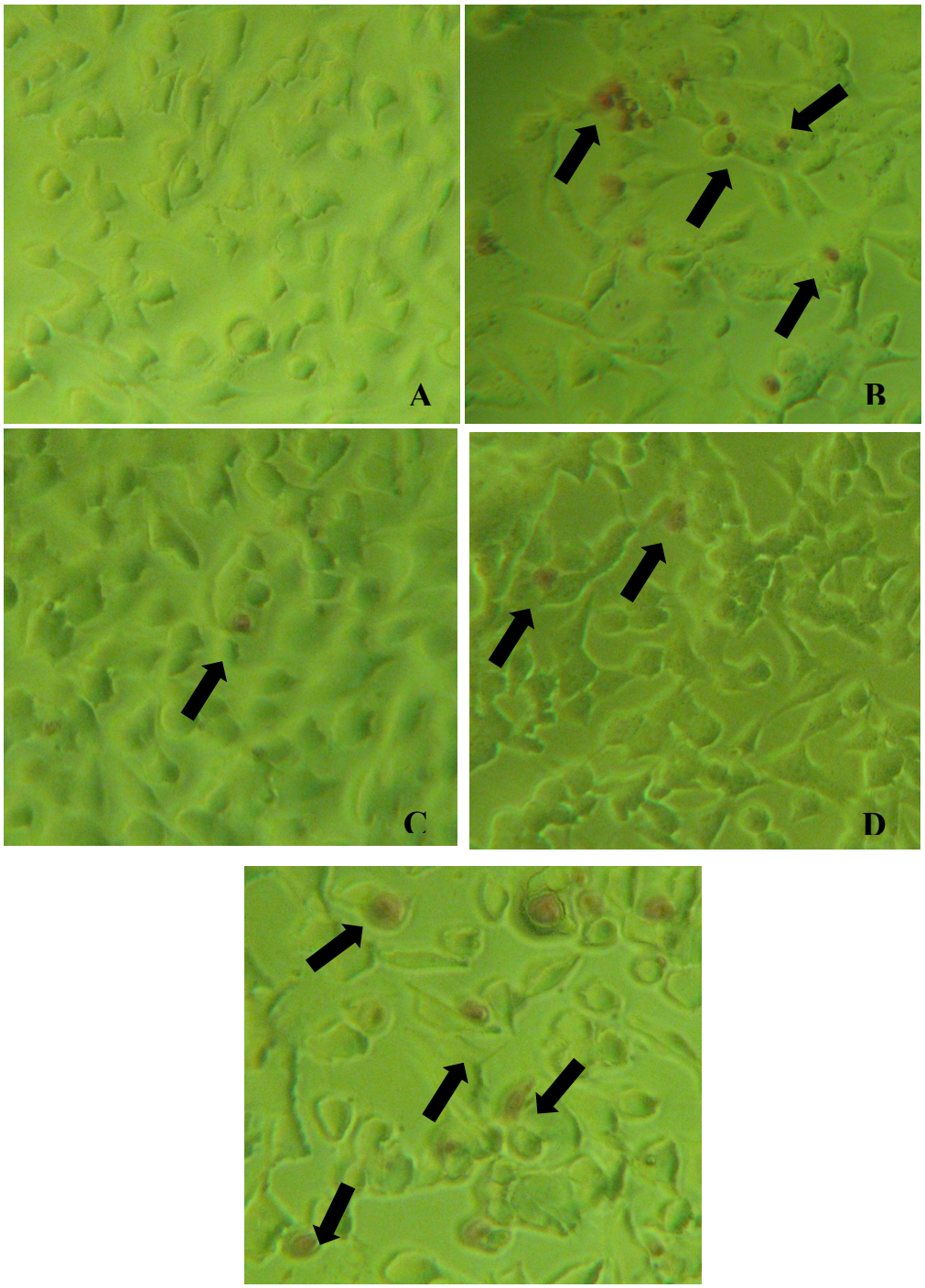


Figure 4.11. APOPercentage™ staining for phosphotidylserine in RGC-5 cells shows (A) control RGC-5 cells in culture, (B) H_2O_2 400μM caused many RGC-5 cells to die by apoptosis as indicated by pink staining (black arrows) of phosphotidylserine in apoptotic cells. Pre-treatment with EC 50μM (C) and EGCG 50μM (D) clearly blunts the effect of H_2O_2 400μM with very few apoptotic cells, whereas genistein 10μM has no effect in attenuating apoptosis (E).

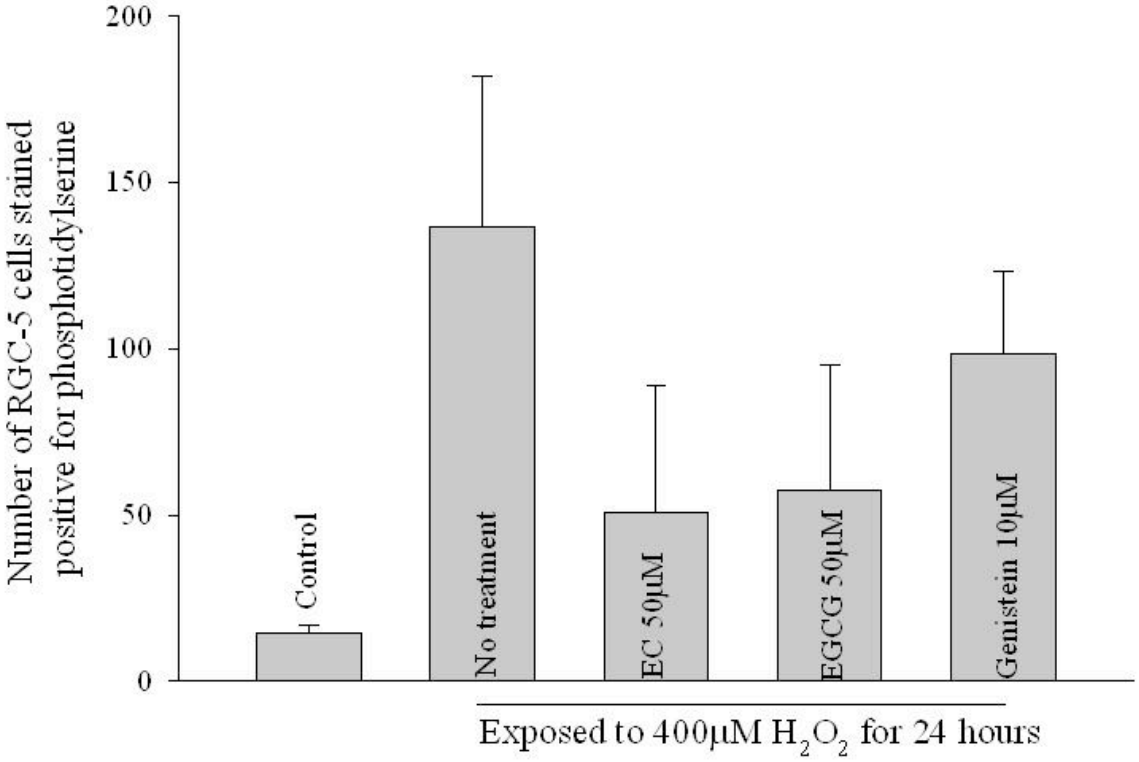


Figure 4.12 Quantitative analysis revealed that the number of apoptotic cells staining positive for phosphotidylserine using the APOPercentage^{TM} staining kit is reduced in RGC-5 cells pre-treated with EC 50μM and EGCG 50μM for an hour before further incubation with H_2O_2 400μM for 24 hours. Results are expressed in mean number of cells ± SEM.

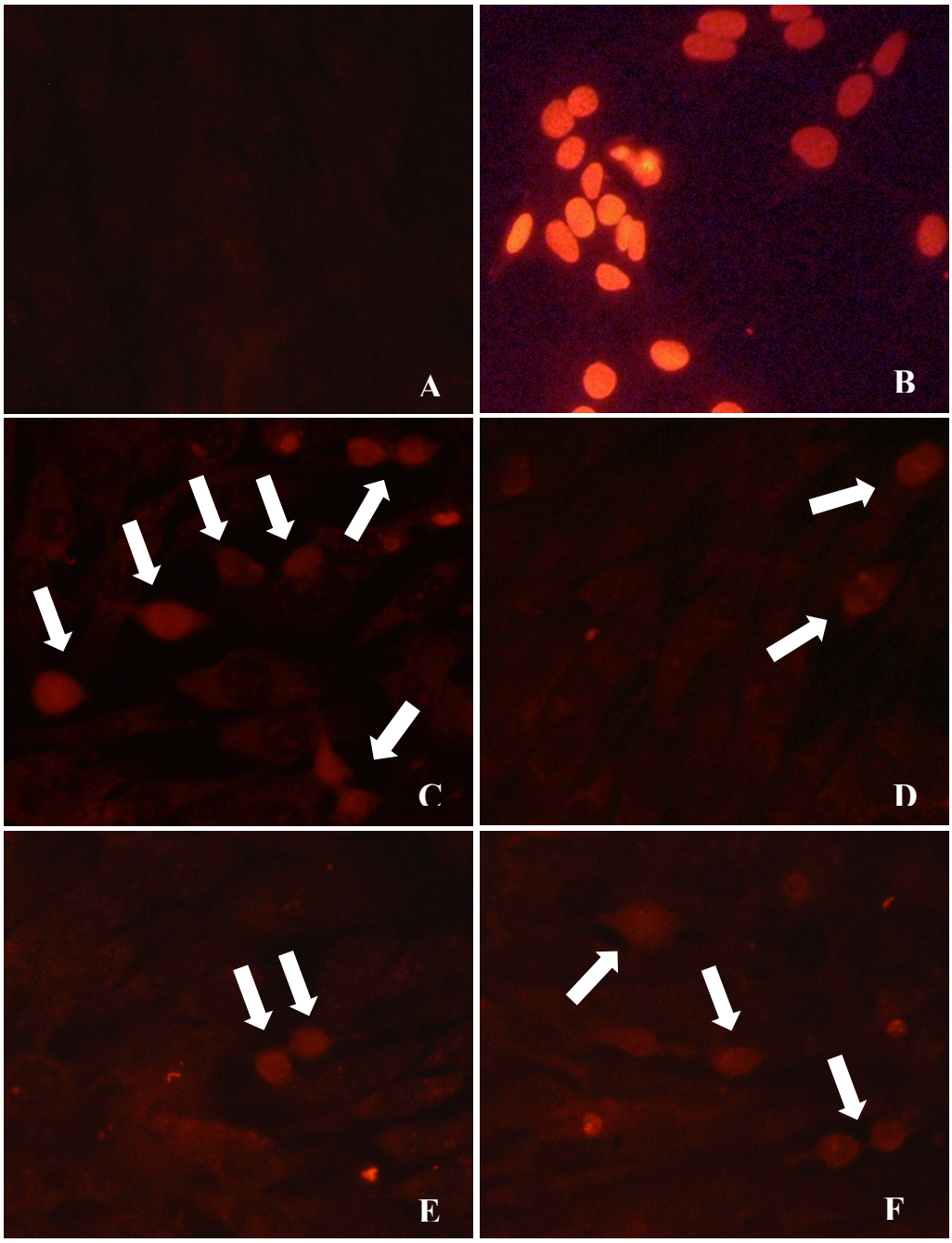


Figure 4.13. Occurrence of DNA breakdown, as indicated by TUNEL labelling in RGC-5 cells subjected to H_2O_2. 400μM. DNA breakdown was hardly seen in control cells (A) compared to positive control (B) where cells were treated with DNAse I and TUNEL staining was seen in every cell. RGC-5 cells exposed to H_2O_2 (C) showed increased TUNEL staining (white arrows) suggesting cell death by apoptosis. Pre-treatment with EC 50μM (D) and EGCG 50μM (E) concentration significantly reduced DNA breakdown in cells as shown by TUNEL staining. This effect was not seen in cells pre-treated with genistein 10μM (F).

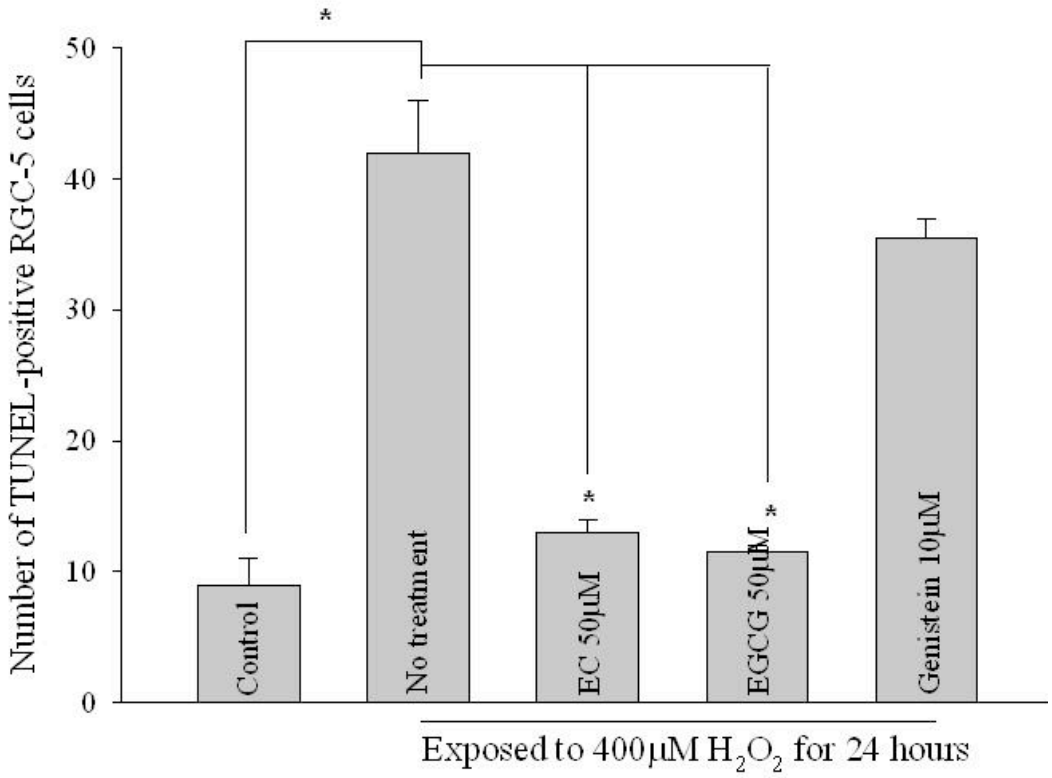


Figure 4.14 Quantitative analysis revealed that the number of TUNEL-positive RGC-5 cells is reduced in RGC-5 cells pre-treated with EC 50μM and EGCG 50μM for an hour before further incubation with H_2O_2 400μM for 24 hours. Results are expressed in mean number of cells ± SEM, where * $p<0.05$.

4.2.4 Glutamate/BSO-induced toxicity

4.2.4.1 MTT assay

The effects of increasing concentrations (0.1, 1, 5 and 10mM) of glutamate with and without co-treatment with L- buthionine sulfoximine (BSO) on RGC-5 cell viability as assessed by MTT assay, are summarized in figure 4.13. BSO is a specific inhibitor of –glutamylcysteine synthetase (Griffith & Meister 1979), which is the initial step in glutathione (GSH) synthesis. GSH is a major thiol in mammalian cells, and is involved in the cellular antioxidative defense by serving as an electron donor for the reduction of reactive oxygen species such as peroxides, producing its oxidized form, glutathione disulphide (GSSG). The balance between GSH and GSSG concentrations is believed to be a determinant in the cellular capability to cope with an oxidative stressful stimulus. In these studies, RGC-5 cells were plated on 96-well plates and exposed to increasing concentrations of glutamate with and without adding 1mM BSO for 24 hours while the control cells were exposed to vehicle alone. Glutamate-induced RGC-5 cell death occurs in a dose-dependent manner, either with or without co-treatment with BSO. Without co-treatment with BSO, RGC-5 cells were resistant to glutamate toxicity, achieving significant cell death only at higher concentrations. However, the addition of 1mM BSO increases the RGC-5 cells to glutamate toxicity, causing approximately 26% reduction in cell viability when exposed to 1mM glutamate, as shown in figure 4.15. This was the dose used in subsequent experiments with glutamate-induced toxicity.

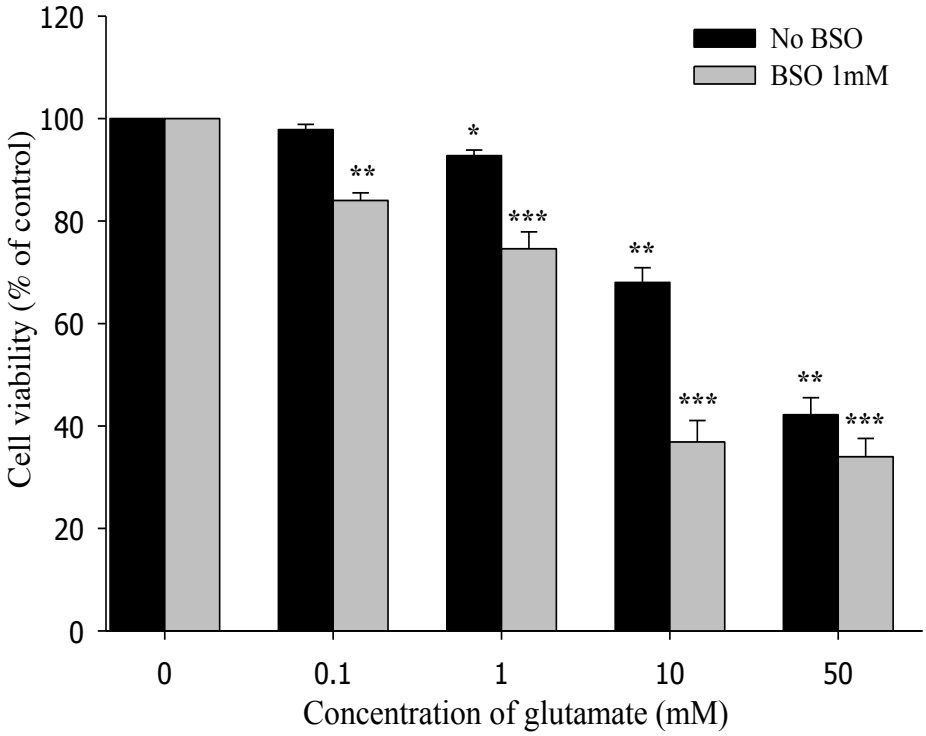


Figure 4.15 show the effect of glutamate-induced toxicity on the viability of RGC-5 cells in culture as measured by the MTT assay. The addition of 1mM BSO (grey bars) increased RGC-5 cells sensitivity to glutamate toxicity. RGC-5 cell death caused by 1mM glutamate and 1mM BSO caused approximately 26% reduction in cell viability, and this was the concentration used for subsequent experiments. Values are expressed as percentage of control and are the mean ± SEM of at least 5 individual experiments. Statistical significance was calculated using unpaired *t*-test compared to control (*p<0.05, **p<0.05,***p<0.001).

As shown in figure 4.16 below, only EC 50μM significantly attenuates glutamate-induced RGC-5 cell death, whereas the same effect was not seen with EGCG (50μM or 75μM) or genistein (1μM or 10μM).

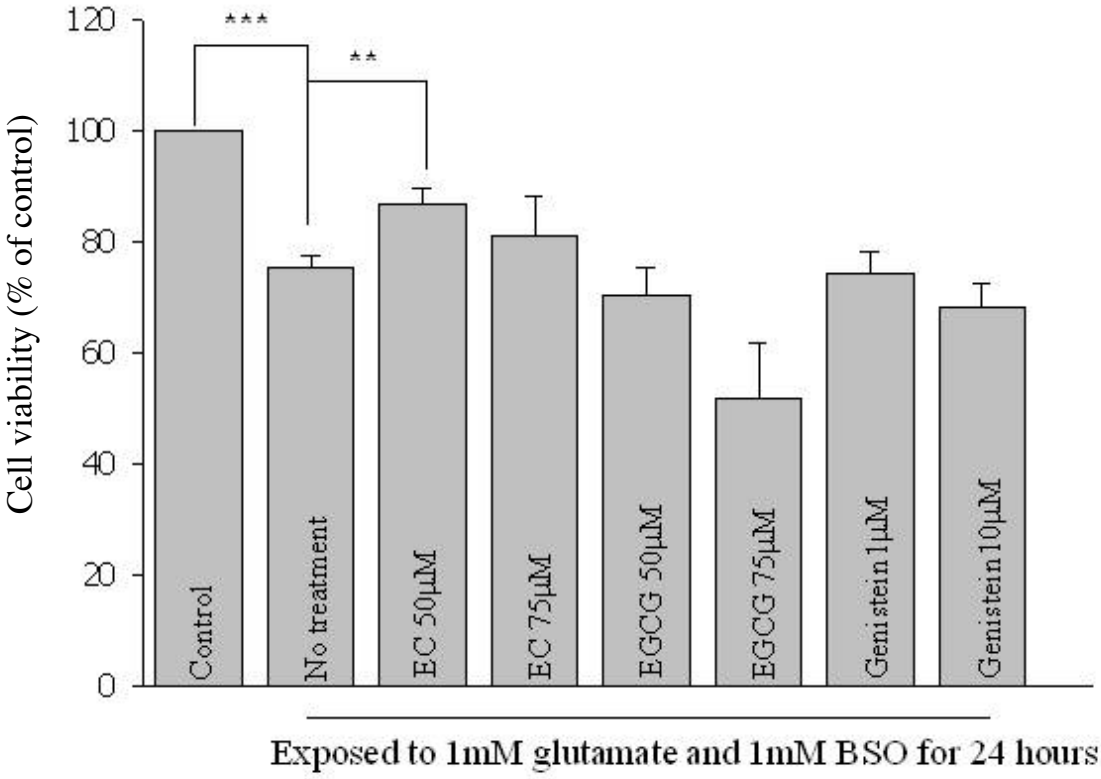


Figure 4.16 In these studies, 96-well plates with RGC-5 cells were incubated with EC (50μM and 75μM), EGCG (50μM and 75μM) and genistein (1μM and 10μM) before exposed to glutamate 1mM and BSO 1mM for 24 hours. In untreated cells, glutamate-induced toxicity caused approximately 25% reduction in RGC-5 cell viability as measured by MTT assay, and only EC 50μM was shown to significantly reduce this effect. Interestingly, neither EGCG nor genistein have the same positive effect on glutamate-induced RGC-5 cell death. Values are expressed as percentage of control and are the mean ± SEM of at least 5 individual experiments. Statistical significance was calculated using unpaired *t*-test compared to control (**$p<0.05$, ***$p<0.001$).

4.2.4.2 WST-1 assay

The effects of glutamate on the activity of mitochondrial dehydrogenase in RGC-5 cells were carried out using WST-1 assay and the results are shown in figure 4.17. Glutamate-induced toxicity in the presence of 1mM BSO reduced RGC-5 cell mitochondrial dehydrogenase activity by almost 40%. Only EC50μM attenuate this effect compared to EGCG 50μM and genistein 10μM.

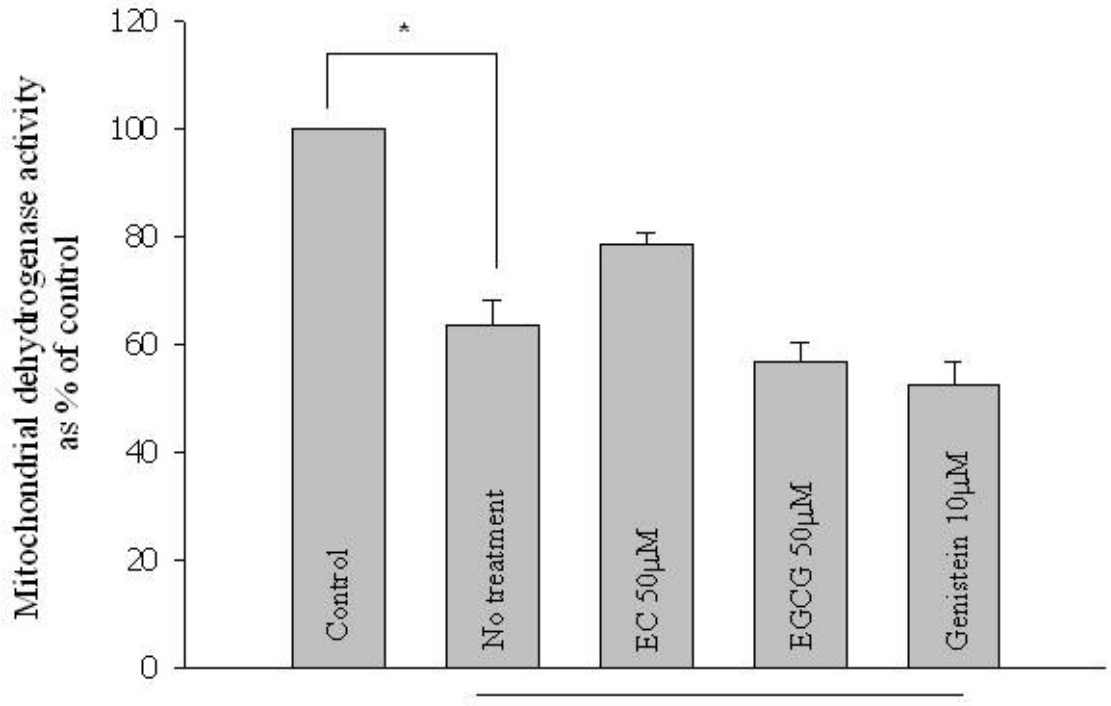


Figure 4.17 In these studies, RGC-5 cells grown in 96-well plates were treated with EGCG 50μM, EC 50μM and genistein 10μM for 1 hours before exposed to 1mM glutamate for 24 hours. To increase RGC-5 cells sensitivity to glutamate-induced toxicity, 1mM BSO was added. Only EC 50μM blunt the effects of glutamate on mitochondrial dehydrogenase activity in RGC-5 cells, although this change did not achieve statistical significance. Values are expressed as percentage of control and are the mean ± SEM of at least 4 individual experiments. (*p<0.05)

4.2.4.3 Apoptotic membrane alteration with the APOPercentage™ assay

Compared to control RGC-5 cells (figure 4.18A), 1mM glutamate in the presence of 1mM BSO cause a marked increase in apoptotic cells, as shown by the pink staining of phosphotidylserine on cell membranes (figure 4.18B). The number of apoptotic cells is clearly reduced when RGC-5 cells were pre-treated to EC50μM an hour before exposure to glutamate (figure 4.18C). In comparison, EGCG 50μM and genistein 10μM has no effect on reducing glutamate-induced apoptosis in RGC-5 cells (figures 4.18D and E, respectively). The corresponding quantitative analysis of cells counted from at least 3 different random field of view, is shown in figure 4.19.

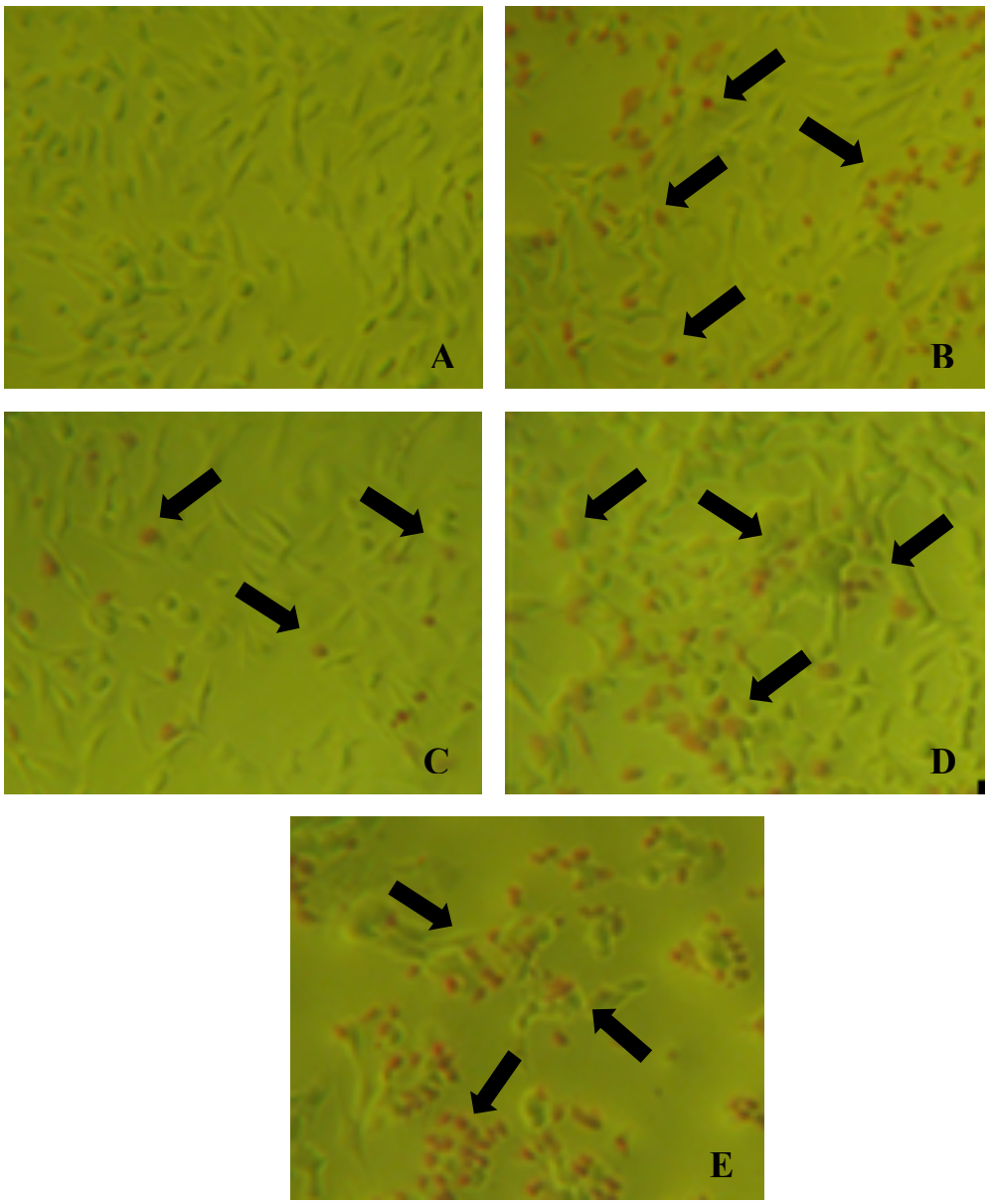


Figure 4.18 APOPercentage™ staining for phosphotidylserine in RGC-5 cells. Glutamate-induced toxicity caused many RGC-5 cells to die by apoptosis as indicated by pink staining (B) of phosphotidylserine in apoptotic cells compared to control cells (A) where no apoptotic cells were seen. This effect is clearly blunted by 50μM EC (C) but not by 50μM EGCG (D) or genistein 10μM (E).

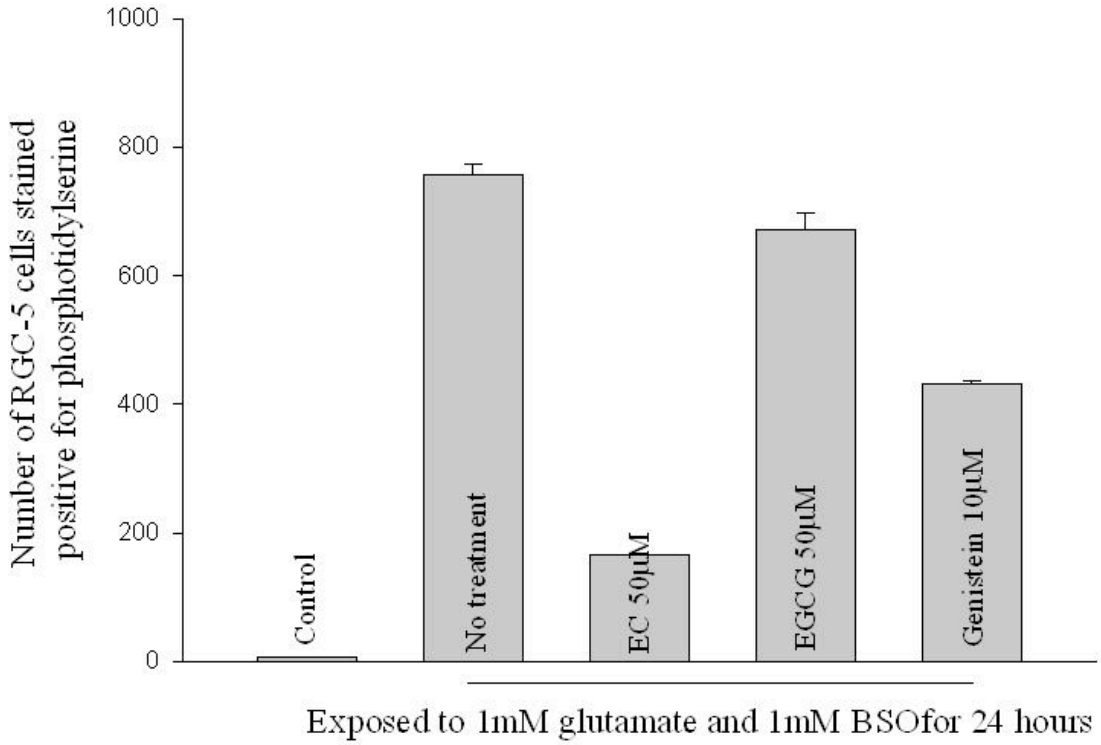


Figure 4.19 Quantitative analysis revealed that the number of apoptotic cells staining positive for phosphotidylserine using the APOPercentage^{TM} staining kit is only reduced in RGC-5 cells pre-treated with EC 50µM for an hour before further incubation with 1mM glutamate and 1mM BSO for 24 hours. Results are expressed in mean number of cells ± SEM.

4.2.5 Serum deprivation-induced toxicity

4.2.5.1 MTT assay

RGC-5 cells were plated in 96-well plates for overnight before, and were rinsed twice with serum-derived medium and incubated in serum-deprived medium for another 24, 48 and 72 hours. Cell viability was measured using MTT assay. Serum-deprivation caused a reduction in RGC-5 cell viability in a time-dependent manner, causing approximately 38% cell death after 48 hours, as shown in figure 4.20. This was the exposure time used in subsequent experiments to achieve significant RGC-5 cell death.

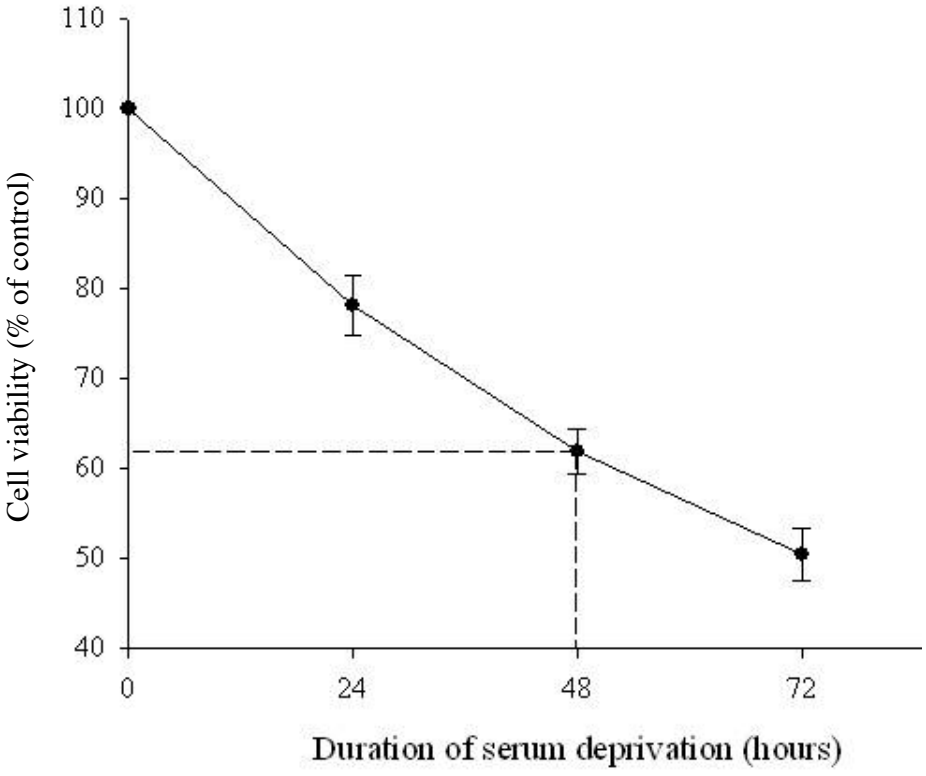


Figure 4.20. Graph showing increasing RGC-5 cell death in serum-deprived conditions in a time-dependent manner. Serum-deprived conditions caused approximately 30% RGC-5 cell death after 48 hours, causing 50% cell death after 72 hours. Values are expressed as percentage of control and are the mean ± SEM of at least 3 individual experiments.

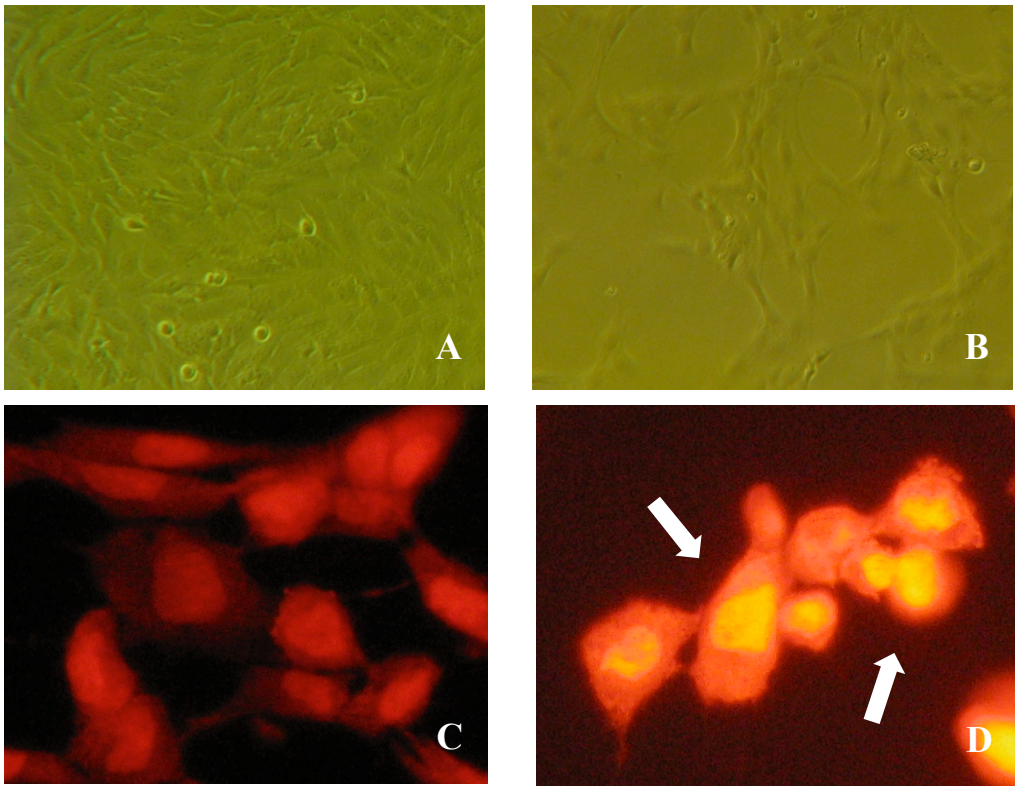


Figure 4.21 Effects of serum deprivation on RGC-5 cells in culture after 48 hours. Figures (A) and (B) show unstained RGC-5 cells as viewed under epifluoresence microscope, while figures (C) and (D) show DHE staining for ROS. In control conditions (A), RGC-5 cells multiply rapidly, growing to almost complete cell confluence. In contrast, RGC-5 cells exposed to serum-deprived medium grow sparsely as shown in (B). In contrast to control RGC-5 cells stained for ROS (C), serum deprivation caused ROS production in RGC-5 cells after 48 hours, as indicated by the presence of yellow fluorescence (D).

Figure 4.21 (B) shows the reduced density of RGC-5 cells following exposure to serum deprivation for 48 hours by almost 50%. DHE staining indicated increased ROS production in RGC-5 cells caused by serum deprivation (C control, D serum deprivation).

To assess the effects of flavonoids on RGC-5 cell survival in serum-deprived conditions, cells were treated with EC (10 μM and 50μM), EGCG (10 μM and 50 μM) and genistein (10 μM) after rinsing with serum-free medium in 96-well plates. The cells were incubated at 37°C for another 48 hours, and cell viability was measured using MTT assay. As shown in figure 4.22, serum-deprivation caused almost 40% reduction in RGC-5 cell viability after 48 hours, and this reduction is statistically significant. However, none of the selected flavonoids increased RGC-5 cell survival after 48 hours. Both EC 50μM and EGCG 50μM increased RGC-5 cell death in serum-deprived conditions.

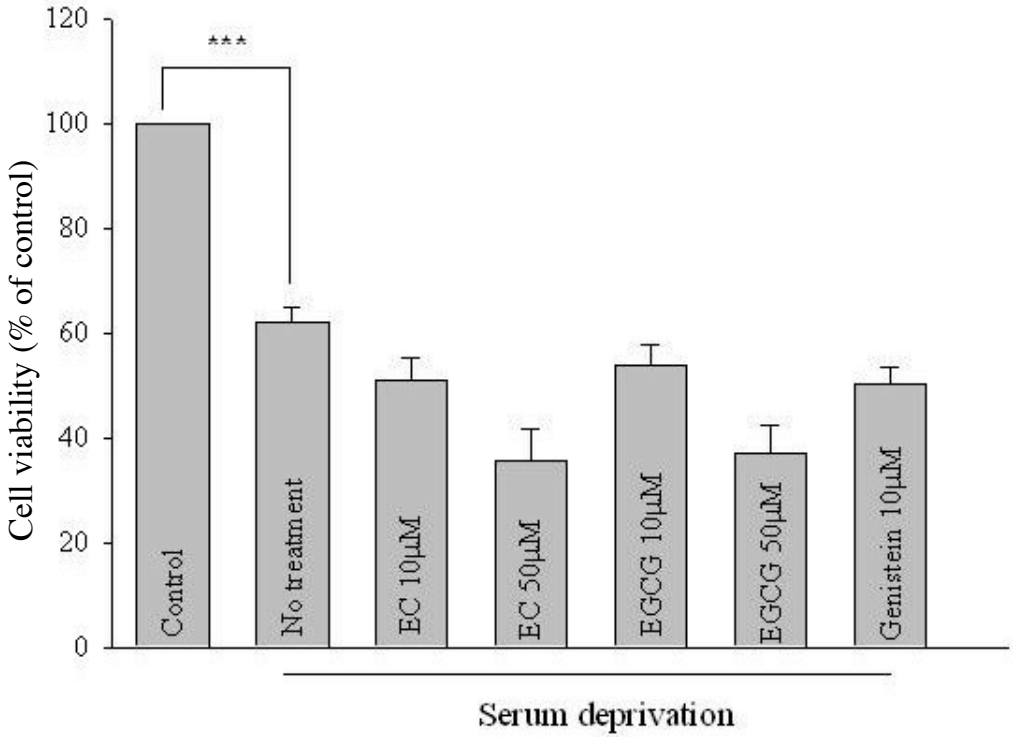


Figure 4.22. In these studies, 96-well plates with RGC-5 cells were rinsed twice with serum-free medium after plated overnight. EC (10μM and 50μM), EGCG (10 μM and 50μM) and genistein (10μM) were added into each well and the cells were incubated for another 48 hours in serum-deprived medium. Serum-deprivation caused 40% RGC-5 cell death, and this effect is not negated by any of the selected flavonoids at the chosen concentrations. Values are expressed as percentage of control and are the mean ± SEM of at least 5 individual experiments. Statistical significance was calculated using unpaired *t*-test compared to control (***$p<0.001$).

4.2.5.2 Western blot analysis

To further elucidate the signaling pathway of serum-induced RGC-5 cell death, protein was extracted from RGC-5 cell lysates exposed to increasing duration of serum deprivation conditions. Figure 4.23A shows that serum deprivation causes up-regulation of phosphorylated p38 (P-p38) proteins of the MAPK pathway as early as 30 minutes of exposure and peaking at 24 hours. At 72 hours, P-p38 band is hardly detectable. Serum deprivation did not up-regulate any of the c-Jun proteins, as shown by the lack of phosphorylated c-Jun band. Mitochondrial signaling pathway is up-regulated in serum-deprived conditions as shown by the increase in Bax levels after 24 hours which remained up-regulated for 96 hours (see figure 4.23B).

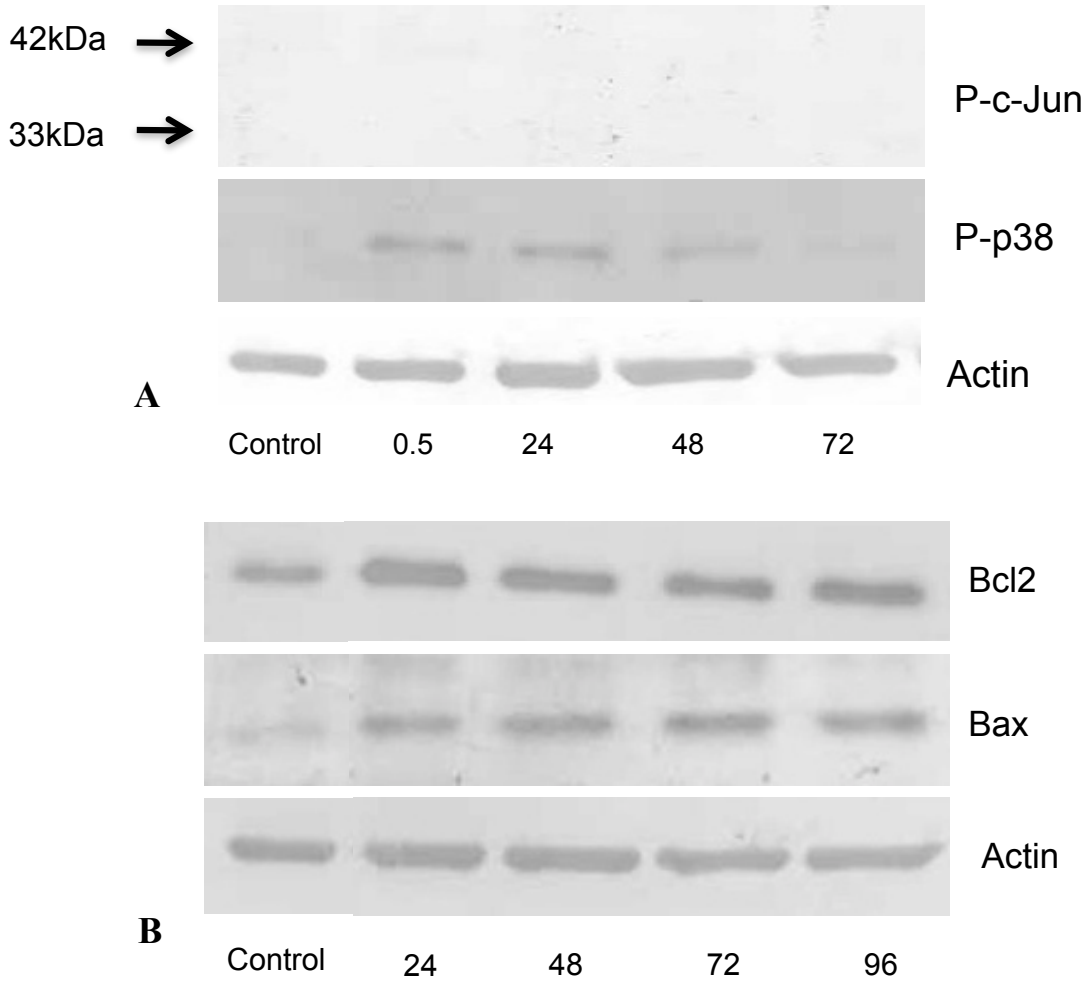
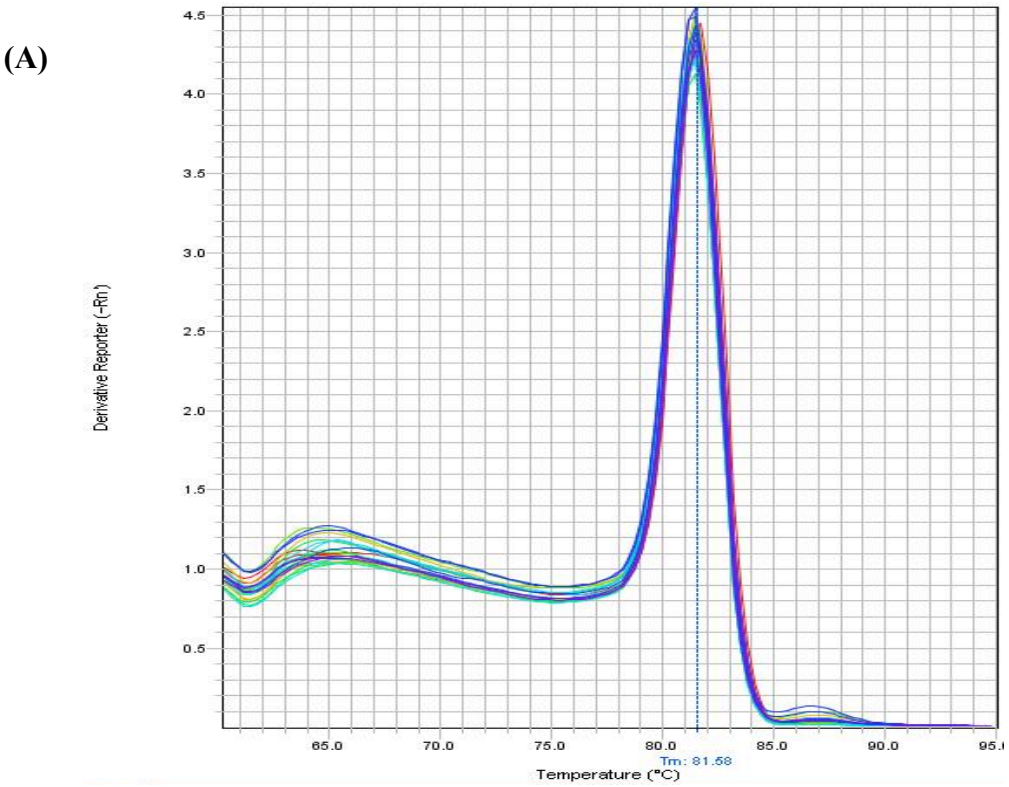


Figure 4.23 Western blot analysis showed P-p38 is up-regulated after 30 minutes following serum deprivation, peaking at 24 hours before reducing to almost undetectable levels after 72 hours (A). Serum deprivation conditions clearly did not up-regulate any of the P-c-Jun proteins (33-42kDa). (B) Serum-deprivation caused activation of Bax protein (23 kDa) after 24 hours and remained up-regulated after 96 hours. There is an initial increased in Bcl-2 (26kDa) proteins after 24 hours, followed by a slight decrease after 48 hours onwards (n=3).

4.2.5.3 qPCR analysis

To further analyse the mechanism of RGC-5 cell death by serum deprivation, RGC-5 cell lysates exposed to serum were collected for mRNA extraction and cDNA synthesis, as described previously in section 2.2.13.3 in chapter 2. In order to normalise the mRNA samples, three housekeeping genes were used, namely beta-actin (actin), actin-related protein (ARP) and beta-2-microglobulin (B_2M). To optimize all the primers, the melt curves were obtained (figures 4.21A and 4.22A) and melting temperatures (T_m) for each primers was determined, as shown table 4.1. Optimal temperatures were then calculated (i.e. 2.5°C below T_m) for maximal fluorescence measurement during each cycle of qPCR. Two examples of melt curves are shown in figure 4.24A for the B_2M gene with a size of 120bp, and in figure 4.25A for the Bax gene with a size of 365bp. To further validate each primers, the generated PCR products were separated on agarose gel and visualized using UV gel analyser. A single band at the corresponding expected molecular size for each primer suggest specificity of the primers with no non-specific PCR products amplified, as shown in figures 4.24B and 4.25B.



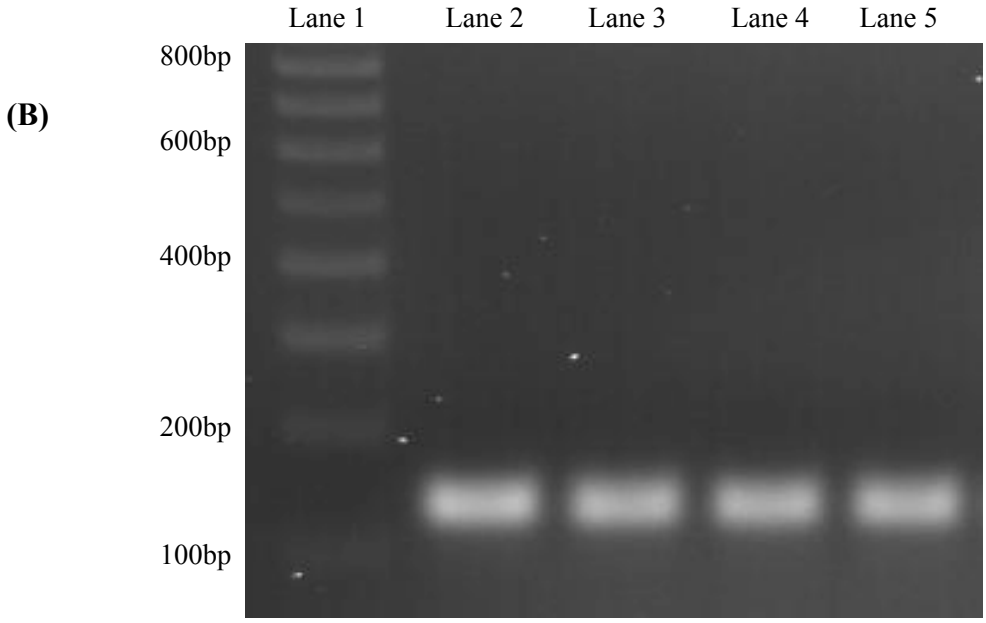


Figure 4.24: Amplification of B_2M gene. (A) Graph showing a melt curve during primer optimization step for B_2M gene. One major peak was observed at 81.6^{o}C which indicate the specificity of the primers used, with no non-specific PCR product amplified. This result corroborate with findings in (B) where the generated PCR product was further separated on the ethidium bromide-stained agarose gel. A single and clear band was observed both in control and in sample lanes (lanes 2, 3, 4 & 5) at the correct expected molecular size (120bp). Lane 2 represents cDNA from controlRGC-5 cell lysates while lanes 3, 4 and 5 represents RGC-5 cells exposed to 48, 72 and 96 hours duration of serum deprivation respectively.

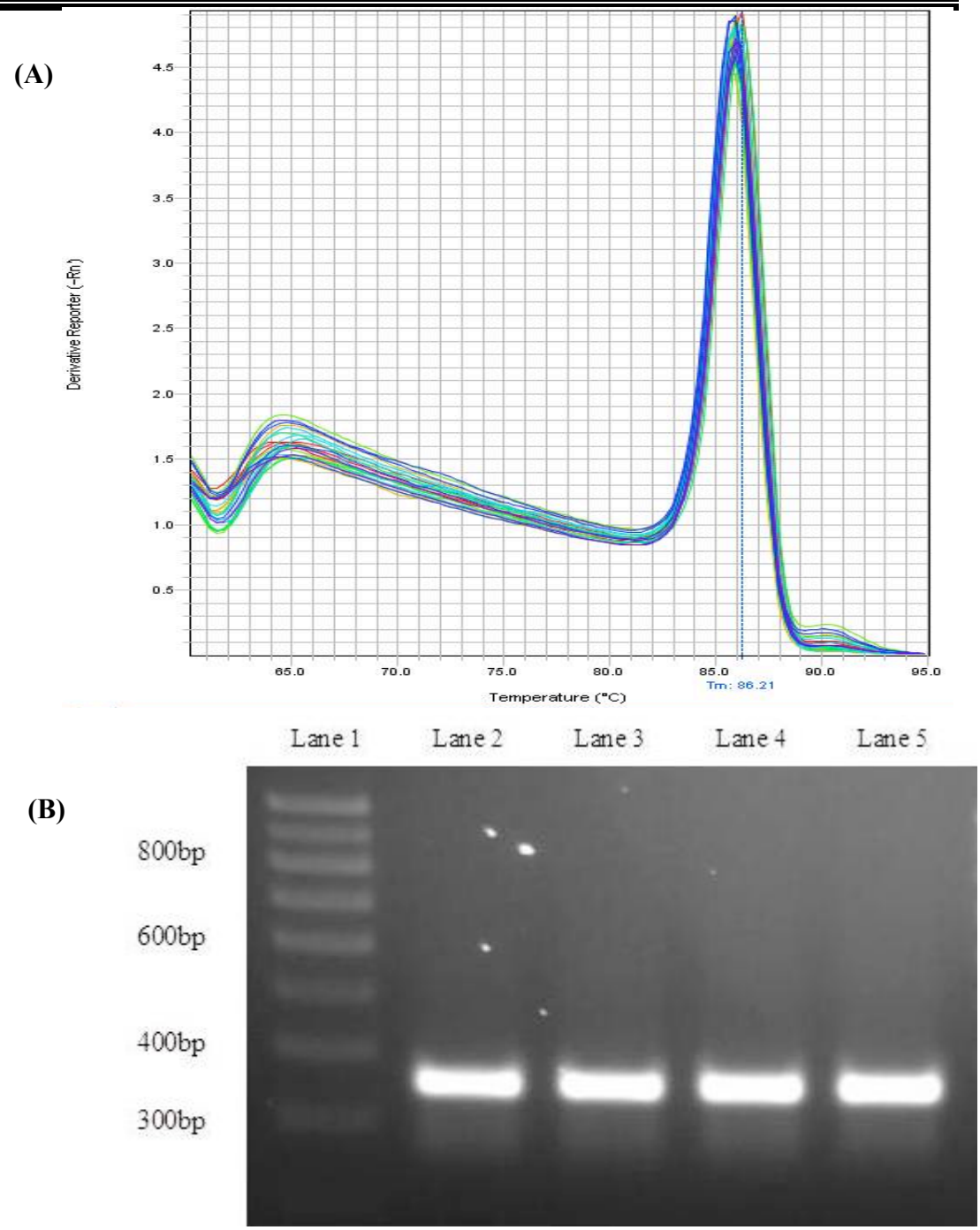


Figure 4.25: Amplification of Bax gene. (A) Graph showing a melt curve during primer optimization step for Bax gene. One major peak was observed at temperature > 80^{o}C (86.2 ^{o}C) which indicate the specificity of the primers used, with no non-specific PCR product amplified. This result was supported as in (B). When the generated PCR product was further separated on the ethidium bromide-stained agarose gel, a single and clear band was observed both in control and in sample lanes (lanes 2, 3, 4 & 5) at the correct expected molecular size (365bp). Lane 2 represents cDNA from control RGC-5 cell lysates while lanes 3, 4 and 5 represents RGC-5 cells exposed to 48, 72 and 96 hours duration of serum deprivation respectively.

Primers	T_m (°C)	Size (bp)
Genes of interest:		
Bcl-2	85.1	293
Bax	86.2	365
HO-1	84.0	285
Nrf-2	82.2	597
Housekeeping genes:		
Actin	86.3	514
B_2M	81.6	120
ARP	78.5	317

Table 4.1 showing the melting temperatures (T_m) and the sizes measured in basepairs (bp) for each primer used in qpCR analysis.

The samples were measured for Bax and Bcl-2 genes expression compared to untreated control. Figure 4.26 shows that serum deprivation decreases Bcl-2 but increases Bax gene expression after 48 hours, peaking at almost 2-fold change after 72 hours. The Bax/Bcl-2 ratio is maximal after 72 hours, however these changes were not statistically significant.

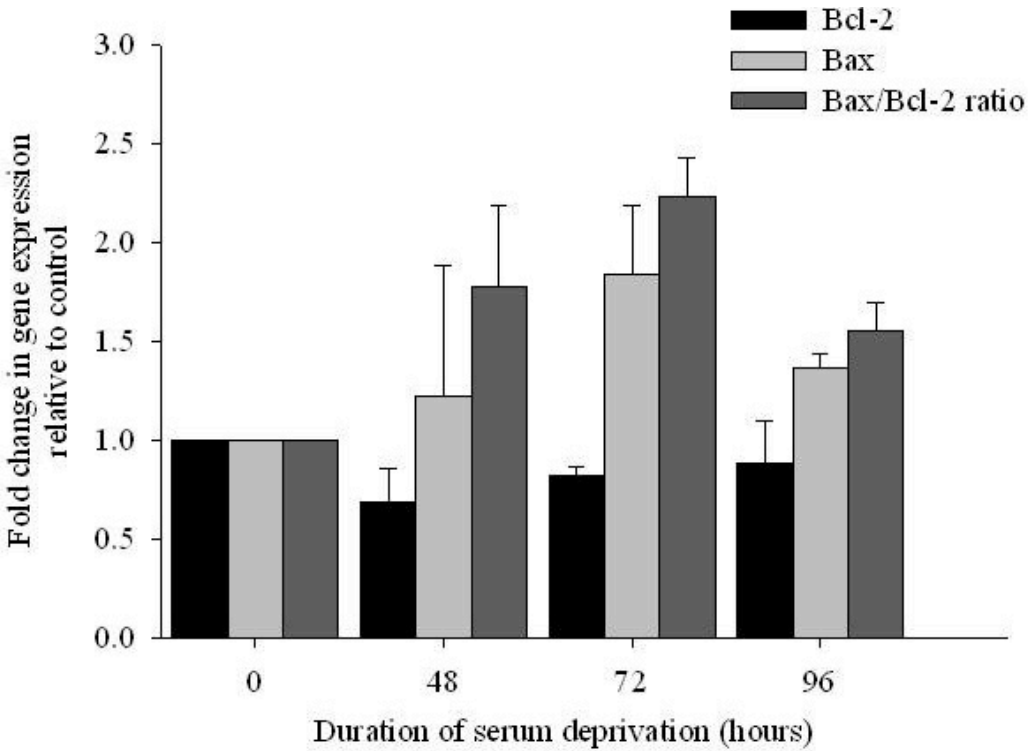


Figure 4.26. RGC-5 cells were exposed to serum deprivation in a time-dependent manner and analysed for Bax and Bcl-2 gene expression using qPCR. Serum deprivation caused a decrease in Bcl-2 but an increase in Bax gene expression. Values are calculated as mean fold change ± SEM of at least 3 experiments.

4.2.6 Effects of flavonoids alone on RGC-5 cells

In order to assess the early effects of genistein, EC and EGCG on RGC-5 cells, mRNA was extracted from cell lysates after 9 hours incubation followed by cDNA synthesis for downstream processing. Each sample was tested in duplicates. The relative difference was expressed as x-fold change of flavonoid-treated RGC-5 cells over control samples by using the $2^{-\Delta\Delta C}{}_T$ method. Agarose gel electrophoresis was used to confirm the reaction products had the expected size. The bands were visualised under UV light as shown in figure 4.27. The formation of a single product was also confirmed by observing the melting curve graph that was generated by the sequence-detection system for each reaction.

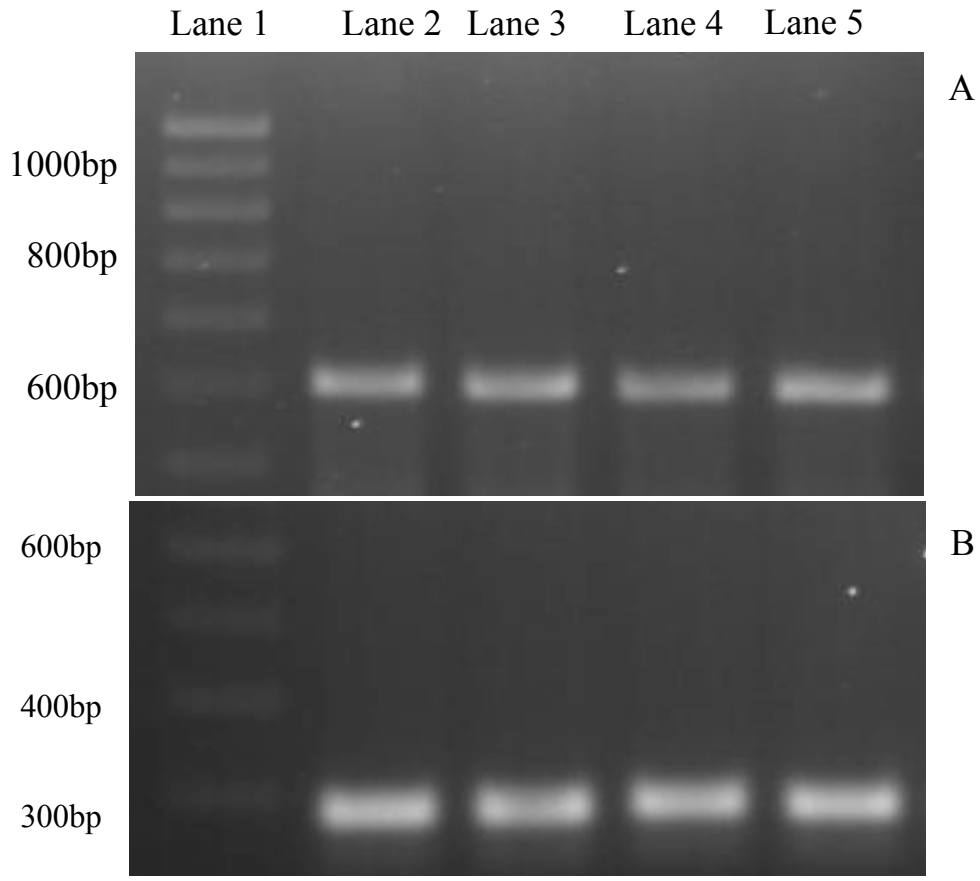


Figure 4.27 To validate each primers, the generated amplified PCR products were separated on 2% agarose gel and visualized using UV gel analyser. A single product is seen as a single band at the corresponding expected molecular size for each primer suggests specificity of the primers with no non-specific PCR products amplified. Representative bands which correspond to the respective molecular sizes of each primer: are shown above: (A) Nrf-2 (597bp) and (B) Bcl-2 (293bp). The bands are not analysed using densitometry but serve only as a representative of the amplified PCR products. Lane 1: molecular marker, lane 2: control, lane 3: genistein 10μM, lane 4: EC 50μM and lane 5: EGCG 50μM.

There was no statistically significant change in mRNA levels of Nrf-2, HO-1 and Bcl-2 in RGC-5 cells after 9 hours of exposure to genistein 10μM, EC 50μM and EGCG 50μM as shown in Figure 4.28. However EC 50μM showed almost 2-fold increase in Nrf-2 mRNA expression and 1.4-fold increase in HO-1 expression. Genistein and EGCG cause only a slight increase of HO-1 mRNA expression in RGC-5 cells. There was no significant change in the Bcl-2 mRNA level observed.

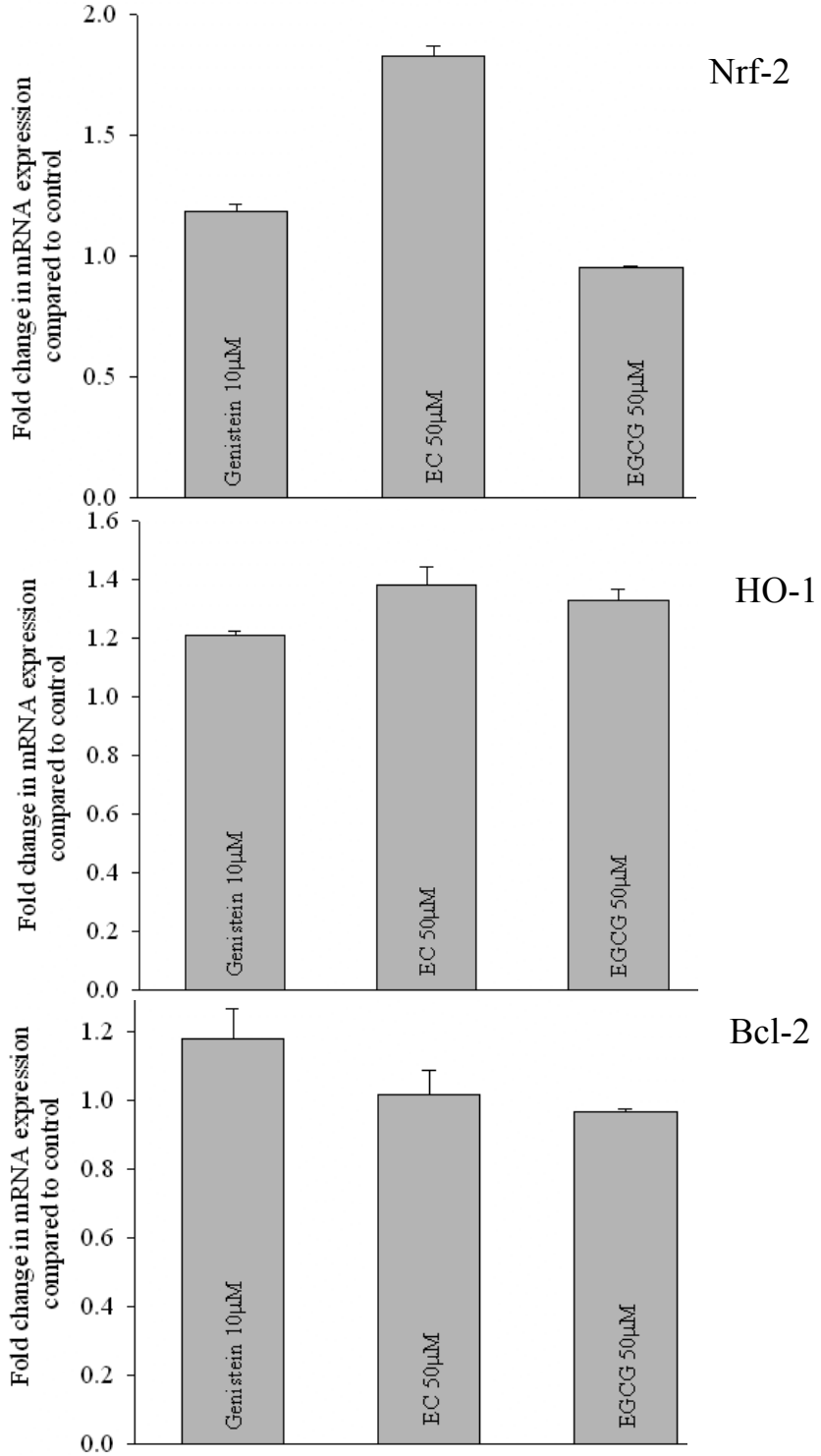


Figure 4.28 Expressions of mRNA of Nrf-2, HO-1, and Bcl-2 in RGC-5 cell cultures after 9-hour exposure to genistein 10µM, EC 50µM and EGCG 50µM were calculated using the $2^{-\Delta\Delta C}{}_T$ method and compared to untreated control. Samples were analysed in duplicates and data is expressed as fold in gene expression compared to control values (mean ± SD). Genistein and EC increased Nrf-2 mRNA expression, however the change is not statistically significant. All three flavonoids increased the HO-1 mRNA expression slightly and only genistein cause a slight increase in Bcl-2 expression.

4.3 Discussion

Lipid peroxidation studies showed that EGCG, EC and genistein have antioxidant properties (see figures 4.2-4.4). Lipid peroxidation occurs as a result of oxidative stress-induced damage to the lipid contents in biological membranes, such as cholesterol and fatty acid moieties. Thiobarbituric acid (TBA) reactivity is considered an index of lipid peroxidation, and is measured by the level of carbonyl by-products of which, the most important is believed to be 3-carbon aldehyde, malonaldehyde (MDA) (Girotti 1985). Janero showed that the MDA-TBA reactivity provide a diagnostic index to detect and measure lipid peroxidation and peroxidative tissue injury (Janero 1990). In the present study, rat brain homogenates were used as a source of lipids for the MDA-TBA reaction. Sodium nitroprusside (SNP) has been shown previously to be a potent oxidant in stimulating lipid peroxidation (Osborne & Wood 2004). It acts by donating nitrous oxide (NO) in an aqueous environment, which subsequently leads to the excessive production of free radicals (Kishnani & Fung 1996). A paper by Zhang and Osborne reported that EGCG effectively inhibit SNP-induced TBARS formation with an IC_{50} value of 0.8μM (Zhang & Osborne 2006). In the present study we show that EC (IC_{50} value 1.5μM) and EGCG (IC_{50} value 2.5μM) are approximately 20-fold more potent as antioxidants compared to genistein (IC_{50} value 39μM). Thus based on the lipid peroxidation data one might expect that the order of effectiveness for the individual flavonoid as an antioxidant is EC>EGCG>genistein.

In this chapter, we showed that among the three flavonoids, EGCG and EC are the safest compounds, having no detrimental effects on RGC-5 cells in culture at

concentrations below 100μM. In contrast, genistein caused significant reduction of RGC-5 cell survival after 24 hours at concentrations of 25μM upwards.

It is generally thought than oxidative stress plays a part in the pathogenesis of glaucoma (Izzotti *et al* 2006, Tezel 2006) initiated by ischemia to the optic nerve head components (Flammer & Orgul 1998, Osborne *et al* 2001) because of a reduced optic nerve head blood supply (Flammer & Orgul 1998). An increase in lipid peroxidation products (Birich *et al* 1986) and decrease in glutathione (Gherghel *et al* 2005) occur in the serum of POAG patients. Lipid peroxidation assays provide an insight into the mechanism by which a substance may alleviate oxidative stress, especially in intact cell systems. To deliver an insult that selectively causes oxidative stress to retinal ganglion cells *in situ* is virtually impossible. Nevertheless, it is possible to obtain partial knowledge on the effects of defined insults on retinal ganglion cells by using a cell culture system where a selective oxidative stress may be delivered. The retinal ganglion cell line RGC-5 (Krishnamoorthy *et al* 2001) enabled studies of H_2O_2-induced oxidative stress in such a cell system to be carried out. Our data confirms that exposure of RGC-5 cells to H_2O_2 results cell death in a dose-dependent manner (figure 4.8A), causes ROS generation (figure 4.10) and cell death by apoptosis (figures 4.11 & 4.13), as previously reported (Li & Osborne 2008). It also shows that EC attenuates this process to a similar degree to EGCG (Zhang *et al* 2007). However, genistein did not show any protective effect on RGC-5 cell survival at a non-toxic concentration of 10μM. These findings corroborate the lipid peroxidation results that showed that genistein has the weakest antioxidant activity out of the three flavonoids.

Glutamate has been implicated as a mechanism of RGC death in glaucoma (Dreyer *et al* 1996, Osborne *et al* 1999, Levin 2003, Lotery 2005, Salt & Cordeiro 2006).

Glutamate causes excitotoxicity by overstimulation of glutamate receptor, N-methyl-D aspartate (NMDA) (Frandsen *et al* 1989), generating a cascade of events resulting in an overload of intracellular calcium (Choi 1987, Frandsen *et al* 1989) and release of nitric oxide (Hoyt *et al* 1992, Luo *et al* 1993), which subsequently leads to generation of reactive oxygen species and cell death. Krishnamoorthy et al (Krishnamoorthy *et al* 2001) demonstrated that RGC-5 cells are resistant to glutamate toxicity in its undifferentiated form. In these experiments, we used undifferentiated RGC-5 cells, and found that their sensitivity to glutamate toxicity is increased with the concomitant use of 1mM buthionine sulfoximine (BSO), which is an inhibitor of GSH production. In the early stages of glutamate neurotoxicity in the cerebral cortex, GSH levels are reduced with an increase in peroxynitrite production (Kumar *et al* 2010). This explains the increased sensitivity of RGC-5 cells to glutamate neurotoxicity when co-treated with BSO. Glutamate causes RGC-5 cell death by apoptosis (figure 4.18) in a dose-dependent manner (figure 4.15). Mitochondrial dysfunction has been implicated in glutamate-induced cell death (Dugan *et al* 1995, Schinder *et al* 1996, White & Reynolds 1996, Castilho *et al* 1999), and this is confirmed by the reduction of mitochondrial dehydrogenase activity in RGC-5 cells caused by glutamate toxicity (figure 4.17). Interestingly, we found that there is a differential effect between the two green tea flavonoids, EGCG and EC in ameliorating glutamate-induced toxicity in RGC-5 cells. The results showed that only EC 50μM was able to significantly attenuate glutamate-induced RGC-5 cell death (figure 4.16), and preserve mitochondrial dehydrogenase activity (figure 4.17). However, neither EGCG nor genistein have any protective effect on RGC-5 cells against glutamate-induced cell death.

The different effects of the two green tea flavonoids, EC and EGCG, and genistein in attenuating glutamate-induced cell death, may be partly explained by the possible specificity of the structure-activity relationship. Ishige *et al* (Ishige *et al* 2001) suggested that three structural features of flavonoids are required for protection against glutamate neurotoxicity: hydroxylated C3, an unsaturated C ring and hydrophobicity. Among the three flavonoids, genistein does not contain hydroxylated C3, although it has an unsaturated C ring. On the other hand, although both EC and EGCG contain a saturated C ring, EC is more hydrophobic relative to EGCG and has a higher affinity towards lipid bilayers (Nakayama *et al* 2000, Kajiya *et al* 2002).

Genistein has been shown to reduce glutamate-induced cell death in the primary mouse hippocampal culture (Kajta *et al* 2007) and the human cortical cell line HCN 1-A (Occhiuto *et al* 2008). Genistein exerts its neuroprotective effects by binding to estrogenic receptors on the neuronal cells (Bang *et al* 2004, Kajta *et al* 2007), specifically to the beta subtype of the estrogen receptor, ERβ (Donzelli *et al* 2010). Genistein is a relatively selective ERβ agonist and binds to ERα at seven to eight times lower affinity compared to ERβ (Kuiper *et al* 1998). Kumar *et al* demonstrated that the ERβ subtype is scarce compared to Erα which is present in abundance in RGC-5 cells (Kumar *et al* 2005). This may explain, in part, the results of our study which showed that genistein does not demonstrate any neuroprotective activity against glutamate-induced cell death.

Reduced neurotrophic support is one of the insults that might cause retinal ganglion cell death in glaucoma, as a result of obstruction of axonal transport within the optic nerve head (Quigley & Addicks 1980, Aguayo *et al* 1996, Nickells 1996, Fawcett *et al* 1998, Pease *et al* 2000). In fact, Wadia and colleagues hypothesized that trophic

withdrawal was a primary cause in the pathogenesis of glaucoma (Wadia *et al* 1998). Therefore, an insult of serum deprivation was used to simulate the effect of reduced neurotrophic support to retinal ganglion cells *in situ*, and to study the neuroprotective effects of the selected flavonoids in attenuating cell death. Cell viability studies showed that serum deprivation caused RGC-5 cell death in a time-dependent manner, causing almost 40% cell death after 48 hours (figure 4.20). We confirmed the results of earlier studies that showed serum deprivation caused oxidative stress as shown by the increased ROS production in RGC-5 cells in figure 4.21D (Jung *et al* 2008). Neuronal cell death caused by serum deprivation has been shown to occur by apoptosis (Liu & Zhu 1999, Charles *et al* 2005, Jung *et al* 2008) involving mitochondrial signaling pathways (Liu & Zhu 1999, Charles *et al* 2005). It is also known that serum deprivation causes activation of the mitogen-activated protein kinase pathways (MAPK) leading to apoptotic cell death (Yeste-Velasco *et al* 2009, Lee *et al* 2010). Western blot analysis showed that serum deprivation caused RGC-5 cell death by p38 and mitochondrial signaling pathways. Figure 4.23 shows that serum deprivation causes up-regulation of phosphorylated p38 (P-p38) but not the JNK pathway (P-c-Jun). Serum deprivation also causes up-regulation of Bax protein, which is a pro-apoptotic mitochondrial protein. This was further confirmed by real-time PCR analysis which showed almost 2-fold increase in Bax/Bcl-2 ratio after 72 hours of serum deprivation (Figure 4.26). These findings corroborate with previous reports on serum deprivation-induced cell death in RGC-5 cells (Charles *et al* 2005, Shao *et al* 2012) and primary cortical neurons (Liu & Zhu 1999) involving up-regulation of Bax with down-regulation of Bcl-2 proteins. As shown in figure 4.22, none of the selected flavonoids showed any protection against serum deprivation-

induced RGC-5 cell death. This seems to suggest that flavonoids do not depend solely on their anti-oxidant capabilities to exert neuroprotective effects but instead have multiple modes of actions that encourage neuronal cell survival.

Alteration of cellular redox balance as a result of elevated levels of ROS and/or reduced endogenous antioxidant capacity appears to trigger a transcriptional response to induce the gene expression of cytoprotective enzymes (Friling *et al* 1990). This response is mediated by a DNA element that regulates basal expression of genes encoding antioxidant enzymes such as glutathione-S-transferase (GST), and is called "antioxidant response element" (ARE) (Dhakshinamoorthy *et al* 2000, Jaiswal 2000, Bloom *et al* 2001). Nuclear factor erythroid 2-related factor 2, or Nrf-2, is a transcription factor that binds to ARE in response to oxidative stress and activates the ARE-mediated induction of antioxidant enzyme gene expression (Kang *et al* 2004, Wakabayashi *et al* 2004). In our study, real-time PCR analysis showed that EC caused a 1.8-fold increase in Nrf-2 gene expression after 9 hours in RGC-5 cells compared to a small increase caused by genistein (figure 4.25). EGCG did not affect Nrf-2 gene expression after 9 hours. Work from other laboratories has demonstrated that activation of the Nrf-2-ARE pathway provides protection from glutamate- and H_2O_2-induced cell death (Shih *et al* 2003, Kraft *et al* 2004). This may explain in part, the ability of EC to protect RGC-5 cell death from glutamate-induced cell death compared to genistein and EGCG (figure 4.16).

The microsomal enzyme heme oxygenase (HO) was first reported by Schmid and colleagues in 1968, who described the enzymatic conversion of heme to bilirubin using microsomal fractions from various tissues (Tenhunen *et al* 1968, Tenhunen *et al* 1969b, Tenhunen *et al* 1969a). HO is the rate-limiting enzyme in heme degradation to

CO, iron and biliverdin. There are 3 isoforms of HO, namely HO-1, HO-2 and HO-3. HO-1, also known as heat shock protein 32 (HSP32), exists at undetectable levels in most tissues and cell types until a stress condition arises, whereas HO-2 and HO-3 may exist at detectable levels in most tissues in the absence of stress. Several evidences have shown that HO-1 confers cellular protection against oxidative stress through anti-oxidative, anti-apoptotic and anti-inflammatory actions (Vile *et al* 1994, Abraham *et al* 1995, Otterbein *et al* 2000, Petrache *et al* 2000). HO-1 has been shown to be up-regulated in response to oxidative stress induced by increased hydrostatic pressure in retinal ganglion cells both *in vitro* and *in vivo* (Liu *et al* 2007). Evidence that HO-1 is involved in glaucoma was given by Peng and colleagues (Peng *et al* 2008) who demonstrated that overexpression of HO-1 was able to protect retinal ganglion cells against ischaemia/reperfusion injury (Hegazy *et al* 2000, Peng *et al* 2008). An increase in HO-1 gene expression was seen in RGC-5 cells treated with genistein and EGCG as shown in Figure 4.26. EGCG has been reported to up-regulate HO-1 via the MAPK kinase pathways (Wu *et al* 2006a, Wu *et al* 2006b, Pullikotil *et al* 2011). These findings corroborate with previous results that showed retinal ganglion cell protection by both genistein (Chapter 3) (Kamalden *et al* 2011) and EGCG against ischaemia/reperfusion injury (Zhang *et al* 2008).

The findings of this chapter demonstrate that EC, EGCG and genistein have differential effects on RGC-5 cells when exposed to defined oxidative stress *in vitro*. It can be concluded that the protective effects of flavonoids do not depend solely on their antioxidant capacity, but instead act by activating multiple signaling pathways.

CHAPTER 5

ROTENONE-INDUCED DEATH OF CULTURED RGC-5 CELLS IS CASPASE INDEPENDENT, INVOLVES THE JNK AND p38 PATHWAYS AND IS ATTENUATED BY SPECIFIC GREEN TEA FLAVONOIDS

5.1 Introduction

5.1.1 Aim

A] To characterise the death process of RGC-5 cells following inhibition of mitochondrial complex I using rotenone. **B]** To examine the possible neuroprotective properties of the flavonoids genistein, epigallocatechin gallate (EGCG), epicatechin (EC) and baicalin.

5.1.2 Brief overview

Retinal ganglion cell (RGC) axons within the human eye have a very rich supply of mitochondria (Bristow *et al* 2002, Munemasa *et al* 2010) and abundant evidence exists to show that optimum mitochondrial function is necessary for neuronal survival (Ankarcrona *et al* 2010, Patten *et al* 2010). Mitochondrial dysfunctions have a strong link for the cause of neuronal death in various CNS diseases that include glaucoma (Lee *et al* 2011). For example, RGC intra-axonal mitochondria are directly affected in a rat animal model of glaucoma (Munemasa *et al* 2010). Moreover, light has been proposed to be a risk factor in patients with glaucoma (Osborne *et al* 2006) and is known to cause cell death *in vitro* by directly interacting with their mitochondria (Osborne *et al* 2008).

The proton-translocating NADH-quinone oxidoreductase or complex I (DiMauro & Schon 2003) is the first of four enzyme complexes in the mammalian mitochondrial respiratory chain. Significantly, a dysfunction in complex I occurs in a large number of human diseases such as myopathies (DiMauro *et al* 1985, Acsadi *et al* 2009, Cordero *et al* 2010, Schon *et al* 2010), stroke-like syndrome (DiMauro & Schon 2003, Santa 2010, Witte *et al* 2010) and Leber's hereditary optic neuropathy (Wallace *et al* 1988, Qi *et al* 2007). A diminution of complex I also occurs in certain

neurodegenerative diseases, such as Parkinson's disease where the amount of complex I in the brain is reduced (Schapira *et al* 1998, Chinta & Andersen 2011). In addition, a selective loss of brain dopamine pathways, formation of Lewy bodies and motor tremor are associated with a rat animal model of Parkinson's disease following appropriate administration of 1-methyl-4-phenylpyridinium ion (MPTP) or rotenone that selectively inhibit complex I (Ramsay *et al* 1986, Betarbet *et al* 2000, Alam & Schmidt 2002, Hirsch *et al* 2003).

Inhibition of complex 1 by intravitreal injection of the rotenone into the mouse eye more-or-less selectively causes a loss of RGCs in the retina (Zhang *et al* 2002, Zhang *et al* 2006). Studies on this animal model have been carried out in an attempt to learn more about Leber's hereditary optic neuropathy where RGC death occurs because of a genetic defect in complex I (Yu-Wai-Man *et al* 2011). Experiments have also been conducted on primary rat retinal cultures (Beretta *et al* 2006, Kretz *et al* 2007) in an attempt to understand more clearly the mechanism by which inhibition of complex I with rotenone result in RGC death. However, unequivocal biochemical data on primary retinal cell cultures can be difficult to achieve because of varying numbers of RGCs and the existence of other retinal cell-types. We have therefore used a pure cell line (RGC-5) which while having limited RGC properties does allow for a more precise understanding of the mechanism by which cells die following complex I inhibition. It also allows us to compare information from previous studies where the death mechanisms of RGC-5 cells caused by sodium azide (inhibitor complex IV) and light have been described and shown to be different (Ji *et al* 2011). Another aim of the present studies was to determine whether certain types of flavonoids are better than others at blunting the negative influence of rotenone to RGC-5 cells. Flavonoids are present in various fruits, vegetables, grains, coffee and tea, can be tolerated when

consumed in fairly significant amounts and have known medicinal benefits to man for a number of diseases and conditions (Cody 1988, Kuppusamy *et al* 1990). The possibility of using such substances to treat a chronic disease like glaucoma where RGCs die is one worthy of consideration.

5.1.3 Summary of results

The result of the studies in this chapter can be summarized as follows:

1) Rotenone reduced cell viability of RGC-5 cells in a dose-dependent manner.
2) Rotenone-induced death of RGC-5 cells results in a generation of ROS, the breakdown of DNA, translocation of membrane phosphatidylserine, and is unaffected by necrostatin-1, z-VAD-fmk or NU1025.
3) Rotenone-induced toxicity of RGC-5 cells causes an activation of mitogen-activated kinases (MAPKs) indicated by an up-regulation of P-p38 and an increase and translocation into mitochondria of P-c-Jun and P-JNK. Exposure of RGC-5 cells to rotenone does not affect apoptosis inducing factor (AIF) or significantly stimulate caspase-3 activity.
4) EGCG and EC both significantly blunted rotenone toxicity of RGC-5 cells at concentrations of 10μM while genistein and baicalin were without effect.
5) Genistein attenuates lipid peroxidation less efficaciously than EC and EGCG and does not affect rotenone toxicity of RGC-5 cells.

5.2 Results

5.2.1 Assessment of cell viability

All studies were conducted on RGC-5 cells, grown overnight to desired confluence in 96- or 6-well plates or on coverslips in 24-well plates. The effect of rotenone on the viability of RGC-5 cells in culture over 24 hours was assessed using an MTT assay. As shown in Figure 5.1, rotenone significantly reduces cell viability in a dose-dependent manner with 10μM rotenone causing 28% cell death over 24 hours.

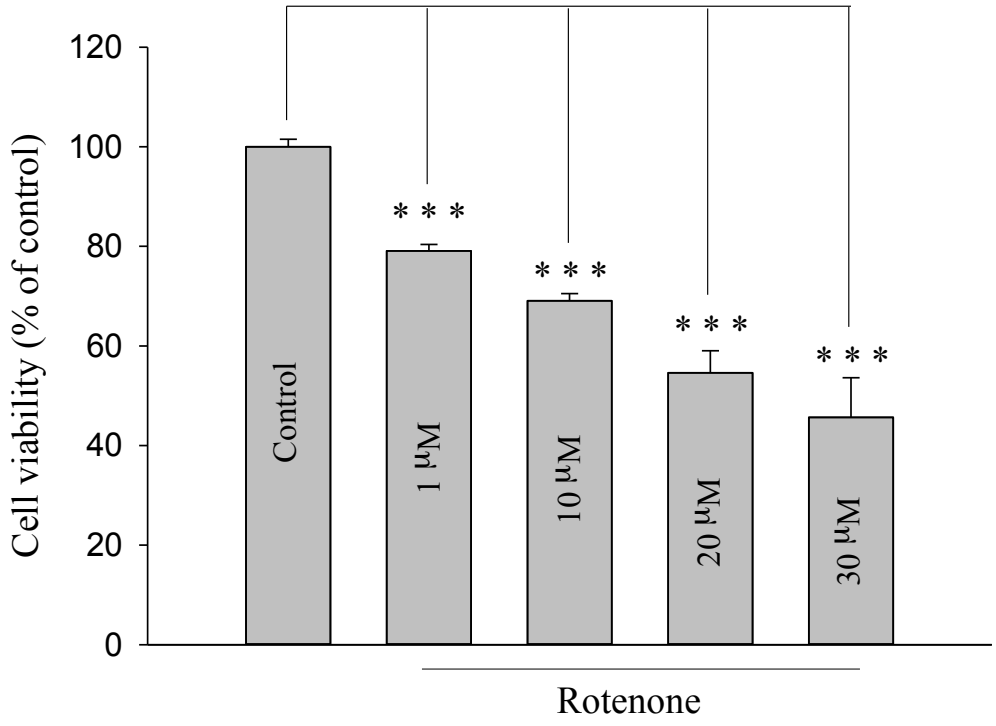


Figure 5.1. In these studies, 96-well plates were plated with RGC-5 cells and left overnight before being exposed to increasing concentrations of rotenone for 24 hours. Cell viability was measured by MTT assay. It is very clear that rotenone causes a dose-dependent reduction of RGC-5 cell viability compared to untreated (control) cells. At a concentration of 10μM, rotenone reduced the RGC-5 cell viability by 28%. Values are expressed as percentage of control and are the mean ± SEM of 5 individual experiments, each analysed at least in triplicates. Significant differences (***$p<0.001$) are calculated by one-way ANOVA followed by Tukey multiple comparative test.

Since 10μM rotenone caused approximately 28% loss of RGC-5 cell viability over a period of 24 hours this amount of rotenone was used in subsequent experiments. Figures 5.2 and 5.3 show that EGCG and EC significantly attenuated RGC-5 cell death caused by 10μM rotenone between concentrations of 10-75μM peaking slightly in each case at 50μM. Moreover, 50μM EGCG, EC or 2mM trolox were in all intensive purposes equally effective at nullifying rotenone-induced loss of cell viability. In contrast to EC 50μM and EGCG 50μM, the flavonoids baicalin and genistein at 10μM each were without effect (figure 5.4).

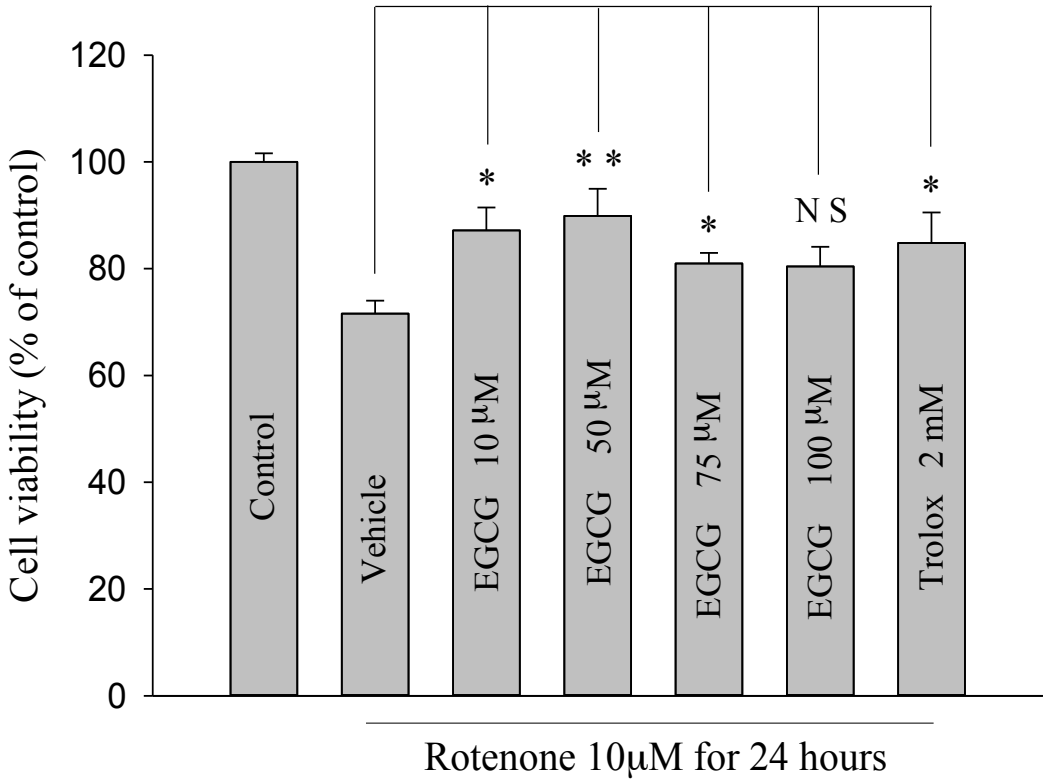


Figure 5.2. This figure shows the effect of EGCG in attenuating the effects of rotenone on RGC-5 cell cultures. Cell viability was measured using a MTT assay. Compared to rotenone-treated cells alone (vehicle), EGCG significantly increased cell viability in a dose-dependent manner, peaking at 50μM. In this study, 2mM trolox (vitamin E analogue) was used as a positive control, significantly attenuated rotenone-induced reduction in cell viability. Values are expressed as means ± SEM of at least 5 independent experiments. Statistical differences (***$p<0.001$) were calculated by a one-way ANOVA followed by Tukey multiple comparative test. (NS = not significant)

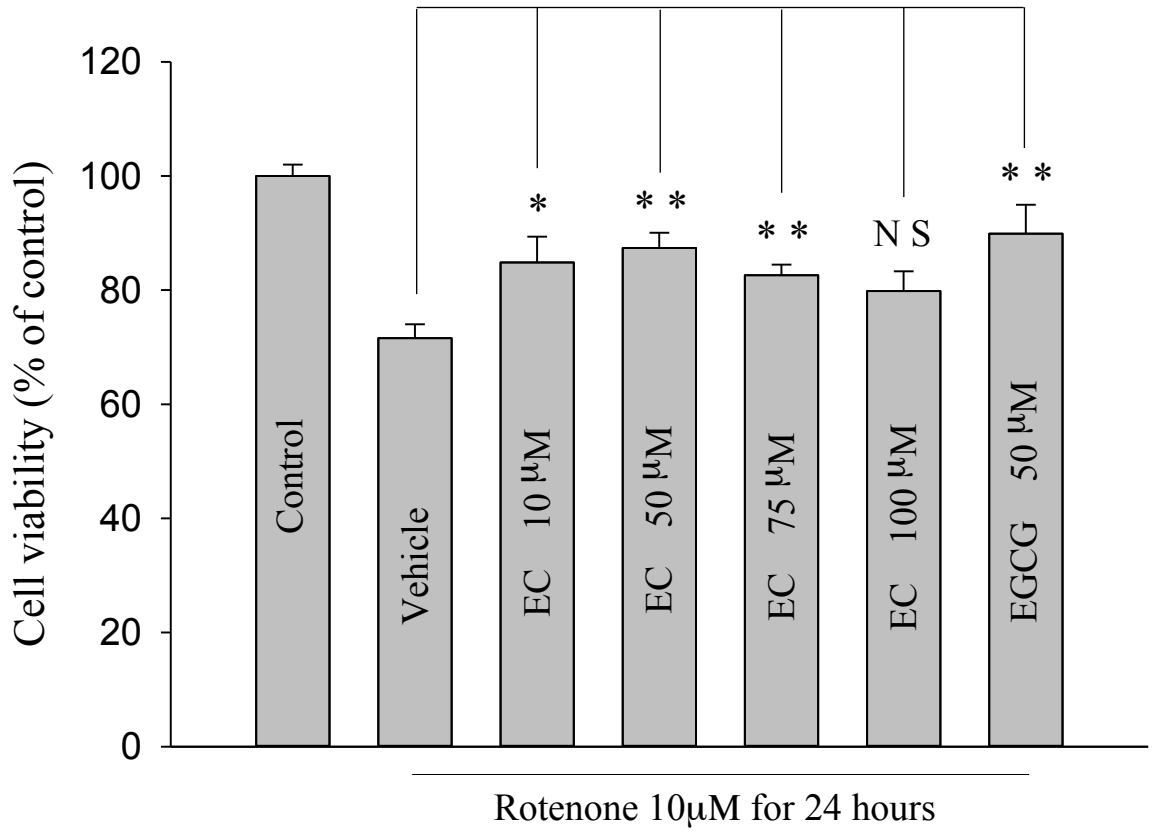


Figure 5.3. This figure shows the effect of EC in attenuating the effect of rotenone on RGC-5 cell cultures over 24 hours. Cell viability was measured using a MTT assay. Compared to rotenone-treated cells alone (vehicle), EC significantly increased cell viability in a dose-dependent manner, peaking at 50μM. In this study, EGCG was used as a positive control, and significantly attenuated rotenone-induced reduction in cell viability. Values are expressed as means, ± SEM of at least 5 independent experiments. Statistical differences (***$p<0.001$) were calculated by one-way ANOVA followed by a Tukey multiple comparative test. (NS = not significant)

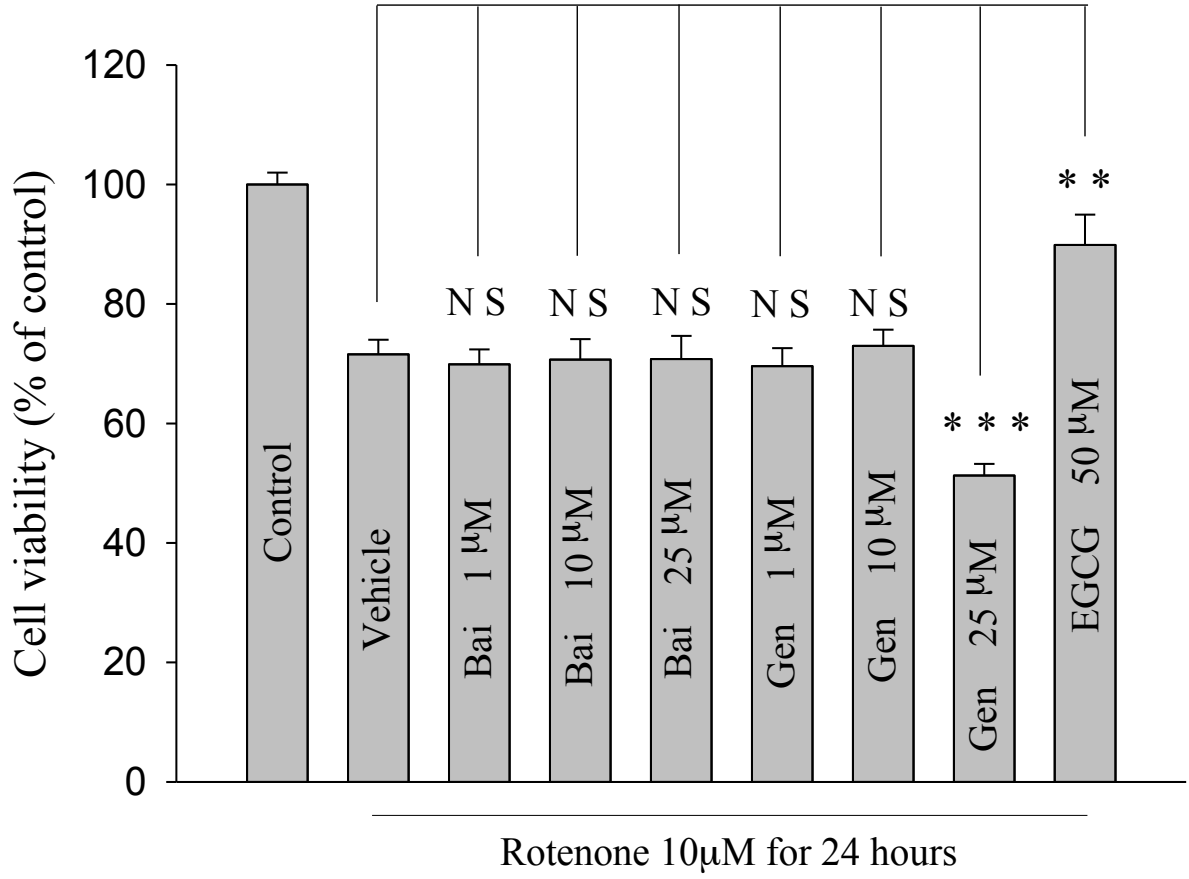


Figure 5.4. This figure shows the effects of baicalin and genistein on RGC-5 cell cultures exposed to rotenone for 24 hours. Cell viability was measured using a MTT assay. EGCG (50μM) was used as a comparative control significantly attenuating the influence of rotenone. Both baicalin (1-25 μM) and genistein (1-10 μM) had no effect at attenuating the influence of rotenone. Moreover, genistein 25μM caused a further reduction in cell viability caused by rotenone. Values are expressed as mean ± SEM of at least 5 independent experiments. Statistical differences (***$p<0.001$) are calculated by one-way ANOVA followed by a Tukey multiple comparative test. (NS = not significant)

Rotenone-induced loss of cell viability is significantly attenuated by 100-200μM of the JNK inhibitor SP600125 but to a lesser extent than in comparison with EC 50μM, as shown in figure 5.5. In contrast to JNK inhibitor, the pan-caspase inhibitor, z-VAD-fmk (figure 5.6), the PARP inhibitor, NU1025 (figure 5.7) and the necroptosis inhibitor, necrostatin-1 (figure 5.8) were without influence on rotenone-induced toxicity at all concentrations tested when compared with EC 50μM.

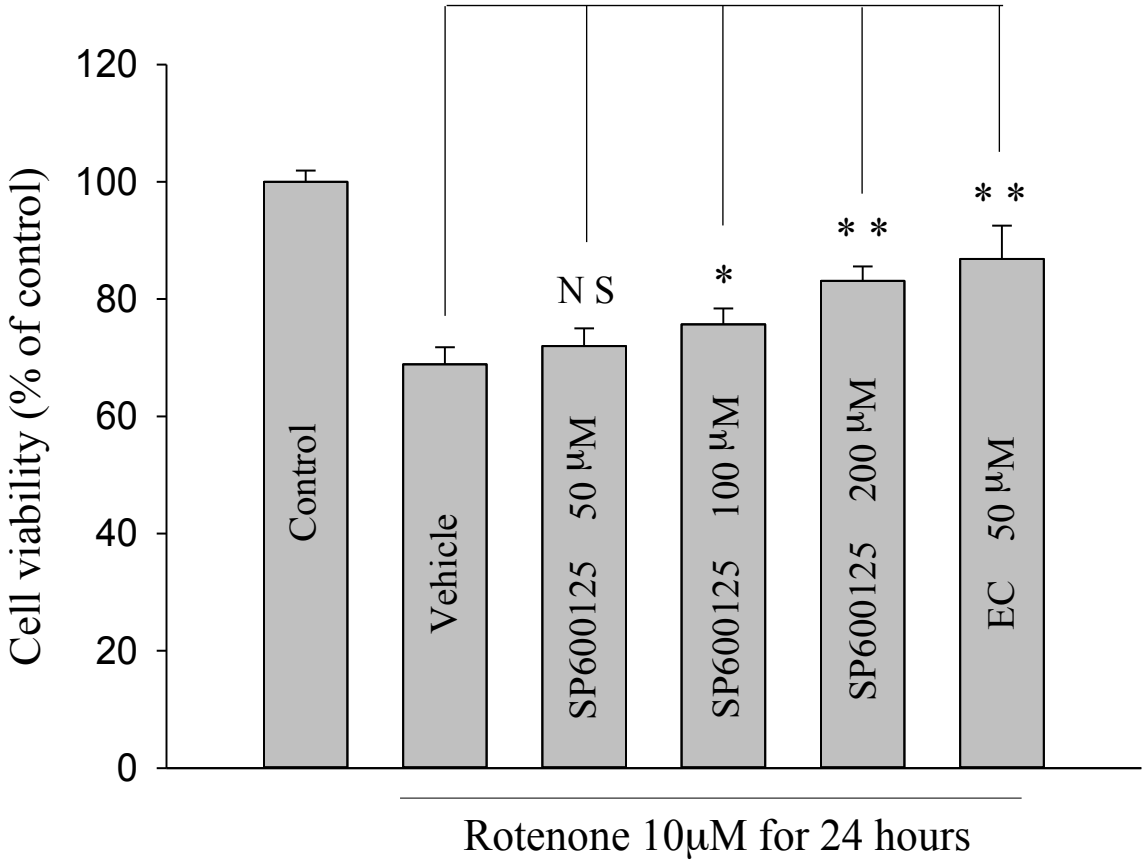


Figure 5.5. This figure shows the effect of JNK inhibitor, SP600125 on RGC-5 cell cultures exposed to rotenone for 24 hours. Cell viability was measured using a MTT assay. In this study, EC 50μM was used as a comparative control, and significantly attenuated rotenone-induced reduction of cell viability. The effect of rotenone is also significantly attenuated by SP600125 at 100μM and 200μM. Values are expressed as means, ± SEM of at least 5 independent experiments. Statistical differences (* $p<0.05$, ** $p<0.01$, *** $p<0.001$) were calculated by one-way ANOVA followed by a Tukey multiple comparative test. (NS = not significant)

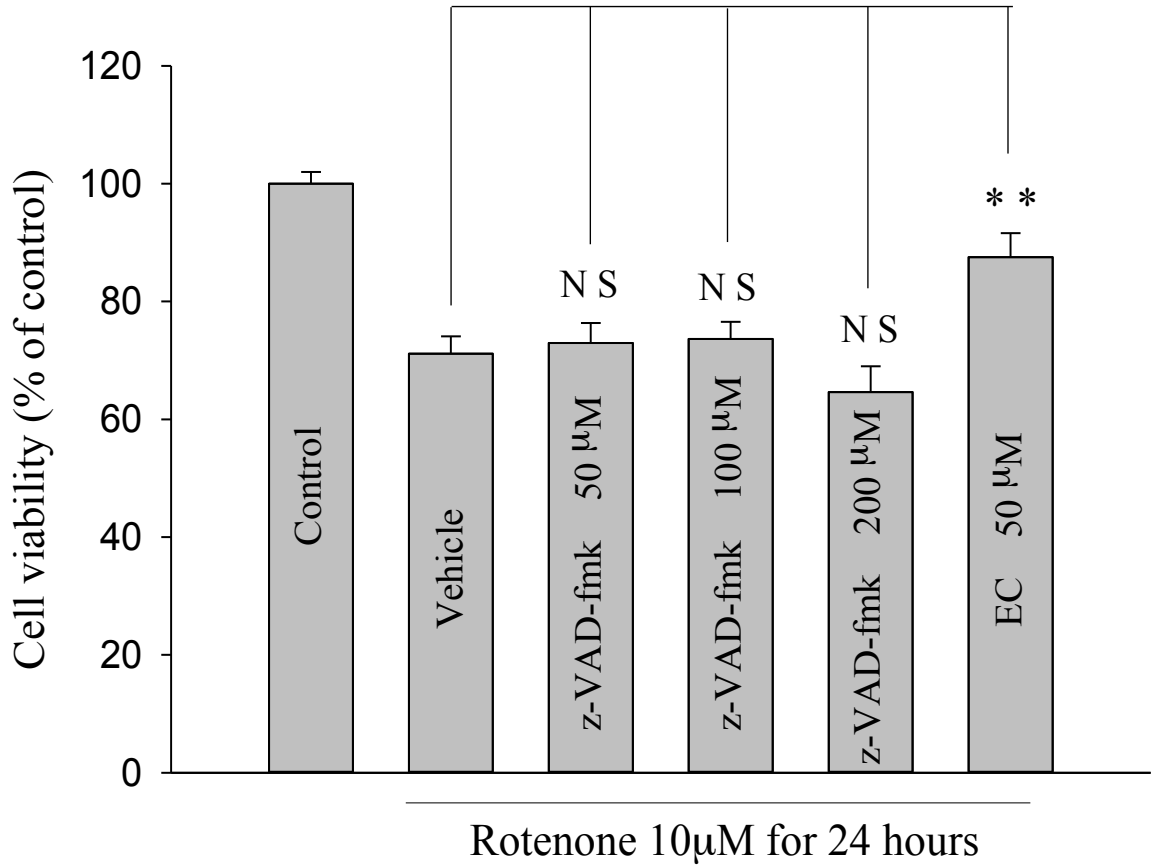


Figure 5.6. This figure shows the effect of a pan-caspase inhibitor, z-VAD-fmk in RGC-5 cell cultures exposed to rotenone for 24 hours. Cell viability is measured using MTT assay. In this study, EC 50μM is used as positive control, and significantly attenuated rotenone-induced reduction in cell viability. The pan-caspase inhibitor did not enhance cell survival at all concentrations tested. Values are expressed as means ± SEM of at least 5 independent experiments. Statistical differences **$p<0.01$ are calculated by one-way ANOVA followed by Tukey multiple comparative test. (NS = not significant)

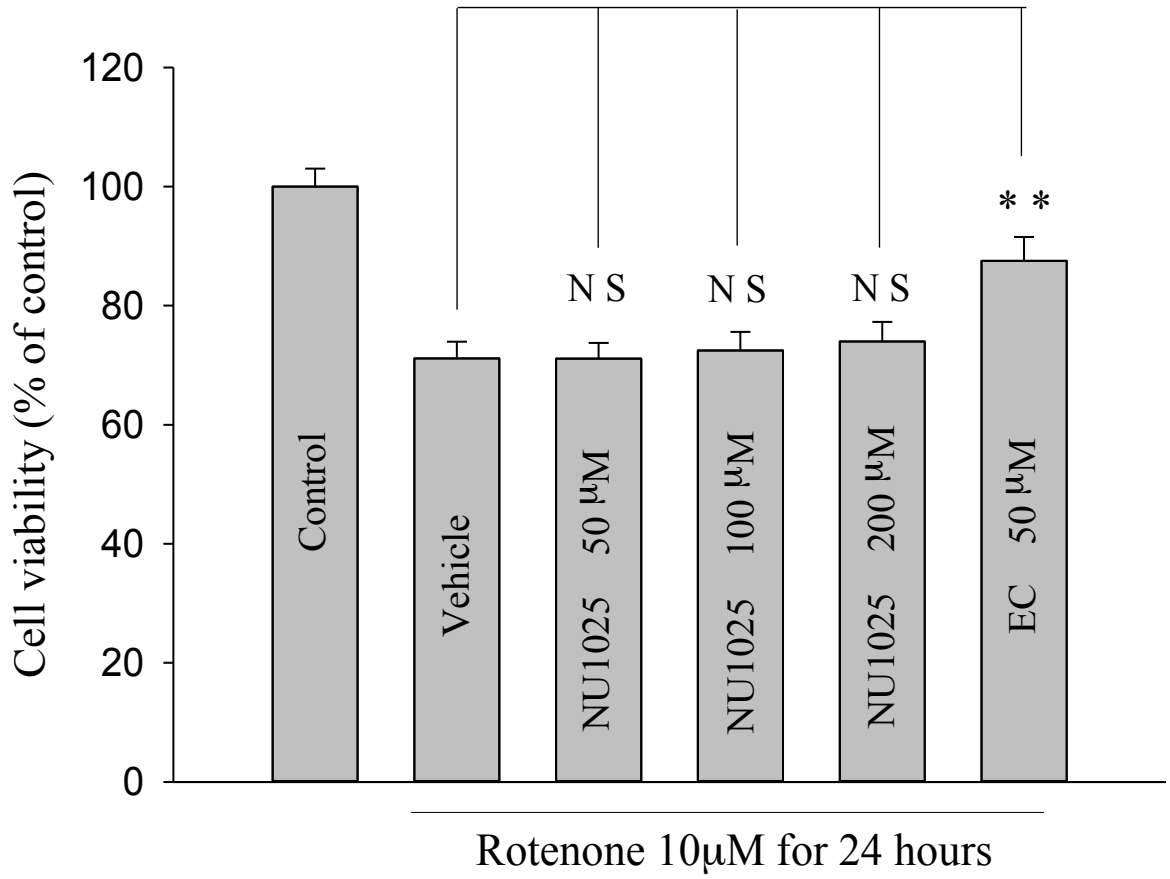


Figure 5.7. This figure shows the effect of PARP inhibitor, NU1025 in RGC-5 cell cultures exposed to rotenone for 24 hours. Cell viability is measured using MTT assay. In this study, EC 50μM is used as positive control, and significantly attenuated rotenone-induced reduction in cell viability. The PARP inhibitor has no effect in attenuating rotenone-induced loss in RGC-5 cell viability. Values are expressed as means ± SEM of at least 5 independent experiments. Statistical differences **$p<0.01$ are calculated by one-way ANOVA followed by Tukey multiple comparative test. (NS= not significant)

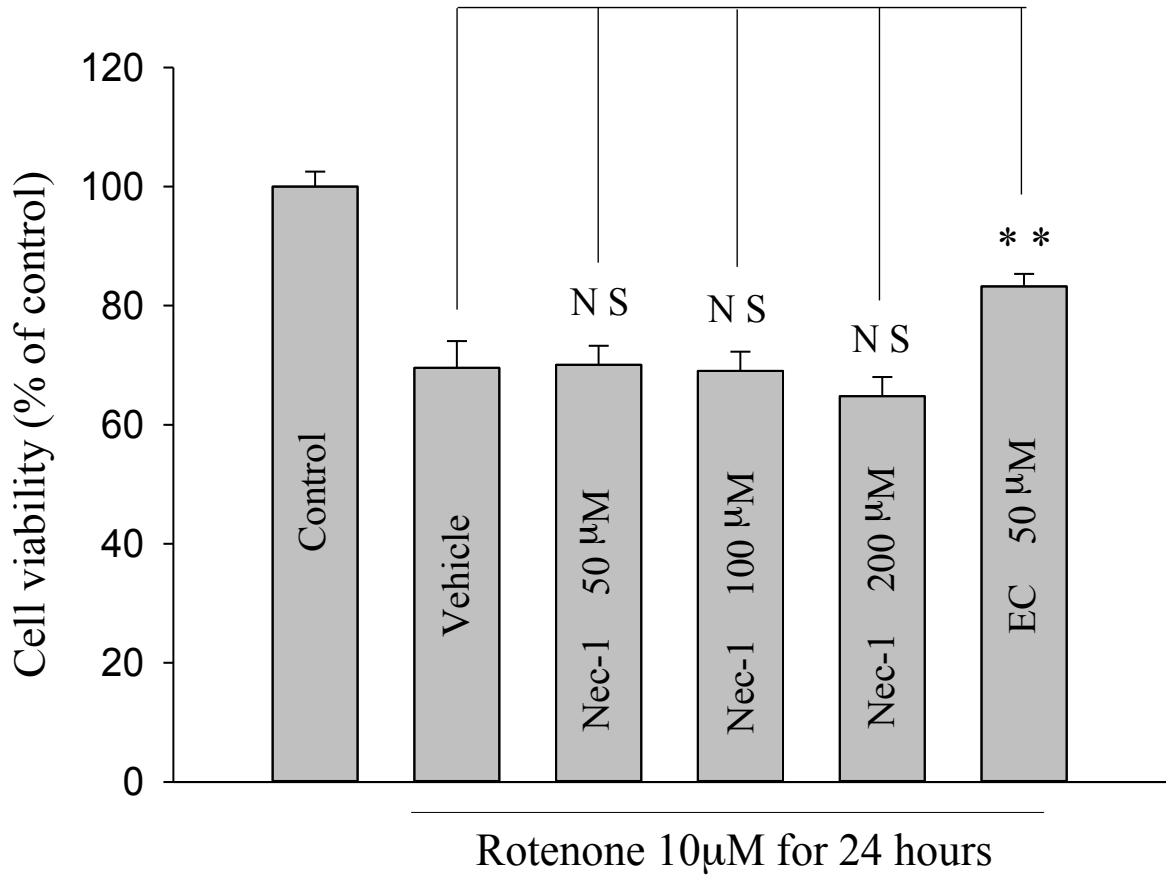


Figure 5.8. This figure shows the effect of necrostatin inhibitor, Nec-1 in RGC-5 cell cultures exposed to rotenone for 24 hours. Cell viability is measured using MTT assay. In this study, EC 50μM is used as positive control, and significantly attenuated rotenone-induced reduction in cell viability. Nec-1 has no effect in attenuating rotenone-induced loss in RGC-5 cell viability. Values are expressed as mean ± SEM of at least 5 independent experiments. Statistical differences **$p<0.01$ are calculated by one-way ANOVA followed by Tukey multiple comparative test. (NS = not significant)

5.2.2 Assessment of caspase-3 activity

Support for the view that rotenone-induced toxicity of RGC-5 cells did not involve the stimulation specifically of caspase-3 is shown in figure 5.9. In this study RGC-5 cells were exposed to rotenone (10µM) or staurosporine (500nM) for 24 hours and caspase-3 activity thereafter determined. Caspase-3 activity was significantly increased following exposure to staurosporine while the slighter increase in caspase-3 caused by rotenone did not reach significance.

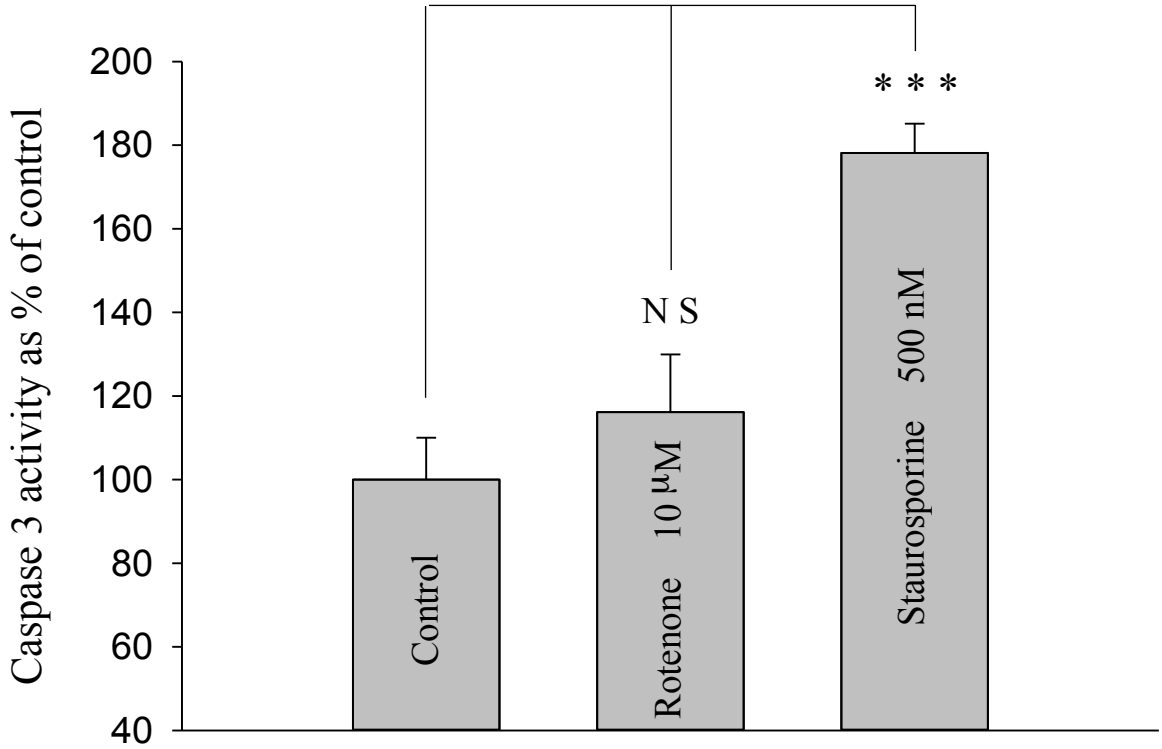


Figure 5.9. Exposure of RGC-5 cells to staurosporine (500nM) for 24 hours causes a significant stimulation of caspase-3 activity in cell lysates. A slight increase in caspase-3 activity also occurs when RGC-5 cells are exposed to rotenone (10µM) but the influence is non-significant. Results are mean values ± SEM on at least three independent experiments. Significant differences (***$p<0.001$) were calculated by one-way ANOVA followed by a Tukey multiple comparative test. (NS=not significant).

5.2.3 Assessment of reactive oxygen species (ROS) production

Yellow fluorescence staining for DHE as an indicator for ROS production in RGC-5 cells is shown in figure 5.10. No yellow fluorescence is seen in control cells (figure 5.10A), whereas cells exposed to 10μM rotenone for 24 hours shows intense yellow fluorescence particularly associated with nuclei (white arrows) (figure 5.10B). However, this rotenone-induced stimulation of ROS is significantly reduced in the presence of EC 50μM (figure 5.10C) or EGCG 50μM (figure 5.10D) indicated by decreases in the intensity of yellow fluorescence. In contrast, rotenone-induced ROS formation appears not to be attenuated by 10μM of either genistein (figure 5.10E) or baicalin (figure 5.10F).

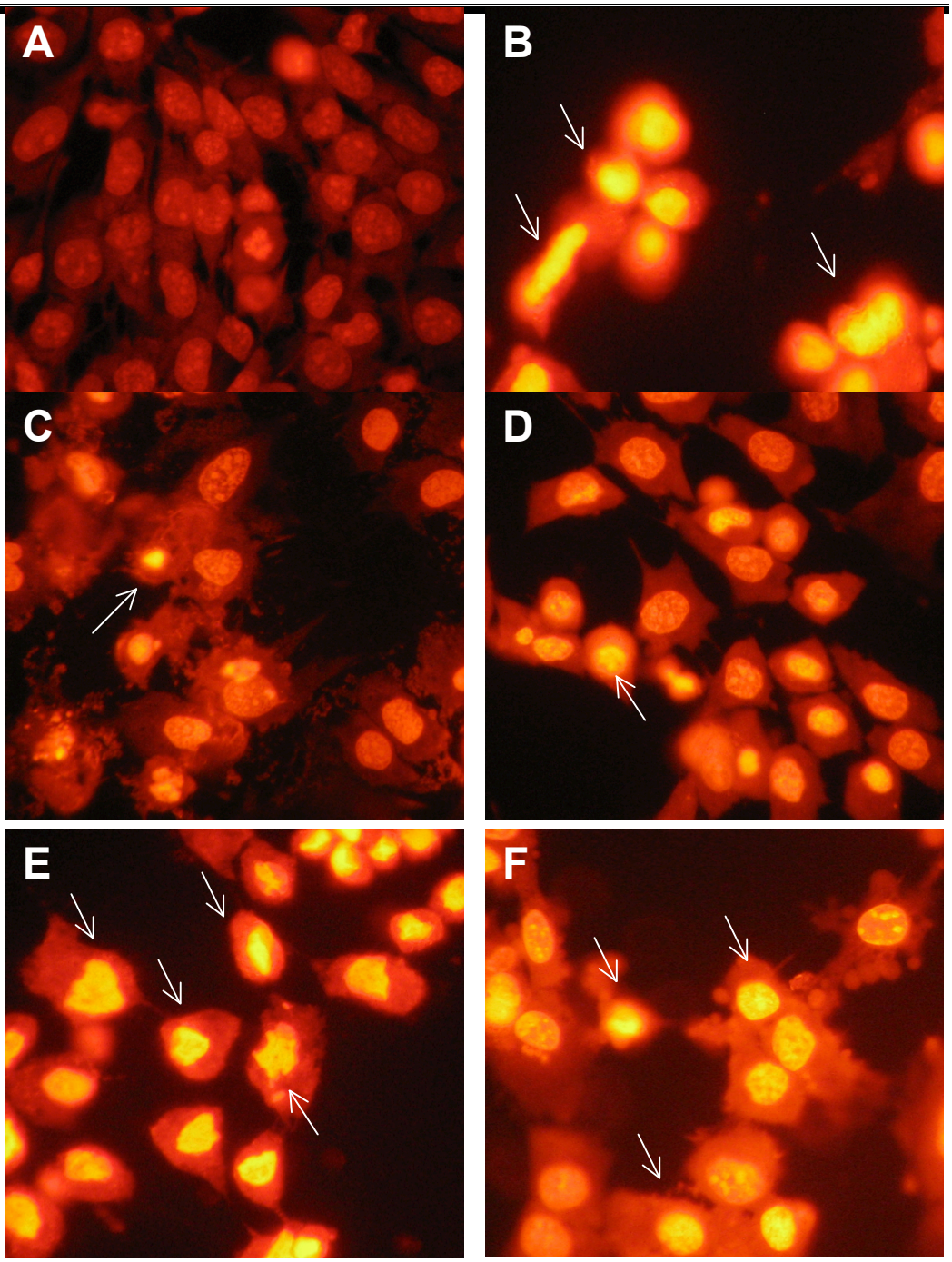


Figure 5.10. Representative DHE staining for ROS in RGC-5 cells, from four different experiments. In control (vehicle-treated) cells (A), DHE production is hardly seen as shown by the absence of yellow fluorescence which indicates ROS production. ROS production is clearly seen when exposed to rotenone 10μM for 24 hours (B), and this effect is attenuated by EC 50μM (C) and EGCG 50μM (D), while baicalin 10μM (E) or genistein 10μM (F) had no obvious influence.

5.2.4 Assessment of apoptosis by APOPercentage™ and TUNEL staining

Rotenone-induced RGC-5 cell death resulted in membranes staining positively for phosphatidylserime (using APOPercentage™ staining kit). In healthy cells, phosphotidylserine is maintained within cellular membranes by an energy dependent process. In apoptotic-committed cells, this process is compromised causing phosphotidylserine to be exposed over membranes and able to be stained by use of APOPercentage™ Dye. As the process of apoptosis advances so cell volume shrinks, with more phosphatidylserine to be exposed resulting in a more intense staining with the dye. As shown in figure 5.11A, control cells do not stain for phosphotidylserine indicated by the absence of pink cellular staining. In contrast, RGC-5 cells exposed to rotenone 10μM for 24 hours show multiple apoptotic cells staining pink (white arrows) as demonstrated in figure 5.11B. The number of pink apoptotic cells is reduced in cells pre-treated for an hour with EC 50μM and EGCG 50μM, but not with baicalin 10μM or genistein 10μM (figures 5.11 C-F). The quantification of RGC-5 cells which stained positive for phosphotidylserine is shown in figure 5.12.

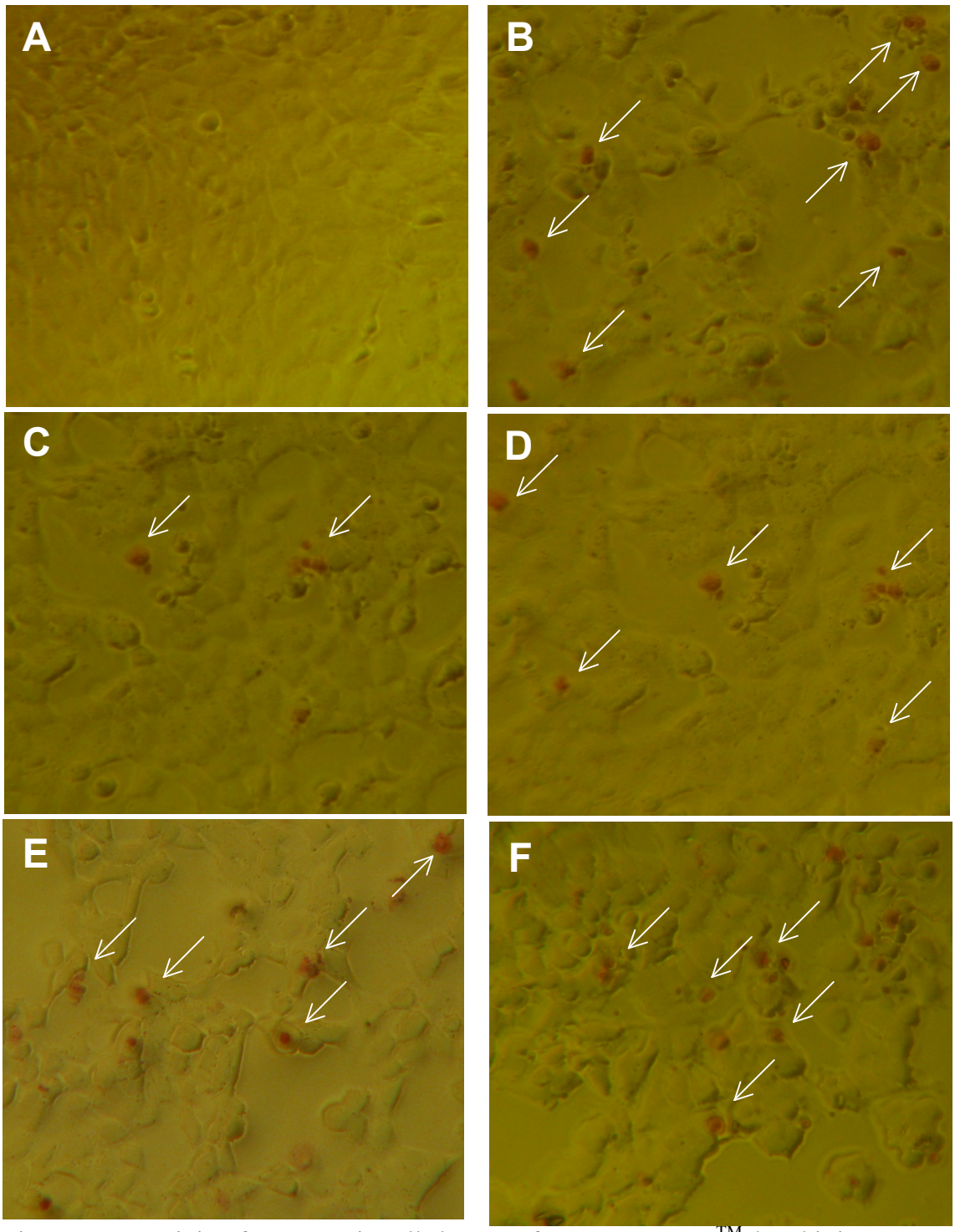


Figure 5.11. Staining for apoptotic cells by use of APOPercentage™ dye kit in RGC-5 cell cultures. In control (vehicle-treated) cultures (A), there is little evidence for apoptosis because of an absence of pink staining. However, evidence for apoptosis (arrows) is clearly seen when cultures are exposed to rotenone 10μM for 24 hours (B), and this process is partially blunted in the presence of EC 50μM (C) or EGCG 50μM (D). In contrast, there was no evidence for baicalin 10μM (E) or genistein 10μM (F) attenuating the negative effect of rotenone. These findings were repeated and confirmed to occur in three separate experiments.

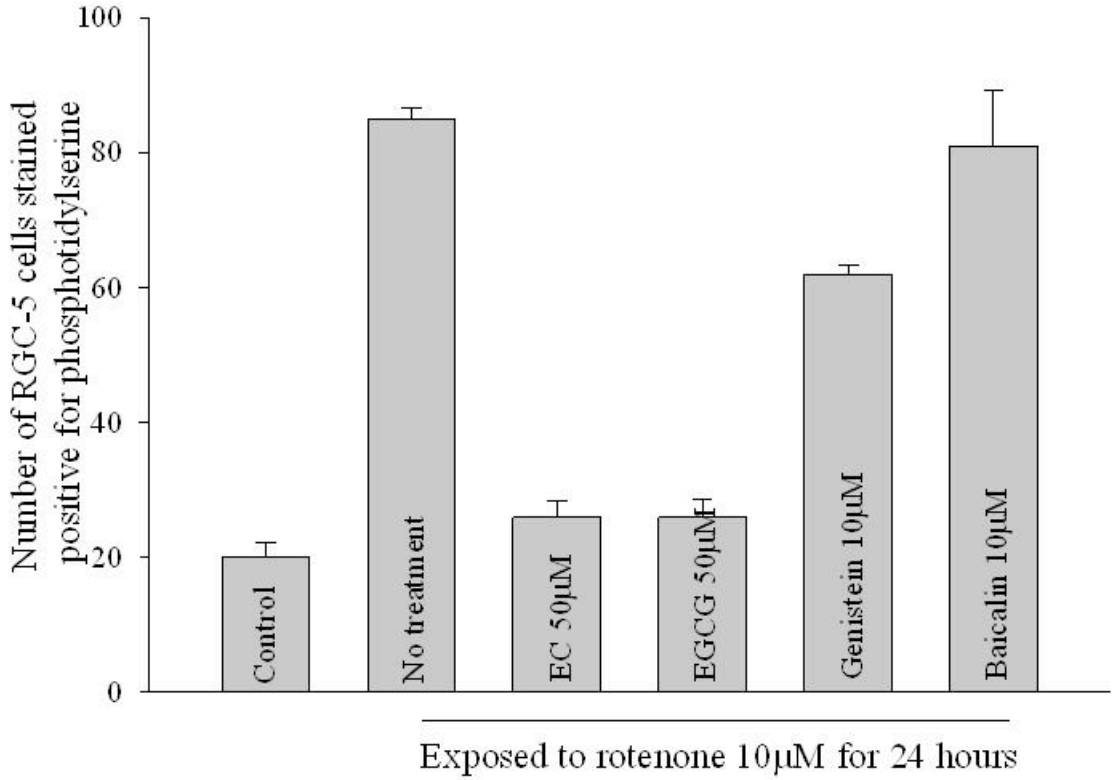


Figure 5.12 Quantitative analysis reveals that the number of apoptotic cells staining positive for phosphotidylserine using the APOPercentage^{TM} staining kit is reduced in RGC-5 cells pre-treated with EC 50μM and EGCG 50μM for an hour before further incubation with rotenone 10μM for 24 hours. Results are expressed in mean number of cells ± SEM.

Further evidence showing that rotenone-induced RGC-5 cell death was by apoptosis was obtained by staining for DNA breakdown using TUNEL staining technique (figure 5.13). RGC-5 cells grown on cover slips in 24-well plates were treated with vehicle (figure 5.13A), rotenone 10μM (figure 5.13B) with and without pre-treatment with EGCG, EC, baicalin or genistein (figure 5.13C-F). Figure 5.13A shows absence of red TUNEL staining associated with apoptotic cells. TUNEL positive cells were much enhanced when RGC-5 cells were exposed to rotenone 10μM for 24 hours (figure 5.13B). Pre-treatment of RGC-5 cells with EC 50μM and EGCG 50μM for an hour before exposure to rotenone 10μM for another 24 hours, showed significant reduction of apoptotic cells (figure 5.13C and D). However, pre-treatment with either baicalin 10μM or genistein 10μM did not attenuate rotenone-induced apoptosis in RGC-5 cells (figure 5.13E and F). Figure 5.14 shows the quantitative analysis of TUNEL-positive RGC-5 cells from at least 3 different random fields of view.

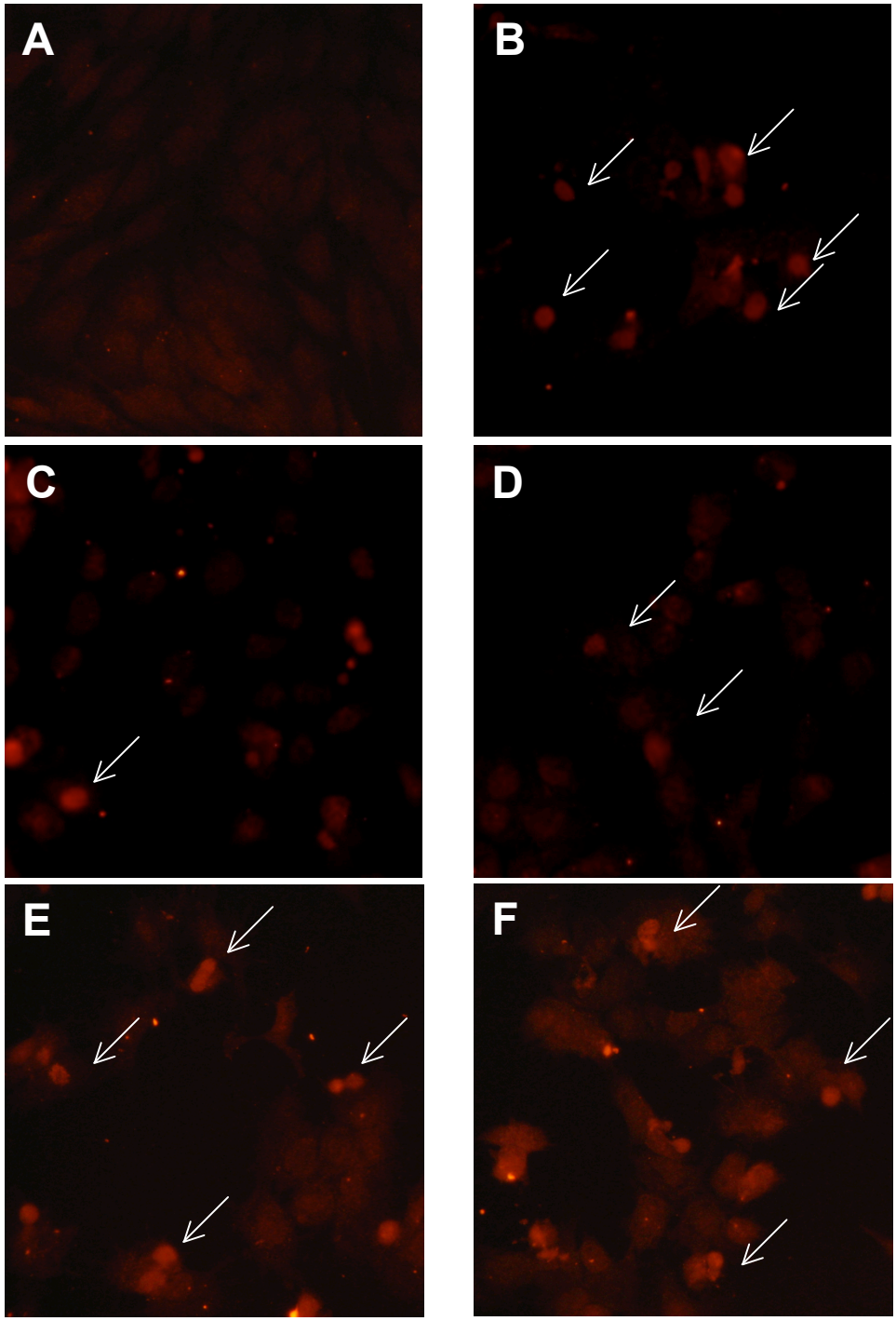


Figure 5.13. Red TUNEL staining for DNA breakdown (arrows) as an indication of apoptosis occurs in RGC-5 cell cultures (B) following exposure to 10μM of rotenone for 24 hours. No red fluorescence TUNEL positive cells occur in control vehicle-treated cultures (A). Cultures exposed to rotenone in the presence of 50μM of either EC (C) or EGCG (D) showed a decrease of TUNEL positive red cells when compared with rotenone 10μM alone (figure 4.14B). However, this was not the case when RGC-5 cells were pre-treated with baicalin 10μM (E) or genistein 10μM (F).

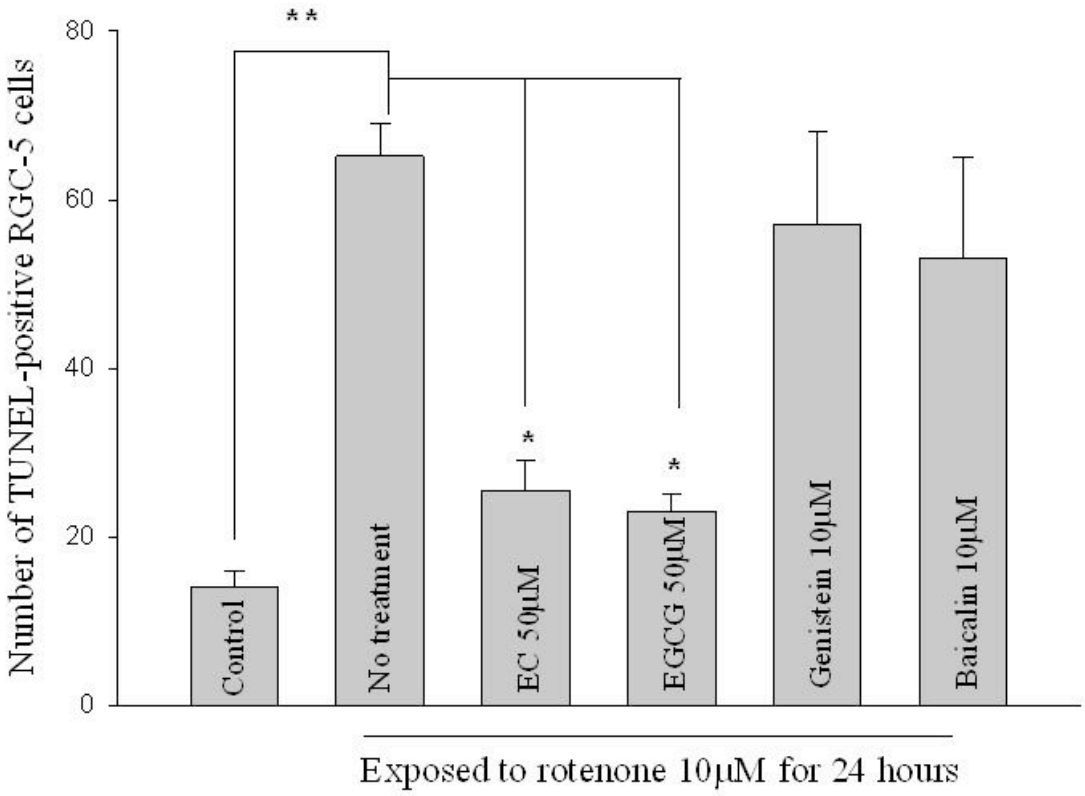


Figure 5.14 Quantitative analysis shows that the number of TUNEL-positive cells is reduced in RGC-5 cells pre-treated with EC 50μM and EGCG 50μM for an hour prior to further incubation with rotenone 10μM for 24 hours. Results are expressed as mean number of cells ± SEM where *p<0.05 and **p<0.01.

5.2.5 Role of MAPK kinase pathway in rotenone-induced RGC-5 cell death

Mitogen-activated protein kinase pathway (MAPK) form a highly complex signalling pathway which regulates many cellular processes including cell death. There are three MAPK families identified: the p38MAP kinase, the c-jun amino-terminal kinase (JNK) and the extracellular-regulating kinase (ERK) (see figure 1.11, chapter 1). The p38 signalling pathway has been implicated in retinal ganglion cell apoptosis (Kikuchi *et al* 2000) and neurodegenerative conditions such as Alzheimer's disease (Ando *et al* 2011).

To study the involvement of p38 signalling pathway in rotenone-induced cell death, immunocytochemistry studies were carried out on RGC-5 cells which were grown on cover slips in 24-well plates and exposed to rotenone 10μM for 24 hours (figure 5.135). RGC-5 cells exposed to rotenone 10μM in 6-well plates were collected and processed for phosphorylated p38 (P-p38) proteins using for immunoblotting studies. Immunocytochemistry studies showed that very little P-p38 exists in control RGC-5 cells (figure 5.15A and D). Rotenone 10μM caused up-regulation of P-p38 proteins as shown in figure 5.15B and D. Western blot analysis showed that P-p38 up-regulation occurred as early as 30 minutes following rotenone exposure and continues to be up-regulated for 24 hours, as shown in figure 5.16.

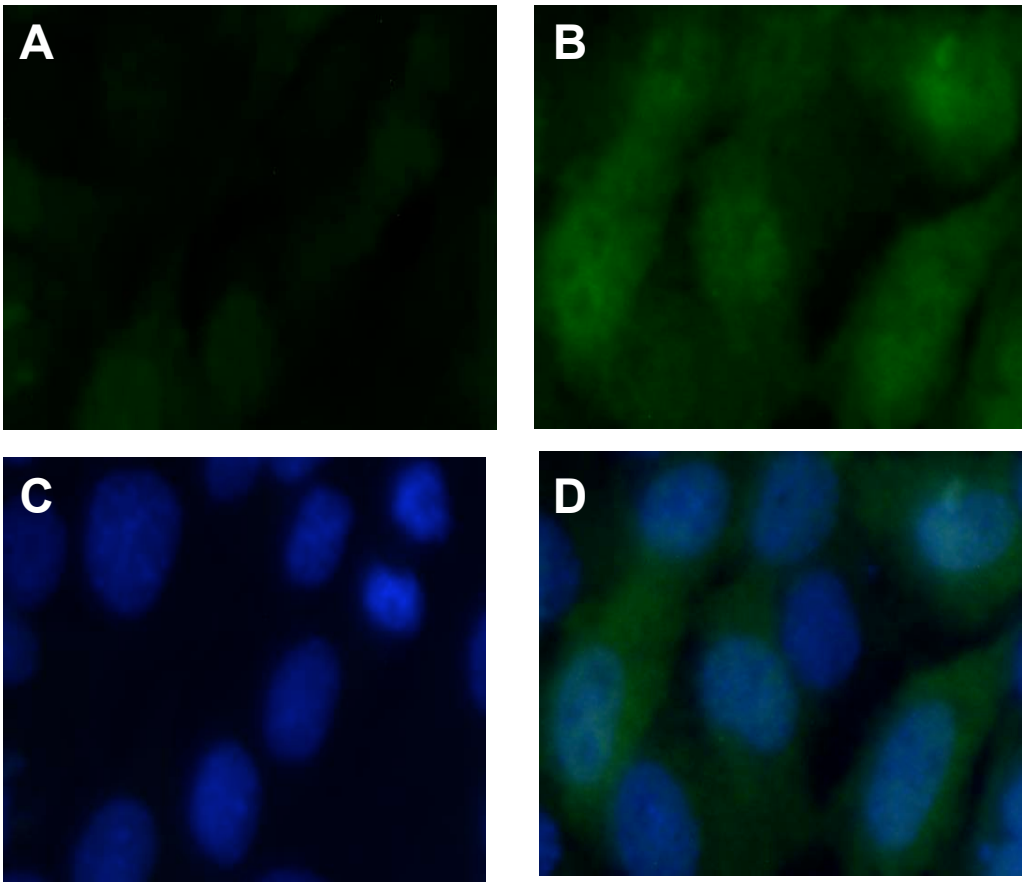


Figure 5.15 Immunocytochemistry studies show that very little P-p38 is detected in RGC-5 cells under control conditions (A and C). After exposure to rotenone 10μM for 24 hours, P-p38 is up-regulated in the cytoplasm and nuclei (B and D). Figures A and B show localisation of pp38 alone, while cells in figures C and D are counterstained with DAPI to stain nuclei.

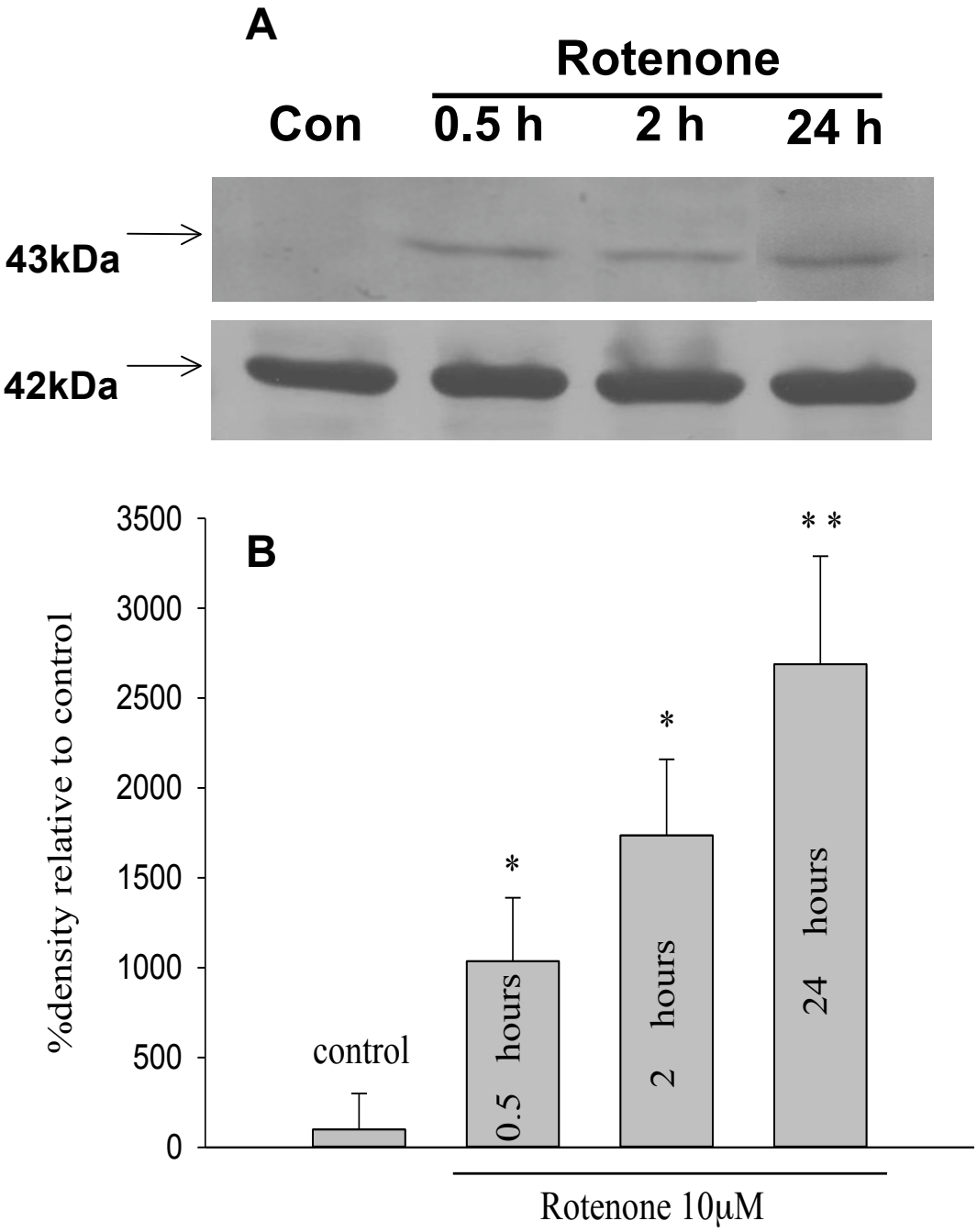


Figure 5.16. Western blot analysis (A) showed that P-p38 (43kDa) is up-regulated in RGC-5 cell cultures as early as 30 minutes after exposure to rotenone 10μM and remained up-regulated for 24 hours. The error bars in (B) are mean percentage density ± SEM where n=4 separate experiments; *p<0.05, **p<0.01. Statistical significances were calculated by an unpaired t-test.

JNK stress signaling pathway is involved in many cellular processes including cell proliferation and apoptosis (Nishina *et al* 2004). Following activation, JNK phosphorylates substrates such as c-Jun, ATF-2 and Bcl-2 (Lei & Davis 2003). Xia and colleagues were the first to report that JNK signaling pathway is required for neuronal apoptosis and showed that inhibitors of JNK pathway block apoptosis (Xia *et al* 1995). To determine if c-Jun is activated in rotenone-induced cell death, RGC-5 cells were plated overnight on cover slips in 24-well plates before treated with rotenone 10μM. After 24 hours cells were fixed with 4% paraformaldehyde and analysed for phosphorylated c-Jun (P-c-Jun) proteins using immunocytochemistry. Rotenone-induced RGC-5 cell death caused up-regulation of P-c-Jun both in the cytoplasm and nuclei, as shown in figure 5.17B and D.

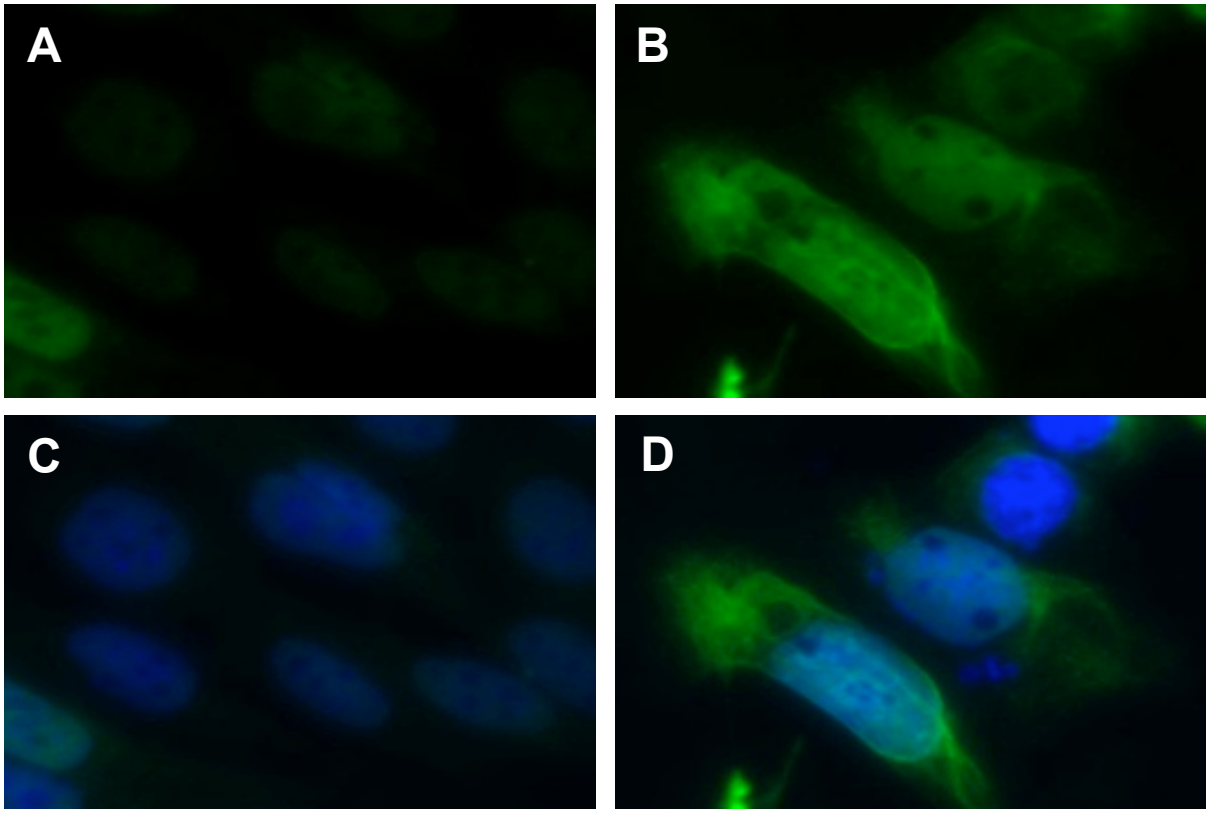


Figure 5.17. RGC-5 cells were grown on cover slips and exposed to rotenone 10μM for 24 hours before stained for P-c-Jun proteins (upper panel, A and D) and counterstaining with DAPI nuclei staining (lower panel, C and D). Very minimal P-c-Jun protein can be detected in control RGC-5 cells (A and C). Rotenone 10μM caused up-regulation of P-c-Jun proteins both in the cytoplasm and nuclei of RGC-5 cells (B and D).

RGC-5 cell lysates were separated into nucleus, cytoplasm and mitochondrial fractions by subcellular fractionation methods (section 2.2.3). Briefly, RGC-5 cells in 6-well plates were scraped and cell lysates were homogenized and separated into crude subcellular fractions by differential centrifugation. Western blot analysis of the subcellular fractions showed that P-JNK (46kDa) and P-c-Jun (33 and 47kDa) proteins can be detected in the nucleus and cytoplasm fractions but exist in a small amount in the mitochondria fraction of control RGC-5 cells. Following 24-hour exposure to a high dose of rotenone (20μM), there appeared to be an up-regulation of

P-JNK and P-c-Jun proteins (especially the 33kDa protein) in the nucleus and mitochondria. This suggests that rotenone caused translocation of both P-c-Jun and P-JNK proteins from the nucleus into the mitochondria (figure 5.18).

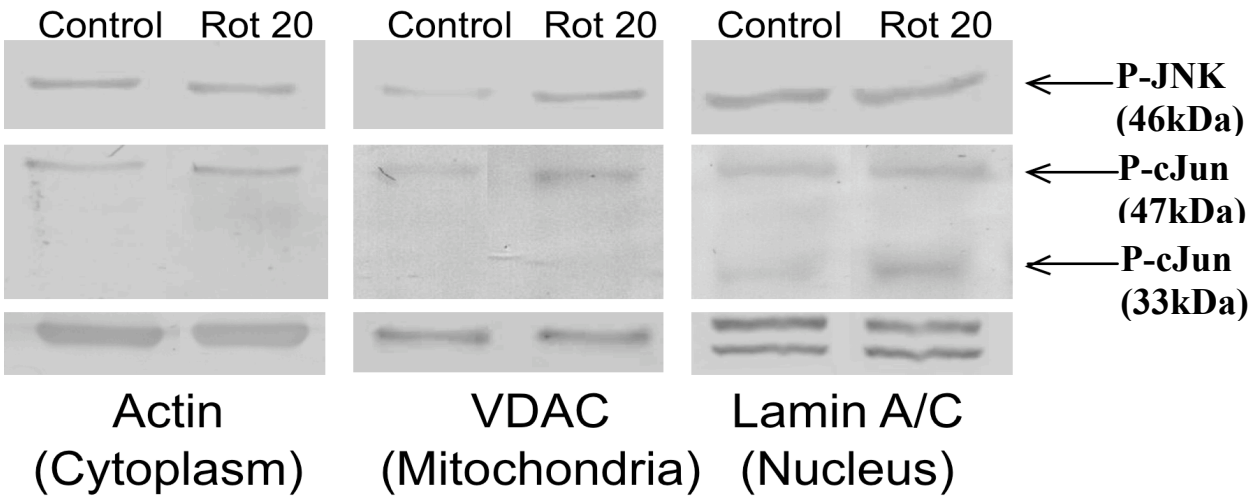


Figure 5.18. Western blots of P-c-Jun (33kDa and 47kDa) and P-JNK (46kDa) in fractionated control RGC-5 cells and cells exposed to rotenone 20μM (Rot 20) for 24 hours. A clear up-regulation of mitochondrial P-c-Jun and P-JNK occurs following exposure of RGC-5 cells to rotenone. Also an up-regulation of a 33kDa band occurred in the nucleus in blots stained for P-JNK. Antibodies used to normalise proteins located to different compartments were actin for cytoplasm (42kDa), voltage-dependent channel antibody for mitochondria (33kDa) and lamin A/C for nuclei (62kDa and 69kDa). These data summarise results from three separate experiments.

Apoptosis-inducing factor (AIF) is a flavoprotein acting as a NADH oxidase. Under normal physiological conditions, the AIF precursor (67kDa) is transported from the cytoplasmic ribosomes where it is synthesized, into mitochondria, where it is involved in oxidative phosphorylation. In caspase-independent apoptosis, AIF is cleaved into a 57kDa form which is released into the cytosol where it translocates into the nucleus to contribute to DNA fragmentation (Susin *et al* 1999).

In the present studies, AIF was detected in its 67kDa form in control RGC-5 cells (figure 5.19). However, when exposed to rotenone 10μM for 24 hours or light 1000lux for 96 hours, only light insult caused cleavage of AIF, consistent with caspase-independent apoptosis as previously reported (Li & Osborne 2008).

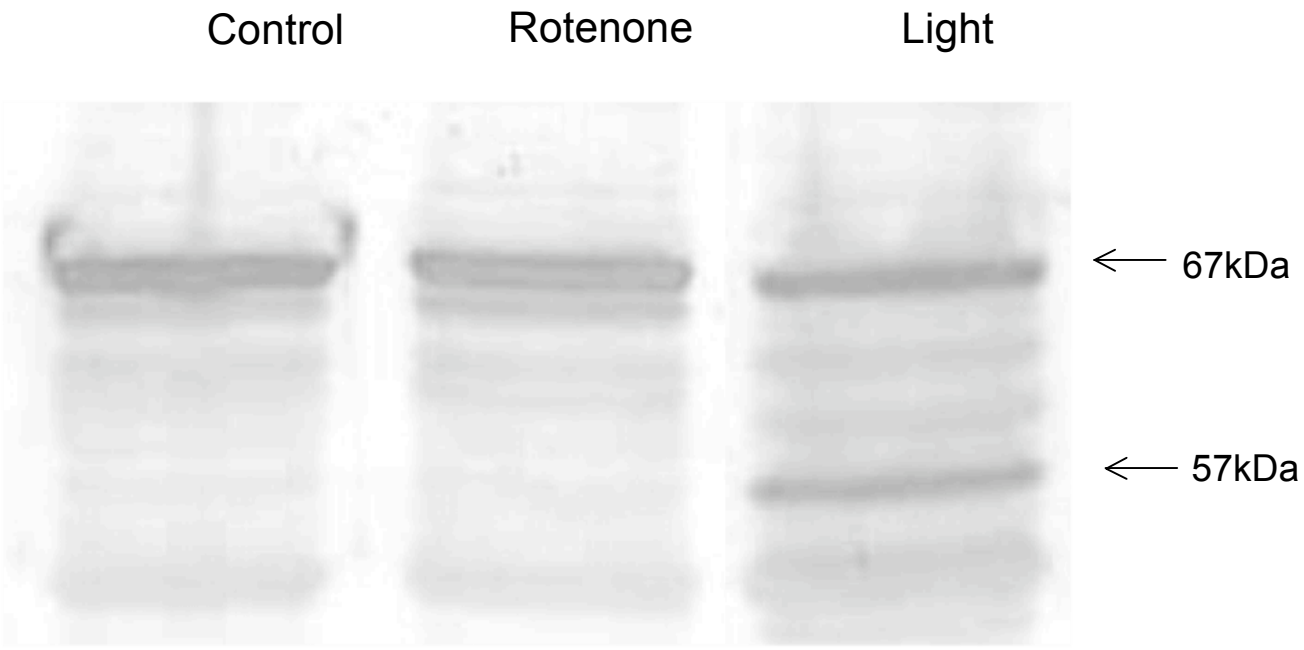


Figure 5.19. Western blot analysis of proteins from RGC-5 cells exposed to 10μM rotenone for 24 hours. Two controls were used in these experiments. Normal RGC-5 cells exposed to vehicle (Control) or to white light for 96hours (for details of method used see Ji *et al* 2011). AIF appears as two bands (67kDa and 57kDa) in light exposed samples but this does not occur in protein samples of cells exposed to rotenone or vehicle.

5.3 Discussion

Inhibition of the proton-translocating NADH-quinone oxidoreductase (complex 1) of mitochondria with rotenone results in cell death. However, the cascade of events that leads to cell death following complex 1 inhibition remains unclear. Reduction of complex 1 activity results in the formation of ROS (Sherer *et al* 2002) thought to be due to inhibition of electron transfer (Kussmaul & Hirst 2006), reverse electron transport (Adam-Vizi & Chinopoulos 2006) and when the $NADH/NAD^+$ ratio is significantly high (Kussmaul & Hirst 2006). It is also known that complex 1 inhibition provokes a number of events that includes activation of various kinase pathways and a release of a variety of proapoptotic factors but the traditional caspase pathway does not seem to be involved because caspase-3 activation is generally not observed (Li *et al* 2005, Marella *et al* 2007). In this respect, the present study supports this view where rotenone-induced death of RGC-5 cells does not involve a significant activation of caspase-3 as compared with the influence of staurosporine.

Significantly, the mechanism by which RGC-5 cell death occurs because of rotenone exposure is not dissimilar to what occurs following a light insult (Osborne *et al* 2008, Ji *et al* 2011) or induced by inhibition of mitochondrial complex IVwith sodium azide (Ji *et al* 2011). Death of RGC-5 cells caused by all three insults causes a stimulation of ROS, the breakdown of DNA, the translocation of membrane phosphotidylserine and an up-regulation of P-p38. However, despite this similarity important differences also exist. Rotenone-induced toxicity to RGC-5 cells is insensitive to necrostatin-1 and the pan-caspase inhibitor z-VAD-fmk and does not involve the activation of apoptosis inducing factor (AIF). In contrast light-induced toxicity is blunted by necrostatin-1 and involves the activation of AIF while cell death caused by sodium azide toxicity is inhibited by z-VAD-fmk (Ji *et al* 2011).

Necrostatin-1 inhibits a death process termed necroptosis, which shares features common to apoptosis, necrosis and type-2 autophagy (Degterev *et al* 2005, Hitomi *et al* 2008). While the same death receptor agonist may trigger necroptosis and apoptosis, necroptosis can be differentiated from apoptosis morphologically and functionally and by inhibition with necrostatin-1 (Degterev *et al* 2005, Hitomi *et al* 2008). Necrostatin-1 targets a serine/threonine kinase receptor that interacts with protein kinase-1 (RIP1) which is specifically involved in necroptosis (Degterev *et al* 2005, Kroemer *et al* 2009) and is known to trigger the activation and cleavage of AIF (Delavallee *et al* 2011). Death mechanisms involving apoptosis generally involve a stimulation of caspases and z-VAD-fmk is a potent inhibitor of this process (Galluzzi & Kroemer 2008). Thus the results from this and a previous study (Ji *et al* 2011) show that the precise mechanisms by which rotenone, sodium azide and light cause RGC-5 cell death have common similarities but are nevertheless distinctive.

Rotenone as well as light and sodium azide-induced death of RGC-5 cells all involves an activation of mitogen-activated protein kinases (MAPKs). MAPKs involve the extracellular signal regulators kinase (ERK), c-Jun N-terminal kinase (JNK) and p38 MAPK and are linked with a diverse range of biological activities including regulation of programmed cell death (Ono & Han 2000). Activation of ERKs typically contributes to cell differentiation, proliferation and survival (Ono & Han 2000) whereas JNK and p38 MAPK, in contrast, are activated by pro-inflammatory cytokines and environmental stress and also can promote apoptosis (Davies *et al* 2000). Our present results show that exposure of RGC-5 cells to rotenone results in an up-regulation of phosphorylated products of c-Jun and JNK and their translocation into mitochondria. One might therefore speculate that the activation of P-c-Jun and P-JNK is associated with inflammation and this occurs when cells die. Significantly,

when the activation of JNK by rotenone is inhibited by use of the JNK inhibitor SP600125 cell death is inhibited. The protein for p-p38 only occurs in trace amounts in healthy RGC-5 cells but is also up-regulated significantly following exposure to rotenone. This protein is located to both the nuclei and cytoplasm of RGC-5. Thus it appears as if rotenone-induced toxicity of RGC-5 cells causes an activation of p38 and JNK pathways, with the latter causing a phosphorylation of c-Jun and inhibition of JNK with SP600125 increases cell survival.

One aim of the present studies was to determine whether any of three different flavonoids (EGCG, EC, genistein, baicalin) are particularly effective at blunting the negative effect of rotenone on RGC-5 cell survival. Flavonoids have numerous beneficial physiological effects in for example cancer and cardiovascular and neurodegenerative diseases (Cody 1988, Kuppusamy *et al* 1990, Gao *et al* 2001, Lee *et al* 2003, Mandel *et al* 2005). These positive effects are mainly, but not exclusively, attributed to the antioxidant activity of flavonoids. Moreover, the mechanisms by which the individual flavonoids act as antioxidants are almost certainly not identical. This study also showed that at non-toxic doses, EC and EGCG are equally effective at attenuating rotenone-induced toxicity but baicalin and genistein were without influence. Such data suggest that the causes for EC and EGCG having neuroprotective effects are not solely linked to their strong antioxidant properties but are likely to be associated with their additional properties. It is clear from such data that if RGC cell death in glaucoma is associated with complex I dysfunction then it is likely that EC or EGCG are more likely to be effective neuroprotective flavonoids that either genistein or baicalin.

CHAPTER 6

LIGHT- AND SODIUM AXIDE-INDUCED DEATH OF RGC-5 CELLS IN CULTURE OCCURS VIA DIFFERENT MECHANISMS AND IS ATTENUATED BY EPIGALLOCATECHIN GALLATE

6.1 Introduction

6.1.1 Aim

There were two main aims of the studies presented in this section: **A]** to compare the effect of EGCG at attenuating cell death in RGC-5 cultures caused by either a mitochondrial complex IV inhibitor, sodium azide or a defined light insult, and **B]** to compare the mechanisms of cell death caused by the two types of insults.

6.1.2 Brief overview

Mitochondria are involved in numerous metabolic functions that include maintaining intracellular pH and the production of reactive oxygen species (ROS) which promote and regulate apoptosis (Chan 2006). The production of ROS such as hydroxyl free radicals, singlet oxygen, hydrogen peroxide, nitric oxide and peroxynitrite is finely balanced with sophisticated antioxidant and repair systems located within mitochondria (Christophe & Nicolas 2006, Lin & Beal 2006). Sustained or intense insults such as occurs as a result of ageing (Chan 2006) and ischemia (Lin & Beal 2006, Osborne *et al* 2006) cause mitochondria to produce ROS in excess of their capacity to detoxify such species and this can lead to neuronal death. A variety of studies have also shown that light impinging on the retina (400–760 nm) *in situ* can interact with mitochondrial chromophores to generate ROS (King *et al* 2004, Godley *et al* 2005, Osborne *et al* 2006). For example, mitochondrial cytochrome oxidase (COX) absorbs light in the blue part of the spectrum in both its oxidized and reduced states (Bell JE 1981). Another mitochondrial enzyme, cytochrome P450 absorbs light at wavelengths near 450 nm when bound to carbon monoxide (Montellano 1995). Also, flavins such as riboflavin and flavoprotein nucleotides are essential components

of numerous cytosolic and mitochondria enzyme systems and they absorb light at 450–520 nm to generate hydrogen peroxide (Garcia & Silva 1997, Hockberger *et al* 1999). Significantly, mitochondria associated with brain neurons are never exposed to visible light, but this is not the case for the retina. Outer retinal cells are to some extent protected from visible light by the macular pigments but this is not the case for inner retinal neurones. Of importance in this context is the observation that ganglion cell axons in the non-myelinated intraocular portions of their axons are laden with many mitochondria (Barron *et al* 2004, Carelli *et al* 2004). Osborne and collaborators linked this fact with laboratory studies which showed that light negatively affects mitochondrial functions and causes cells in culture to die (Osborne *et al* 2006, Lascaratos *et al* 2007, Wood *et al* 2007, Osborne *et al* 2008, Osborne 2010). It was therefore hypothesised that light (particularly the blue component) is a risk factor for retinal ganglion cells *in situ* when their homeostasis is already compromised, as it might be in the case of glaucoma, diabetes and the ageing retina. It has now been clearly shown that exposure of cell cultures to light (400–760 nm) causes them to die in an intensity dependent manner by an apoptotic-type mechanism (Osborne *et al* 2006, Lascaratos *et al* 2007, Wood *et al* 2007, Osborne *et al* 2008). The light-induced death process involves the generation of ROS and the activation of apoptosis inducing factor (AIF) and polyADP-ribose polymerase-1 (PARP), whereas caspase-3 is unaffected. Moreover, for the light-induced death process to occur, a functional mitochondrial electron respiratory transport chain is necessary. This was demonstrated in cultures of fibroblasts (BJhTERT cells) where some were maintained in ethidium bromide for 50 days to deplete their mitochondrial DNA and to disturb their mitochondrial respiratory chain function (BJhTERT rh0 cells). Only the BJhTERT

cells with an intact mitochondrial respiratory chain function were affected by a light insult (Osborne *et al* 2008).

The mitochondrial electron transport chain is composed of a series of electron carriers (flavoproteins, iron-sulphur proteins, ubiquinone and cytochromes) that are spatially arranged according to their redox potentials and organized into four complexes where excess ROS can be generated. Studies on isolated mitochondria and cell cultures show that certain toxins can specifically inhibit the different mitochondrial complexes. For example rotenone, antimycin A and sodium azide are inhibitors of complexes I, III and IV, respectively. It is of interest to note that in a recent study by Liu and Schubert (2009), it was demonstrated that certain antioxidants are better than others at scavenging ROS that were generated by the inhibition of individual mitochondrial complexes.

One aim was to gain further insight into the mechanism by which a light insult (400–760 nm) to cells in culture causes oxidative stress and apoptotic-like death. Since it was suggested that light might have a direct effect on complex IV of the electron transport chain (King *et al* 2004, Godley *et al* 2005) we compared the effect of a light insult with that provided by sodium azide. Sodium azide inhibits complex IV by binding with molecular iron associated with cytochrome oxidase and prevents the production of ATP (Ellenhorn 1988, Leary *et al* 2002, Safiulina *et al* 2006). Our results showed that the cell death mechanisms elicited by sodium azide and light are dissimilar, suggesting that light insults do not solely involve the inhibition of mitochondrial complex IV.

6.1.3 Summary of results

The mode of RGC-5 cell death caused by light and sodium azide are not the same suggesting that manner by which EGCG attenuates each death process are likely not to be identical. The similarities and differences between the two insults are summarised below:

1) The following similarities exist between light and sodium azide-induced cell death: a) both processes are attenuated by epigallocatechin gallate (EGCG), b) both processes cause a generation of reactive oxygen species (ROS), c) both insults cause a translocation of phosphatidylserine and the breakdown of DNA, and d) both insults cause an activation of p38MAPK and its translocation from the nucleus to the cytoplasm.
2) The following differences are associated with each of the insults:

   a] Light-induced death of RGC-5 cells is inhibited by necrostatin-1, unaffected by alpha fodrin or caspase inhibition and causes an activation of apoptosis inducing factor (AIF), JNK, c-Jun and HO-1.

   b] Sodium azide-induced cell death is unaffected by necrostatin-1 and involves the activation of alpha-fodrin and the caspase-3 without influencing AIF, JNK, c-Jun or HO-1.

6.2 Results

6.2.1 Cell viability

The degree of reduction in the viability of RGC-5 cells using the resazurin-reduction assay is dependent on the duration of light insult at an intensity of 1000 lux (figure 6.1). Compared with dark conditions, 1000 lux of light for 24 hours had no significant effect on cell survival. In contrast, a doubling of exposure time to 48 hours causes an approximate 25% reduction in cell viability. Increasing the exposure time to light caused a greater negative time-dependent effect on cell viability. After 120 hours, most of the RGC-5 cells are dead. The duration of light exposure used for subsequent experiments was 48 hours.

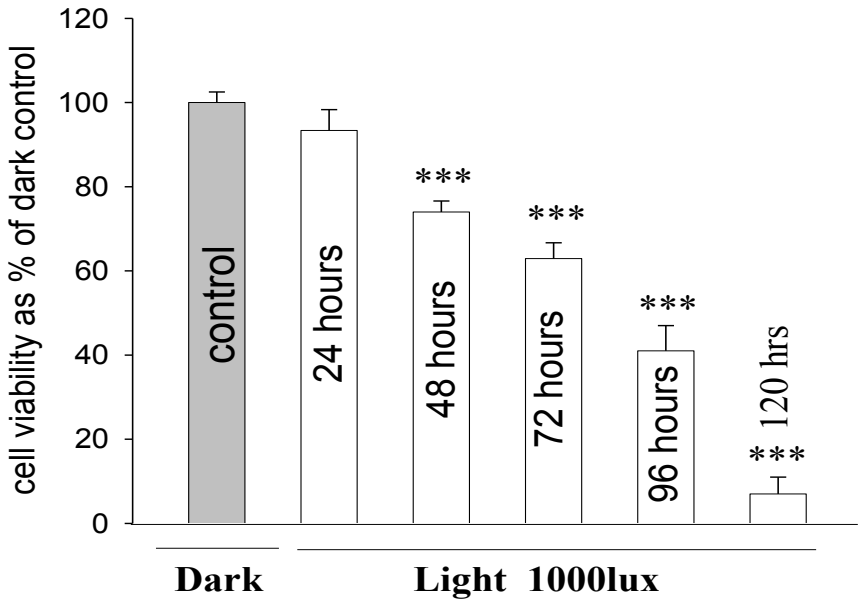


Figure 6.1. This figure shows the effect of increasing duration of light exposure time for 24, 48, 76, 96 and 120 hours on RGC-5 cell viability cell using resazurin-reduction procedure. In these studies, 96-well plates with RGC-5 cells are exposed to different times at an intensity of 1000 lux, while the control plate is covered with white paper to set up a dark condition in the same environment in the incubator. Compared with dark conditions, light causes a time-dependent reduction in cell viability. Values are expressed as percentage of control (dark conditions) and are the mean ± SEM of 5 individual experiments, each analysed at least in triplicates. Statistical differences ***$p<0.001$ are calculated by one-way ANOVA followed by TUKEY multiple comparative test.

The effects of increasing the dose of sodium azide on RGC-5 cell viability (using the resazurin-reduction assay) is shown in figure 6.2. In these studies, RGC-5 cells in 96-well plates were exposed to increasing concentrations of sodium azide for 24 hours. Compared to control, sodium azide-induced reduction in RGC-5 cell viability is dose-dependent. At 5mM concentration, cell viability is reduced by approximately 26% and this concentration chosen for subsequent experiments in this study.

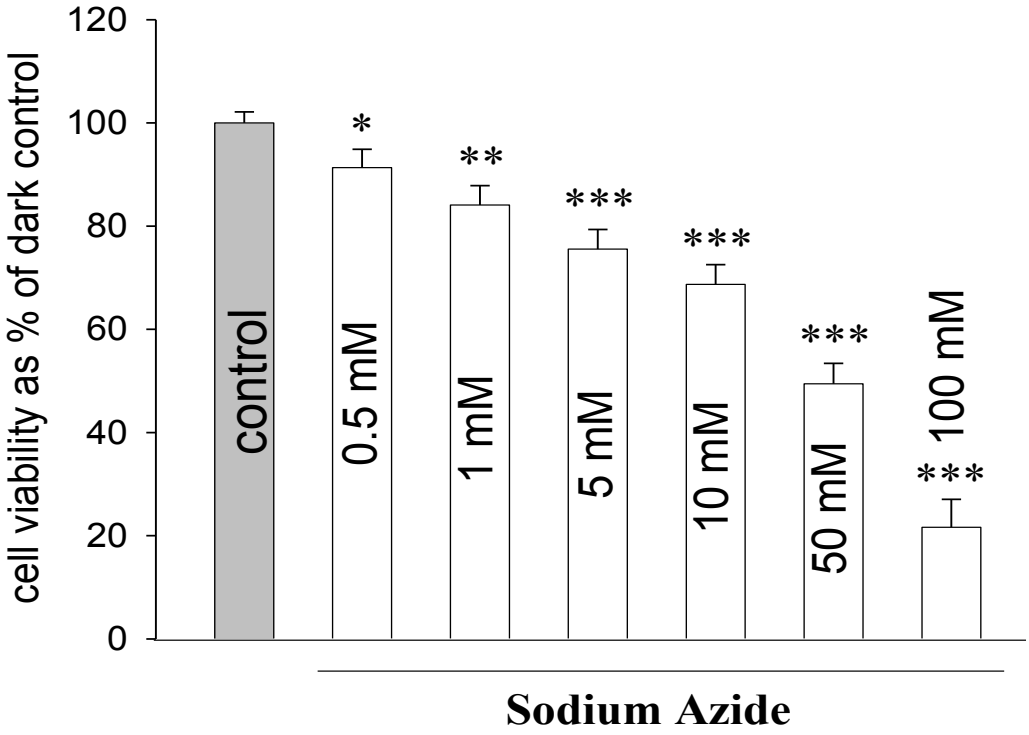


Figure 6.2. This figure shows the effect on increasing the dose of sodium azide for 24 hours on RGC-5 cell viability using resazurin-reduction assay. In these studies, RGC-5 cells in 96-well plates are exposed to increasing concentrations of sodium azide ((0.5mM, 1mM, 5mM, 10mM, 50mM and 100mM). After 24 hours, 5mM of sodium azide caused about 26% reduction in cell viability. Values are expressed as percentage of control and are the mean ± SEM of 5 individual experiments, each analysed at least in triplicates. Statistical differences ***$p<0.001$ are calculated by one-way ANOVA followed by TUKEY multiple comparative test.

The effect of epigallocatechin gallate (EGCG) in attenuating the light-induced RGC-5 cell loss is shown in figure 6.3. In this experiment, RGC-5 cells in 96-well plates were treated with EGCG in increasing concentrations (10μM, 20μM and 50μM) for 1 hours in dark conditions before being exposed to a further 48 hours in the dark (for control cells) or light at an intensity of 1000 lux. Cell viability was then assessed using resazurin-reduction assay. EGCG at low concentrations (10μM & 20μM) significantly attenuates light-induced damage to RGC-5 cells, but is ineffective at a higher concentration (50μM).

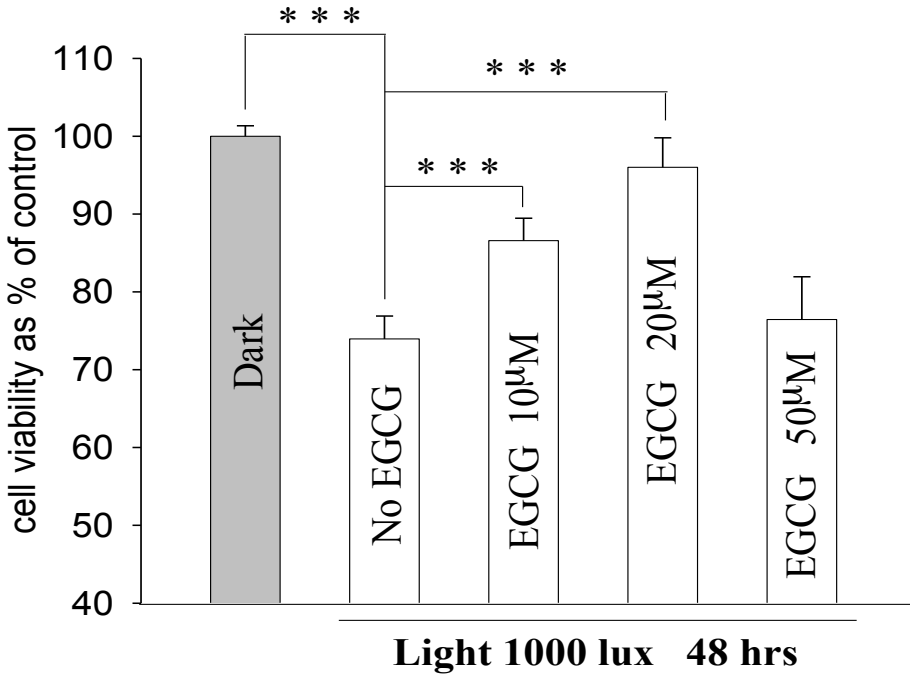


Figure 6.3. This figure shows the effect of EGCG in attenuating light-induced RGC-5 cell loss. After 48 hours, EGCG at 10μM and 20μM increased cell viability compared with vehicle-treated cells (labelled as No EGCG). However at 50μM concentration, this positive effect of EGCG on cell viability is not seen. Values are expressed as percentage of control (dark conditions) and are the mean ± SEM of 5 individual experiments, each analysed at least in triplicates. Statistical differences ***$p<0.001$ are calculated by one-way ANOVA followed by TUKEY multiple comparative test.

To assess the effects of EGCG in RGC-5 cell loss induced by sodium azide, cells were treated with increasing concentrations of EGCG for 1 hour before being exposed to sodium azide for a further 24 hours. The results of the cell viability studies carried out by resazurin-reduction assay are shown in figure 6.4 below. EGCG dose-dependently attenuated the loss cell loss induced by 5mM sodium azide.

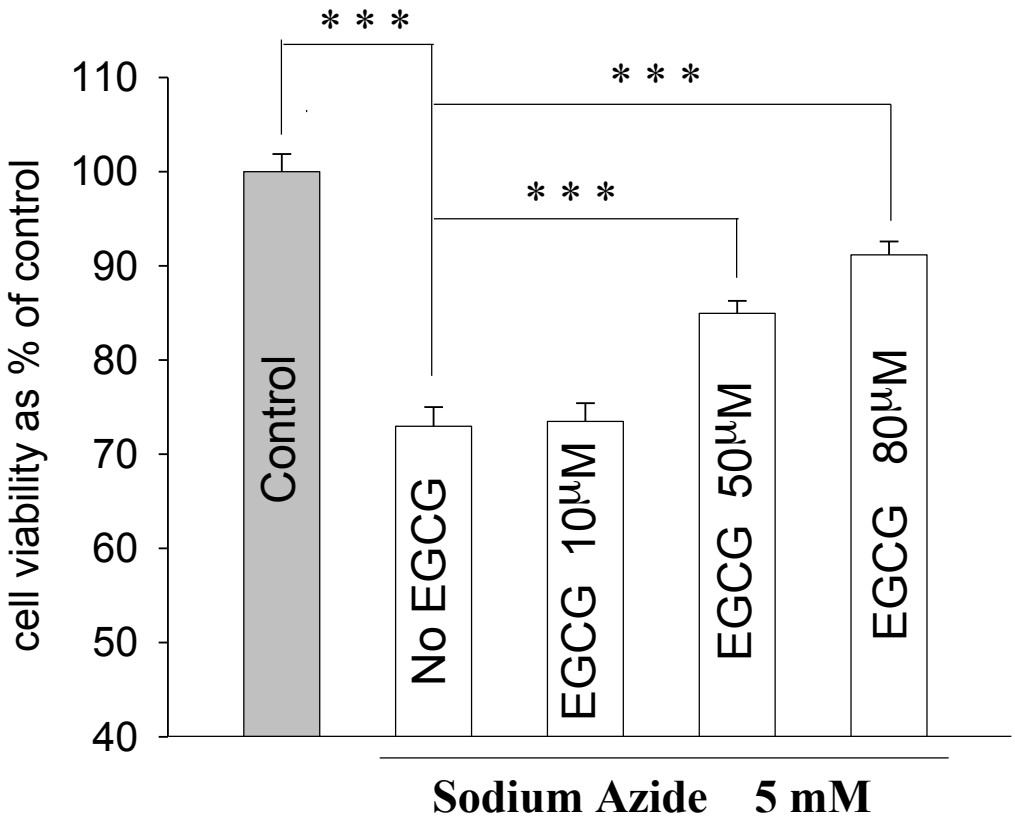


Figure 6.4. This figure shows the effect of EGCG in attenuating sodium azide-induced RGC-5 cell loss using the resazurin-reduction assay. EGCG significantly increased cell viability in a dose-dependent manner, peaking at 80μM. Values are expressed as percentage of control and are the mean ± SEM of 5 individual experiments, each analysed at least in triplicates. Statistical differences ***$p<0.001$ are calculated by one-way ANOVA followed by TUKEY multiple comparative test.

Mitochondrial dehydrogenase activity is related to mitochondrial energy production, and a fall in activity implies a reduced energy production. The effect of EGCG on the activity of mitochondrial dehydrogenase in light-induced cell damage is shown in figure 6.5. After 48 hours, light significantly reduces mitochondrial activity by approximately 30%, and this effect is attenuated by EGCG at 10μM and 20μM concentrations.

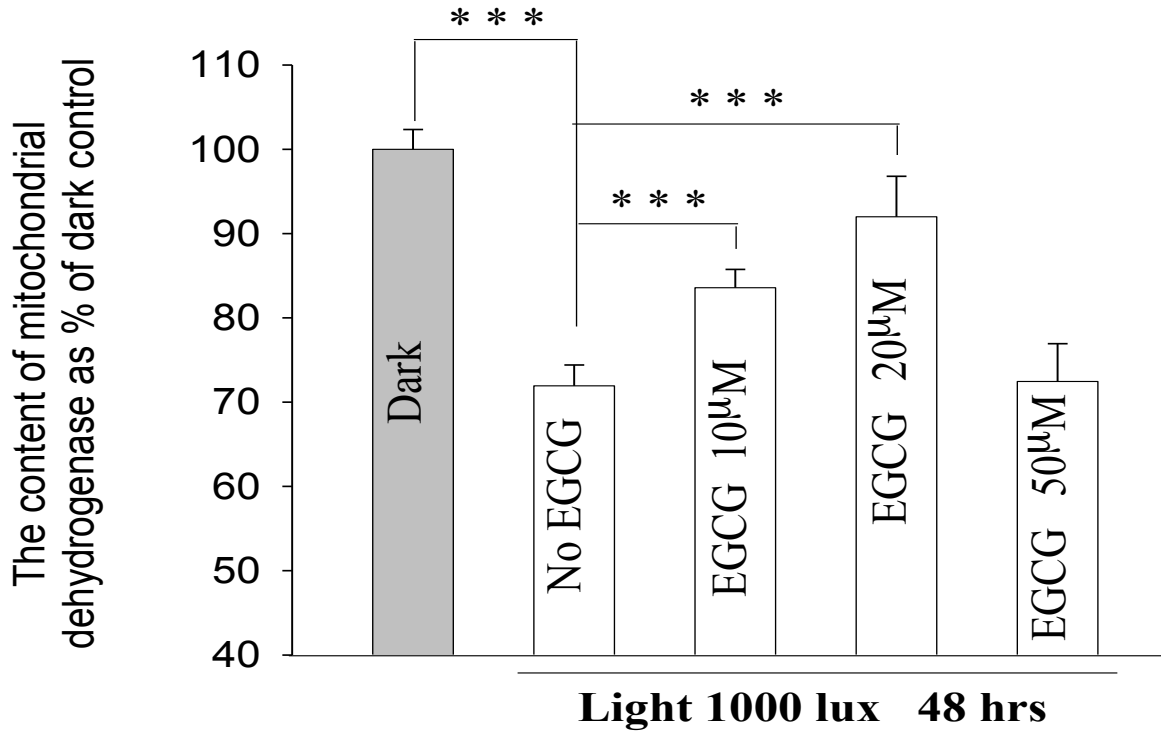


Figure 6.5. In these studies, 96-well plates with RGC-5 cells were treated to three different concentrations of EGCG (10μM, 20μM & 50μM) for 1 hour before being exposed to light (1000lux) for a further 48 hours. Mitochondrial dehydrogenase activity was measured by WST-1 assay. EGCG at 10μM and 20μM significantly attenuate light-induced reduction of mitochondrial dehydrogenase activity after 48 hours. However, this positive effect on the mitochondria is not seen at 50μM concentration. Values are expressed as percentage of control (dark conditions) and are the mean ± SEM of 5 individual experiments, each analysed at least in triplicates. Statistical differences ***$p<0.001$ are calculated by one-way ANOVA followed by TUKEY multiple comparative test.

To compare these findings to the effects of EGCG on mitochondrial dehydrogenase activity in sodium azide-induced cell death, RGC-5 cells pre-treated with EGCG was exposed to 5mM sodium azide for 24 hours and analysed using WST-1 assay. The results are shown in figure 6.6 below. Sodium azide at 5mM significantly reduced mitochondrial dehydrogenase activity by almost 30%. This negative effect is significantly attenuated by EGCG in a dose-dependent manner.

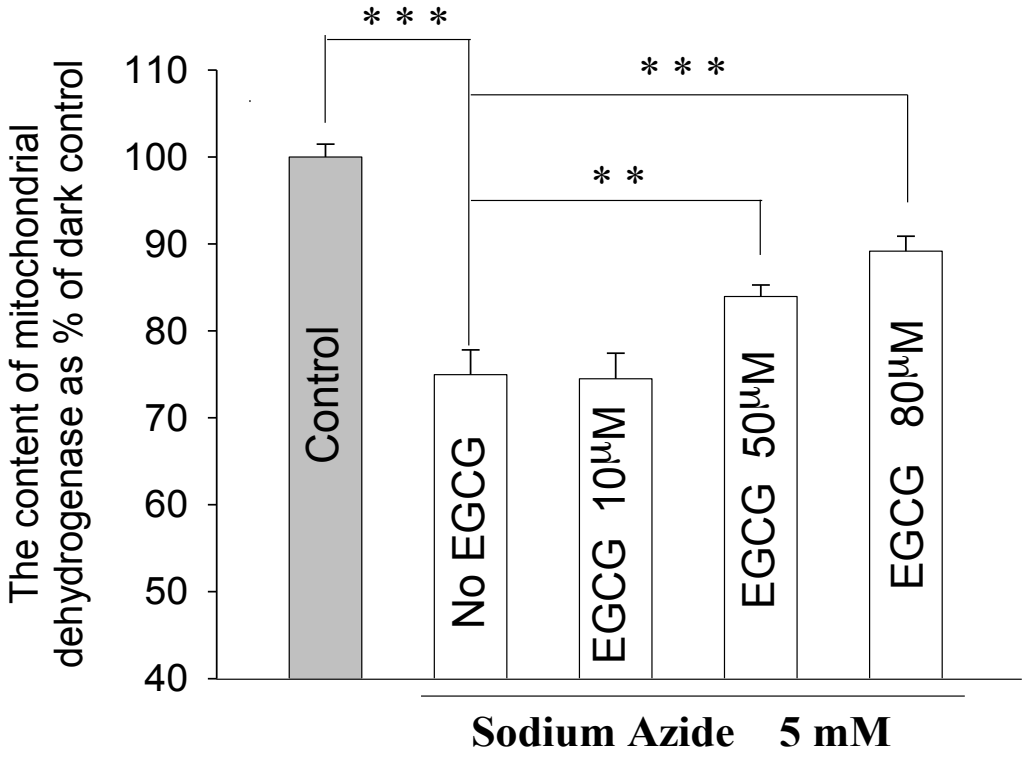


Figure 6.6. This figure shows that the effects of sodium azide on mitochondrial dehydrogenase activity using the WST-1 assay. Sodium azide caused almost 30% reduction in the activity, and this effect is significantly attenuated by EGCG in a dose-dependent manner. Values are expressed as percentage of control and are the mean ± SEM of 5 individual experiments, each analysed at least in triplicates. Statistical differences **p<0.01, ***p<0.001 are calculated by one-way ANOVA followed by TUKEY multiple comparative test.

To further compare the mechanism by which light and sodium azide cause RGC-5 cell death, cell viability studies were carried out using a caspase signaling pathway inhibitors, pan-caspase inhibitor (z-VAD-fmk). The cell viability studies were carried out using the resazurin-reduction assay. Figure 6.7 show that after 48 hours, the pan-caspase inhibitor has no effect on light-induced cell death in RGC-5 cells.

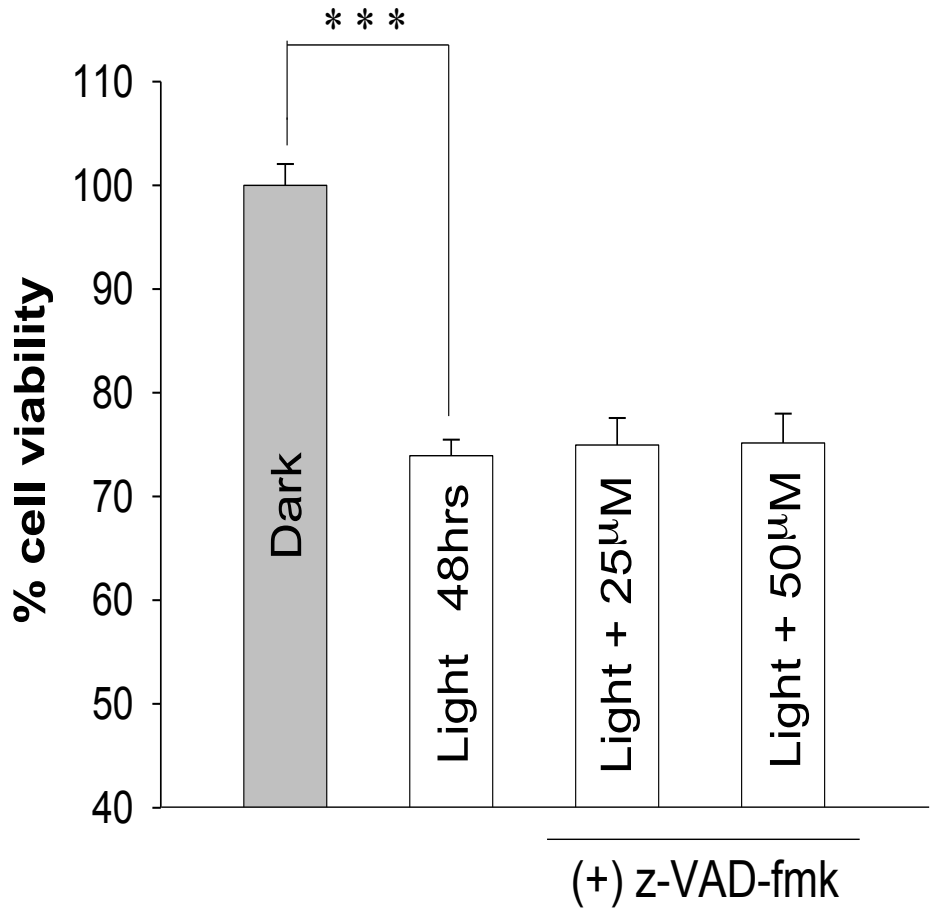


Figure 6.7. Cell viability studies using resazurin-reduction assay show that light-induced RGC-5 cell death is not attenuated by a pan-caspase inhibitor, z-VAD-fmk at the concentrations used. Values are expressed as percentage of control and are the mean ± SEM of 5 individual experiments, each analysed at least in triplicates. Statistical differences ***$p<0.001$ are calculated by one-way ANOVA followed by TUKEY multiple comparative test.

In contrast to light-induced RGC-5 cell death, cell loss caused by sodium azide at 5mM is significantly attenuated by pan-caspase inhibitor, as shown in figure 6.8. Using the resazurin-reduction assay to assess for cell viability, RGC-5 cell survival is significantly increased by pan caspase inhibitor (z-VAD-fmk) at increasing concentrations of 25 and 50μM.

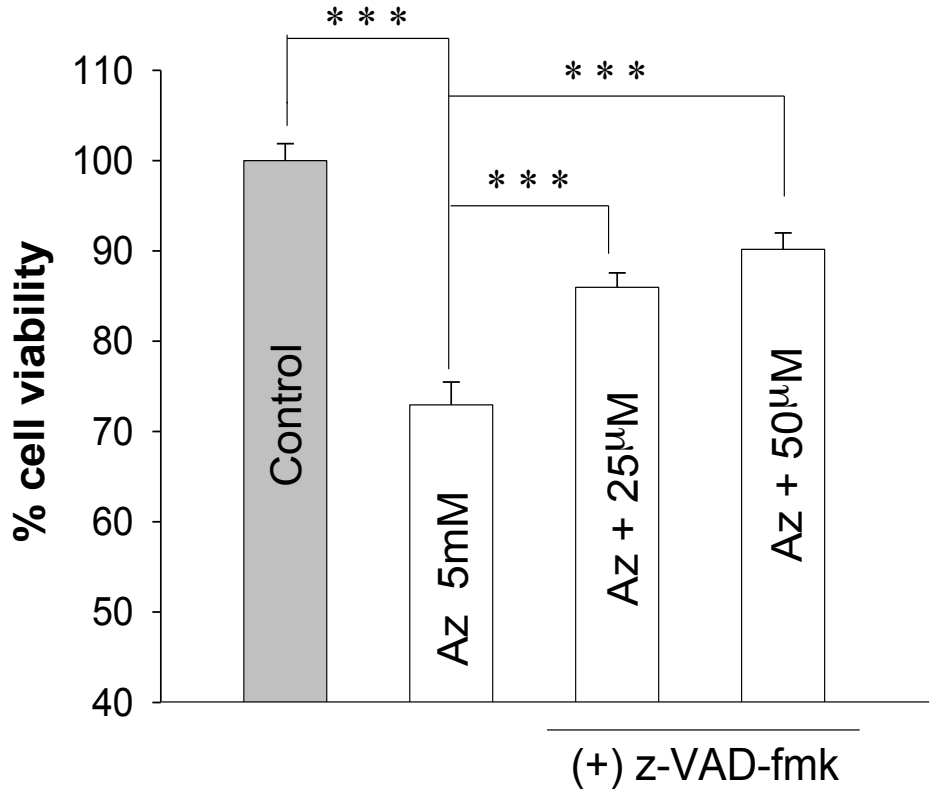


Figure 6.8. In the cell viability studies above, RGC-5 cell loss induced by sodium azide (5mM) is significantly attenuated by a pan-caspase inhibitor, z-VAD-fmk in a dose-dependent manner (25μM & 50μM). Values are expressed as percentage of control and are the mean ± SEM of 5 individual experiments, each analysed at least in triplicates. Statistical differences ***$p<0.001$ are calculated by one-way ANOVA followed by TUKEY multiple comparative test.

To confirm the involvement of caspase pathway in both light- and sodium azide-induced RGC-5 cell death, caspase-3 activity was carried out using the caspase-3 assay. The results are shown in figure 6.9. Consistent with the observations in the cell viability studies, caspase-3 activity was elevated by sodium azide and staurosporine (positive control) but not by light. This findings suggest that in contrast to light, sodium azide-induced cell death involves caspase signaling pathway.

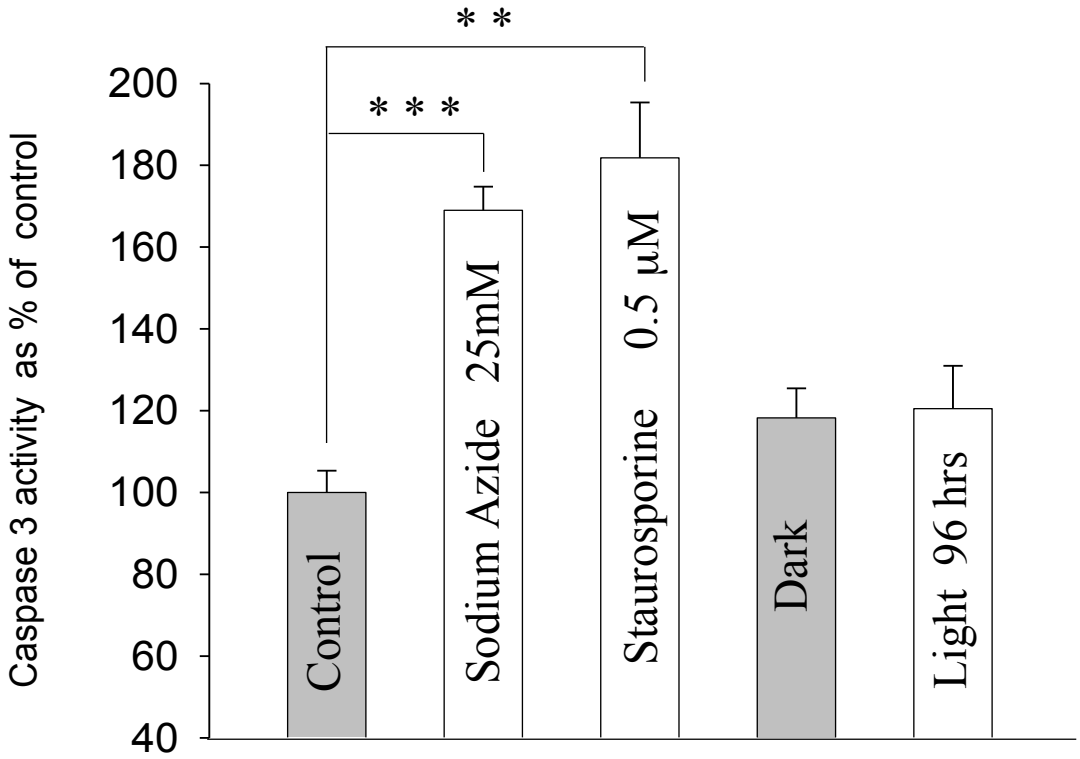


Figure 6.9. In the caspase-3 studies, RGC-5 cells in 6-well plates are treated with sodium azide (5mM) or staurosporine (0.5μM) for 24 hours, or exposed to dark (control) or light (1000 lux) conditions for 48 hours. The cells pellets are lysed before being analysed using caspase-3 colorimetric assay as described in section 2.2.11. Staurosporine is used as positive control in this assay. Caspase-3 activity is significantly increased by sodium azide, but is not affected by light after 96 hours. Values are expressed as percentage of control and are the mean ± SEM of 5 individual experiments, each analysed at least in triplicates. Statistical differences **$p<0.01$, ***$p<0.001$ are calculated by one-way ANOVA followed by TUKEY multiple comparative test.

To determine if light-induced cell death occur by necroptosis, RGC-5 cells in 96-well plates were pre-treated with necroptosis inhibitor, necrostatin-1 at 25μM and 50μM concentrations, before exposed to light treatment 1000lux for 48 hours. Cell viability studies are carried out using resazurin-reduction assay. As shown in figure 6.10 below, light-induced RGC-5 cell death is significantly attenuated by necrostatin-1 at both concentrations used. This finding suggests that light cause cell death by necroptosis.

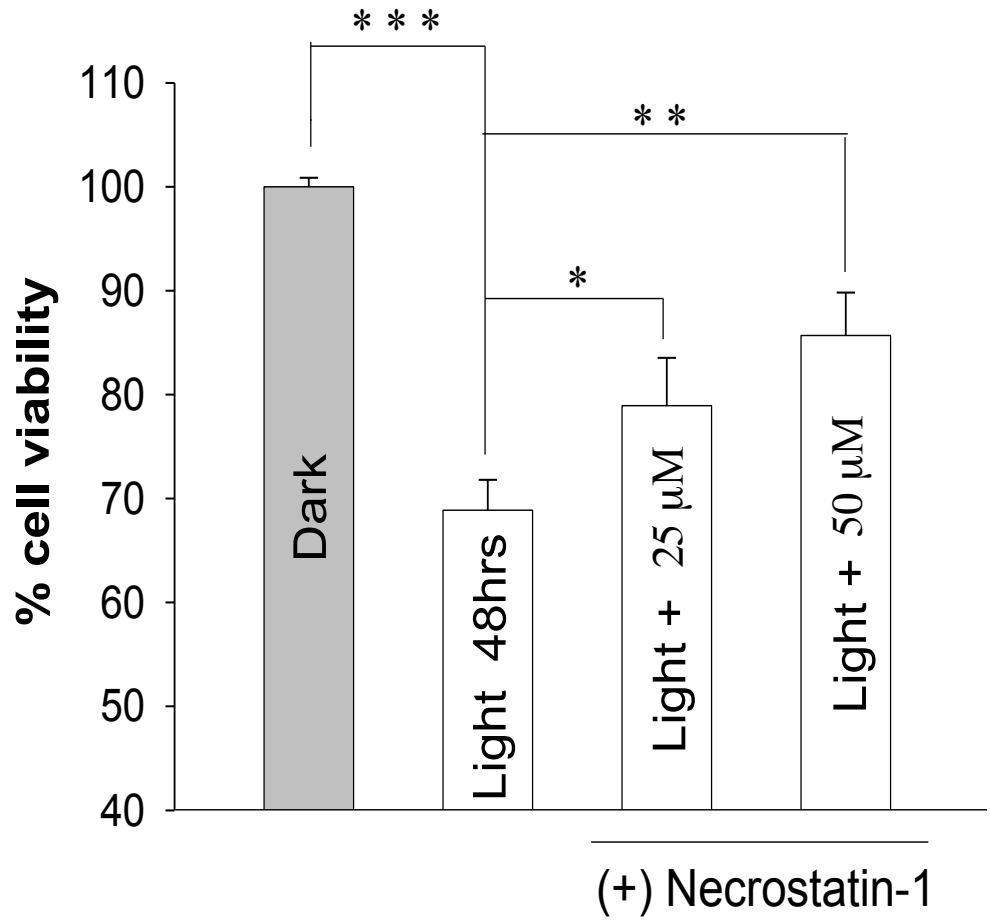


Figure 6.10. In the cell viability studies above, RGC-5 cell loss induced by light (1000lux, 96 hours) is significantly attenuated by a necroptosis inhibitor, necrostatin-1, in a dose-dependent manner (25μM & 50μM). Values are expressed as percentage of control and are the mean ± SEM of 5 individual experiments, each analysed at least in triplicates. Statistical differences ***$p<0.001$ are calculated by one-way ANOVA followed by TUKEY multiple comparative test.

To compare the mode of cell death by necroptosis, cell viability studies are carried out on RGC-5 cells exposed to sodium azide (5mM, 24 hours) after pre-treatment for an hour with necropstatin-1. Figure 6.11 shows that cell death in RGC-5 cell death caused by sodium azide is not affected by necrostatin-1, implying that necroptosis is not involved in sodium azide-induced cell death.

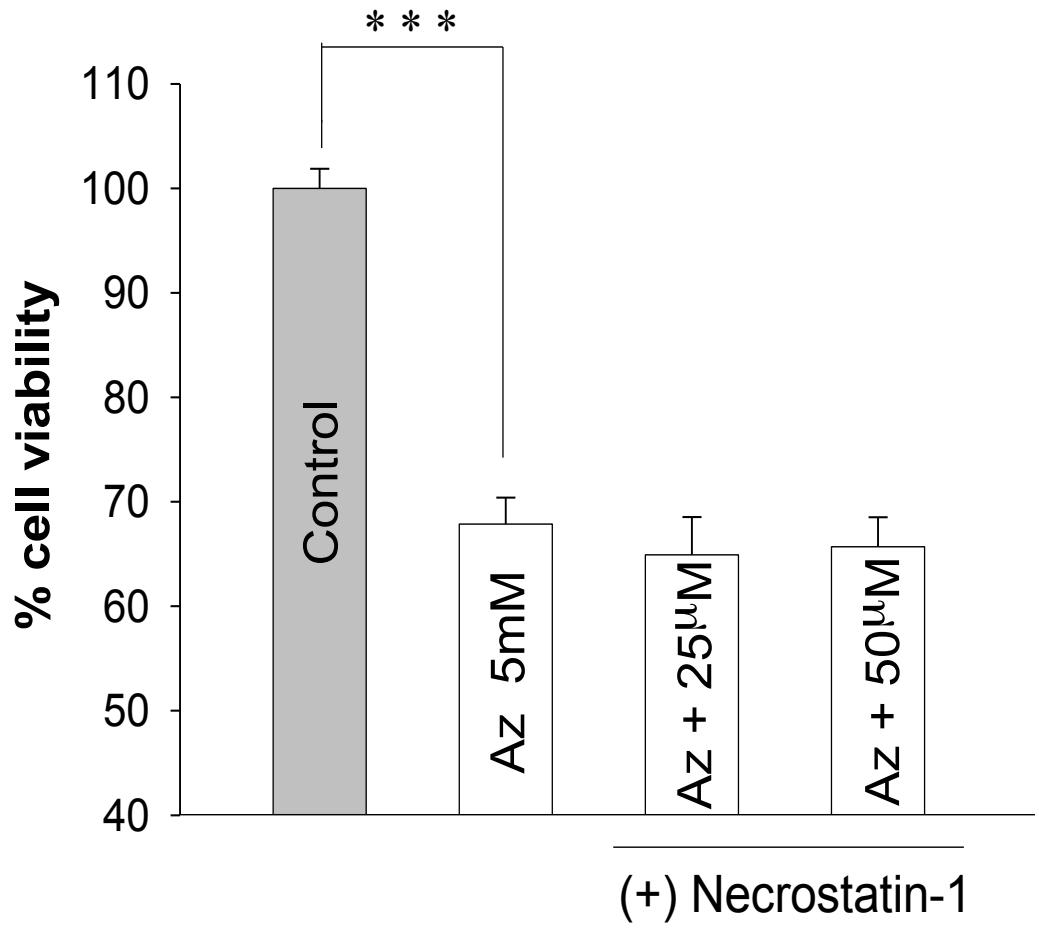


Figure 6.11. In the cell viability studies above, necrostatin-1, a necroptosis inhibitor, does not have any effect on RGC-5 cell loss induced by sodium azide (5mM, 24 hours) Values are expressed as percentage of control and are the mean ± SEM of 5 individual experiments, each analysed at least in triplicates. Statistical differences ***$p<0.001$ are calculated by one-way ANOVA followed by TUKEY multiple comparative test.

6.3.2 Production of reactive oxygen species (ROS)

To compare the production of reactive oxygen species (ROS) in light- and sodium azide-induced RGC-5 cell damage, DHE staining is used as an indicator of ROS production. ROS production is shown by a yellow fluorescence against a dark red background. As shown in figure 6.12, ROS production is marked when RGC-5 cells are exposed to sodium azide 5mM for 24 hours and light 1000 lux for 48 hours. However, these effects are ROS production is significantly reduced when cells were pre-treated with EGCG 20μM (for light experiments) and 80μM (for sodium azide experiments).

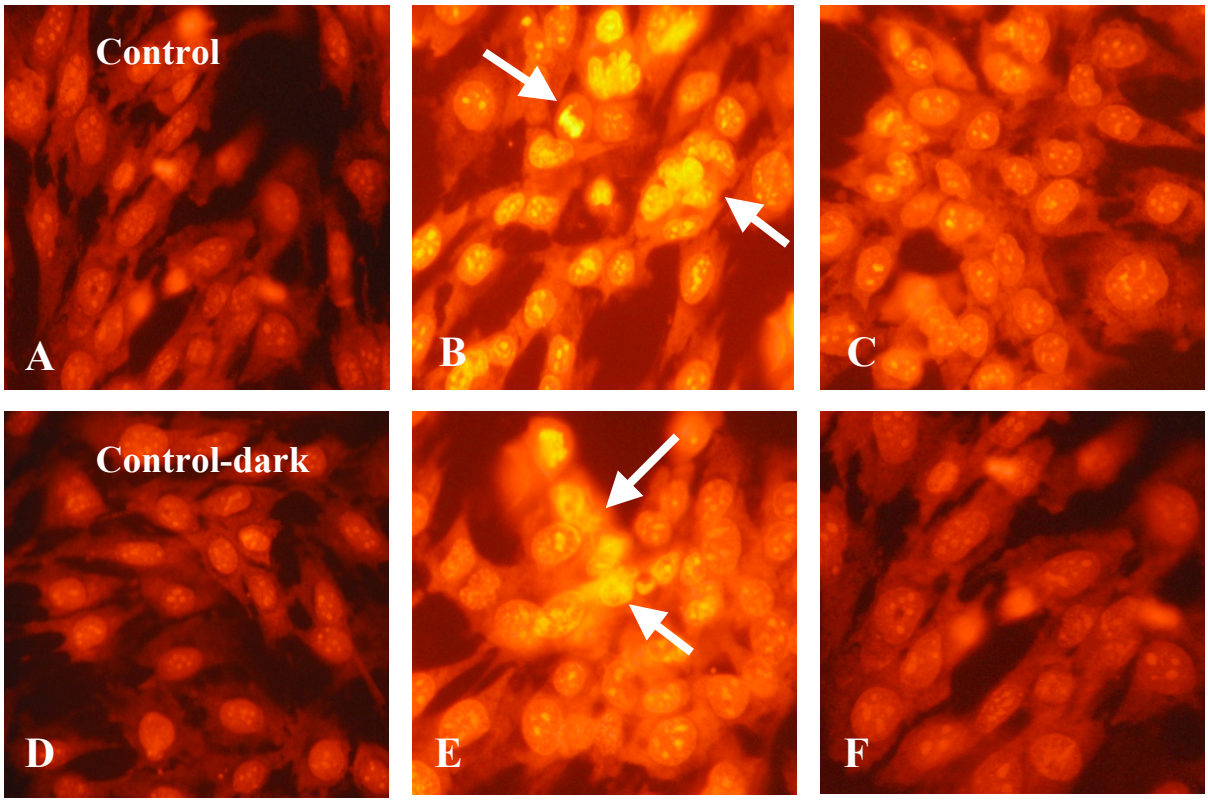


Figure 6.12. DHE staining for ROS production in RGC-5 cells. In the upper panel (A-C), cells are exposed to sodium azide or vehicle (control), and in the lower panel (D-F), cells are exposed to dark conditions (control) or light (1000lux) for 48 hours. In contrast to control, ROS production as indicated by yellow fluorescence (white arrows) is markedly en hanced by sodium azide and light (B & E). This effect is significantly reduced when cells are pre-treated for 1 hour with EGCG 80μM as shown by the absence of yellow fluorescence in C and F. These findings were confirmed in three separate experiments.

6.3.3 Dead/live cell assay with propidium iodide (PI)

A cell live-death assay was used to stain RGC-5 cell death induced by light and sodium azide. Fluoroscein diacetate stains live cells fluorescent green while propidium iodide stains dead cells red. Following pre-treatment for 1 hour with EGCG 20μM (for light experiments) and 80μM (for sodium azide experiments), cells were exposed to light 1000 lux for 48 hours or sodium azide 5mM for 24 hours, RGC-5 cells on coverslips in 24-well plates are incubated with fluorescein diacetate (FDA) at 5μM for 2 minutes before counterstaining with 3μM propidium iodide for 30 minutes. Cells are rinsed before examined under fluorescence microscopy. Figure 6.13 shows that when exposed to soidm azide or light, some cells died and this effect was partially blunted by EGCG.

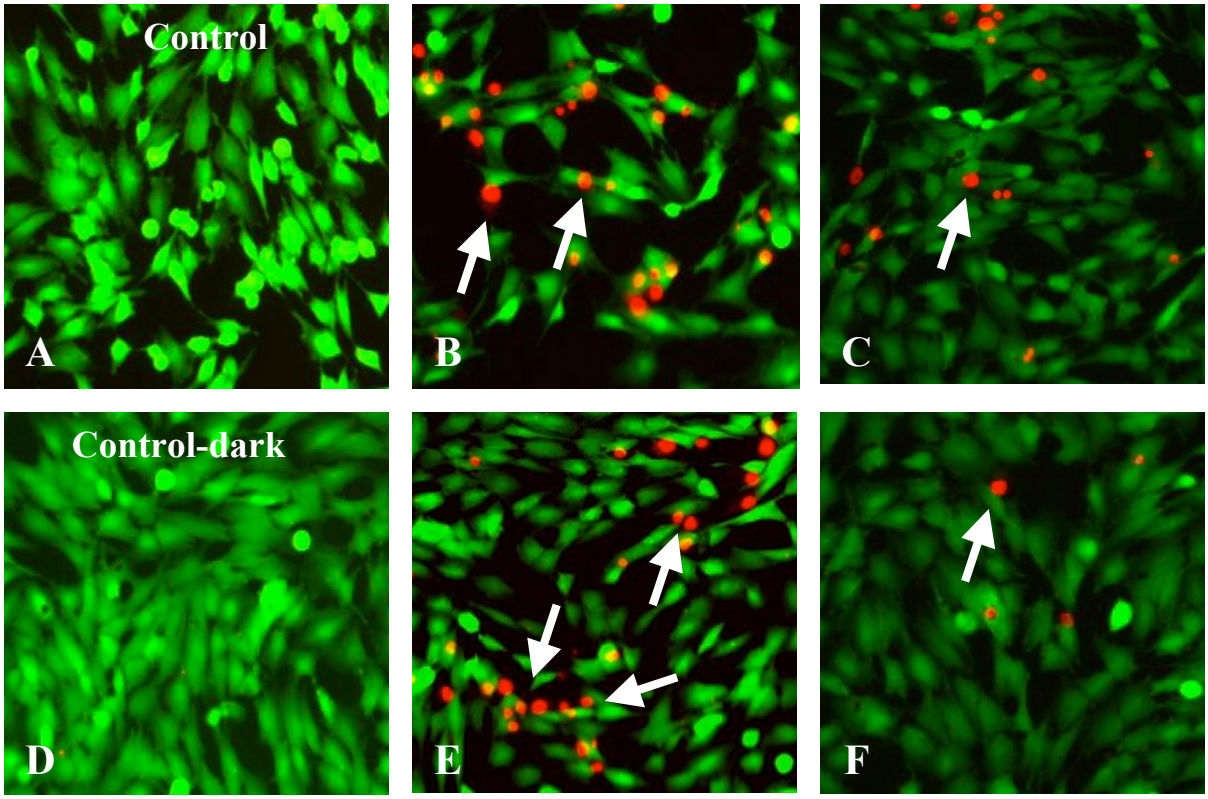


Figure 6.13. FDA/PI cell live-death counterstaining in RGC-5 cell cultures. In the upper panel (A-C), cells are exposed to sodium azide or vehicle (control), and in the lower panel (D-F), cells are exposed to dark conditions (control) or light (1000 lux) for 48 hours. In contrast to control, cell death as indicated by red staining (white arrows) is increased by sodium azide and light (B & E). This effect is blunted when cells are pre-treated for 1 hour with EGCG 20μM (in light) and 80μM (in sodium azide) (figures C&F). These findings were confirmed in three separate experiments.

6.3.4 Apoptosis by APOPercentage™ and TUNEL methods

Both light and sodium azide caused RGC-5 cell death by apoptosis as shown by the translocation of phosphotidylserine as identified by APOPercentageTM staining method in figure 6.14. The number of apoptotic cells as indicated by pink staining, is increased when cells are exposed to light insult 1000 lux for 48 hours, or 5mM sodium azide insult for 24 hours. When pre-treated with EGCG 20μM and 80μM for 1 hour before exposure to the insults, the number of apoptotic cells is markedly reduced.

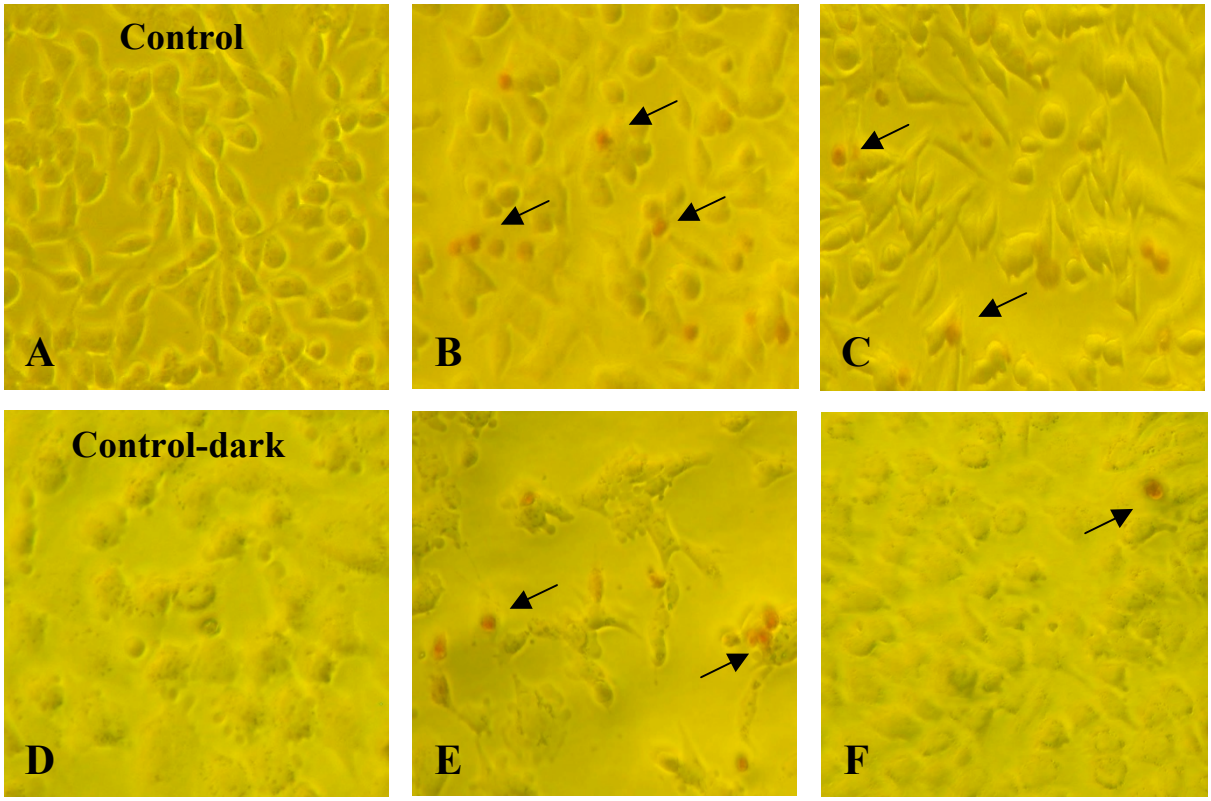


Figure 6.14. APOPercentage™ staining for phosphotidylcholine translocation in RGC-5 cells. In the upper panel (A-C), cells are exposed to sodium azide or vehicle (control), and in the lower panel (D-F), cells are exposed to dark conditions (control) or light (1000 lux) for 48 hours. In contrast to control, apoptosis as indicated by pink staining (black arrows) is increased by sodium azide and light (B & E). This effect is blunted when cells are pre-treated for 1 hour with EGCG 20μM (in light) and 80μM (in sodium azide) (figures C&F). These findings were confirmed in three separate experiments.

The findings with TUNEL staining for DNA breakdown in apoptotic cells in RGC-5 cells corroborated the APOPercentage^{TM} staining, as shown in figure 6.15. Light and sodium azide caused cell death by apoptotic cells are shown by the increase in cells with DNA breakdown (figures 6.15B & E). When pre-treated with EGCG 20μM and 80μM in light and sodium azide experiments respectively, the number of apoptotic cells are markedly reduced (figures 6.15C & F)

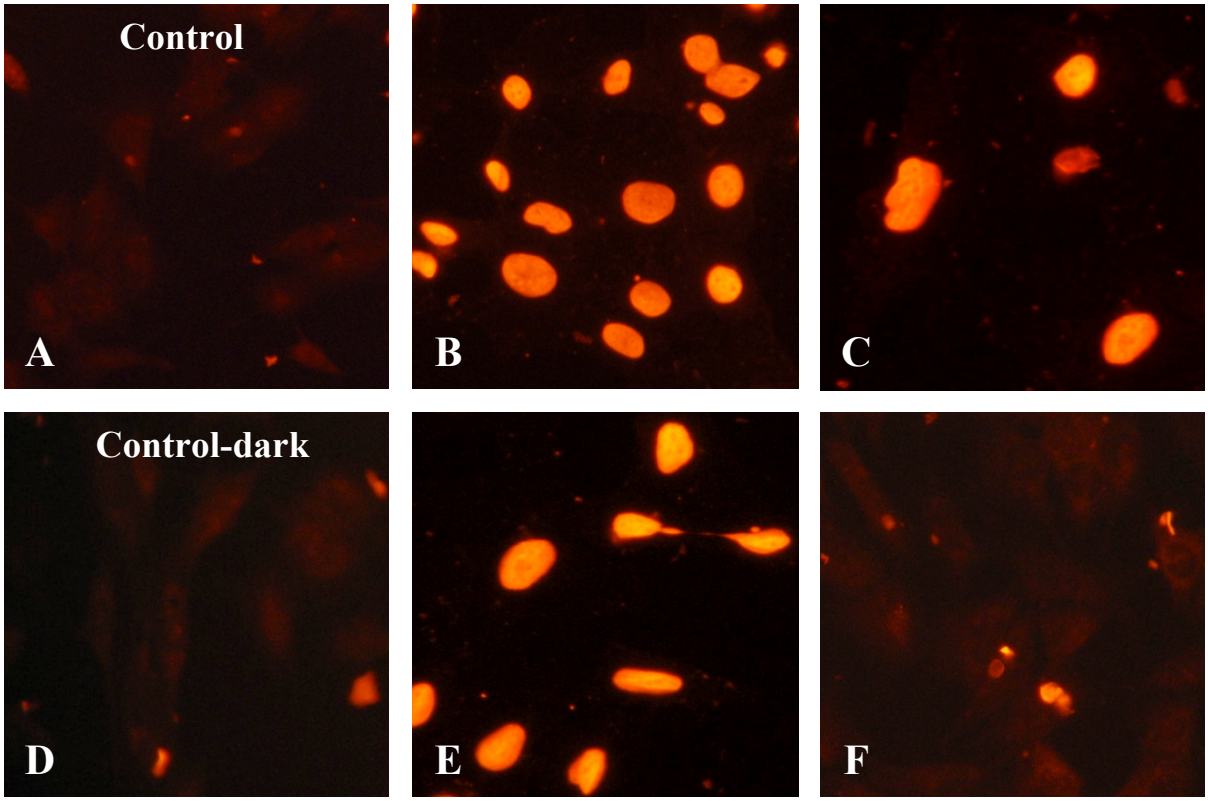
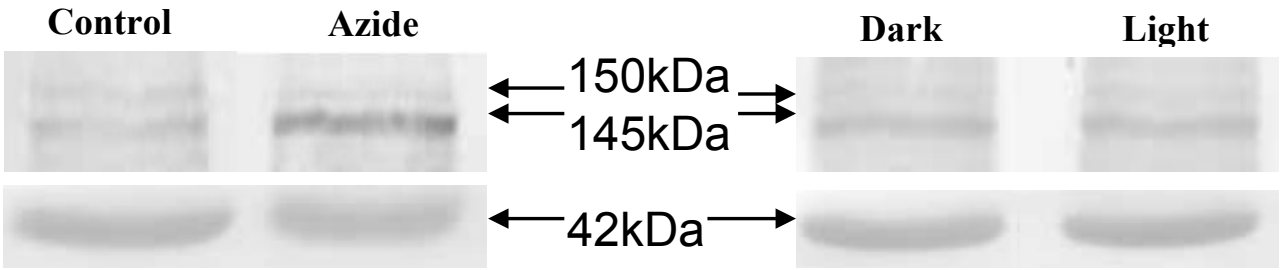


Figure 6.15. TUNEL staining for DNA breakdown indicating apoptosis in RGC-5 cells. In the upper panel (A-C), cells are exposed to sodium azide or vehicle (control), and in the lower panel (D-F), cells are exposed to dark conditions (control) or light (1000 lux) for 48 hours. In contrast to control, apoptosis as indicated by bright reddish-yellow staining is increased by sodium azide and light (B & E). This effect is blunted when cells are pre-treated for 1 hour with EGCG 20μM (in light) and 80μM (in sodium azide) (figures C&F). These findings were confirmed in three separate experiments.

6.3.5 Western blot analysis

Results from western blot analysis of RGC-5 cell extracts processed for alpha fodrin proteins after exposure to either light or sodium azide insult, are shown in figure 6.16. Alpha fodrin is a member of the spectrin family of filamentous proteins that is cleaved in apoptosis initiated by insults such as staurosporine. After respective treatment with light (1000lux, 96 hours) and sodium azide (5mM, 24 hours), RGC-5 cells in 6-well plates are collected and extracted for proteins. Immunostaining using alpha fodrin antibodies showed two protein species with molecular weights of 150 and 145kDa. Only the 145kDa protein is significantly up-regulated by sodium azide whereas this effect is not seen in light insult.



Figrue 6.16 The figure shows two protein bands for alpha-fodrin (150kDa and 145kDa, upper panel) are detected in control and dark conditions. However, only the 145kDa species is up-regulated in sodium azide (Azide, 5mM at 24 hours). This effect is not seen in light-treated cells (1000lux, 96 hours). Identical amounts of total protein for each sample are analysed to allow for the 145kDa alpha fodrin protein to be related to actin (42kDa, lower panel).

Relative to actin (42kDa), densitometry studies shows that sodium azide cause a significant increase in levels of the 145kDa alpha fodrin protein by approximately 100% as shown in figure 6.17A. In contrast, there is no difference in the levels of the cleaved alpha fodrin protein in light-induced cell damage.

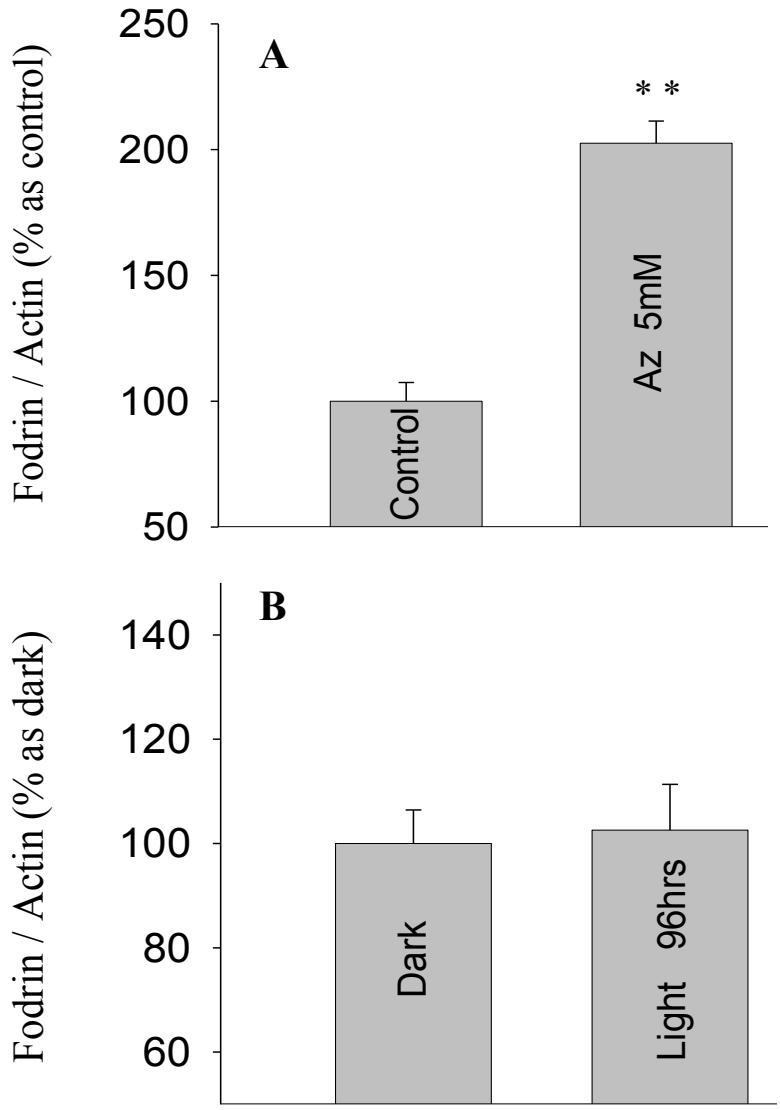


Figure 6.17. Quantitative analysis, relative to actin, of the 145kDa alpha fodrin protein are shown above. RGC-5 cell extracts are analysed after treatment with sodium azide (5mM, 24 hours) or light (1000lux, 96 hours). The 145kDa protein is up-regulated only in sodium azide-treated cells. Results are expressed as mean values ± SEMs for three separate experiments.

In contrast to the findings in alpha fodrin, apoptosis inducing factor (AIF) which occur as a major (67kDa) and minor (62kDa) product, is only affected by light and not by sodium azide. Figure 6.18 shows an AIF-cleaved component with a molecular weight of 57kDa is induced by light (1000 lux, 96 hours) but not by sodium azide (azide, 5mM for 24 hours)).

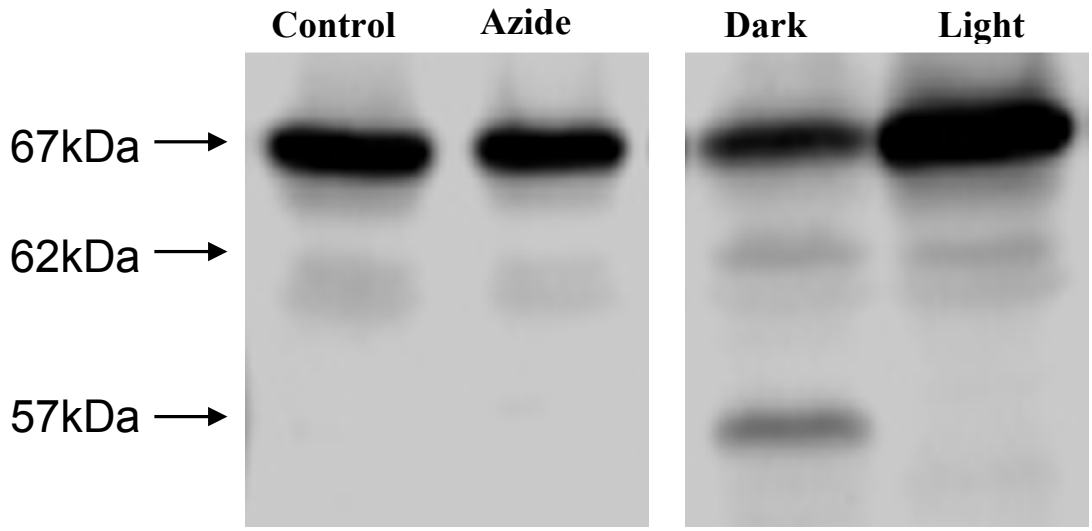


Figure 6.18. Western blots of identical amounts of total fractionated proteins stained using an AIF antibody. In control RGC-5 cells (Control or Dark) a major (67kDa) and a minor (62kDa) proteins are detected. However, when the cultures are exposed to light (1000lux for 96 hours) an additional 57kDa protein band is detected. This finding is not seen when cells are exposed to 5mM sodium azide (Azide) for 24 hours.

Bcl-2 protein (26kDa), which is involved in the mitochondrial anti-apoptotic signaling pathway, is reduced in RGC-5 cells following an insult of either light or sodium azide as shown in figure 6.19.

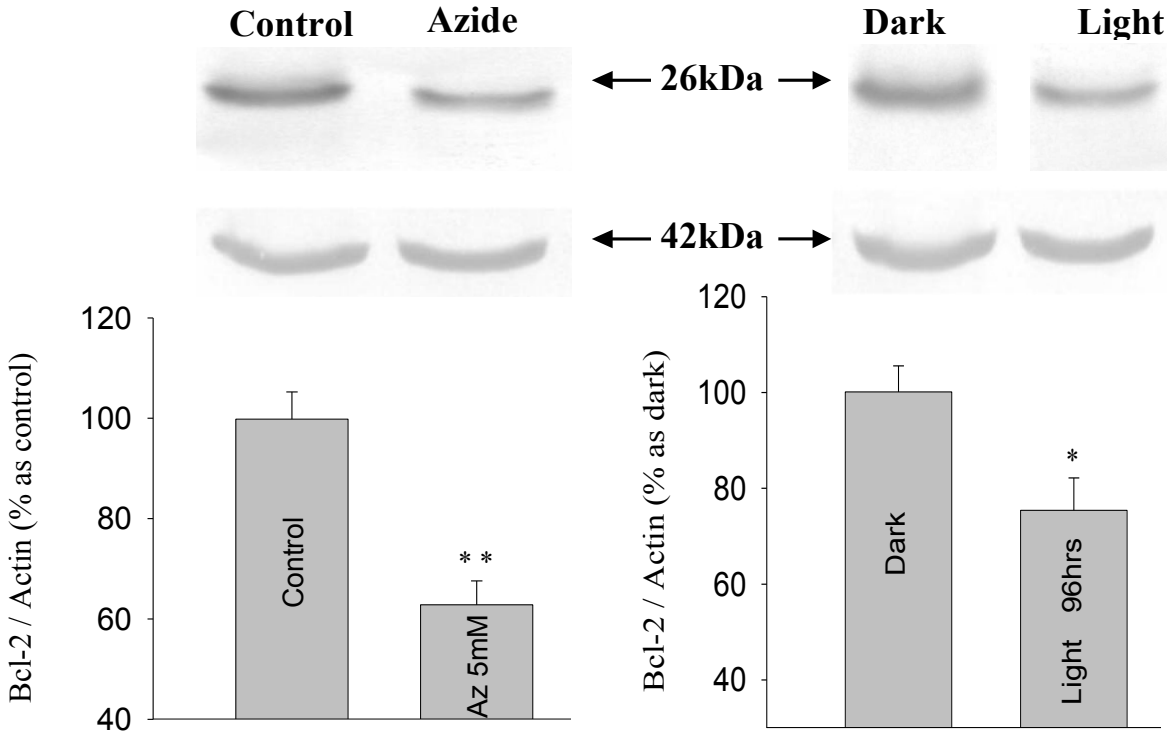


Figure 6.19. Western blots of identical amounts of fractionated proteins stained by antibodies detecting Bcl-2 (26kDa) and actin (42kDa). When related to the amount of actin using densitometry, both light (1000lux, 96 hours) and sodium azide (Azide; 5mM, 24 hours) caused a down-regulation of Bcl-2. Results are expressed as mean values ± SEMs of three different experiments. Statistical significance is analysed using student's unpaired *t*-test, *p<0.05, **p<0.01.

Heme oxygenase-1 or heat shock protein 32 (Hsp32) is a major heat shock/stress response protein and its up-regulation is associated with cytoprotective response to various stimuli causing cellular stress. Western blot analysis of RGC-5 cell lysates stained with antibody against HO-1 (molecular weight 32kDa) show that only light insult (1000lux, 96 hours) cause up-regulation of HO-1, whereas this finding is not seen sodium azide-treated cells (5mM, 24 hours) (figure 6.20).

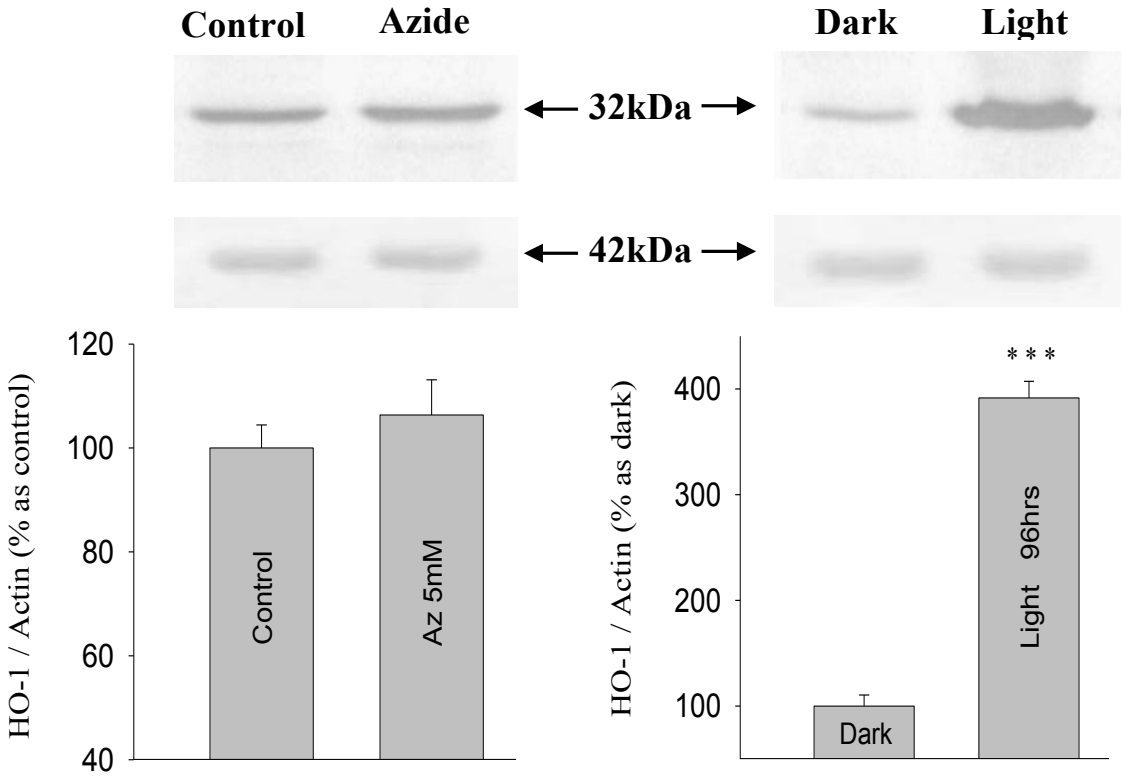


Figure 6.20. Western blots of identical amounts of fractionated proteins stained by antibodies detecting HO-1 (32kDa) and actin (42kDa). When related to the amount of actin using densitometry, only light (1000lux, 96 hours) in comparison to sodium azide (Azide; 5mM, 24 hours) caused a four-fold increase in HO-1 levels. Results are expressed as mean values ± SEMs of three different experiments. Statistical significance is analysed using student's unpaired *t*-test, ***$p<0.001$.

The antibody to P-JNK revealed a major protein component of a molecular weight of 46kDa in control RGC-5 cell extracts (figure 6.21) and an additional minor protein species of 52kDa in cells exposed to light (1000lux, 96 hours). This minor P-JNK protein species is absent in RGC-5 extracts exposed to sodium zide (5mM, 24 hours). Protein species corresponding to P-c-Jun (molecular weight 37kDa) and P-p38 (molecular weight 43kDa) are not evident in control RGC-5 cell extracts. However, P-c-Jun protein is evident in RGC-5 cells only after exposure to light insult (1000lux, 96 hours) while P-p-38 MAPK is up-regulated in cells exposed to both light (1000lux, 96 hours) and sodium azide (5mM, 24 hours) insults.

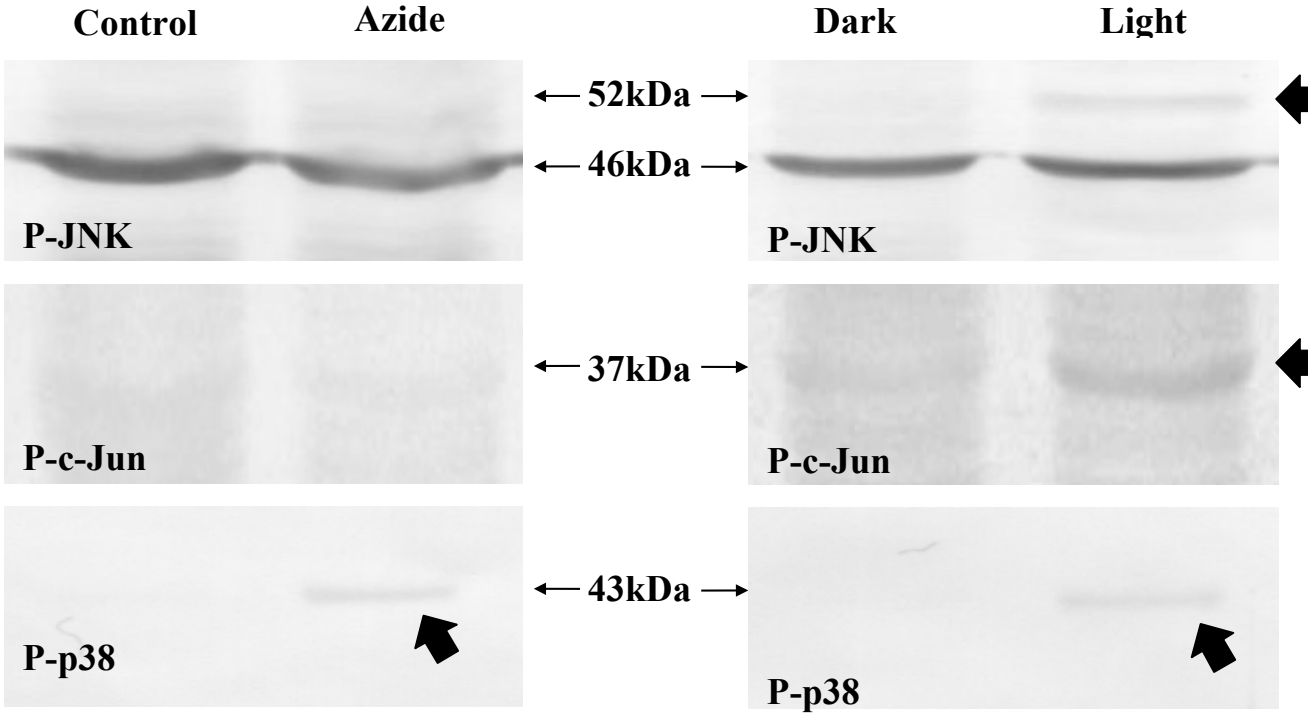


Figure 6.21. Western blots of identical amounts of total fractionated proteins stained by antibodies for detecting P-JNK (46 and 52kDa), its substrate P-c-Jun (37kDa) and another MAPK family protein, P-p38 (43kDa). In the control samples (Control and Dark), staining for the 52kDa species of P-JNK, P-c-Jun and P-p38 MAPK are barely detectable. Following sodium azide insult (Azide; 5mM, 24 hours), only the P-p38 MAPK protein (wide black arrow) is up-regulated. In contrast, all three proteins namely P-JNK (52kDa), P-c-Jun and P-p38 MAPK (wide black arrows) are up-regulated following light insult (1000lux, 96 hours).

6.3.6 Immunocytochemistry

In these studies, RGC-5 cells are plated on cover slips in 24-well plates and exposed to either sodium azide (5mM, 24 hours) or light (1000lux, 96 hours) insults. After fixation, cells are stained using antibodies against P-p38 MAPK and p-c-Jun proteins. In order to stain the nuclei for co-localisation of proteins, DAPI staining is used. Figure 6.22 show that P-p38 MAPK protein is activated by both sodium azide and light insults, which confirms the western blot results in figure 6.21. It can be observed that P-p38 MAPK is located in the cytoplasm of RGC-5 cells.

Figure 6.23 show that only light insult causes the activation of P-c-Jun, resulting in these phosphorylated proteins being translocated from the nucleus to the cytoplasm. There is no difference in P-c-Jun immunostaining between vehicle-treated cells (control) and sodium azide-treated cells, which corroborate the western blot analysis of RGC-5 cell extracts as shown in figure 6.21.

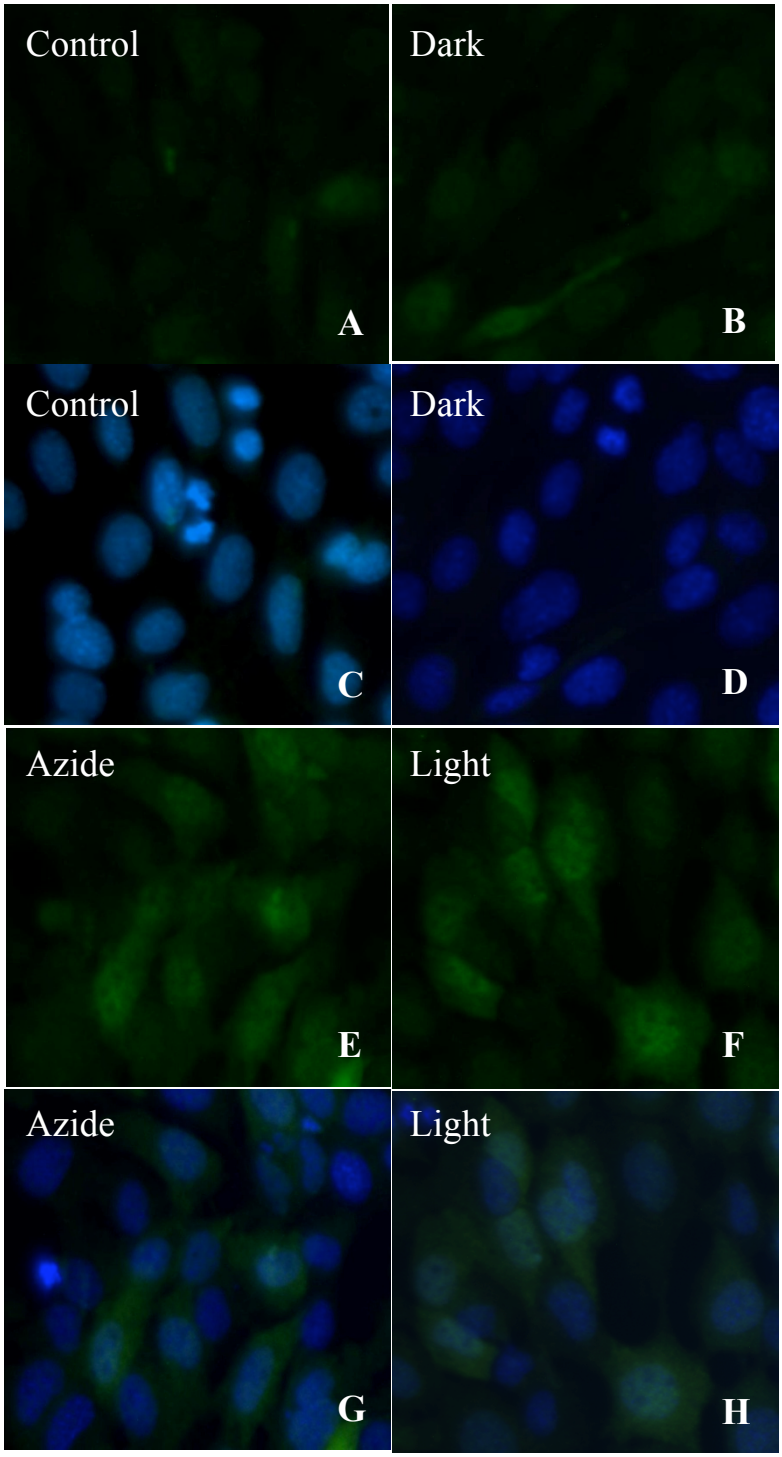


Figure 6.22. In these studies, RGC-5 cells are plated on cover slips and stained for P-p38 MAPK protein. DAPI staining is used to stain the nuclei (C&D). In control cells (Control and Dark), P-p38 is hardly seen (A&B), but following an insult with either sodium azide (Azide; 5mM, 24 hours) or light (1000lux, 96 hours), some P-p38 can be clearly located in the cytoplasm. Figures G and H show superimposed images with DAPI staining for co-localisation of protein in cells.

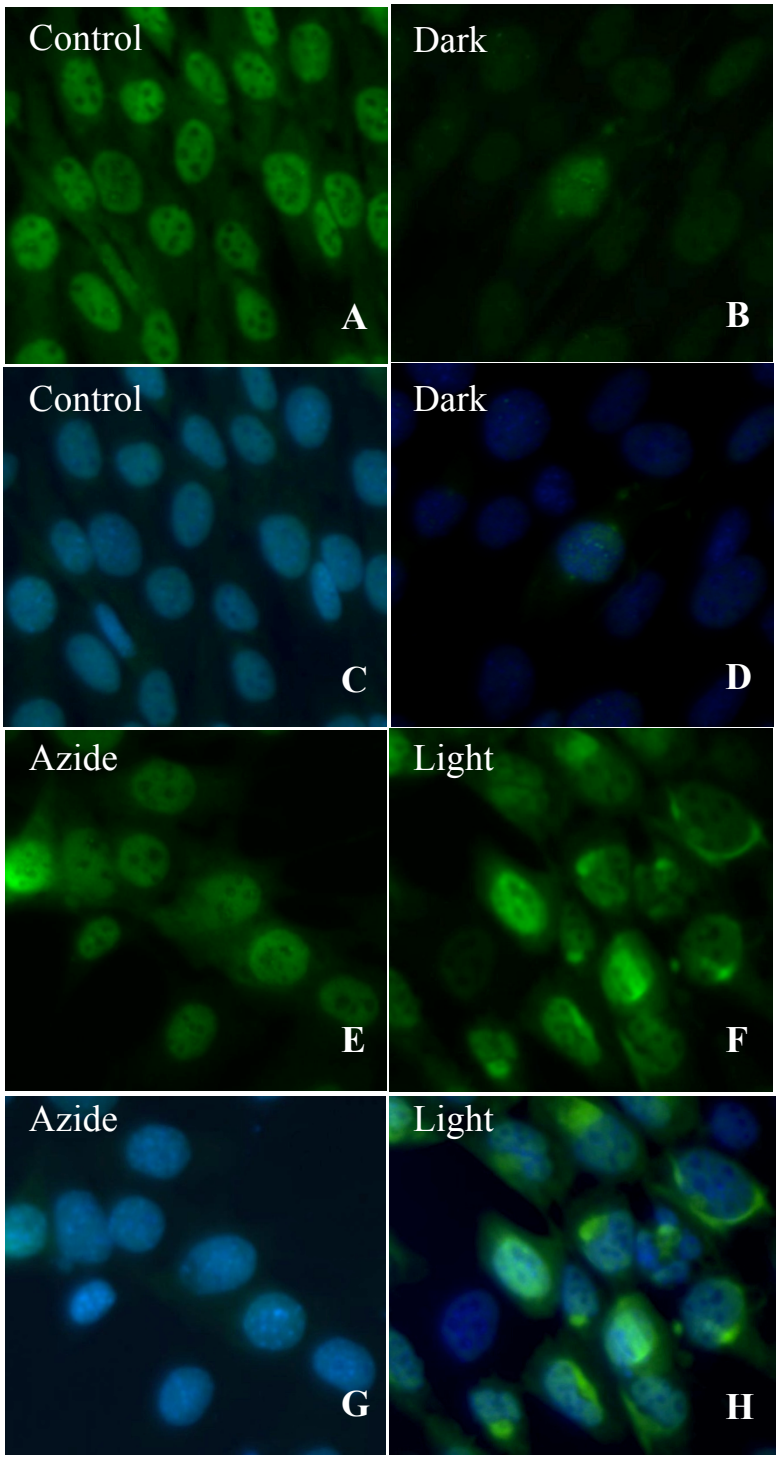


Figure 6.23. In these immunocytochemistry studies, RGC-5 cells are plated on cover slips and stained for P-c-Jun protein. DAPI staining is used to stain the nuclei (C&D). In RGC-5 cells exposed to sodium azide insult (Azide; 5mM, 24 hours), there is no difference in appearance from control cells (Control). However, P-c-Jun is up-regulated in some cells when exposed to light insult (1000lux, 96 hours) compared with cells in dark conditions (Dark). Figures G and H show superimposed images with DAPI staining for co-localisation of P-c-Jun protein in cells.

6.4 Discussion

Light (400–760 nm) impinging on the retina in situ has the potential to act on mitochondria and cause neuronal death (Osborne *et al* 2006, Lascaratos *et al* 2007, Wood *et al* 2007, Osborne *et al* 2008, Osborne 2010). Light is absorbed by different flurophores and its interaction particularly with mitochondrial COX/complex IV might be of importance in relation to cell death (Garcia & Silva 1997, Barron *et al* 2004). In the present study we showed that inhibition of COX/complex IV with sodium azide resulted in RGC-5 cells dying via mechanisms that were different in detail from those caused by light. However, it should be noted that while the evidence for sodium azide affecting complex IV by inhibition of the electron transfer between COX and oxygen (Ellenhorn 1988, Leary *et al* 2002, Safiulina *et al* 2006) is overwhelming, other modes of action cannot be excluded. For example, sodium azide has been described as stimulating nitric oxide synthesis (Bennett *et al* 1996) to activate potassium channels (Qamirani *et al* 2006), affecting Na^+/K^+-ATPase (Qamirani *et al* 2006) and influencing intracellular calcium concentrations (Marino *et al* 2007). It is of significance to note that our preliminary studies show that 1 mM potassium cyanide kills RGC-5 cells by a process that appears to be identical to that of sodium azide. Potassium cyanide is also thought to primarily inhibit COX (Hargreaves *et al* 2007). The present study was designed to compare the mode of death of RGC-5 cells by light or sodium azide insults in similar numbers of affected cells (figures 6.1-6.8). Such insults caused a number of similar effects that included the stimulation of ROS (figure 6.13), the breakdown of DNA (figure 6.15), the translocation of membrane phosphatidylserine (figure 6.14) and the activation of P-p38 MAPK (figures 6.21 and 6.22). Moreover, many of these effects were significantly attenuated by EGCG. EGCG is a flavonoid that is able to

counteract inflammation and oxidative stress and it also causes a down-regulation of certain apoptotic genes, and thus functions as a powerful neuroprotectant (Higdon & Frei 2003, Mandel *et al* 2005, Zhang *et al* 2008). However, when comparing the influence of z-VAD-fmk and necrostatin-1 at attenuating the insults of sodium azide or light to RGC-5 cells, differences in their actions were detected. Necrostatin-1 specifically reduced the detrimental influence of light, whereas z-VAD-fmk only nullified the influence of sodium azide (figures 6.7, 6.8, 6.10 and 6.11). Necrostatin-1 inhibits the death process termed necroptosis, which shares features common to apoptosis, necrosis and type-2 autophagy (Degterev *et al* 2005, Hitomi *et al* 2008). Although the same death receptor agonist may trigger necroptosis and apoptosis, necroptosis can be differentiated from apoptosis morphologically and functionally and by inhibition with necrostatin-1 (Degterev *et al* 2005, Hitomi *et al* 2008). Necrostatin-1 targets a serine/threonine kinase receptor that interacts with protein kinase-1 (RIP1), which is specifically involved in necroptosis (Degterev *et al* 2005, Kroemer *et al* 2009). Death mechanisms involving apoptosis generally involve a stimulation of caspases and z-VAD-fmk is a potent inhibitor of this process (Galluzzi & Kroemer 2008). Our results strongly suggest that the mechanism by which sodium azide causes cell death, as opposed to light, is by a process that was attenuated by z-VAD-fmk. Moreover, sodium azide but not light has the capacity to enhance caspase-3 activity (figure 6.9). Staurosporine-induced cell death is known to involve the stimulation of caspase-3 (Maher & Hanneken 2005), and this was also shown to be the case in RGC-5 cells. As expected both sodium azide- and light induced cell deaths resulted in a down-regulation of Bcl-2 (figure 6.19). However in the case of heme oxygenase-1 (HO-1) (figure 6.20), only light caused an up-regulation of this protein.

Heme oxygenase-1 or Hsp32 is a major heat shock/stress response protein and its activity is known to be increased several fold by various stimuli that induce cellular stress, and there is also data to suggest that its up-regulation contributes to the protection against cytotoxic actions of peroxynitrite and superoxide anions (Foresti *et al* 1999). Over expression of HO-1 is also known to protect neurones and non-neuronal cells from oxidative stress and glutamate toxicity (Satoh *et al* 2003). The death pathway resulting from a light insult, but not from sodium azide might therefore be connected with a stimulation of an endogenous neuroprotective pathway that involves an up-regulation of HO-1. Another possibility relates to the molecular structure of HO-1 which consists of a heme structure sandwiched between two helices (Xia *et al* 2004) allowing for the possibility of light directly acting on the enzyme.

Distinctive death pathways for the light insult and that for sodium azide were revealed by analysis of the western blots in which antibodies for alpha fodrin (figure 6.16 and 6.17), AIF (figure 6.18), P-c-Jun, P-p38 MAPK and P-JNK (figure 6.21) were used. Alpha fodrin is a member of the spectrin family of filamentous proteins and has been shown to be cleaved during apoptosis initiated by insults such as staurosporine, ceramide and ischemia (Nath *et al* 2000, Arboleda *et al* 2007). Therefore, the finding that a cleaved alpha fodrin product was up regulated by sodium azide is consistent with the view that the mechanism of death is by a process that is different from that caused by a light insult. Moreover, the fact that a cleaved product (57 KDa) for AIF only occurred after a light insult provides further evidence that the death mechanisms for light and sodium azide are different. The cleaved 57 kDa AIF species that was only generated after a light insult is thought to be caused by activated calpains and/or cathepsins (Otera *et al* 2005, Polster *et al* 2005) and translocated from the

mitochondria into the nucleus (Otera *et al* 2005, Yu *et al* 2006, Osborne *et al* 2008) to cause DNA fragmentation. This type of death mechanism is caspase-independent, occurs in necroptosis and is not associated with an insult induced by sodium azide.

Mitogen-activated protein kinases (MAPKs) including extracellular signal-regulated kinase (ERK), c-Jun, N-terminal kinase (JNK) and p38 MAPK are linked with a diverse range of biological activities including regulation of programmed cell death (Ono & Han 2000). Activation of ERKs typically contributes to cell differentiation, proliferation and survival (Ono & Han 2000) whereas JNK and p38 MAPK, in contrast, are activated by pro inflammatory cytokines and environmental stress and also can promote apoptosis (Davies *et al* 2000). The present results show that the exposure of RGC-5 cells to light, but not to sodium azide, resulted in the occurrence of phosphorylated products of c-Jun and JNK. One might therefore speculate that the activation of P-c-Jun and P-JNK is associated with inflammation and that this occurs when cells die as in necroptosis. A protein for P-p38 MAPK was also located in the nuclei of RGC-5 cells and when activated by both light and sodium azide was also found to be in the cytoplasm (figure 6.22). Thus both sodium azide and light cause up-regulation and translocation of a phosphorylated product of p38 MAPK, showing the close link between necroptosis and apoptosis. The present results favour the view that light does not exclusively affect cytochrome oxidase in the mitochondrial electron transport chain, causing cell death. Such a conclusion is based on the premise that sodium azide causes cell death by an action primarily on cytochrome oxidase and that this death process is different from the mechanism by which cells die when exposed to light. Therefore, we suggest that light affects a cell's function by an action on a

number of mitochondrial flurophores such as cytochrome P450, flavins and flavoproteins, and not just on cytochrome oxidase.

In summary, the present study shows that the death mechanisms caused by insults of light and sodium azide are dissimilar but display some common features. These common features include the generation of ROS, the expression of phosphatidylserine, the breakdown of DNA and the activation of P-p38 MAPK. However, the death process caused by light is only inhibited by necrostatin-1, whereas the death process induced by sodium azide is specifically inhibited by z-VAD-fmk. Moreover, light causes an activation of AIF, c-Jun, JNK and HO-1, but at the same time it does not affect alpha fodrin or caspase-3 production. In contrast, sodium azide causes the activation of alpha fodrin and stimulates caspase-3 production, but it does not affect AIF, c-Jun, JNK or HO-1.

CHAPTER 7

GENERAL DISCUSSION

7.1 General discussion

This study shows that EGCG, EC and genistein are potent antioxidants as evidenced by lipid peroxidation results (figures 4.2-4.4). Lipid peroxidation occurs as a result of oxidative stress-induced damage to the lipid contents in biological membranes, such as cholesterol and fatty acid moieties. Thiobarbituric acid (TBA) reactivity is generally considered an index of lipid peroxidation and is measured by carbonyl by-products, the most important of which is believed to be 3-carbon aldehyde, malonaldehyde (MDA) (Girotti 1985). The MDA-TBA reactivity has been shown to provide a diagnostic index to detect and measure lipid peroxidation and peroxidative tissue injury (Janero 1990). In the present study, rat brain homogenates were used as a source of lipids for the MDA-TBA reaction. Sodium nitroprusside (SNP) has been shown previously to be a potent oxidant in stimulating lipid peroxidation (Osborne & Wood 2004). It acts by donating nitrous oxide, NO in an aqueous environment, which subsequently leads to the excessive production of free radicals (Kishnani & Fung 1996). A 2006 paper by Zhang and Osborne reported an IC_{50} value of 0.8μM for EGCG inhibiting SNP-induced TBARS formation (Zhang & Osborne 2006). In the present study we show that EC (IC_{50} value 1.5μM) and EGCG (IC_{50} value 2.5μM) are approximately 20-fold more efficacious as an antioxidant than genistein (IC_{50} value 39μM). Thus based on the lipid peroxidation data one might expect that the order of effectiveness for the individual flavonoid as an antioxidant is EC>EGCG>genistein.

In this chapter, we showed that among the three flavonoids, EGCG and EC are the safest compounds, having no detrimental effects on RGC-5 cells in culture at concentrations below 100μM. In contrast, genistein caused significant reduction of RGC-5 cell survival after 24 hours at concentrations of 25μM upwards.

It is generally thought than oxidative stress plays a part in the pathogenesis of glaucoma (Izzotti *et al* 2006, Tezel 2006) initiated by ischemia to the optic nerve head components (Flammer & Orgul 1998, Osborne *et al* 2001) because of a reduced optic nerve head blood supply (Flammer & Orgul 1998). An increase in lipid peroxidation products (Birich *et al* 1986) and decrease in glutathione (Gherghel *et al* 2005) occur in the serum of POAG patients. Lipid peroxidation assays provide an insight into the mechanism by which a substance may alleviate oxidative stress, especially in intact cell systems. To deliver an insult that selectively causes oxidative stress to retinal ganglion cells *in situ* is virtually impossible. Nevertheless, partial knowledge of the effects of a selective insult is made possible by using a cell culture system where a selective oxidative stress may be delivered. A retinal ganglion cell line (RGC-5) (Krishnamoorthy *et al* 2001) enabled studies using various oxidative stressors in such a cell system to be carried out. We proceeded to establish the neuroprotective actions of the selected flavonoids in RGC-5 cells subjected to H_2O_2, glutamate, serum deprivation, rotenone, sodium azide and light toxicities. A summary of the neuroprotective effects of the selected flavonoids are detailed in Table 7.1.Our data confirms that exposure of RGC-5 cells to H_2O_2 results cell death in a dose-dependent manner (figure 4.8A), causes ROS generation (Figure 4.10) and cell death by apoptosis (figures 4.12 and 4.13), as previously reported (Li & Osborne 2008). It also shows that EC attenuates this process to a similar degree to EGCG (Zhang *et al* 2007). However, genistein did not show any protective effect on RGC-5 cell survival at a non-toxic concentration of 10μM. These findings corroborate the lipid peroxidation results that showed that genistein has the weakest antioxidant activity out of the three flavonoids.

FLAVONOIDS / INSULTS	Genistein	EGCG	EC	Baicalin
Retinal ischaemia	Y	-	-	-
Hydrogen peroxide	N	Y	Y	-
Glutamate toxicity	N	N	Y	-
Serum deprivation	N	N	N	-
Rotenone	N	Y	Y	N
Sodium azide	-	Y	-	-
Light	-	Y	-	-

Table 7.1 A summary of the neuroprotective effects of selected flavonoids against various oxidative stressors. (Y: shows neuroprotective effects, N: no neuroprotective effects shown)

Glutamate has been implicated as a mechanism of RGC death in glaucoma (Dreyer *et al* 1996, Osborne *et al* 1999, Levin 2003, Lotery 2005, Salt & Cordeiro 2006). Glutamate causes excitotoxicity by overstimulation of glutamate receptor, N-methyl-D aspartate (NMDA) (Frandsen *et al* 1989), generating a cascade of events resulting in an overload of intracellular calcium (Choi 1987, Frandsen *et al* 1989) and release of nitric oxide (Hoyt *et al* 1992, Luo *et al* 1993), which subsequently leads to generation of reactive oxygen species and cell death. Krishnamoorthy *et al* (Krishnamoorthy *et al* 2001) demonstrated that RGC-5 cells are resistant to glutamate toxicity in its undifferentiated form. In these experiments, we used undifferentiated RGC-5 cells, and found that their sensitivity to glutamate toxicity is increased with the concomitant use of 1mM buthionine sulfoximine (BSO), which is an inhibitor of GSH production. In the early stages of glutamate neurotoxicity in the cerebral cortex, GSH levels are reduced with an increase in peroxynitrite production (Kumar *et al*

2010). This explains the increased sensitivity of RGC-5 cells to glutamate neurotoxicity when co-treated with BSO. Glutamate causes RGC-5 cell death by apoptosis (Figure 4.16) in a dose-dependent manner (Figure 4.13). Mitochondrial dysfunction has been implicated in glutamate-induced cell death (Dugan *et al* 1995, Schinder *et al* 1996, White & Reynolds 1996, Castilho *et al* 1999), and this is confirmed by the reduction of mitochondrial dehydrogenase activity in RGC-5 cells caused by glutamate toxicity (Figure 4.15). Interestingly, we found that there is a differential effect between the two green tea flavonoids, EGCG and EC in ameliorating glutamate-induced toxicity in RGC-5 cells. The results showed that only EC 50μM was able to significantly attenuate glutamate-induced RGC-5 cell death (figure 4.14), and preserve mitochondrial dehydrogenase activity (figure 4.15). However, neither EGCG nor genistein have any protective effect on RGC-5 cells against glutamate-induced cell death.

The different effects of the two green tea flavonoids, EC and EGCG, and genistein in attenuating glutamate-induced cell death, may be partly explained by the possible specificity of the structure-activity relationship. Ishige *et al* (Ishige *et al* 2001) suggested that three structural features of flavonoids are required for protection against glutamate neurotoxicity: hydroxylated C3, an unsaturated C ring and hydrophobicity. Among the three flavonoids, genistein does not contain hydroxylated C3, although it has an unsaturated C ring. On the other hand, although both EC and EGCG contain a saturated C ring, EC is more hydrophobic relative to EGCG and has a higher affinity towards lipid bilayers (Nakayama *et al* 2000, Kajiya *et al* 2002).

Increasing evidence suggests the role of mitochondria in the pathogenesis of glaucoma. Mitochondrial DNA mutations have been linked to POAG (Abu-Amero &

Bosley 2006) and NTG (Mabuchi *et al* 2007, Wolf *et al* 2009). Both types of glaucoma show evidence of oxidative stress involving the mitochondrial electron transport chain (Tezel 2006). Moreover, the proposed mechanism of RGC cell death in glaucoma is similar to that of mitochondrial optic neuropathies such as autosomal dominant optic atrophy (ADOA) (Kerrigan *et al* 1997, Calandrella *et al* 2007). Mitochondrial dysfunction is often demonstrated by oxidative stress, caused by an overproduction of ROS, which has been implicated in the development of glaucoma (Tezel 2006). Reactive oxygen species are generated primarily from electron leakage of Complex I and III of the mitochondrial respiratory chain (Cadenas & Davies 2000). Taken together, it can be deduced that mitochondrial dysfunction is implicated in RGC cell death in glaucoma.

Like in other neurons, the main source of energy for cellular metabolism in RGCs is the mitochondria, which are unevenly distributed in the axon, corresponding to the local energy requirement (Bristow *et al* 2002, Carelli *et al* 2004). Unmyelinated RGC axons within the globe are laden with mitochondria that are located in varicosities along their length, which meets the high energy demand for nerve conduction. This is in contrast to the myelinated portion of the RGC axons that contains fewer mitochondria, where salutatory nerve conduction requires less energy (Bristow *et al* 2002, Carelli *et al* 2004). The mitochondria in the unmyelinated portion of RGC axon are not protected from light, and light insult has been shown to adversely affect the function of mitochondria in cultured cells by generating ROS (Osborne *et al* 2008). In a normal situation, ROS generated by light are likely to be effectively removed by intracellular antioxidant mechanisms. However, it is postulated that with increasing age, the ability of the cell to overcome ROS

production is reduced as the RGCs may be energetically compromised (Osborne 2010). As a result, excessive ROS may be generated by light which is absorbed by the photosensitizers in the mitochondrial respiratory chain enzymes, the flavin and cytochrome C oxidases (Godley *et al* 2005). In this situation, it is plausible that the radical scavenging activity of RGCs may be overwhelmed by the overproduction of ROS, leading to RGC cell damage and ultimately death. This implies that light may be a potential risk factor for glaucoma where the remaining functioning RGCs are energetically compromised (Osborne *et al* 2006, Osborne 2010). Therefore, another aim of this study was to compare the mode of RGC-5 cell death caused by mitochondrial dysfunction to that caused by light insult, and determine the effects of flavonoids in attenuating these insults (Chapters 5 and 6). Mitochondrial complex inhibitors, rotenone (for complex I) and sodium azide (for complex IV) were used to inhibit the oxidative phosphorylation pathways in RGC-5 cells to simulate mitochondrial dysfunction. These studies showed that rotenone, sodium azide and light cause cell death by mechanisms that are similar but distinct in several ways. All three insults cause stimulation of ROS, the breakdown of DNA, the translocation of membrane phosphotidylserine and the activation of MAPK. Rotenone and light-induced RGC-5 cell death are similar in that they both cause up-regulation on HO-1, P-JNK and its substrate, P-c-Jun, which is not the case in sodium azide-induced cell death. A summary of the cytokines and pathway involved in RGC-5 cell death induced by the various oxidative stressors used in this study is shown in Table 7.2.

Insults / Cytokines activated	Ischaemia	Serum deprivation	Rotenone	Sodium azide	Light
Alpha fodrin	-	-	-	Y	N
AIF	-	-	N	N	Y
Bax	-	Y	-	-	-
Caspase 3	Y	-	N	Y	N
Caspase 8	Y	-	-	-	-
GFAP	Y	-	-	-	-
HO-1	-	-	-	N	Y
PARP	Y	-	-	-	-
P-c-Jun	-	-	Y	N	Y
P-JNK	-	-	Y	N	Y
P-p38	-	-	Y	Y	Y
Necroptosis pathway	-	-	-	N	Y

Table 7.2 A summary of the cytokines or pathway activated by the various types of oxidative stressors. (Y;yes, N:n)

Apoptotic cell death generally involves a stimulation of caspases and z-VAD-fmk is a potent inhibitor of this process (Galluzzi & Kroemer 2008). Rotenone- and light-induced cell death are not inhibited by pan-caspase inhibitor, suggesting that caspase does not play a major role in the mechanism of cell death induced by these two insults. This is in contrast with sodium azide-induced cell death, is attenuated by pan-caspase inhibitor implying cell death involving the caspase pathway. Necroptosis and apoptosis cell death can be differentiated both morphologically and functionally and by inhibition with necrostation-1 (Degterev *et al* 2005, Hitomi *et al* 2008). Our results show that only light insult is inhibited by necrostatin-1, which is not the case in cell death caused by rotenone or sodium azide. Moreover, the fact that a cleaved product of AIF only occurred after light insult provides further evidence that light-induced RGC-5 cell death occurs by a caspase-independent pathway and occurs by necroptosis.

The distinctive death pathway that occurs in sodium azide-induced cell death was revealed by analysis of western blots in which a cleaved alpha-fodrin product was up-regulated. Alpha fodrin is a member of the spectrin family of proteins and has been shown to be activated during apoptosis caused by staurosporine (Nath *et al* 2000). Staurosporine has been known to activate the caspase pathway in order to cause neuronal cell death (Maher & Hanneken 2005, Grishchuk *et al* 2011). Further evidence that sodium azide causes caspase-dependent cell death is provided by the inhibition of RGC-5 cell death by z-VAD-fmk.

Flavonoids have numerous beneficial physiological effects in cancer, cardiovascular and neurodegenerative diseases (Kuppusamy *et al* 1990, Lee *et al* 2003, Mandel *et al* 2005). Flavonoids have multiple modes of action, and the mechanism by which

flavonoids act as neuroprotectants relates mostly, but not exclusively, to their antioxidant activity. In this study, mitochondrial dysfunction, caused by rotenone or sodium azide, and causing RGC-5 cell death, is attenuated by EGCG and EC, but not by genistein or baicalin. Furthermore, although light insult has been show to act on the mitochondria to cause cell death (Osborne *et al* 2008), these flavonoids have no similar attenuating effects against light-induced RGC-5 cell death.

The studies presented in this thesis show that flavonoids have different modes of action in protecting the RGC against various oxidative stressors both *in vivo* and *in vitro*, but the precise mechanisms of action of individual flavonoids remain largely undefined. Future work may focus on the more detailed molecular mechanism of action of these flavonoids. The flavonoids used in this study are worthy of consideration for the treatment of glaucoma, based on their wide safety profile, wide availability, and multiple modes of action and neuroprotective efficacy.

CHAPTER 8

REFERENCES

Abib RT, Quincozes-Santos A, Nardin P, Wofchuk ST, Perry ML, et al. 2008. Epicatechin gallate increases glutamate uptake and S100B secretion in C6 cell lineage. *Mol Cell Biochem* 310: 153-8

Abraham NG, Lavrovsky Y, Schwartzman ML, Stoltz RA, Levere RD, et al. 1995. Transfection of the human heme oxygenase gene into rabbit coronary microvessel endothelial cells: protective effect against heme and hemoglobin toxicity. *Proc Natl Acad Sci U S A* 92: 6798-802

Abu-Amero KK, Bosley TM. 2006. Mitochondrial abnormalities in patients with LHON-like optic neuropathies. *Invest Ophthalmol Vis Sci* 47: 4211-20

Acsadi G, Lee I, Li X, Khaidakov M, Pecinova A, et al. 2009. Mitochondrial dysfunction in a neural cell model of spinal muscular atrophy. *J Neurosci Res* 87: 2748-56

Adam-Vizi V, Chinopoulos C. 2006. Bioenergetics and the formation of mitochondrial reactive oxygen species. *Trends Pharmacol Sci* 27: 639-45

Adlercreutz H, Yamada T, Wahala K, Watanabe S. 1999. Maternal and neonatal phytoestrogens in Japanese women during birth. *Am J Obstet Gynecol* 180: 737-43

Agarwal N, Agarwal R, Kumar DM, Ondricek A, Clark AF, et al. 2007. Comparison of expression profile of neurotrophins and their receptors in primary and transformed rat retinal ganglion cells. *Mol Vis* 13: 1311-8

Aguayo AJ, Clarke DB, Jelsma TN, Kittlerova P, Friedman HC, Bray GM. 1996. Effects of neurotrophins on the survival and regrowth of injured retinal neurons. *Ciba Found Symp* 196: 135-44; discussion 44-8

Akiyama T, Ishida J, Nakagawa S, Ogawara H, Watanabe S, et al. 1987. Genistein, a specific inhibitor of tyrosine-specific protein kinases. *J Biol Chem* 262: 5592-5

Alam M, Schmidt WJ. 2002. Rotenone destroys dopaminergic neurons and induces parkinsonian symptoms in rats. *Behav Brain Res* 136: 317-24

Amin A, Buratovich M. 2007. The Anti-Cancer Charm of Flavonoids: A Cup-of-Tea Will Do! *Recent patents on anti-cancer drug discovery* 2: 109-17

Ando K, Uemura K, Kuzuya A, Maesako M, Asada-Utsugi M, et al. 2011. N-cadherin regulates p38 MAPK signaling via association with JNK-associated leucine zipper protein: implications for neurodegeneration in Alzheimer disease. *J Biol Chem* 286: 7619-28

Anglade P, Vyas S, Javoy-Agid F, Herrero MT, Michel PP, et al. 1997. Apoptosis and autophagy in nigral neurons of patients with Parkinson's disease. *Histol Histopathol* 12: 25-31

Ankarcrona M, Mangialasche F, Winblad B. 2010. Rethinking Alzheimer's disease therapy: are mitochondria the key? *J Alzheimers Dis* 20 Suppl 2: S579-90

Arboleda G, Waters C, Gibson R. 2007. Inhibition of caspases but not of calpains temporarily protect against C2-ceramide-induced death of CAD cells. *Neurosci Lett* 421: 245-9

Arnold S, Beyer C. 2009. Neuroprotection by estrogen in the brain: the mitochondrial compartment as presumed therapeutic target. *J Neurochem* 110: 1-11

Arts IC, Hollman PC. 2005. Polyphenols and disease risk in epidemiologic studies. *The American journal of clinical nutrition* 81: 317S-25S

Atalar PT, Atalar E, Kilic H, Abbasoglu OE, Ozer N, et al. 2006. Impaired systemic endothelial function in patients with pseudoexfoliation syndrome. *Int Heart J* 47: 77-84

Azcoitia I, Moreno A, Carrero P, Palacios S, Garcia-Segura LM. 2006. Neuroprotective effects of soy phytoestrogens in the rat brain. *Gynecol Endocrinol* 22: 63-9

Bae JH, Mun KC, Park WK, Lee SR, Suh SI, et al. 2002. EGCG attenuates AMPA-induced intracellular calcium increase in hippocampal neurons. *Biochem Biophys Res Commun* 290: 1506-12

Baluchnejadmojarad T, Roghani M, Nadoushan MR, Bagheri M. 2009. Neuroprotective effect of genistein in 6-hydroxydopamine hemi-parkinsonian rat model. *Phytother Res* 23: 132-5

Banerjee S, Li Y, Wang Z, Sarkar FH. 2008. Multi-targeted therapy of cancer by genistein. *Cancer Lett* 269: 226-42

Bang OY, Hong HS, Kim DH, Kim H, Boo JH, et al. 2004. Neuroprotective effect of genistein against beta amyloid-induced neurotoxicity. *Neurobiol Dis* 16: 21-8

Barclay AN, Hyden H. 1978. Localizatin of the Thy-1 antigen in rat brain and spinal cord by immunofluorescence. *J Neurochem* 31: 1375-91

Barnes S, Boersma B, Patel R, Kirk M, Darley-Usmar VM, et al. 2000. Isoflavonoids and chronic disease: mechanisms of action. *Biofactors* 12: 209-15

Barnstable CJ, Drager UC. 1984. Thy-1 antigen: a ganglion cell specific marker in rodent retina. *Neuroscience* 11: 847-55

Barres BA, Silverstein BE, Corey DP, Chun LL. 1988. Immunological, morphological, and electrophysiological variation among retinal ganglion cells purified by panning. *Neuron* 1: 791-803

Barron MJ, Griffiths P, Turnbull DM, Bates D, Nichols P. 2004. The distributions of mitochondria and sodium channels reflect the specific energy requirements and conduction properties of the human optic nerve head. *Br J Ophthalmol* 88: 286-90

Bastianetto S, Yao ZX, Papadopoulos V, Quirion R. 2006. Neuroprotective effects of green and black teas and their catechin gallate esters against beta-amyloid-induced toxicity. *Eur J Neurosci* 23: 55-64

Beale R, Osborne NN. 1982. Localization of the Thy-1 antigen to the surfaces of rat retinal ganglion cells. *Neurochem Int* 4: 587-95

Bell JE HC. 1981. Spectroscopy in biochemstry In *Hemoproteins*, ed. B JE, pp. 42-46. FL: CRC Press Inc, Boca Raton

Bendotti C, Bao Cutrona M, Cheroni C, Grignaschi G, Lo Coco D, et al. 2005. Inter- and intracellular signaling in amyotrophic lateral sclerosis: role of p38 mitogen-activated protein kinase. *Neurodegener Dis* 2: 128-34

Bennett MC, Mlady GW, Kwon YH, Rose GM. 1996. Chronic in vivo sodium azide infusion induces selective and stable inhibition of cytochrome c oxidase. *J Neurochem* 66: 2606-11

Beretta S, Wood JP, Derham B, Sala G, Tremolizzo L, et al. 2006. Partial mitochondrial complex I inhibition induces oxidative damage and perturbs glutamate transport in primary retinal cultures. Relevance to Leber Hereditary Optic Neuropathy (LHON). *Neurobiol Dis* 24: 308-17

Berliner JA, Heinecke JW. 1996. The role of oxidized lipoproteins in atherogenesis. *Free Radic Biol Med* 20: 707-27

Betarbet R, Sherer TB, MacKenzie G, Garcia-Osuna M, Panov AV, Greenamyre JT. 2000. Chronic systemic pesticide exposure reproduces features of Parkinson's disease. *Nat Neurosci* 3: 1301-6

Birich TV, Birich TA, Marchenko LN, Remizonova DB, Fedulov AS. 1986. [Lipid peroxidation in the blood of primary glaucoma patients]. *Vestn Oftalmol* 102: 13-5

Block ML, Zecca L, Hong JS. 2007. Microglia-mediated neurotoxicity: uncovering the molecular mechanisms. *Nat Rev Neurosci* 8: 57-69

Bloom D, Dhakshinamoorthy S, Wang W, Celli CM, Jaiswal AK. 2001. Role of NF-E2 related factors in oxidative stress. In *Cell and molecular response to stress*, ed. KB Storey, JM Storey, pp. 229-38. Amsterdam: Elsevier

Bok D. 1985. Retinal photoreceptor-pigment epithelium interactions. Friedenwald lecture. *Invest Ophthalmol Vis Sci* 26: 1659-94

Boland MV, Quigley HA. 2007. Risk factors and open-angle glaucoma: classification and application. *J Glaucoma* 16: 406-18

Borras C, Gambini J, Gomez-Cabrera MC, Sastre J, Pallardo FV, et al. 2006. Genistein, a soy isoflavone, up-regulates expression of antioxidant genes: involvement of estrogen receptors, ERK1/2, and NFkappaB. *Faseb J* 20: 2136-8

Bors W, Heller W, Michel C, Saran M. 1990. Flavonoids as antioxidants: determination of radical-scavenging efficiencies. *Methods Enzymol* 186: 343-55

Bors W, Michel C, Saran M. 1994. Flavonoid antioxidants: rate constants for reactions with oxygen radicals. *Methods Enzymol* 234: 420-9

Borsello T, Clarke PG, Hirt L, Vercelli A, Repici M, et al. 2003. A peptide inhibitor of c-Jun N-terminal kinase protects against excitotoxicity and cerebral ischemia. *Nat Med* 9: 1180-6

Bosco A, Steele MR, Vetter ML. 2011. Early microglia activation in a mouse model of chronic glaucoma. *J Comp Neurol* 519: 599-620

Boulton M, Docchio F, Dayhaw-Barker P, Ramponi R, Cubeddu R. 1990. Age-related changes in the morphology, absorption and fluorescence of melanosomes and lipofuscin granules of the retinal pigment epithelium. *Vision Res* 30: 1291-303

Bowmaker JK, Dartnall HJ. 1980. Visual pigments of rods and cones in a human retina. *J Physiol* 298: 501-11

Brass LM. 2004. Estrogens and Stroke: Use of Oral Contraceptives and Postmenopausal Use of Estrogen: Current Recommendations. *Curr Treat Options Neurol* 6: 459-67

Bringmann A, Pannicke T, Grosche J, Francke M, Wiedemann P, et al. 2006. Muller cells in the healthy and diseased retina. *Prog Retin Eye Res* 25: 397-424

Bristow EA, Griffiths PG, Andrews RM, Johnson MA, Turnbull DM. 2002. The distribution of mitochondrial activity in relation to optic nerve structure. *Arch Ophthalmol* 120: 791-6

Bron A, Tripathi R, Tripathi B. 1997. The Retina In *Wolff's Anatomy of the Eye and Orbit*, pp. 487. London: Chapman & Hall Medical

Burguete MC, Torregrosa G, Perez-Asensio FJ, Castello-Ruiz M, Salom JB, et al. 2006. Dietary phytoestrogens improve stroke outcome after transient focal cerebral ischemia in rats. *Eur J Neurosci* 23: 703-10

Bussow H. 1980. The astrocytes in the retina and optic nerve head of mammals: a special glia for the ganglion cell axons. *Cell Tissue Res* 206: 367-78

Busto R, Globus MY, Neary JT, Ginsberg MD. 1994. Regional alterations of protein kinase C activity following transient cerebral ischemia: effects of intraischemic brain temperature modulation. *J Neurochem* 63: 1095-103

Buttemeyer R, Philipp AW, Schlenzka L, Mall JW, Beissenhirtz M, Lisdat F. 2003. Epigallocatechin gallate can significantly decrease free oxygen radicals in the reperfusion injury in vivo. *Transplant Proc* 35: 3116-20

Caccamo D, Campisi A, Curro M, Bramanti V, Tringali M, et al. 2005. Antioxidant treatment inhibited glutamate-evoked NF-kappaB activation in primary astroglial cell cultures. *Neurotoxicology* 26: 915-21

Cadenas E, Davies KJ. 2000. Mitochondrial free radical generation, oxidative stress, and aging. *Free Radic Biol Med* 29: 222-30

Cai Q, Wei H. 1996. Effect of dietary genistein on antioxidant enzyme activities in SENCAR mice. *Nutr Cancer* 25: 1-7

Calandrella N, Scarsella G, Pescosolido N, Risuleo G. 2007. Degenerative and apoptotic events at retinal and optic nerve level after experimental induction of ocular hypertension. *Mol Cell Biochem* 301: 155-63

Cao G, Chen M, Song Q, Liu Y, Xie L, et al. 2012. EGCG protects against UVB-induced apoptosis via oxidative stress and the JNK1/c-Jun pathway in ARPE19 cells. *Mol Med Report* 5: 54-9

Carballo M, Conde M, El Bekay R, Martin-Nieto J, Camacho MJ, et al. 1999. Oxidative stress triggers STAT3 tyrosine phosphorylation and nuclear translocation in human lymphocytes. *J Biol Chem* 274: 17580-6

Cardell M, Wieloch T. 1993. Time course of the translocation and inhibition of protein kinase C during complete cerebral ischemia in the rat. *J Neurochem* 61: 1308-14

Carelli V, Ghelli A, Bucchi L, Montagna P, De Negri A, et al. 1999. Biochemical features of mtDNA 14484 (ND6/M64V) point mutation associated with Leber's hereditary optic neuropathy. *Ann Neurol* 45: 320-8

Carelli V, Ghelli A, Ratta M, Bacchilega E, Sangiorgi S, et al. 1997. Leber's hereditary optic neuropathy: biochemical effect of 11778/ND4 and 3460/ND1 mutations and correlation with the mitochondrial genotype. *Neurology* 48: 1623-32

Carelli V, Ross-Cisneros FN, Sadun AA. 2004. Mitochondrial dysfunction as a cause of optic neuropathies. *Prog Retin Eye Res* 23: 53-89

Carter WO, Narayanan PK, Robinson JP. 1994. Intracellular hydrogen peroxide and superoxide anion detection in endothelial cells. *J Leukoc Biol* 55: 253-8

Cassidy A, de Pascual Teresa S, Rimbach G. 2003. Molecular mechanisms by which dietary isoflavones potentially prevent atherosclerosis. *Expert Rev Mol Med* 5: 1-15

Casson RJ, Liu L, Graham SL, Morgan WH, Grigg JR, et al. 2009. Efficacy and safety of bimatoprost as replacement for latanoprost in patients with glaucoma or ocular hypertension: a uniocular switch study. *J Glaucoma* 18: 582-8

Castilho RF, Ward MW, Nicholls DG. 1999. Oxidative stress, mitochondrial function, and acute glutamate excitotoxicity in cultured cerebellar granule cells. *J Neurochem* 72: 1394-401

Chakrabarti S, Ghanekar Y, Kaur K, Kaur I, Mandal AK, et al. 2010. A polymorphism in the CYP1B1 promoter is functionally associated with primary congenital glaucoma. *Hum Mol Genet* 19: 4083-90

Chan DC. 2006. Mitochondria: dynamic organelles in disease, aging, and development. *Cell* 125: 1241-52

Chang D, Sha Q, Zhang X, Liu P, Rong S, et al. 2011. The evaluation of the oxidative stress parameters in patients with primary angle-closure glaucoma. *PLoS One* 6: e27218

Charles I, Khalyfa A, Kumar DM, Krishnamoorthy RR, Roque RS, et al. 2005. Serum deprivation induces apoptotic cell death of transformed rat retinal ganglion cells via mitochondrial signaling pathways. *Invest Ophthalmol Vis Sci* 46: 1330-8

Chen J, Lin H, Hu M. 2003a. Metabolism of flavonoids via enteric recycling: role of intestinal disposition. *J Pharmacol Exp Ther* 304: 1228-35

Chen L, Lee MJ, Li H, Yang CS. 1997. Absorption, distribution, elimination of tea polyphenols in rats. *Drug Metab Dispos* 25: 1045-50

Chen L, Yang X, Jiao H, Zhao B. 2003b. Tea catechins protect against lead-induced ROS formation, mitochondrial dysfunction, and calcium dysregulation in PC12 cells. *Chem Res Toxicol* 16: 1155-61

Cherdshewasart W, Sriwatcharakul S. 2007. Major isoflavonoid contents of the 1-year-cultivated phytoestrogen-rich herb, Pueraria mirifica. *Biosci Biotechnol Biochem* 71: 2527-33

Chidlow G, Casson R, Sobrado-Calvo P, Vidal-Sanz M, Osborne NN. 2005. Measurement of retinal injury in the rat after optic nerve transection: an RT-PCR study. *Mol Vis* 11: 387-96

Chidlow G, Osborne NN. 2003. Rat retinal ganglion cell loss caused by kainate, NMDA and ischemia correlates with a reduction in mRNA and protein of Thy-1 and neurofilament light. *Brain Res* 963: 298-306

Chidlow G, Wood JP, Casson RJ. 2007. Pharmacological neuroprotection for glaucoma. *Drugs* 67: 725-59

Chinta SJ, Andersen JK. 2011. Nitrosylation and nitration of mitochondrial complex I in Parkinson's disease. *Free Radic Res* 45: 53-8

Choi DW. 1987. Ionic dependence of glutamate neurotoxicity. *J Neurosci* 7: 369-79

Choi YB, Kim YI, Lee KS, Kim BS, Kim DJ. 2004. Protective effect of epigallocatechin gallate on brain damage after transient middle cerebral artery occlusion in rats. *Brain Res* 1019: 47-54

Chow HH, Cai Y, Alberts DS, Hakim I, Dorr R, et al. 2001. Phase I pharmacokinetic study of tea polyphenols following single-dose administration of epigallocatechin gallate and polyphenon E. *Cancer Epidemiol Biomarkers Prev* 10: 53-8

Christophe M, Nicolas S. 2006. Mitochondria: a target for neuroprotective interventions in cerebral ischemia-reperfusion. *Curr Pharm Des* 12: 739-57

Chung LY, Cheung TC, Kong SK, Fung KP, Choy YM, et al. 2001. Induction of apoptosis by green tea catechins in human prostate cancer DU145 cells. *Life Sci* 68: 1207-14

Citirik M, Acaroglu G, Batman C, Yildiran L, Zilelioglu O. 2007. A possible link between the pseudoexfoliation syndrome and coronary artery disease. *Eye (Lond)* 21: 11-5

Cockburn DM. 1983. Does reduction of intraocular pressure (IOP) prevent visual field loss in glaucoma? *Am J Optom Physiol Opt* 60: 705-11

Cody V. 1988. Crystal and molecular structures of flavonoids. *Prog Clin Biol Res* 280: 29-44

Constable PA, Lawrenson JG. 2009. Glial cell factors and the outer blood retinal barrier. *Ophthalmic Physiol Opt* 29: 557-64

Cordero MD, de Miguel M, Carmona-Lopez I, Bonal P, Campa F, Moreno-Fernandez AM. 2010. Oxidative stress and mitochondrial dysfunction in fibromyalgia. *Neuro Endocrinol Lett* 31: 169-73

Costa BL, Fawcett R, Li GY, Safa R, Osborne NN. 2008. Orally administered epigallocatechin gallate attenuates light-induced photoreceptor damage. *Brain Res Bull* 76: 412-23

Crispo JA, Ansell DR, Piche M, Eibl JK, Khaper N, et al. 2010. Protective effects of polyphenolic compounds on oxidative stress-induced cytotoxicity in PC12 cells. *Can J Physiol Pharmacol* 88: 429-38

Curcio CA, Sloan KR, Kalina RE, Hendrickson AE. 1990. Human photoreceptor topography. *J Comp Neurol* 292: 497-523

Dacey DM. 1993. The mosaic of midget ganglion cells in the human retina. *J Neurosci* 13: 5334-55

Dacey DM. 1994. Physiology, morphology and spatial densities of identified ganglion cell types in primate retina. *Ciba Found Symp* 184: 12-28; discussion 28-34, 63-70

Dacey DM, Liao HW, Peterson BB, Robinson FR, Smith VC, et al. 2005. Melanopsin-expressing ganglion cells in primate retina signal colour and irradiance and project to the LGN. *Nature* 433: 749-54

Danias J, Shen F, Kavalarakis M, Chen B, Goldblum D, et al. 2006. Characterization of retinal damage in the episcleral vein cauterization rat glaucoma model. *Exp Eye Res* 82: 219-28

Danila AM, Kotani A, Hakamata H, Kusu F. 2007. Determination of rutin, catechin, epicatechin, and epicatechin gallate in buckwheat Fagopyrum esculentum Moench by micro-high-performance liquid chromatography with electrochemical detection. *J Agric Food Chem* 55: 1139-43

Davies SP, Reddy H, Caivano M, Cohen P. 2000. Specificity and mechanism of action of some commonly used protein kinase inhibitors. *Biochem J* 351: 95-105

Davis RJ. 1995. Transcriptional regulation by MAP kinases. *Mol Reprod Dev* 42: 459-67

Daw NW, Jensen RJ, Brunken WJ. 1990. Rod pathways in mammalian retinae. *Trends Neurosci* 13: 110-5

Dawson VL, Dawson TM. 2004. Deadly conversations: nuclear-mitochondrial cross-talk. *J Bioenerg Biomembr* 36: 287-94

Day AJ, Canada FJ, Diaz JC, Kroon PA, McLauchlan R, et al. 2000. Dietary flavonoid and isoflavone glycosides are hydrolysed by the lactase site of lactase phlorizin hydrolase. *FEBS Lett* 468: 166-70

De Robertis E. 1956. Electron microscope observations on the submicroscopic organization of the retinal rods. *J Biophys Biochem Cytol* 2: 319-30

Degterev A, Huang Z, Boyce M, Li Y, Jagtap P, et al. 2005. Chemical inhibitor of nonapoptotic cell death with therapeutic potential for ischemic brain injury. *Nat Chem Biol* 1: 112-9

del Rio Hortega P, Penfield W. 1927. Cerebral cicatrix. The reaction of neuroglia and microglia to brain wounds. *Bull Johns Hopkins Hosp* 41: 278-82

Delavallee L, Cabon L, Galan-Malo P, Lorenzo HK, Susin SA. 2011. AIF-mediated caspase-independent necroptosis: a new chance for targeted therapeutics. *IUBMB Life* 63: 221-32

Delmulle L, Bellahcene A, Dhooge W, Comhaire F, Roelens F, et al. 2006. Anti-proliferative properties of prenylated flavonoids from hops (Humulus lupulus L.) in human prostate cancer cell lines. *Phytomedicine* 13: 732-4

Derijard B, Hibi M, Wu IH, Barrett T, Su B, et al. 1994. JNK1: a protein kinase stimulated by UV light and Ha-Ras that binds and phosphorylates the c-Jun activation domain. *Cell* 76: 1025-37

Dhakshinamoorthy S, Long DJ, 2nd, Jaiswal AK. 2000. Antioxidant regulation of genes encoding enzymes that detoxify xenobiotics and carcinogens. *Curr Top Cell Regul* 36: 201-16

DiMauro S, Bonilla E, Zeviani M, Nakagawa M, DeVivo DC. 1985. Mitochondrial myopathies. *Ann Neurol* 17: 521-38

DiMauro S, Schon EA. 2003. Mitochondrial respiratory-chain diseases. *N Engl J Med* 348: 2656-68

Dolga AM, Terpolilli N, Kepura F, Nijholt IM, Knaus HG, et al. 2011. KCa2 channels activation prevents [Ca2+]i deregulation and reduces neuronal death following glutamate toxicity and cerebral ischemia. *Cell Death Dis* 2: e147

Donzelli A, Braida D, Finardi A, Capurro V, Valsecchi AE, et al. 2010. Neuroprotective effects of genistein in Mongolian gerbils: estrogen receptor-beta involvement. *J Pharmacol Sci* 114: 158-67

Dowling JE, Boycott BB. 1966. Organization of the primate retina: electron microscopy. *Proc R Soc Lond B Biol Sci* 166: 80-111

Dreyer EB, Zurakowski D, Schumer RA, Podos SM, Lipton SA. 1996. Elevated glutamate levels in the vitreous body of humans and monkeys with glaucoma. *Arch Ophthalmol* 114: 299-305

Dugan LL, Sensi SL, Canzoniero LM, Handran SD, Rothman SM, et al. 1995. Mitochondrial production of reactive oxygen species in cortical neurons following exposure to N-methyl-D-aspartate. *J Neurosci* 15: 6377-88

Durkin JP, Tremblay R, Chakravarthy B, Mealing G, Morley P, et al. 1997. Evidence that the early loss of membrane protein kinase C is a necessary step in the excitatory amino acid-induced death of primary cortical neurons. *J Neurochem* 68: 1400-12

Ekstrom C. 2010. Risk factors for incident open-angle glaucoma: a population-based 20-year follow-up study. *Acta ophthalmologica*

Elkabes S, DiCicco-Bloom EM, Black IB. 1996. Brain microglia/macrophages express neurotrophins that selectively regulate microglial proliferation and function. *J Neurosci* 16: 2508-21

Ellenhorn M. 1988. Sodium azide In *Diagnosis and treatment of human poisoning*, ed. E MJ, pp. 1385-88. Baltimore: Williams and Wilkins

Ellis RE, Yuan JY, Horvitz HR. 1991. Mechanisms and functions of cell death. *Annu Rev Cell Biol* 7: 663-98

Evans BA, Griffiths K, Morton MS. 1995. Inhibition of 5 alpha-reductase in genital skin fibroblasts and prostate tissue by dietary lignans and isoflavonoids. *J Endocrinol* 147: 295-302

Fadok VA, Voelker DR, Campbell PA, Cohen JJ, Bratton DL, Henson PM. 1992. Exposure of phosphatidylserine on the surface of apoptotic lymphocytes triggers specific recognition and removal by macrophages. *J Immunol* 148: 2207-16

Falsini B, Marangoni D, Salgarello T, Stifano G, Montrone L, et al. 2009. Effect of epigallocatechin-gallate on inner retinal function in ocular hypertension and glaucoma: a short-term study by pattern electroretinogram. *Graefes Arch Clin Exp Ophthalmol* 247: 1223-33

Famiglietti EV, Jr., Kolb H. 1975. A bistratified amacrine cell and synaptic cirucitry in the inner plexiform layer of the retina. *Brain Res* 84: 293-300

Famiglietti EV, Jr., Kolb H. 1976. Structural basis for ON-and OFF-center responses in retinal ganglion cells. *Science* 194: 193-5

Fan BJ, Wang DY, Lam DS, Pang CP. 2006. Gene mapping for primary open angle glaucoma. *Clin Biochem* 39: 249-58

Fansi AA, Papamatheakis DG, Harasymowycz PJ. 2009. Racial variability of glaucoma risk factors between African Caribbeans and Caucasians in a Canadian urban screening population. *Can J Ophthalmol* 44: 576-81

Fawcett JP, Bamji SX, Causing CG, Aloyz R, Ase AR, et al. 1998. Functional evidence that BDNF is an anterograde neuronal trophic factor in the CNS. *J Neurosci* 18: 2808-21

Fernandez-Martinez L, Letteboer S, Mardin CY, Weisschuh N, Gramer E, et al. 2011. Evidence for RPGRIP1 gene as risk factor for primary open angle glaucoma. *Eur J Hum Genet* 19: 445-51

Ferreira SM, Lerner SF, Brunzini R, Evelson PA, Llesuy SF. 2004. Oxidative stress markers in aqueous humor of glaucoma patients. *Am J Ophthalmol* 137: 62-9

Fink SL, Cookson BT. 2005. Apoptosis, pyroptosis, and necrosis: mechanistic description of dead and dying eukaryotic cells. *Infect Immun* 73: 1907-16

Flammer J, Mozaffarieh M. 2007. What is the present pathogenetic concept of glaucomatous optic neuropathy? *Surv Ophthalmol* 52 Suppl 2: S162-73

Flammer J, Orgul S. 1998. Optic nerve blood-flow abnormalities in glaucoma. *Prog Retin Eye Res* 17: 267-89

Flammer J, Orgul S, Costa VP, Orzalesi N, Krieglstein GK, et al. 2002. The impact of ocular blood flow in glaucoma. *Prog Retin Eye Res* 21: 359-93

Foresti R, Sarathchandra P, Clark JE, Green CJ, Motterlini R. 1999. Peroxynitrite induces haem oxygenase-1 in vascular endothelial cells: a link to apoptosis. *Biochem J* 339 (Pt 3): 729-36

Formigli L, Papucci L, Tani A, Schiavone N, Tempestini A, et al. 2000. Aponecrosis: morphological and biochemical exploration of a syncretic process of cell death sharing apoptosis and necrosis. *J Cell Physiol* 182: 41-9

Foster RG, Hankins MW. 2002. Non-rod, non-cone photoreception in the vertebrates. *Prog Retin Eye Res* 21: 507-27

Frandsen A, Drejer J, Schousboe A. 1989. Direct evidence that excitotoxicity in cultured neurons is mediated via N-methyl-D-aspartate (NMDA) as well as non-NMDA receptors. *J Neurochem* 53: 297-9

Frassetto LJ, Schlieve CR, Lieven CJ, Utter AA, Jones MV, et al. 2006. Kinase-dependent differentiation of a retinal ganglion cell precursor. *Invest Ophthalmol Vis Sci* 47: 427-38

Friling RS, Bensimon A, Tichauer Y, Daniel V. 1990. Xenobiotic-inducible expression of murine glutathione S-transferase Ya subunit gene is controlled by an electrophile-responsive element. *Proc Natl Acad Sci U S A* 87: 6258-62

Fujimura Y, Umeda D, Yamada K, Tachibana H. 2008. The impact of the 67kDa laminin receptor on both cell-surface binding and anti-allergic action of tea catechins. *Arch Biochem Biophys* 476: 133-8

Fukutake M, Takahashi M, Ishida K, Kawamura H, Sugimura T, Wakabayashi K. 1996. Quantification of genistein and genistin in soybeans and soybean products. *Food Chem Toxicol* 34: 457-61

Galluzzi L, Kroemer G. 2008. Necroptosis: a specialized pathway of programmed necrosis. *Cell* 135: 1161-3

Ganapathy PS, Dun Y, Ha Y, Duplantier J, Allen JB, et al. 2010. Sensitivity of staurosporine-induced differentiated RGC-5 cells to homocysteine. *Curr Eye Res* 35: 80-90

Gao Z, Huang K, Xu H. 2001. Protective effects of flavonoids in the roots of Scutellaria baicalensis Georgi against hydrogen peroxide-induced oxidative stress in HS-SY5Y cells. *Pharmacol Res* 43: 173-8

Garcia J, Silva E. 1997. Flavin-sensitized photooxidation of amino acids present in a parenteral nutrition infusate: protection by ascorbic acid. *J Nutr Biochem* 8: 341-45

Garcia-Lafuente A, Guillamon E, Villares A, Rostagno MA, Martinez JA. 2009a. Flavonoids as anti-inflammatory agents: implications in cancer and cardiovascular disease. *Inflamm Res* 58: 537-52

Garcia-Lafuente A, Guillamon E, Villares A, Rostagno MA, Martinez JA. 2009b. Flavonoids as anti-inflammatory agents: implications in cancer and cardiovascular disease. *Inflamm Res*

Gavrieli Y, Sherman Y, Ben-Sasson SA. 1992. Identification of programmed cell death in situ via specific labeling of nuclear DNA fragmentation. *J Cell Biol* 119: 493-501

Ghanem AA, Arafa LF, El-Baz A. 2010. Oxidative stress markers in patients with primary open-angle glaucoma. *Curr Eye Res* 35: 295-301

Gherghel D, Griffiths HR, Hilton EJ, Cunliffe IA, Hosking SL. 2005. Systemic reduction in glutathione levels occurs in patients with primary open-angle glaucoma. *Invest Ophthalmol Vis Sci* 46: 877-83

Gibbons S, Moser E, Kaatz GW. 2004. Catechin gallates inhibit multidrug resistance (MDR) in Staphylococcus aureus. *Planta Med* 70: 1240-2

Girotti AW. 1985. Mechanisms of lipid peroxidation. *J Free Radic Biol Med* 1: 87-95

Giulian D, Li J, Leara B, Keenen C. 1994. Phagocytic microglia release cytokines and cytotoxins that regulate the survival of astrocytes and neurons in culture. *Neurochem Int* 25: 227-33

Godley BF, Shamsi FA, Liang FQ, Jarrett SG, Davies S, Boulton M. 2005. Blue light induces mitochondrial DNA damage and free radical production in epithelial cells In *J Biol Chem*, pp. 21061-6

Gokulakrisnan A, Jayachandran Dare B, Thirunavukkarasu C. 2011. Attenuation of the cardiac inflammatory changes and lipid anomalies by (-)-epigallocatechin-gallate in cigarette smoke-exposed rats. *Mol Cell Biochem* 354: 1-10

Goodchild AK, Ghosh KK, Martin PR. 1996. Comparison of photoreceptor spatial density and ganglion cell morphology in the retina of human, macaque monkey, cat, and the marmoset Callithrix jacchus. *J Comp Neurol* 366: 55-75

Goodyear E, Levin LA. 2008. Model systems for experimental studies: retinal ganglion cells in culture. *Prog Brain Res* 173: 279-84

Gottstein N, Ewins BA, Eccleston C, Hubbard GP, Kavanagh IC, et al. 2003. Effect of genistein and daidzein on platelet aggregation and monocyte and endothelial function. *Br J Nutr* 89: 607-16

Graham HN. 1992. Green tea composition, consumption, and polyphenol chemistry. *Prev Med* 21: 334-50

Green DR, Kroemer G. 2004. The pathophysiology of mitochondrial cell death. *Science* 305: 626-9

Griffith OW, Meister A. 1979. Potent and specific inhibition of glutathione synthesis by buthionine sulfoximine (S-n-butyl homocysteine sulfoximine). *J Biol Chem* 254: 7558-60

Grishchuk Y, Ginet V, Truttmann AC, Clarke PG, Puyal J. 2011. Beclin 1-independent autophagy contributes to apoptosis in cortical neurons. *Autophagy* 7: 1115-31

Grutter MG. 2000. Caspases: key players in programmed cell death. *Curr Opin Struct Biol* 10: 649-55

Guan QH, Pei DS, Liu XM, Wang XT, Xu TL, Zhang GY. 2006. Neuroprotection against ischemic brain injury by SP600125 via suppressing the extrinsic and intrinsic pathways of apoptosis. *Brain Res* 1092: 36-46

Guenther E, Schmid S, Grantyn R, Zrenner E. 1994. In vitro identification of retinal ganglion cells in culture without the need of dye labeling. *J Neurosci Methods* 51: 177-81

Guenther E, Schmid S, Reiff D, Zrenner E. 1999. Maturation of intrinsic membrane properties in rat retinal ganglion cells. *Vision Res* 39: 2477-84

Guo Q, Rimbach G, Moini H, Weber S, Packer L. 2002. ESR and cell culture studies on free radical-scavenging and antioxidant activities of isoflavonoids. *Toxicology* 179: 171-80

Gupta S, Barrett T, Whitmarsh AJ, Cavanagh J, Sluss HK, et al. 1996. Selective interaction of JNK protein kinase isoforms with transcription factors. *Embo J* 15: 2760-70

Gutendorf B, Westendorf J. 2001. Comparison of an array of in vitro assays for the assessment of the estrogenic potential of natural and synthetic estrogens, phytoestrogens and xenoestrogens. *Toxicology* 166: 79-89

Haque AM, Hashimoto M, Katakura M, Hara Y, Shido O. 2008. Green tea catechins prevent cognitive deficits caused by Abeta1-40 in rats. *J Nutr Biochem* 19: 619-26

Hargreaves IP, Duncan AJ, Wu L, Agrawal A, Land JM, Heales SJ. 2007. Inhibition of mitochondrial complex IV leads to secondary loss complex II-III activity: implications for the pathogenesis and treatment of mitochondrial encephalomyopathies. *Mitochondrion* 7: 284-7

Hashimoto R, Yaita M, Tanaka K, Hara Y, Kojo S. 2000. Inhibition of radical reaction of apolipoprotein B-100 and alpha-tocopherol in human plasma by green tea catechins. *J Agric Food Chem* 48: 6380-3

Hayashi A, Koroma BM, Imai K, de Juan E, Jr. 1996. Increase of protein tyrosine phosphorylation in rat retina after ischemia-reperfusion injury. *Invest Ophthalmol Vis Sci* 37: 2146-56

Hayashi A, Weinberger AW, Kim HC, de Juan E, Jr. 1997. Genistein, a protein tyrosine kinase inhibitor, ameliorates retinal degeneration after ischemia-reperfusion injury in rat. *Invest Ophthalmol Vis Sci* 38: 1193-202

Hayreh SS. 1969. Blood supply of the optic nerve head and its role in optic atrophy, glaucoma, and oedema of the optic disc. *Br J Ophthalmol* 53: 721-48

Hayreh SS, Revie IH, Edwards J. 1970. Vasogenic origin of visual field defects and optic nerve changes in glaucoma. *Br J Ophthalmol* 54: 461-72

He C, Klionsky DJ. 2009. Regulation mechanisms and signaling pathways of autophagy. *Annu Rev Genet* 43: 67-93

He Y, Leung KW, Zhang YH, Duan S, Zhong XF, et al. 2008. Mitochondrial complex I defect induces ROS release and degeneration in trabecular meshwork cells of POAG patients: protection by antioxidants. *Invest Ophthalmol Vis Sci* 49: 1447-58

He Z, Vingrys AJ, Armitage JA, Bui BV. 2011. The role of blood pressure in glaucoma. *Clin Exp Optom* 94: 133-49

Hegazy KA, Dunn MW, Sharma SC. 2000. Functional human heme oxygenase has a neuroprotective effect on adult rat ganglion cells after pressure-induced ischemia. *Neuroreport* 11: 1185-9

Heijl A. 1989. Effect of IOP on the visual field in ocuLar hypertension and glaucoma. *Int Ophthalmol* 13: 119-24

Heijnen CG, Haenen GR, van Acker FA, van der Vijgh WJ, Bast A. 2001. Flavonoids as peroxynitrite scavengers: the role of the hydroxyl groups. *Toxicol In Vitro* 15: 3-6

Henneberry RC. 1989. The role of neuronal energy in the neurotoxicity of excitatory amino acids. *Neurobiol Aging* 10: 611-3; discussion 18-20

Hernandez M, Urcola JH, Vecino E. 2008. Retinal ganglion cell neuroprotection in a rat model of glaucoma following brimonidine, latanoprost or combined treatments. *Exp Eye Res* 86: 798-806

Hernandez MR, Pena JD. 1997. The optic nerve head in glaucomatous optic neuropathy. *Arch Ophthalmol* 115: 389-95

Hershenson M, Naureckas E, Li J. 1997. Mitogen-activated signalling in cultured airway smooth muscle cells. *Can J Physiol. Pharmacol* 75: 898-910

Higdon JV, Frei B. 2003. Tea catechins and polyphenols: health effects, metabolism, and antioxidant functions. *Crit Rev Food Sci Nutr* 43: 89-143

Hirsch JA, Martinez LM, Pillai C, Alonso JM, Wang Q, Sommer FT. 2003. Functionally distinct inhibitory neurons at the first stage of visual cortical processing. *Nat Neurosci* 6: 1300-8

Hitomi J, Christofferson DE, Ng A, Yao J, Degterev A, et al. 2008. Identification of a molecular signaling network that regulates a cellular necrotic cell death pathway. *Cell* 135: 1311-23

Ho CT, Lee CY, Huan MT. 1992. *Phenolic compounds in Food and Their Effects on Health II. Antioxidants and Cancer Prevention*. Washington, DC: American Chemical Society.

Ho KP, Li L, Zhao L, Qian ZM. 2003. Genistein protects primary cortical neurons from iron-induced lipid peroxidation. *Mol Cell Biochem* 247: 219-22

Hockberger PE, Skimina TA, Centonze VE, Lavin C, Chu S, et al. 1999. Activation of flavin-containing oxidases underlies light-induced production of H2O2 in mammalian cells. *Proc Natl Acad Sci U S A* 96: 6255-60

Holler N, Zaru R, Micheau O, Thome M, Attinger A, et al. 2000. Fas triggers an alternative, caspase-8-independent cell death pathway using the kinase RIP as effector molecule. *Nat Immunol* 1: 489-95

Hollman PC, Katan MB. 1998. Bioavailability and health effects of dietary flavonols in man. *Arch Toxicol Suppl* 20: 237-48

Hong SJ, Dawson TM, Dawson VL. 2004. Nuclear and mitochondrial conversations in cell death: PARP-1 and AIF signaling. *Trends Pharmacol Sci* 25: 259-64

Hou RR, Chen JZ, Chen H, Kang XG, Li MG, Wang BR. 2008. Neuroprotective effects of (-)-epigallocatechin-3-gallate (EGCG) on paraquat-induced apoptosis in PC12 cells. *Cell Biol Int* 32: 22-30

Hoyt KR, Tang LH, Aizenman E, Reynolds IJ. 1992. Nitric oxide modulates NMDA-induced increases in intracellular Ca2+ in cultured rat forebrain neurons. *Brain Res* 592: 310-6

Hsu YC, Liou YM. 2011. The anti-cancer effects of (-)-epigallocatechin-3-gallate on the signaling pathways associated with membrane receptors in MCF-7 cells. *J Cell Physiol* 226: 2721-30

Hu DN, Ritch R. 1997. Tissue culture of adult human retinal ganglion cells. *J Glaucoma* 6: 37-43

Huang CC, Wu WB, Fang JY, Chiang HS, Chen SK, et al. 2007. (-)-Epicatechin-3-gallate, a green tea polyphenol is a potent agent against UVB-induced damage in HaCaT keratinocytes. *Molecules* 12: 1845-58

Huang J, Nasr M, Kim Y, Matthews HR. 1992. Genistein inhibits protein histidine kinase. *J Biol Chem* 267: 15511-5

Hunter T. 1987. A thousand and one protein kinases. *Cell* 50: 823-9

Husain SC, J; Cillard, P. 1987. Hydroxyl radical scavenging activity of flavonoids. *Phytochemistry* 26

Hwang J, Sevanian A, Hodis HN, Ursini F. 2000. Synergistic inhibition of LDL oxidation by phytoestrogens and ascorbic acid. *Free Radic Biol Med* 29: 79-89

Hwang SL, Shih PH, Yen GC. 2012. Neuroprotective effects of citrus flavonoids. *J Agric Food Chem* 60: 877-85

Imai M, Kikuchi H, Denda T, Ohyama K, Hirobe C, Toyoda H. 2009. Cytotoxic effects of flavonoids against a human colon cancer derived cell line, COLO 201: a potential natural anti-cancer substance. *Cancer letters* 276: 74-80

Isbrucker RA, Edwards JA, Wolz E, Davidovich A, Bausch J. 2006. Safety studies on epigallocatechin gallate (EGCG) preparations. Part 2: dermal, acute and short-term toxicity studies. *Food Chem Toxicol* 44: 636-50

Ishida A. 1995. Ion channel components of retinal ganglion cells. *Prog Retinal Eye Res* 15: 261-80

Ishida AT, Stell WK, Lightfoot DO. 1980. Rod and cone inputs to bipolar cells in goldfish retina. *J Comp Neurol* 191: 315-35

Ishige K, Schubert D, Sagara Y. 2001. Flavonoids protect neuronal cells from oxidative stress by three distinct mechanisms. *Free Radic Biol Med* 30: 433-46

Izzotti A, Bagnis A, Sacca SC. 2006. The role of oxidative stress in glaucoma. *Mutat Res* 612: 105-14

Izzotti A, Longobardi M, Cartiglia C, Sacca SC. 2011. Mitochondrial damage in the trabecular meshwork occurs only in primary open-angle glaucoma and in pseudoexfoliative glaucoma. *PLoS One* 6: e14567

Jaiswal AK. 2000. Regulation of genes encoding NAD(P)H:quinone oxidoreductases. *Free Radic Biol Med* 29: 254-62

Janero DR. 1990. Malondialdehyde and thiobarbituric acid-reactivity as diagnostic indices of lipid peroxidation and peroxidative tissue injury. *Free Radic Biol Med* 9: 515-40

Janzer RC, Raff MC. 1987. Astrocytes induce blood-brain barrier properties in endothelial cells. *Nature* 325: 253-7

Jehle T, Wingert K, Dimitriu C, Meschede W, Lasseck J, et al. 2008. Quantification of ischemic damage in the rat retina: a comparative study using evoked potentials, electroretinography, and histology. *Invest Ophthalmol Vis Sci* 49: 1056-64

Ji D, Kamalden TA, del Olmo-Aguado S, Osborne NN. 2011. Light- and sodium azide-induced death of RGC-5 cells in culture occurs via different mechanisms. *Apoptosis* 16: 425-37

Ji D, Li GY, Osborne NN. 2008. Nicotinamide attenuates retinal ischemia and light insults to neurones. *Neurochem Int* 52: 786-98

John SW. 2005. Mechanistic insights into glaucoma provided by experimental genetics the cogan lecture. *Invest Ophthalmol Vis Sci* 46: 2649-61

Johnson EC, Deppmeier LM, Wentzien SK, Hsu I, Morrison JC. 2000. Chronology of optic nerve head and retinal responses to elevated intraocular pressure. *Invest Ophthalmol Vis Sci* 41: 431-42

Johnson GL, Lapadat R. 2002. Mitogen-activated protein kinase pathways mediated by ERK, JNK, and p38 protein kinases. *Science* 298: 1911-2

Jones KH, Senft JA. 1985. An improved method to determine cell viability by simultaneous staining with fluorescein diacetate-propidium iodide. *J Histochem Cytochem* 33: 77-9

Ju WK, Kim KY, Angert M, Duong-Polk KX, Lindsey JD, et al. 2009. Memantine blocks mitochondrial OPA1 and cytochrome c release and subsequent apoptotic cell death in glaucomatous retina. *Invest Ophthalmol Vis Sci* 50: 707-16

Ju WK, Kim KY, Lindsey JD, Angert M, Duong-Polk KX, et al. 2008. Intraocular pressure elevation induces mitochondrial fission and triggers OPA1 release in glaucomatous optic nerve. *Invest Ophthalmol Vis Sci* 49: 4903-11

Ju WK, Misaka T, Kushnareva Y, Nakagomi S, Agarwal N, et al. 2005. OPA1 expression in the normal rat retina and optic nerve. *J Comp Neurol* 488: 1-10

Jung SH, Kang KD, Ji D, Fawcett RJ, Safa R, et al. 2008. The flavonoid baicalin counteracts ischemic and oxidative insults to retinal cells and lipid peroxidation to brain membranes. *Neurochem Int* 53: 325-37

Justicia C, Gabriel C, Planas AM. 2000. Activation of the JAK/STAT pathway following transient focal cerebral ischemia: signaling through Jak1 and Stat3 in astrocytes. *Glia* 30: 253-70

Kajiya K, Kumazawa S, Nakayama T. 2002. Effects of external factors on the interaction of tea catechins with lipid bilayers. *Biosci Biotechnol Biochem* 66: 2330-5

Kajta M, Domin H, Grynkiewicz G, Lason W. 2007. Genistein inhibits glutamate-induced apoptotic processes in primary neuronal cell cultures: an involvement of aryl hydrocarbon receptor and estrogen receptor/glycogen synthase kinase-3beta intracellular signaling pathway. *Neuroscience* 145: 592-604

Kamalden TA, Ji D, Fawcett RJ, Osborne NN. 2011. Genistein blunts the negative effect of ischaemia to the retina caused by an elevation of intraocular pressure. *Ophthalmic Res* 45: 65-72

Kamruzzaman SM, Endale M, Oh WJ, Park SC, Kim KS, et al. 2010. Inhibitory effects of Bulnesia sarmienti aqueous extract on agonist-induced platelet activation and thrombus formation involves mitogen-activated protein kinases. *J Ethnopharmacol* 130: 614-20

Kaneko A. 1970. Physiological and morphological identification of horizontal, bipolar and amacrine cells in goldfish retina. *J Physiol* 207: 623-33

Kang MI, Kobayashi A, Wakabayashi N, Kim SG, Yamamoto M. 2004. Scaffolding of Keap1 to the actin cytoskeleton controls the function of Nrf2 as key regulator of cytoprotective phase 2 genes. *Proc Natl Acad Sci U S A* 101: 2046-51

Kang WS, Lim IH, Yuk DY, Chung KH, Park JB, et al. 1999. Antithrombotic activities of green tea catechins and (-)-epigallocatechin gallate. *Thromb Res* 96: 229-37

Kaplan DR, Miller FD. 2000. Neurotrophin signal transduction in the nervous system. *Curr Opin Neurobiol* 10: 381-91

Kaplan E, Lee B, Shapley R. 1990. New views of primate retinal function. *Prog Retinal Res* 7: 273-336

Kapoor M, Howard R, Hall I, Appleton I. 2004. Effects of epicatechin gallate on wound healing and scar formation in a full thickness incisional wound healing model in rats. *Am J Pathol* 165: 299-307

Karwoski CJ, Lu HK, Newman EA. 1989. Spatial buffering of light-evoked potassium increases by retinal Muller (glial) cells. *Science* 244: 578-80

Kashima M. 1999. Effects of catechins on superoxide nad hydroxyl radical. *Chem Pharm Bull (Tokyo)* 47: 279-83

Kashimoto R, Kurimoto T, Miyoshi T, Okamoto N, Tagami Y, et al. 2008. Cilostazol promotes survival of axotomized retinal ganglion cells in adult rats. *Neurosci Lett* 436: 116-9

Katai N, Yoshimura N. 1999. Apoptotic retinal neuronal death by ischemia-reperfusion is executed by two distinct caspase family proteases. *Invest Ophthalmol Vis Sci* 40: 2697-705

Katiyar S, Mukhtar H. 1996. Tea in chemoprevention of cancer. *Int J Oncol* 8: 221-38

Kawai Y, Tanaka H, Murota K, Naito M, Terao J. 2008. (-)-Epicatechin gallate accumulates in foamy macrophages in human atherosclerotic aorta: implication in the anti-atherosclerotic actions of tea catechins. *Biochem Biophys Res Commun* 374: 527-32

Kendell KR, Quigley HA, Kerrigan LA, Pease ME, Quigley EN. 1995. Primary open-angle glaucoma is not associated with photoreceptor loss. *Invest Ophthalmol Vis Sci* 36: 200-5

Kerr JF, Wyllie AH, Currie AR. 1972. Apoptosis: a basic biological phenomenon with wide-ranging implications in tissue kinetics. *Br J Cancer* 26: 239-57

Kerrigan LA, Zack DJ, Quigley HA, Smith SD, Pease ME. 1997. TUNEL-positive ganglion cells in human primary open-angle glaucoma. *Arch Ophthalmol* 115: 1031-5

Kidd MN, O'Connor M. 1985. Progression of field loss after trabeculectomy: a five-year follow-up. *Br J Ophthalmol* 69: 827-31

Kikuchi M, Tenneti L, Lipton SA. 2000. Role of p38 mitogen-activated protein kinase in axotomy-induced apoptosis of rat retinal ganglion cells. *J Neurosci* 20: 5037-44

Kim GS, Hong JS, Kim SW, Koh JM, An CS, et al. 2003. Leptin induces apoptosis via ERK/cPLA2/cytochrome c pathway in human bone marrow stromal cells. *J Biol Chem* 278: 21920-9

Kim JH, Yu YS, Kim DH, Kim KW. 2009. Recruitment of pericytes and astrocytes is closely related to the formation of tight junction in developing retinal vessels. *J Neurosci Res* 87: 653-9

Kim MH, Ryu SY, Bae MA, Choi JS, Min YK, Kim SH. 2008. Baicalein inhibits osteoclast differentiation and induces mature osteoclast apoptosis. *Food Chem Toxicol* 46: 3375-82

Kindy MS. 1993. Inhibition of tyrosine phosphorylation prevents delayed neuronal death following cerebral ischemia. *J Cereb Blood Flow Metab* 13: 372-7

King A, Gottlieb E, Brooks DG, Murphy MP, Dunaief JL. 2004. Mitochondria-derived reactive oxygen species mediate blue light-induced death of retinal pigment epithelial cells. *Photochem Photobiol* 79: 470-5

King RA, Bursill DB. 1998. Plasma and urinary kinetics of the isoflavones daidzein and genistein after a single soy meal in humans. *Am J Clin Nutr* 67: 867-72

Kischkel FC, Hellbardt S, Behrmann I, Germer M, Pawlita M, et al. 1995. Cytotoxicity-dependent APO-1 (Fas/CD95)-associated proteins form a death-inducing signaling complex (DISC) with the receptor. *Embo J* 14: 5579-88

Kishnani NS, Fung HL. 1996. Nitric oxide generation from pharmacological nitric oxide donors. *Methods Enzymol* 268: 259-65

Kitanaka C, Kuchino Y. 1999. Caspase-independent programmed cell death with necrotic morphology. *Cell Death Differ* 6: 508-15

Klionsky DJ, Emr SD. 2000. Autophagy as a regulated pathway of cellular degradation. *Science* 290: 1717-21

Kofuji P, Ceelen P, Zahs KR, Surbeck LW, Lester HA, Newman EA. 2000. Genetic inactivation of an inwardly rectifying potassium channel (Kir4.1 subunit) in mice: phenotypic impact in retina. *J Neurosci* 20: 5733-40

Koh SH, Lee SM, Kim HY, Lee KY, Lee YJ, et al. 2006. The effect of epigallocatechin gallate on suppressing disease progression of ALS model mice. *Neurosci Lett* 395: 103-7

Kolb H. 1970. Organization of the outer plexiform layer of the primate retina: electron microscopy of Golgi-impregnated cells. *Philos Trans R Soc Lond B Biol Sci* 258: 261-83

Kolb H, Famiglietti EV. 1974. Rod and cone pathways in the inner plexiform layer of cat retina. *Science* 186: 47-9

Kölliker R. 1854. *Mikr. Anat. oder Gewebelehre d. Menschen 2* Part 2: 605

Kondo K, Kurihara M, Miyata N, Suzuki T, Toyoda M. 1999. Scavenging mechanisms of (-)-epigallocatechin gallate and (-)-epicatechin gallate on peroxyl radicals and formation of superoxide during the inhibitory action. *Free Radic Biol Med* 27: 855-63

Kong WC, Cho EY. 1999. Antibodies against neurofilament subunits label retinal ganglion cells but not displaced amacrine cells of hamsters. *Life Sci* 64: 1773-8

Koo SI, Noh SK. 2007. Green tea as inhibitor of the intestinal absorption of lipids: potential mechanism for its lipid-lowering effect. *J Nutr Biochem* 18: 179-83

Kraft AD, Johnson DA, Johnson JA. 2004. Nuclear factor E2-related factor 2-dependent antioxidant response element activation by tert-butylhydroquinone and sulforaphane occurring preferentially in astrocytes conditions neurons against oxidative insult. *J Neurosci* 24: 1101-12

Krammer PH. 2000. CD95's deadly mission in the immune system. *Nature* 407: 789-95

Krammer PH, Arnold R, Lavrik IN. 2007. Life and death in peripheral T cells. *Nat Rev Immunol* 7: 532-42

Kretz A, Marticke JK, Happold CJ, Schmeer C, Isenmann S. 2007. A primary culture technique of adult retina for regeneration studies on adult CNS neurons. *Nat Protoc* 2: 131-40

Krinsky NI, Landrum JT, Bone RA. 2003. Biologic mechanisms of the protective role of lutein and zeaxanthin in the eye. *Annu Rev Nutr* 23: 171-201

Krishnamoorthy RR, Agarwal P, Prasanna G, Vopat K, Lambert W, et al. 2001. Characterization of a transformed rat retinal ganglion cell line. *Brain Res Mol Brain Res* 86: 1-12

Kroemer G, Galluzzi L, Vandenabeele P, Abrams J, Alnemri ES, et al. 2009a. Classification of cell death: Nomenclature Committee on Cell Death 2009. *Cell Death Differ* 16: 3-11

Kroemer G, Galluzzi L, Vandenabeele P, Abrams J, Alnemri ES, et al. 2009b. Classification of cell death: recommendations of the Nomenclature Committtee on cell death 2009. *Cell Death Differ*: 3-11

Kroemer G, Petit P, Zamzami N, Vayssiere JL, Mignotte B. 1995. The biochemistry of programmed cell death. *Faseb J* 9: 1277-87

Kroemer G, Reed JC. 2000. Mitochondrial control of cell death. *Nat Med* 6: 513-9

Kruse FE, Joussen AM, Fotsis T, Schweigerer L, Rohrschneider K, Volcker HE. 1997. [Inhibition of neovascularization of the eye by dietary factors exemplified by isoflavonoids]. *Ophthalmologe* 94: 152-6

Kuiper GG, Lemmen JG, Carlsson B, Corton JC, Safe SH, et al. 1998. Interaction of estrogenic chemicals and phytoestrogens with estrogen receptor beta. *Endocrinology* 139: 4252-63

Kumar A, Singh RL, Babu GN. 2010. Cell death mechanisms in the early stages of acute glutamate neurotoxicity. *Neurosci Res* 66: 271-8

Kumar DM, Perez E, Cai ZY, Aoun P, Brun-Zinkernagel AM, et al. 2005. Role of nonfeminizing estrogen analogues in neuroprotection of rat retinal ganglion cells against glutamate-induced cytotoxicity. *Free Radic Biol Med* 38: 1152-63

Kuppusamy UR, Khoo HE, Das NP. 1990. Structure-activity studies of flavonoids as inhibitors of hyaluronidase. *Biochem Pharmacol* 40: 397-401

Kurbitz C, Heise D, Redmer T, Goumas F, Arlt A, et al. 2011. Epicatechin gallate and catechin gallate are superior to epigallocatechin gallate in growth suppression and anti-inflammatory activities in pancreatic tumor cells. *Cancer Sci* 102: 728-34

Kurzer MS, Xu X. 1997. Dietary phytoestrogens. *Annu Rev Nutr* 17: 353-81

Kussmaul L, Hirst J. 2006. The mechanism of superoxide production by NADH:ubiquinone oxidoreductase (complex I) from bovine heart mitochondria. *Proc Natl Acad Sci U S A* 103: 7607-12

Kwak N, Okamoto N, Wood JM, Campochiaro PA. 2000. VEGF is major stimulator in model of choroidal neovascularization. *Invest Ophthalmol Vis Sci* 41: 3158-64

Kwong JM, Caprioli J. 2006. Expression of phosphorylated c-Jun N-terminal protein kinase (JNK) in experimental glaucoma in rats. *Exp Eye Res* 82: 576-82

Kyriakis JM, Avruch J. 1990. pp54 microtubule-associated protein 2 kinase. A novel serine/threonine protein kinase regulated by phosphorylation and stimulated by poly-L-lysine. *J Biol Chem* 265: 17355-63

Kyriakis JM, Avruch J. 2001. Mammalian mitogen-activated protein kinase signal transduction pathways activated by stress and inflammation. *Physiol Rev* 81: 807-69

Laemmli UK. 1970. Cleavage of structural proteins during the assembly of the head of bacteriophage T4. *Nature* 227: 680-5

Lambert JD, Sang S, Lu AY, Yang CS. 2007. Metabolism of dietary polyphenols and possible interactions with drugs. *Curr Drug Metab* 8: 499-507

Lambert JD, Yang CS. 2003. Cancer chemopreventive activity and bioavailability of tea and tea polyphenols. *Mutat Res* 523-524: 201-8

Lascaratos G, Ji D, Wood JP, Osborne NN. 2007. Visible light affects mitochondrial function and induces neuronal death in retinal cell cultures. *Vision Res* 47: 1191-201

Leary SC, Hill BC, Lyons CN, Carlson CG, Michaud D, et al. 2002. Chronic treatment with azide in situ leads to an irreversible loss of cytochrome c oxidase activity via holoenzyme dissociation. *J Biol Chem* 277: 11321-8

Lee H, Bae JH, Lee SR. 2004a. Protective effect of green tea polyphenol EGCG against neuronal damage and brain edema after unilateral cerebral ischemia in gerbils. *J Neurosci Res* 77: 892-900

Lee HH, Yang LL, Wang CC, Hu SY, Chang SF, Lee YH. 2003. Differential effects of natural polyphenols on neuronal survival in primary cultured central neurons against glutamate- and glucose deprivation-induced neuronal death. *Brain Res* 986: 103-13

Lee KN, Seo MC, Bae IH, Oh SH, Jang WG, et al. 2010. COMP-Ang1, a variant of angiopoietin 1, inhibits serum-deprived apoptosis of mesenchymal cells via PI3K/Akt and mitogen-activated protein kinase pathways. *Pharmacology* 86: 327-35

Lee MJ, Maliakal P, Chen L, Meng X, Bondoc FY, et al. 2002. Pharmacokinetics of tea catechins after ingestion of green tea and (-)-epigallocatechin-3-gallate by humans: formation of different metabolites and individual variability. *Cancer Epidemiol Biomarkers Prev* 11: 1025-32

Lee S, Van Bergen NJ, Kong GY, Chrysostomou V, Waugh HS, et al. 2011. Mitochondrial dysfunction in glaucoma and emerging bioenergetic therapies. *Exp Eye Res* 93: 204-12

Lee YB, Lee HJ, Won MH, Hwang IK, Kang TC, et al. 2004b. Soy isoflavones improve spatial delayed matching-to-place performance and reduce cholinergic neuron loss in elderly male rats. *J Nutr* 134: 1827-31

Lee YB, Schrader JW, Kim SU. 2000. p38 map kinase regulates TNF-alpha production in human astrocytes and microglia by multiple mechanisms. *Cytokine* 12: 874-80

Lei K, Davis RJ. 2003. JNK phosphorylation of Bim-related members of the Bcl2 family induces Bax-dependent apoptosis. *Proc Natl Acad Sci U S A* 100: 2432-7

Leifer D, Lipton SA, Barnstable CJ, Masland RH. 1984. Monoclonal antibody to Thy-1 enhances regeneration of processes by rat retinal ganglion cells in culture. *Science* 224: 303-6

Levin LA. 2003. Retinal ganglion cells and neuroprotection for glaucoma. *Surv Ophthalmol* 48 Suppl 1: S21-4

Levites Y, Amit T, Mandel S, Youdim MB. 2003. Neuroprotection and neurorescue against Abeta toxicity and PKC-dependent release of nonamyloidogenic soluble precursor protein by green tea polyphenol (-)-epigallocatechin-3-gallate. *Faseb J* 17: 952-4

Levites Y, Amit T, Youdim MB, Mandel S. 2002. Involvement of protein kinase C activation and cell survival/ cell cycle genes in green tea polyphenol (-)-epigallocatechin 3-gallate neuroprotective action. *J Biol Chem* 277: 30574-80

Levkovitch-Verbin H, Harizman N, Dardik R, Nisgav Y, Vander S, Melamed S. 2007. Regulation of cell death and survival pathways in experimental glaucoma. *Exp Eye Res* 85: 250-8

Levkovitch-Verbin H, Quigley HA, Kerrigan-Baumrind LA, D'Anna SA, Kerrigan D, Pease ME. 2001. Optic nerve transection in monkeys may result in secondary degeneration of retinal ganglion cells. *Invest Ophthalmol Vis Sci* 42: 975-82

Levkovitch-Verbin H, Quigley HA, Martin KR, Harizman N, Valenta DF, et al. 2005. The transcription factor c-jun is activated in retinal ganglion cells in experimental rat glaucoma. *Exp Eye Res* 80: 663-70

Levkovitch-Verbin H, Quigley HA, Martin KR, Valenta D, Baumrind LA, Pease ME. 2002. Translimbal laser photocoagulation to the trabecular meshwork as a model of glaucoma in rats. *Invest Ophthalmol Vis Sci* 43: 402-10

Li GY, Osborne NN. 2008. Oxidative-induced apoptosis to an immortalized ganglion cell line is caspase independent but involves the activation of poly(ADP-ribose)polymerase and apoptosis-inducing factor. *Brain Res* 1188: 35-43

Li HC, Zhang GY. 2003. Inhibitory effect of genistein on activation of STAT3 induced by brain ischemia/reperfusion in rat hippocampus. *Acta Pharmacol Sin* 24: 1131-6

Li J, Spletter ML, Johnson DA, Wright LS, Svendsen CN, Johnson JA. 2005. Rotenone-induced caspase 9/3-independent and -dependent cell death in undifferentiated and differentiated human neural stem cells. *J Neurochem* 92: 462-76

Li X, Valencia A, Sapp E, Masso N, Alexander J, et al. 2010. Aberrant Rab11-dependent trafficking of the neuronal glutamate transporter EAAC1 causes oxidative stress and cell death in Huntington's disease. *J Neurosci* 30: 4552-61

Li Y, Sarkar FH. 2002. Inhibition of nuclear factor kappaB activation in PC3 cells by genistein is mediated via Akt signaling pathway. *Clin Cancer Res* 8: 2369-77

Li YM, Chan HY, Huang Y, Chen ZY. 2007. Green tea catechins upregulate superoxide dismutase and catalase in fruit flies. *Mol Nutr Food Res* 51: 546-54

Liang HW, Qiu SF, Shen J, Sun LN, Wang JY, et al. 2008. Genistein attenuates oxidative stress and neuronal damage following transient global cerebral ischemia in rat hippocampus. *Neurosci Lett* 438: 116-20

Lieven CJ, Millet LE, Hoegger MJ, Levin LA. 2007. Induction of axon and dendrite formation during early RGC-5 cell differentiation. *Exp Eye Res* 85: 678-83

Lin MT, Beal MF. 2006. Mitochondrial dysfunction and oxidative stress in neurodegenerative diseases. *Nature* 443: 787-95

Lindsey JD, Weinreb RN. 2005. Elevated intraocular pressure and transgenic applications in the mouse. *J Glaucoma* 14: 318-20

Linford NJ, Dorsa DM. 2002. 17beta-Estradiol and the phytoestrogen genistein attenuate neuronal apoptosis induced by the endoplasmic reticulum calcium-ATPase inhibitor thapsigargin. *Steroids* 67: 1029-40

Lipton SA, Tauck DL. 1987. Voltage-dependent conductances of solitary ganglion cells dissociated from the rat retina. *J Physiol* 385: 361-91

Liu Q, Ju WK, Crowston JG, Xie F, Perry G, et al. 2007. Oxidative stress is an early event in hydrostatic pressure induced retinal ganglion cell damage. *Invest Ophthalmol Vis Sci* 48: 4580-9

Liu X, Zhu XZ. 1999. Roles of p53, c-Myc, Bcl-2, Bax and caspases in serum deprivation-induced neuronal apoptosis: a possible neuroprotective mechanism of basic fibroblast growth factor. *Neuroreport* 10: 3087-91

Liu Y, Hu M. 2002. Absorption and metabolism of flavonoids in the caco-2 cell culture model and a perused rat intestinal model. *Drug Metab Dispos* 30: 370-7

Liu Y, Schubert DR. 2009. The specificity of neuroprotection by antioxidants. *J Biomed Sci* 16: 98

Lobner D. 2000. Comparison of the LDH and MTT assays for quantifying cell death: validity for neuronal apoptosis? *J Neurosci Methods* 96: 147-52

Lorenz M, Wessler S, Follmann E, Michaelis W, Dusterhoft T, et al. 2004. A constituent of green tea, epigallocatechin-3-gallate, activates endothelial nitric oxide synthase by a phosphatidylinositol-3-OH-kinase-, cAMP-dependent

protein kinase-, and Akt-dependent pathway and leads to endothelial-dependent vasorelaxation. *J Biol Chem* 279: 6190-5

Lotery AJ. 2005. Glutamate excitotoxicity in glaucoma: truth or fiction? *Eye (Lond)* 19: 369-70

Lu H, Meng X, Li C, Sang S, Patten C, et al. 2003. Glucuronides of tea catechins: enzymology of biosynthesis and biological activities. *Drug Metab Dispos* 31: 452-61

Lu LJ, Grady JJ, Marshall MV, Ramanujam VM, Anderson KE. 1995. Altered time course of urinary daidzein and genistein excretion during chronic soya diet in healthy male subjects. *Nutr Cancer* 24: 311-23

Luo D, Knezevich S, Vincent SR. 1993. N-methyl-D-aspartate-induced nitric oxide release: an in vivo microdialysis study. *Neuroscience* 57: 897-900

Ma Y, Sullivan JC, Schreihofer DA. 2010. Dietary genistein and equol (4', 7 isoflavandiol) reduce oxidative stress and protect rats against focal cerebral ischemia. *Am J Physiol Regul Integr Comp Physiol* 299: R871-7

Mabuchi F, Tang S, Kashiwagi K, Yamagata Z, Iijima H, Tsukahara S. 2007. The OPA1 gene polymorphism is associated with normal tension and high tension glaucoma. *Am J Ophthalmol* 143: 125-30

Maggiolini M, Bonofiglio D, Marsico S, Panno ML, Cenni B, et al. 2001. Estrogen receptor alpha mediates the proliferative but not the cytotoxic dose-dependent effects of two major phytoestrogens on human breast cancer cells. *Mol Pharmacol* 60: 595-602

Maher P. 2001. How protein kinase C activation protects nerve cells from oxidative stress-induced cell death. *J Neurosci* 21: 2929-38

Maher P, Hanneken A. 2005. The molecular basis of oxidative stress-induced cell death in an immortalized retinal ganglion cell line. *Invest Ophthalmol Vis Sci* 46: 749-57

Maher P, Hanneken A. 2008. Flavonoids protect retinal ganglion cells from ischemia in vitro. *Exp Eye Res* 86: 366-74

Majji AB, Hayashi A, Kim HC, Grebe RR, de Juan E, Jr. 1999. Inhibition of choriocapillaris regeneration with genistein. *Invest Ophthalmol Vis Sci* 40: 1477-86

Majno G, Joris I. 1995. Apoptosis, oncosis, and necrosis. An overview of cell death. *Am J Pathol* 146: 3-15

Majsterek I, Malinowska K, Stanczyk M, Kowalski M, Blaszczyk J, et al. 2011. Evaluation of oxidative stress markers in pathogenesis of primary open-angle glaucoma. *Exp Mol Pathol* 90: 231-7

Manach C, Donovan JL. 2004. Pharmacokinetics and metabolism of dietary flavonoids in humans. *Free Radic Res* 38: 771-85

Mandel S, Reznichenko L, Amit T, Youdim MB. 2003. Green tea polyphenol (-)-epigallocatechin-3-gallate protects rat PC12 cells from apoptosis induced by serum withdrawal independent of P13-Akt pathway. *Neurotox Res* 5: 419-24

Mandel SA, Avramovich-Tirosh Y, Reznichenko L, Zheng H, Weinreb O, et al. 2005. Multifunctional activities of green tea catechins in neuroprotection. Modulation of cell survival genes, iron-dependent oxidative stress and PKC signaling pathway. *Neurosignals* 14: 46-60

Mansour-Robaey S, Clarke DB, Wang YC, Bray GM, Aguayo AJ. 1994. Effects of ocular injury and administration of brain-derived neurotrophic factor on survival and regrowth of axotomized retinal ganglion cells. *Proc Natl Acad Sci U S A* 91: 1632-6

Mardon J, Mathey J, Kati-Coulibaly S, Puel C, Davicco MJ, et al. 2008. Influence of lifelong soy isoflavones consumption on bone mass in the rat. *Experimental biology and medicine (Maywood, N.J* 233: 229-37

Marella M, Seo BB, Matsuno-Yagi A, Yagi T. 2007. Mechanism of cell death caused by complex I defects in a rat dopaminergic cell line. *J Biol Chem* 282: 24146-56

Margrain TH, Boulton M, Marshall J, Sliney DH. 2004. Do blue light filters confer protection against age-related macular degeneration? *Prog Retin Eye Res* 23: 523-31

Marino S, Marani L, Nazzaro C, Beani L, Siniscalchi A. 2007. Mechanisms of sodium azide-induced changes in intracellular calcium concentration in rat primary cortical neurons. *Neurotoxicology* 28: 622-9

Martin SJ, Reutelingsperger CP, McGahon AJ, Rader JA, van Schie RC, et al. 1995. Early redistribution of plasma membrane phosphatidylserine is a general feature of apoptosis regardless of the initiating stimulus: inhibition by overexpression of Bcl-2 and Abl. *J Exp Med* 182: 1545-56

Mathews MK, Merges C, McLeod DS, Lutty GA. 1997. Vascular endothelial growth factor and vascular permeability changes in human diabetic retinopathy. *Invest Ophthalmol Vis Sci* 38: 2729-41

Matsuda H, Chisaka T, Kubomura Y, Yamahara J, Sawada T, et al. 1986. Effects of crude drugs on experimental hypercholesterolemia. I. Tea and its active principles. *J Ethnopharmacol* 17: 213-24

Maubach J, Bracke ME, Heyerick A, Depypere HT, Serreyn RF, et al. 2003. Quantitation of soy-derived phytoestrogens in human breast tissue and biological fluids by high-performance liquid chromatography. *J Chromatogr B Analyt Technol Biomed Life Sci* 784: 137-44

McConkey DJ, Orrenius S, Jondal M. 1990. Cellular signalling in programmed cell death (apoptosis). *Immunol Today* 11: 120-1

McDowell ML, Das A, Smith JA, Varma AK, Ray SK, Banik NL. 2011. Neuroprotective effects of genistein in VSC4.1 motoneurons exposed to activated microglial cytokines. *Neurochem Int* 59: 175-84

McElnea EM, Quill B, Docherty NG, Irnaten M, Siah WF, et al. 2011. Oxidative stress, mitochondrial dysfunction and calcium overload in human lamina cribrosa cells from glaucoma donors. *Mol Vis* 17: 1182-91

McKernan DP, Guerin MB, O'Brien CJ, Cotter TG. 2007. A key role for calpains in retinal ganglion cell death. *Invest Ophthalmol Vis Sci* 48: 5420-30

Messina MJ, Loprinzi CL. 2001. Soy for breast cancer survivors: a critical review of the literature. *J Nutr* 131: 3095S-108S

Minden A, Lin A, Smeal T, Derijard B, Cobb M, et al. 1994. c-Jun N-terminal phosphorylation correlates with activation of the JNK subgroup but not the ERK subgroup of mitogen-activated protein kinases. *Mol Cell Biol* 14: 6683-8

Mitjans M, del Campo J, Abajo C, Martinez V, Selga A, et al. 2004. Immunomodulatory activity of a new family of antioxidants obtained from grape polyphenols. *J Agric Food Chem* 52: 7297-9

Miwa T, Furukawa S, Nakajima K, Furukawa Y, Kohsaka S. 1997. Lipopolysaccharide enhances synthesis of brain-derived neurotrophic factor in cultured rat microglia. *J Neurosci Res* 50: 1023-9

Molteni A, Brizio-Molteni L, Persky V. 1995. In vitro hormonal effects of soybean isoflavones. *J Nutr* 125: 751S-56S

Montellano Od. 1995. The 1994 Bernard B.Brodie award lecture. Stucture, mechanism and inhibition of cytochorme P450. *Drug Metab Dispos* 23: 1181-87

Moon YJ, Sagawa K, Frederick K, Zhang S, Morris ME. 2006. Pharmacokinetics and bioavailability of the isoflavone biochanin A in rats. *Aaps J* 8: E433-42

Moorhouse AJ, Li S, Vickery RM, Hill MA, Morley JW. 2004. A patch-clamp investigation of membrane currents in a novel mammalian retinal ganglion cell line. *Brain Res* 1003: 205-8

Morita O, Knapp JF, Tamaki Y, Stump DG, Moore JS, Nemec MD. 2009. Effects of green tea catechin on embryo/fetal development in rats. *Food Chem Toxicol* 47: 1296-303

Mosmann T. 1983. Rapid colorimetric assay for cellular growth and survival: application to proliferation and cytotoxicity assays. *J Immunol Methods* 65: 55-63

Mukai D, Matsuda N, Yoshioka Y, Sato M, Yamasaki T. 2008. Potential anthelmintics: polyphenols from the tea plant Camellia sinensis L. are lethally toxic to Caenorhabditis elegans. *J Nat Med* 62: 155-9

Mukhtar H, Ahmad N. 2000. Tea polyphenols: prevention of cancer and optimizing health. *Am J Clin Nutr* 71: 1698S-702S; discussion 703S-4S

Müller F, Wassle H, Voigt T. 1988. Pharmacological modulation of the rod pathway in the cat retina. *J Neurophysiol* 59: 1657-72

Müller H. 1851. Zur Histologie der Netzhaut. *Z. Wiss Zool*: 234

Munemasa Y, Kitaoka Y, Kuribayashi J, Ueno S. 2010. Modulation of mitochondria in the axon and soma of retinal ganglion cells in a rat glaucoma model. *J Neurochem* 115: 1508-19

Munemasa Y, Ohtani-Kaneko R, Kitaoka Y, Kumai T, Hayashi Y, et al. 2006. Pro-apoptotic role of c-Jun in NMDA-induced neurotoxicity in the rat retina. *J Neurosci Res* 83: 907-18

Murata T, Ishibashi T, Khalil A, Hata Y, Yoshikawa H, Inomata H. 1995. Vascular endothelial growth factor plays a role in hyperpermeability of diabetic retinal vessels. *Ophthalmic Res* 27: 48-52

Nagahiro S, Uno M, Sato K, Goto S, Morioka M, Ushio Y. 1998. Pathophysiology and treatment of cerebral ischemia. *J Med Invest* 45: 57-70

Nagai K, Jiang MH, Hada J, Nagata T, Yajima Y, et al. 2002. (-)-Epigallocatechin gallate protects against NO stress-induced neuronal damage after ischemia by acting as an anti-oxidant. *Brain Res* 956: 319-22

Nakagawa T, Yokozawa T. 2002. Direct scavenging of nitric oxide and superoxide by green tea. *Food Chem Toxicol* 40: 1745-50

Nakagawa T, Yokozawa T, Terasawa K, Shu S, Juneja LR. 2002. Protective activity of green tea against free radical- and glucose-mediated protein damage. *J Agric Food Chem* 50: 2418-22

Nakajima M, Cooney MJ, Tu AH, Chang KY, Cao J, et al. 2001. Normalization of retinal vascular permeability in experimental diabetes with genistein. *Invest Ophthalmol Vis Sci* 42: 2110-4

Nakayama T, Hashimoto T, Kajiya K, Kumazawa S. 2000. Affinity of polyphenols for lipid bilayers. *Biofactors* 13: 147-51

Nakazawa T, Shimura M, Ryu M, Himori N, Nitta F, et al. 2012. Progression of Visual Field Defects in Eyes With Different Optic Disc Appearances in Patients With Normal Tension Glaucoma. *J Glaucoma*

Nanjo F, Goto K, Seto R, Suzuki M, Sakai M, Hara Y. 1996. Scavenging effects of tea catechins and their derivatives on 1,1-diphenyl-2-picrylhydrazyl radical. *Free Radic Biol Med* 21: 895-902

Nash MS, Osborne NN. 1999. Assessment of Thy-1 mRNA levels as an index of retinal ganglion cell damage. *Invest Ophthalmol Vis Sci* 40: 1293-8

Nath R, Huggins M, Glantz SB, Morrow JS, McGinnis K, et al. 2000. Development and characterization of antibodies specific to caspase-3-produced alpha II-spectrin 120 kDa breakdown product: marker for neuronal apoptosis. *Neurochem Int* 37: 351-61

Nelson R. 1982. AII amacrine cells quicken time course of rod signals in the cat retina. *J Neurophysiol* 47: 928-47

Nelson R, Connaughton V. 2005. Bipolar cell pathways in the vertebrate retina. In *The Organization of the Retina and Visual system*, ed. H Kolb, E Fernandez, R Nelson. Salt Lake City: University of Utah Health Sciences Center

Nelson R, Famiglietti EV, Jr., Kolb H. 1978. Intracellular staining reveals different levels of stratification for on- and off-center ganglion cells in cat retina. *J Neurophysiol* 41: 472-83

Neuhouser ML. 2004a. Dietary flavonoids and cancer risk: evidence from human population studies. *Nutr Cancer* 50: 1-7

Neuhouser ML. 2004b. Dietary flavonoids and cancer risk: evidence from human population studies. *Nutrition and cancer* 50: 1-7

Newman EA. 1994. A physiological measure of carbonic anhydrase in Muller cells. *Glia* 11: 291-9

Newman EA, Frambach DA, Odette LL. 1984. Control of extracellular potassium levels by retinal glial cell K+ siphoning. *Science* 225: 1174-5

Nicholson DW, Ali A, Thornberry NA, Vaillancourt JP, Ding CK, et al. 1995. Identification and inhibition of the ICE/CED-3 protease necessary for mammalian apoptosis. *Nature* 376: 37-43

Nickells RW. 1996. Retinal ganglion cell death in glaucoma: the how, the why, and the maybe. *J Glaucoma* 5: 345-56

Nie G, Jin C, Cao Y, Shen S, Zhao B. 2002. Distinct effects of tea catechins on 6-hydroxydopamine-induced apoptosis in PC12 cells. *Arch Biochem Biophys* 397: 84-90

Nielsen F, Mikkelsen BB, Nielsen JB, Andersen HR, Grandjean P. 1997. Plasma malondialdehyde as biomarker for oxidative stress: reference interval and effects of life-style factors. *Clin Chem* 43: 1209-14

Nieto PS, Acosta-Rodriguez VA, Valdez DJ, Guido ME. 2010. Differential responses of the mammalian retinal ganglion cell line RGC-5 to physiological stimuli and trophic factors. *Neurochem Int* 57: 216-26

Nishina H, Wada T, Katada T. 2004. Physiological roles of SAPK/JNK signaling pathway. *J Biochem* 136: 123-6

Nongpiur ME, Ku JY, Aung T. 2011. Angle closure glaucoma: a mechanistic review. *Curr Opin Ophthalmol* 22: 96-101

Oakley B, 2nd, Katz BJ, Xu Z, Zheng J. 1992. Spatial buffering of extracellular potassium by Muller (glial) cells in the toad retina. *Exp Eye Res* 55: 539-50

Occhiuto F, Zangla G, Samperi S, Palumbo DR, Pino A, et al. 2008. The phytoestrogenic isoflavones from Trifolium pratense L. (Red clover) protects human cortical neurons from glutamate toxicity. *Phytomedicine* 15: 676-82

Ohkawa H, Ohishi N, Yagi K. 1979. Assay for lipid peroxides in animal tissues by thiobarbituric acid reaction. *Anal Biochem* 95: 351-8

Ohmori Y, Ito M, Kishi M, Mizutani H, Katada T, Konishi H. 1995. Antiallergic constituents from oolong tea stem. *Biol Pharm Bull* 18: 683-6

Okamoto N, Tobe T, Hackett SF, Ozaki H, Vinores MA, et al. 1997. Transgenic mice with increased expression of vascular endothelial growth factor in the retina: a new model of intraretinal and subretinal neovascularization. *Am J Pathol* 151: 281-91

Okuno S, Saito A, Hayashi T, Chan PH. 2004. The c-Jun N-terminal protein kinase signaling pathway mediates Bax activation and subsequent neuronal apoptosis through interaction with Bim after transient focal cerebral ischemia. *J Neurosci* 24: 7879-87

Okura A, Arakawa H, Oka H, Yoshinari T, Monden Y. 1988. Effect of genistein on topoisomerase activity and on the growth of [Val 12]Ha-ras-transformed NIH 3T3 cells. *Biochem Biophys Res Commun* 157: 183-9

Ono K, Han J. 2000. The p38 signal transduction pathway: activation and function. *Cell Signal* 12: 1-13

Organisciak DT, Vaughan DK. 2010. Retinal light damage: mechanisms and protection. *Prog Retin Eye Res* 29: 113-34

Osborne NN. 2009. Recent clinical findings with memantine should not mean that the idea of neuroprotection in glaucoma is abandoned. *Acta ophthalmologica* 87: 450-4

Osborne NN, Casson RJ, Wood JP, Chidlow G, Graham M, Melena J. 2004. Retinal ischemia: mechanisms of damage and potential therapeutic strategies. *Prog Retin Eye Res* 23: 91-147

Osborne NN, Chidlow G, Wood JP. 2006a. Glutamate excitotoxicity in glaucoma: truth or fiction? By AJ Lotery. *Eye (Lond)* 20: 1392-4

Osborne NN, Lascaratos G, Bron AJ, Chidlow G, Wood JP. 2006b. A hypothesis to suggest that light is a risk factor in glaucoma and the mitochondrial optic neuropathies. *Br J Ophthalmol* 90: 237-41

Osborne NN, Li GY, Ji D, Mortiboys HJ, Jackson S. 2008. Light affects mitochondria to cause apoptosis to cultured cells: possible relevance to ganglion cell death in certain optic neuropathies. *J Neurochem* 105: 2013-28

Osborne NN, Melena J, Chidlow G, Wood JP. 2001. A hypothesis to explain ganglion cell death caused by vascular insults at the optic nerve head: possible implication for the treatment of glaucoma. *Br J Ophthalmol* 85: 1252-9

Osborne NN, Ugarte M, Chao M, Chidlow G, Bae JH, et al. 1999. Neuroprotection in relation to retinal ischemia and relevance to glaucoma. *Surv Ophthalmol* 43 Suppl 1: S102-28

Osborne NN, Wood JP. 2004. Metipranolol blunts nitric oxide-induced lipid peroxidation and death of retinal photoreceptors: a comparison with other anti-glaucoma drugs. *Invest Ophthalmol Vis Sci* 45: 3787-95

Osterberg G. 1935. Topography of the layers of rods and cones in the human retina. *Acta Ophthalmol* 13

Otera H, Ohsakaya S, Nagaura Z, Ishihara N, Mihara K. 2005. Export of mitochondrial AIF in response to proapoptotic stimuli depends on processing at the intermembrane space. *Embo J* 24: 1375-86

Otterbein LE, Bach FH, Alam J, Soares M, Tao Lu H, et al. 2000. Carbon monoxide has anti-inflammatory effects involving the mitogen-activated protein kinase pathway. *Nat Med* 6: 422-8

Pannala AS, Rice-Evans CA, Halliwell B, Singh S. 1997. Inhibition of peroxynitrite-mediated tyrosine nitration by catechin polyphenols. *Biochem Biophys Res Commun* 232: 164-8

Papermaster DS, Windle J. 1995. Death at an early age. Apoptosis in inherited retinal degenerations. *Invest Ophthalmol Vis Sci* 36: 977-83

Park DS, Stefanis L, Yan CY, Farinelli SE, Greene LA. 1996. Ordering the cell death pathway. Differential effects of BCL2, an interleukin-1-converting enzyme family protease inhibitor, and other survival agents on JNK activation in serum/nerve growth factor-deprived PC12 cells. *J Biol Chem* 271: 21898-905

Patten DA, Germain M, Kelly MA, Slack RS. 2010. Reactive oxygen species: stuck in the middle of neurodegeneration. *J Alzheimers Dis* 20 Suppl 2: S357-67

Paveto C, Guida MC, Esteva MI, Martino V, Coussio J, et al. 2004. Anti-Trypanosoma cruzi activity of green tea (Camellia sinensis) catechins. *Antimicrob Agents Chemother* 48: 69-74

Pease ME, McKinnon SJ, Quigley HA, Kerrigan-Baumrind LA, Zack DJ. 2000. Obstructed axonal transport of BDNF and its receptor TrkB in experimental glaucoma. *Invest Ophthalmol Vis Sci* 41: 764-74

Pedler C. 1963. The Fine Structure of the Radial Fibres in the Reptile Retina. *Exp Eye Res* 2: 296-303

Pei L, Li Y, Yan JZ, Zhang GY, Cui ZC, Zhu ZM. 2000. Changes and mechanisms of protein-tyrosine kinase and protein-tyrosine phosphatase activities after brain ischemia/reperfusion. *Acta Pharmacol Sin* 21: 715-20

Peng PH, Chiou LF, Chao HM, Lin S, Chen CF, et al. 2010. Effects of epigallocatechin-3-gallate on rat retinal ganglion cells after optic nerve axotomy. *Exp Eye Res* 90: 528-34

Peng PH, Ko ML, Chen CF. 2008a. Epigallocatechin-3-gallate reduces retinal ischemia/reperfusion injury by attenuating neuronal nitric oxide synthase expression and activity. *Exp Eye Res* 86: 637-46

Peng PH, Ko ML, Chen CF, Juan SH. 2008b. Haem oxygenase-1 gene transfer protects retinal ganglion cells from ischaemia/reperfusion injury. *Clin Sci (Lond)* 115: 335-42

Perry V. 1982. The ganglion cell layer of the mammalian retina. *Prog Retinal Res* 1: 53-80

Perry VH, Gordon S. 1988. Macrophages and microglia in the nervous system. *Trends Neurosci* 11: 273-7

Petrache I, Otterbein LE, Alam J, Wiegand GW, Choi AM. 2000. Heme oxygenase-1 inhibits TNF-alpha-induced apoptosis in cultured fibroblasts. *Am J Physiol Lung Cell Mol Physiol* 278: L312-9

Phillis JW, Song D, O'Regan MH. 1996. Inhibition of tyrosine phosphorylation attenuates amino acid neurotransmitter release from the ischemic/reperfused rat cerebral cortex. *Neurosci Lett* 207: 151-4

Polier G, Ding J, Konkimalla BV, Eick D, Ribeiro N, et al. 2011. Wogonin and related natural flavones are inhibitors of CDK9 that induce apoptosis in cancer cells by transcriptional suppression of Mcl-1. *Cell Death Dis* 2: e182

Polster BM, Basanez G, Etxebarria A, Hardwick JM, Nicholls DG. 2005. Calpain I induces cleavage and release of apoptosis-inducing factor from isolated mitochondria. *J Biol Chem* 280: 6447-54

Ponsioen TL, van Luyn MJ, van der Worp RJ, Pas HH, Hooymans JM, Los LI. 2008. Human retinal Muller cells synthesize collagens of the vitreous and vitreoretinal interface in vitro. *Mol Vis* 14: 652-60

Prinz M, Kann O, Draheim HJ, Schumann RR, Kettenmann H, et al. 1999. Microglial activation by components of gram-positive and -negative bacteria: distinct and common routes to the induction of ion channels and cytokines. *J Neuropathol Exp Neurol* 58: 1078-89

Pullikotil P, Chen H, Muniyappa R, Greenberg CC, Yang S, et al. 2011. Epigallocatechin gallate induces expression of heme oxygenase-1 in endothelial cells via p38 MAPK and Nrf-2 that suppresses proinflammatory actions of TNF-alpha. *J Nutr Biochem*

Pulverer BJ, Kyriakis JM, Avruch J, Nikolakaki E, Woodgett JR. 1991. Phosphorylation of c-jun mediated by MAP kinases. *Nature* 353: 670-4

Qamirani E, Razavi HM, Wu X, Davis MJ, Kuo L, Hein TW. 2006. Sodium azide dilates coronary arterioles via activation of inward rectifier K+ channels and Na+-K+-ATPase. *Am J Physiol Heart Circ Physiol* 290: H1617-23

Qi X, Sun L, Lewin AS, Hauswirth WW, Guy J. 2007. The mutant human ND4 subunit of complex I induces optic neuropathy in the mouse. *Invest Ophthalmol Vis Sci* 48: 1-10

Quigley HA. 1999. Neuronal death in glaucoma. *Prog Retin Eye Res* 18: 39-57

Quigley HA, Addicks EM. 1980. Chronic experimental glaucoma in primates. II. Effect of extended intraocular pressure elevation on optic nerve head and axonal transport. *Invest Ophthalmol Vis Sci* 19: 137-52

Quigley HA, Addicks EM, Green WR, Maumenee AE. 1981. Optic nerve damage in human glaucoma. II. The site of injury and susceptibility to damage. *Arch Ophthalmol* 99: 635-49

Quigley HA, Broman AT. 2006. The number of people with glaucoma worldwide in 2010 and 2020. *Br J Ophthalmol* 90: 262-7

Quigley HA, Green WR. 1979. The histology of human glaucoma cupping and optic nerve damage: clinicopathologic correlation in 21 eyes. *Ophthalmology* 86: 1803-30

Quigley HA, McKinnon SJ, Zack DJ, Pease ME, Kerrigan-Baumrind LA, et al. 2000. Retrograde axonal transport of BDNF in retinal ganglion cells is blocked by acute IOP elevation in rats. *Invest Ophthalmol Vis Sci* 41: 3460-6

Ramsay RR, Salach JI, Dadgar J, Singer TP. 1986. Inhibition of mitochondrial NADH dehydrogenase by pyridine derivatives and its possible relation to experimental and idiopathic parkinsonism. *Biochem Biophys Res Commun* 135: 269-75

Ravikumar B, Sarkar S, Davies JE, Futter M, Garcia-Arencibia M, et al. 2010. Regulation of mammalian autophagy in physiology and pathophysiology. *Physiol Rev* 90: 1383-435

Raza H, John A. 2007. In vitro protection of reactive oxygen species-induced degradation of lipids, proteins and 2-deoxyribose by tea catechins. *Food Chem Toxicol* 45: 1814-20

Reese TS, Karnovsky MJ. 1967. Fine structural localization of a blood-brain barrier to exogenous peroxidase. *J Cell Biol* 34: 207-17

Reichenbach A, Stolzenburg JU, Eberhardt W, Chao TI, Dettmer D, Hertz L. 1993. What do retinal muller (glial) cells do for their neuronal 'small siblings'? *J Chem Neuroanat* 6: 201-13

Resnikoff S, Pascolini D, Etya'ale D, Kocur I, Pararajasegaram R, et al. 2004. Global data on visual impairment in the year 2002. *Bull World Health Organ* 82: 844-51

Rezai-Zadeh K, Shytle D, Sun N, Mori T, Hou H, et al. 2005. Green tea epigallocatechin-3-gallate (EGCG) modulates amyloid precursor protein cleavage and reduces cerebral amyloidosis in Alzheimer transgenic mice. *J Neurosci* 25: 8807-14

Reznichenko L, Amit T, Youdim MB, Mandel S. 2005. Green tea polyphenol (-)-epigallocatechin-3-gallate induces neurorescue of long-term serum-deprived PC12 cells and promotes neurite outgrowth. *J Neurochem* 93: 1157-67

Reznichenko L, Kalfon L, Amit T, Youdim MB, Mandel SA. 2010. Low dosage of rasagiline and epigallocatechin gallate synergistically restored the nigrostriatal axis in MPTP-induced parkinsonism. *Neurodegener Dis* 7: 219-31

Rice-Evans CA, Miller NJ, Paganga G. 1996. Structure-antioxidant activity relationships of flavonoids and phenolic acids. *Free Radic Biol Med* 20: 933-56

Rimbach G, Boesch-Saadatmandi C, Frank J, Fuchs D, Wenzel U, et al. 2008a. Dietary isoflavones in the prevention of cardiovascular disease--a molecular perspective. *Food Chem Toxicol* 46: 1308-19

Rimbach G, Boesch-Saadatmandi C, Frank J, Fuchs D, Wenzel U, et al. 2008b. Dietary isoflavones in the prevention of cardiovascular disease--a molecular perspective. *Food Chem Toxicol* 46: 1308-19

Rodieck RW, Watanabe M. 1993. Survey of the morphology of macaque retinal ganglion cells that project to the pretectum, superior colliculus, and parvicellular laminae of the lateral geniculate nucleus. *J Comp Neurol* 338: 289-303

Rodriguez SK, Guo W, Liu L, Band MA, Paulson EK, Meydani M. 2006. Green tea catechin, epigallocatechin-3-gallate, inhibits vascular endothelial growth factor angiogenic signaling by disrupting the formation of a receptor complex. *Int J Cancer* 118: 1635-44

Romano AD, Serviddio G, de Matthaeis A, Bellanti F, Vendemiale G. 2010. Oxidative stress and aging. *J Nephrol* 23 Suppl 15: S29-36

Ross JA, Kasum CM. 2002a. Dietary flavonoids: bioavailability, metabolic effects, and safety. *Annual review of nutrition* 22: 19-34

Ross JA, Kasum CM. 2002b. Dietary flavonoids: bioavailability, metabolic effects, and safety. *Annu Rev Nutr* 22: 19-34

Ruiz-Ederra J, Garcia M, Hicks D, Vecino E. 2004. Comparative study of the three neurofilament subunits within pig and human retinal ganglion cells. *Mol Vis* 10: 83-92

Ruiz-Larrea MB, Mohan AR, Paganga G, Miller NJ, Bolwell GP, Rice-Evans CA. 1997. Antioxidant activity of phytoestrogenic isoflavones. *Free Radic Res* 26: 63-70

Ryan MK, Hendrickson AE. 1987. Interplexiform cells in macaque monkey retina. *Exp Eye Res* 45: 57-66

Sacca SC, Izzotti A, Rossi P, Traverso C. 2007. Glaucomatous outflow pathway and oxidative stress. *Exp Eye Res* 84: 389-99

Safiulina D, Veksler V, Zharkovsky A, Kaasik A. 2006. Loss of mitochondrial membrane potential is associated with increase in mitochondrial volume: physiological role in neurones. *J Cell Physiol* 206: 347-53

Sakamoto K, Kawakami T, Shimada M, Yamaguchi A, Kuwagata M, et al. 2009. Histological protection by cilnidipine, a dual L/N-type Ca(2+) channel blocker, against neurotoxicity induced by ischemia-reperfusion in rat retina. *Exp Eye Res* 88: 974-82

Salah N, Miller NJ, Paganga G, Tijburg L, Bolwell GP, Rice-Evans C. 1995. Polyphenolic flavanols as scavengers of aqueous phase radicals and as chain-breaking antioxidants. *Arch Biochem Biophys* 322: 339-46

Salt TE, Cordeiro MF. 2006. Glutamate excitotoxicity in glaucoma: throwing the baby out with the bathwater? *Eye (Lond)* 20: 730-1; author reply 31-2

Sang S, Yang I, Buckley B, Ho CT, Yang CS. 2007. Autoxidative quinone formation in vitro and metabolite formation in vivo from tea polyphenol (-)-epigallocatechin-3-gallate: studied by real-time mass spectrometry combined with tandem mass ion mapping. *Free Radic Biol Med* 43: 362-71

Sannella AR, Messori L, Casini A, Francesco Vincieri F, Bilia AR, et al. 2007. Antimalarial properties of green tea. *Biochem Biophys Res Commun* 353: 177-81

Santa KM. 2010. Treatment options for mitochondrial myopathy, encephalopathy, lactic acidosis, and stroke-like episodes (MELAS) syndrome. *Pharmacotherapy* 30: 1179-96

Sappington RM, Carlson BJ, Crish SD, Calkins DJ. 2010. The microbead occlusion model: a paradigm for induced ocular hypertension in rats and mice. *Invest Ophthalmol Vis Sci* 51: 207-16

Satoh T, Baba M, Nakatsuka D, Ishikawa Y, Aburatani H, et al. 2003. Role of heme oxygenase-1 protein in the neuroprotective effects of cyclopentenone prostaglandin derivatives under oxidative stress. *Eur J Neurosci* 17: 2249-55

Scalbert A, Williamson G. 2000. Dietary intake and bioavailability of polyphenols. *J Nutr* 130: 2073S-85S

Schapira AH, Gu M, Taanman JW, Tabrizi SJ, Seaton T, et al. 1998. Mitochondria in the etiology and pathogenesis of Parkinson's disease. *Ann Neurol* 44: S89-98

Schenkel J. 2004. Activation of the c-Jun transcription factor following neurodegeneration in vivo. *Neurosci Lett* 361: 36-9

Schinder AF, Olson EC, Spitzer NC, Montal M. 1996. Mitochondrial dysfunction is a primary event in glutamate neurotoxicity. *J Neurosci* 16: 6125-33

Schlotzer-Schrehardt U, Naumann GO. 2006. Ocular and systemic pseudoexfoliation syndrome. *Am J Ophthalmol* 141: 921-37

Schmid S, Guenther E. 1998. Alterations in channel density and kinetic properties of the sodium current in retinal ganglion cells of the rat during in vivo differentiation. *Neuroscience* 85: 249-58

Schnapf JL, Kraft TW, Baylor DA. 1987. Spectral sensitivity of human cone photoreceptors. *Nature* 325: 439-41

Schnitzer J. 1988. Astrocytes in the guinea pig, horse, and monkey retina: their occurrence coincides with the presence of blood vessels. *Glia* 1: 74-89

Scholes JH. 1975. Colour receptors, and their synaptic connexions, in the retina of a cyprinid fish. *Philos Trans R Soc Lond B Biol Sci* 270: 61-118

Schon EA, DiMauro S, Hirano M, Gilkerson RW. 2010. Therapeutic prospects for mitochondrial disease. *Trends Mol Med* 16: 268-76

Schreihofer DA, Do KD, Schreihofer AM. 2005. High-soy diet decreases infarct size after permanent middle cerebral artery occlusion in female rats. *Am J Physiol Regul Integr Comp Physiol* 289: R103-8

Schreihofer DA, Redmond L. 2009. Soy phytoestrogens are neuroprotective against stroke-like injury in vitro. *Neuroscience* 158: 602-9

Schroit AJ, Madsen JW, Tanaka Y. 1985. In vivo recognition and clearance of red blood cells containing phosphatidylserine in their plasma membranes. *J Biol Chem* 260: 5131-8

Schwechter BR, Millet LE, Levin LA. 2007. Histone deacetylase inhibition-mediated differentiation of RGC-5 cells and interaction with survival. *Invest Ophthalmol Vis Sci* 48: 2845-57

Schweichel JU, Merker HJ. 1973. The morphology of various types of cell death in prenatal tissues. *Teratology* 7: 253-66

Setchell KD. 1998. Phytoestrogens: the biochemistry, physiology, and implications for human health of soy isoflavones. *Am J Clin Nutr* 68: 1333S-46S

Setchell KD, Brown NM, Desai PB, Zimmer-Nechimias L, Wolfe B, et al. 2003a. Bioavailability, disposition, and dose-response effects of soy isoflavones when consumed by healthy women at physiologically typical dietary intakes. *J Nutr* 133: 1027-35

Setchell KD, Cassidy A. 1999. Dietary isoflavones: biological effects and relevance to human health. *J Nutr* 129: 758S-67S

Setchell KD, Faughnan MS, Avades T, Zimmer-Nechemias L, Brown NM, et al. 2003b. Comparing the pharmacokinetics of daidzein and genistein with the use of 13C-labeled tracers in premenopausal women. *Am J Clin Nutr* 77: 411-9

Setchell KD, Lydeking-Olsen E. 2003. Dietary phytoestrogens and their effect on bone: evidence from in vitro and in vivo, human observational, and dietary intervention studies. *Am J Clin Nutr* 78: 593S-609S

Shao Z, Shen J, Yang Y, Wu D, Zhou X, Yuan H. 2012. Annexin 1 protects against apoptosis induced by serum deprivation in transformed rat retinal ganglion cells. *Mol Biol Rep* 39: 5543-51

Shapley R, Perry V. 1986. Cat and monkey retina ganglion cells and their visual functional role. *Trends Neurosci* 9: 229-35

Shelnutt SR, Cimino CO, Wiggins PA, Ronis MJ, Badger TM. 2002. Pharmacokinetics of the glucuronide and sulfate conjugates of genistein and daidzein in men and women after consumption of a soy beverage. *Am J Clin Nutr* 76: 588-94

Sherer TB, Betarbet R, Greenamyre JT. 2002. Environment, mitochondria, and Parkinson's disease. *Neuroscientist* 8: 192-7

Shichida Y, Matsuyama T. 2009. Evolution of opsins and phototransduction. *Philos Trans R Soc Lond B Biol Sci* 364: 2881-95

Shih AY, Johnson DA, Wong G, Kraft AD, Jiang L, et al. 2003. Coordinate regulation of glutathione biosynthesis and release by Nrf2-expressing glia potently protects neurons from oxidative stress. *J Neurosci* 23: 3394-406

Shih PH, Wu CH, Yeh CT, Yen GC. 2011. Protective effects of anthocyanins against amyloid beta-peptide-induced damage in neuro-2A cells. *J Agric Food Chem* 59: 1683-9

Shimizu M, Deguchi A, Joe AK, McKoy JF, Moriwaki H, Weinstein IB. 2005. EGCG inhibits activation of HER3 and expression of cyclooxygenase-2 in human colon cancer cells. *J Exp Ther Oncol* 5: 69-78

Sichel G, Corsaro C, Scalia M, Di Bilio AJ, Bonomo RP. 1991. In vitro scavenger activity of some flavonoids and melanins against O2-(.). *Free Radic Biol Med* 11: 1-8

Siesjo BK, Katsura K. 1992. Ischemic brain damage: focus on lipids and lipid mediators. *Adv Exp Med Biol* 318: 41-56

Sigelman J, Ozanics V. 1982. Retina In *Ocular Anatomy, Embryology, and Teratology*, ed. F Jakoobiec, pp. 441. Philadelphia: Harper and Row

Silveira LC, Perry VH. 1991. The topography of magnocellular projecting ganglion cells (M-ganglion cells) in the primate retina. *Neuroscience* 40: 217-37

Singer CA, Figueroa-Masot XA, Batchelor RH, Dorsa DM. 1999. The mitogen-activated protein kinase pathway mediates estrogen neuroprotection after glutamate toxicity in primary cortical neurons. *J Neurosci* 19: 2455-63

Sjostrand FS. 1953. The ultrastructure of the innersegments of the retinal rods of the guinea pig eye as revealed by electron microscopy. *J Cell Physiol* 42: 45-70

Smalheiser NR, Crain SM, Bornstein MB. 1981. Development of ganglion cells and their axons in organized cultures of fetal mouse retinal explants. *Brain Res* 204: 159-78

Song JM, Lee KH, Seong BL. 2005. Antiviral effect of catechins in green tea on influenza virus. *Antiviral Res* 68: 66-74

Stein JD, Kim DS, Niziol LM, Talwar N, Nan B, et al. 2011. Differences in rates of glaucoma among Asian Americans and other racial groups, and among various Asian ethnic groups. *Ophthalmology* 118: 1031-7

Strettoi E, Dacheux RF, Raviola E. 1990. Synaptic connections of rod bipolar cells in the inner plexiform layer of the rabbit retina. *J Comp Neurol* 295: 449-66

Stromberg H, Svensson SP, Hermanson O. 2000. Distribution of the transcription factor signal transducer and activator of transcription 3 in the rat central nervous system and dorsal root ganglia. *Brain Res* 853: 105-14

Sugamura K, Keaney JF, Jr. 2011. Reactive oxygen species in cardiovascular disease. *Free Radic Biol Med*

Suganuma M, Okabe S, Oniyama M, Tada Y, Ito H, Fujiki H. 1998. Wide distribution of [3H](-)-epigallocatechin gallate, a cancer preventive tea polyphenol, in mouse tissue. *Carcinogenesis* 19: 1771-6

Susin SA, Lorenzo HK, Zamzami N, Marzo I, Snow BE, et al. 1999. Molecular characterization of mitochondrial apoptosis-inducing factor. *Nature* 397: 441-6

Suzuki M, Tabuchi M, Ikeda M, Umegaki K, Tomita T. 2004. Protective effects of green tea catechins on cerebral ischemic damage. *Med Sci Monit* 10: BR166-74

Takahashi N, Cummins D, Caprioli J. 1991. Rat retinal ganglion cells in culture. *Exp Eye Res* 53: 565-72

Takahashi S, Abe T, Gotoh J, Fukuuchi Y. 2002. Substrate-dependence of reduction of MTT: a tetrazolium dye differs in cultured astroglia and neurons. *Neurochem Int* 40: 441-8

Tartaglia LA, Ayres TM, Wong GH, Goeddel DV. 1993. A novel domain within the 55 kd TNF receptor signals cell death. *Cell* 74: 845-53

Tedeschi E, Suzuki H, Menegazzi M. 2002. Antiinflammatory action of EGCG, the main component of green tea, through STAT-1 inhibition. *Ann N Y Acad Sci* 973: 435-7

Tenhunen R, Marver HS, Schmid R. 1968. The enzymatic conversion of heme to bilirubin by microsomal heme oxygenase. *Proc Natl Acad Sci U S A* 61: 748-55

Tenhunen R, Marver HS, Schmid R. 1969a. The enzymatic conversion of hemoglobin to bilirubin. *Trans Assoc Am Physicians* 82: 363-71

Tenhunen R, Marver HS, Schmid R. 1969b. Microsomal heme oxygenase. Characterization of the enzyme. *J Biol Chem* 244: 6388-94

Tezel G. 2006. Oxidative stress in glaucomatous neurodegeneration: mechanisms and consequences. *Prog Retin Eye Res* 25: 490-513

Tobe T, Okamoto N, Vinores MA, Derevjanik NL, Vinores SA, et al. 1998. Evolution of neovascularization in mice with overexpression of vascular endothelial growth factor in photoreceptors. *Invest Ophthalmol Vis Sci* 39: 180-8

Toimela T, Tahti H. 2004. Mitochondrial viability and apoptosis induced by aluminum, mercuric mercury and methylmercury in cell lines of neural origin. *Arch Toxicol* 78: 565-74

Topouzis F, Wilson MR, Harris A, Founti P, Yu F, et al. 2011. Risk factors for primary open-angle glaucoma and pseudoexfoliative glaucoma in the thessaloniki eye study. *Am J Ophthalmol* 152: 219-28 e1

Towbin H, Staehelin T, Gordon J. 1979. Electrophoretic transfer of proteins from polyacrylamide gels to nitrocellulose sheets: procedure and some applications. *Proc Natl Acad Sci U S A* 76: 4350-4

Trieu VN, Dong Y, Zheng Y, Uckun FM. 1999. In vivo antioxidant activity of genistein in a murine model of singlet oxygen-induced cerebral stroke. *Radiat Res* 152: 508-16

Trieu VN, Uckun FM. 1999. Genistein is neuroprotective in murine models of familial amyotrophic lateral sclerosis and stroke. *Biochem Biophys Res Commun* 258: 685-8

Tsang F, Fred Wong WS. 2000. Inhibitors of tyrosine kinase signaling cascade attenuated antigen challenge of guinea-pig airways in vitro. *Am J Respir Crit Care Med* 162: 126-33

Uesato S, Kitagawa Y, Kamishimoto M, Kumagai A, Hori H, Nagasawa H. 2001. Inhibition of green tea catechins against the growth of cancerous human colon and hepatic epithelial cells. *Cancer Lett* 170: 41-4

Ullrich A, Schlessinger J. 1990. Signal transduction by receptors with tyrosine kinase activity. *Cell* 61: 203-12

Urusova D, Shim J, Kim DJ, Jung SK, Zykova T, et al. 2011. Epigallocatechin-gallate suppresses tumorigenesis by directly targeting Pin1. *Cancer Prev Res (Phila)*

Valcic S, Burr JA, Timmermann BN, Liebler DC. 2000. Antioxidant chemistry of green tea catechins. New oxidation products of (-)-epigallocatechin gallate and (-)-epigallocatechin from their reactions with peroxyl radicals. *Chem Res Toxicol* 13: 801-10

Valsecchi AE, Franchi S, Panerai AE, Sacerdote P, Trovato AE, Colleoni M. 2008. Genistein, a natural phytoestrogen from soy, relieves neuropathic pain following chronic constriction sciatic nerve injury in mice: anti-inflammatory and antioxidant activity. *J Neurochem* 107: 230-40

Van Bergen NJ, Wood JP, Chidlow G, Trounce IA, Casson RJ, et al. 2009. Recharacterization of the RGC-5 retinal ganglion cell line. *Invest Ophthalmol Vis Sci* 50: 4267-72

Vaney DI, Young HM, Gynther IC. 1991. The rod circuit in the rabbit retina. *Vis Neurosci* 7: 141-54

Vile GF, Basu-Modak S, Waltner C, Tyrrell RM. 1994. Heme oxygenase 1 mediates an adaptive response to oxidative stress in human skin fibroblasts. *Proc Natl Acad Sci U S A* 91: 2607-10

Vitolins M. 2003. Effects of soy protein in menopausal women: a review. *Agro Food Ind High-Tech* 14: 12-16

Vitolins MZ, Anthony M, Burke GL. 2001. Soy protein isoflavones, lipids and arterial disease. *Curr Opin Lipidol* 12: 433-7

Vyas S, Manon B, Vir Singh T, Dev Sharma P, Sharma M. 2011. Potential O-acyl-substituted (-)-Epicatechin gallate prodrugs as inhibitors of DMBA/TPA-

induced squamous cell carcinoma of skin in Swiss albino mice. *Chem Biodivers* 8: 599-613

Wadia JS, Chalmers-Redman RM, Ju WJ, Carlile GW, Phillips JL, et al. 1998. Mitochondrial membrane potential and nuclear changes in apoptosis caused by serum and nerve growth factor withdrawal: time course and modification by (-)-deprenyl. *J Neurosci* 18: 932-47

Wakabayashi N, Dinkova-Kostova AT, Holtzclaw WD, Kang MI, Kobayashi A, et al. 2004. Protection against electrophile and oxidant stress by induction of the phase 2 response: fate of cysteines of the Keap1 sensor modified by inducers. *Proc Natl Acad Sci U S A* 101: 2040-5

Wallace DC, Singh G, Lott MT, Hodge JA, Schurr TG, et al. 1988. Mitochondrial DNA mutation associated with Leber's hereditary optic neuropathy. *Science* 242: 1427-30

Wang GY, Ratto G, Bisti S, Chalupa LM. 1997. Functional development of intrinsic properties in ganglion cells of the mammalian retina. *J Neurophysiol* 78: 2895-903

Wang H, Murphy P. 1994a. Isoflavone content in commercial soybean foods. *J Agri Food Chem* 42: 1666-73

Wang H, Murphy PA. 1994b. Isoflavone composition of American and Japanese soybeans in Iowa: effects of variety, crop year, and location. *Journal of Agriculture and Food Chemistry* 42: 1674-77

Wang J, Santa-Maria I, Ho L, Ksiezak-Reding H, Ono K, et al. 2010. Grape derived polyphenols attenuate tau neuropathology in a mouse model of Alzheimer's disease. *J Alzheimers Dis* 22: 653-61

Wang L, Dong J, Cull G, Fortune B, Cioffi GA. 2003. Varicosities of intraretinal ganglion cell axons in human and nonhuman primates. *Invest Ophthalmol Vis Sci* 44: 2-9

Wang TT, Sathyamoorthy N, Phang JM. 1996. Molecular effects of genistein on estrogen receptor mediated pathways. *Carcinogenesis* 17: 271-5

Wang X, Martindale JL, Holbrook NJ. 2000. Requirement for ERK activation in cisplatin-induced apoptosis. *J Biol Chem* 275: 39435-43

Wassertheil-Smoller S, Hendrix SL, Limacher M, Heiss G, Kooperberg C, et al. 2003. Effect of estrogen plus progestin on stroke in postmenopausal women: the Women's Health Initiative: a randomized trial. *Jama* 289: 2673-84

Wässle H. 1982. Morphological types and central projections of ganglion cells in the cat retina. *Prog Retinal Res* 1: 125-52

Watfa G, Dragonas C, Brosche T, Dittrich R, Sieber CC, et al. 2011. Study of telomere length and different markers of oxidative stress in patients with Parkinson's disease. *J Nutr Health Aging* 15: 277-81

Waxman SG. 1978. Prerequisites for conduction in demyelinated fibers. *Neurology* 28: 27-33

Weber CH, Vincenz C. 2001. The death domain superfamily: a tale of two interfaces? *Trends Biochem Sci* 26: 475-81

Wei H, Bowen R, Cai Q, Barnes S, Wang Y. 1995. Antioxidant and antipromotional effects of the soybean isoflavone genistein. *Proc Soc Exp Biol Med* 208: 124-30

Wei H, Cai Q, Rahn RO. 1996. Inhibition of UV light- and Fenton reaction-induced oxidative DNA damage by the soybean isoflavone genistein. *Carcinogenesis* 17: 73-7

Wei H, Meng Z. 2010. Protective effects of epigallocatechin-3-gallate against lead-induced oxidative damage. *Hum Exp Toxicol*

Wei H, Wei L, Frenkel K, Bowen R, Barnes S. 1993. Inhibition of tumor promoter-induced hydrogen peroxide formation in vitro and in vivo by genistein. *Nutr Cancer* 20: 1-12

Wei H, Zhang X, Wang Y, Lebwohl M. 2002. Inhibition of ultraviolet light-induced oxidative events in the skin and internal organs of hairless mice by isoflavone genistein. *Cancer Lett* 185: 21-9

Wei IH, Wu YC, Wen CY, Shieh JY. 2004. Green tea polyphenol (-)-epigallocatechin gallate attenuates the neuronal NADPH-d/nNOS expression in the nodose ganglion of acute hypoxic rats. *Brain Res* 999: 73-80

Wei YH, Lu CY, Wei CY, Ma YS, Lee HC. 2001. Oxidative stress in human aging and mitochondrial disease-consequences of defective mitochondrial respiration and impaired antioxidant enzyme system. *Chin J Physiol* 44: 1-11

Werblin FS, Dowling JE. 1969. Organization of the retina of the mudpuppy, Necturus maculosus. II. Intracellular recording. *J Neurophysiol* 32: 339-55

Werner EB, Drance SM. 1977. Progression of glaucomatous field defects despite successful filtration. *Can J Ophthalmol* 12: 275-80

Werner EB, Drance SM, Schulzer M. 1977. Trabeculectomy and the progression of glaucomatous visual field loss. *Arch Ophthalmol* 95: 1374-7

White RJ, Reynolds IJ. 1996. Mitochondrial depolarization in glutamate-stimulated neurons: an early signal specific to excitotoxin exposure. *J Neurosci* 16: 5688-97

WHO. 2010. WHO releases the new global estimates on visual impairment. In *Prevention of Blindness and Visual Impairment*, ed. WH Organization

Willbold E, Berger J, Reinicke M, Wolburg H. 1997. On the role of Muller glia cells in histogenesis: only retinal spheroids, but not tectal, telencephalic and cerebellar spheroids develop histotypical patterns. *J Hirnforsch* 38: 383-96

Winter J, Bokkenheuser VD. 1987. Bacterial metabolism of natural and synthetic sex hormones undergoing enterohepatic circulation. *J Steroid Biochem* 27: 1145-9

Wiseman SA, Balentine DA, Frei B. 1997. Antioxidants in tea. *Crit Rev Food Sci Nutr* 37: 705-18

Wisniewska-Knypl JM, Wronska-Nofer T. 1994. Biological markers of oxidative stress induced by ethanol and iron overload in rat. *Int J Occup Med Environ Health* 7: 355-63

Witte ME, Geurts JJ, de Vries HE, van der Valk P, van Horssen J. 2010. Mitochondrial dysfunction: a potential link between neuroinflammation and neurodegeneration? *Mitochondrion* 10: 411-8

Wittstrom E, Ponjavic V, Bondeson ML, Andreasson S. 2011. Anterior Segment Abnormalities and Angle-Closure Glaucoma in a Family with a Mutation in the BEST1 Gene and Best Vitelliform Macular Dystrophy. *Ophthalmic Genet*

Wolf C, Gramer E, Muller-Myhsok B, Pasutto F, Reinthal E, et al. 2009. Evaluation of nine candidate genes in patients with normal tension glaucoma: a case control study. *BMC Med Genet* 10: 91

Wood JP, Chidlow G, Tran T, Crowston JG, Casson RJ. 2010. A comparison of differentiation protocols for RGC-5 cells. *Invest Ophthalmol Vis Sci* 51: 3774-83

Wood JP, Lascaratos G, Bron AJ, Osborne NN. 2007. The influence of visible light exposure on cultured RGC-5 cells. *Mol Vis* 14: 334-44

Wu CC, Hsieh CW, Lai PH, Lin JB, Liu YC, Wung BS. 2006a. Upregulation of endothelial heme oxygenase-1 expression through the activation of the JNK pathway by sublethal concentrations of acrolein. *Toxicol Appl Pharmacol* 214: 244-52

Wu CC, Hsu MC, Hsieh CW, Lin JB, Lai PH, Wung BS. 2006b. Upregulation of heme oxygenase-1 by Epigallocatechin-3-gallate via the phosphatidylinositol 3-kinase/Akt and ERK pathways. *Life Sci* 78: 2889-97

Wu N, Wang YH, Zhao HS, Liu DN, Ying X, et al. 2009. alpha-Crystallin downregulates the expression of TNF-alpha and iNOS by activated rat retinal microglia in vitro and in vivo. *Ophthalmic Res* 42: 21-8

Wygnanski T, Desatnik H, Quigley HA, Glovinsky Y. 1995. Comparison of ganglion cell loss and cone loss in experimental glaucoma. *Am J Ophthalmol* 120: 184-9

Wyllie AH. 1980. Glucocorticoid-induced thymocyte apoptosis is associated with endogenous endonuclease activation. *Nature* 284: 555-6

Wyllie AH, Kerr JF, Currie AR. 1980. Cell death: the significance of apoptosis. *Int Rev Cytol* 68: 251-306

Wyllie AH, Morris RG, Smith AL, Dunlop D. 1984. Chromatin cleavage in apoptosis: association with condensed chromatin morphology and dependence on macromolecular synthesis. *J Pathol* 142: 67-77

Xia Z, Dickens M, Raingeaud J, Davis RJ, Greenberg ME. 1995. Opposing effects of ERK and JNK-p38 MAP kinases on apoptosis. *Science* 270: 1326-31

Xia ZW, Zhou WP, Cui WJ, Zhang XH, Shen QX, et al. 2004. Structure prediction and activity analysis of human heme oxygenase-1 and its mutant. *World J Gastroenterol* 10: 2352-6

Xie J, Jiang L, Zhang T, Jin Y, Yang D, Chen F. 2010. Neuroprotective effects of Epigallocatechin-3-gallate (EGCG) in optic nerve crush model in rats. *Neurosci Lett* 479: 26-30

Xu X, Harris KS, Wang HJ, Murphy PA, Hendrich S. 1995. Bioavailability of soybean isoflavones depends upon gut microflora in women. *J Nutr* 125: 2307-15

Xu X, Wang HJ, Murphy PA, Hendrich S. 2000. Neither background diet nor type of soy food affects short-term isoflavone bioavailability in women. *J Nutr* 130: 798-801

Xu Z, Chen S, Li X, Luo G, Li L, Le W. 2006. Neuroprotective effects of (-)-epigallocatechin-3-gallate in a transgenic mouse model of amyotrophic lateral sclerosis. *Neurochem Res* 31: 1263-9

Yamamoto Y, Matsunaga K, Friedman H. 2004. Protective effects of green tea catechins on alveolar macrophages against bacterial infections. *Biofactors* 21: 119-21

Yang DD, Kuan CY, Whitmarsh AJ, Rincon M, Zheng TS, et al. 1997. Absence of excitotoxicity-induced apoptosis in the hippocampus of mice lacking the Jnk3 gene. *Nature* 389: 865-70

Ye F, Wu J, Dunn T, Yi J, Tong X, Zhang D. 2004. Inhibition of cyclooxygenase-2 activity in head and neck cancer cells by genistein. *Cancer Lett* 211: 39-46

Yeste-Velasco M, Folch J, Casadesus G, Smith MA, Pallas M, Camins A. 2009. Neuroprotection by c-Jun NH2-terminal kinase inhibitor SP600125 against potassium deprivation-induced apoptosis involves the Akt pathway and inhibition of cell cycle reentry. *Neuroscience* 159: 1135-47

Yildirim O, Ates NA, Ercan B, Muslu N, Unlu A, et al. 2005. Role of oxidative stress enzymes in open-angle glaucoma. *Eye (Lond)* 19: 580-3

Yin ST, Tang ML, Su L, Chen L, Hu P, et al. 2008. Effects of Epigallocatechin-3-gallate on lead-induced oxidative damage. *Toxicology* 249: 45-54

Yokozawa T, Nakagawa T, Kitani K. 2002. Antioxidative activity of green tea polyphenol in cholesterol-fed rats. *J Agric Food Chem* 50: 3549-52

Yoo KM, Hwang IK, Moon B. 2009. Comparative flavonoids contents of selected herbs and associations of their radical scavenging activity with antiproliferative actions in V79-4 cells. *J Food Sci* 74: C419-25

Young RW. 1967. The renewal of photoreceptor cell outer segments. *J Cell Biol* 33: 61-72

Young RW, Bok D. 1969. Participation of the retinal pigment epithelium in the rod outer segment renewal process. *J Cell Biol* 42: 392-403

Yu GS, Hu J, Nakagawa H. 1998. Inhibition of beta-amyloid cytotoxicity by midkine. *Neurosci Lett* 254: 125-8

Yu HL, Li L, Zhang XH, Xiang L, Zhang J, et al. 2009. Neuroprotective effects of genistein and folic acid on apoptosis of rat cultured cortical neurons induced by beta-amyloid 31-35. *Br J Nutr* 102: 655-62

Yu SW, Andrabi SA, Wang H, Kim NS, Poirier GG, et al. 2006. Apoptosis-inducing factor mediates poly(ADP-ribose) (PAR) polymer-induced cell death. *Proc Natl Acad Sci U S A* 103: 18314-9

Yu X, Rajala RV, McGinnis JF, Li F, Anderson RE, et al. 2004. Involvement of insulin/phosphoinositide 3-kinase/Akt signal pathway in 17 beta-estradiol-mediated neuroprotection. *J Biol Chem* 279: 13086-94

Yu-Wai-Man P, Griffiths PG, Chinnery PF. 2011. Mitochondrial optic neuropathies - disease mechanisms and therapeutic strategies. *Prog Retin Eye Res* 30: 81-114

Zeng H, Chen Q, Zhao B. 2004. Genistein ameliorates beta-amyloid peptide (25-35)-induced hippocampal neuronal apoptosis. *Free Radic Biol Med* 36: 180-8

Zhang B, Osborne NN. 2006. Oxidative-induced retinal degeneration is attenuated by epigallocatechin gallate. *Brain Res* 1124: 176-87

Zhang B, Rusciano D, Osborne NN. 2008. Orally administered epigallocatechin gallate attenuates retinal neuronal death in vivo and light-induced apoptosis in vitro. *Brain Res* 1198: 141-52

Zhang B, Safa R, Rusciano D, Osborne NN. 2007a. Epigallocatechin gallate, an active ingredient from green tea, attenuates damaging influences to the retina caused by ischemia/reperfusion. *Brain Res* 1159: 40-53

Zhang C, Du F, Shi M, Ye R, Cheng H, et al. 2011. Ginsenoside Rd Protects Neurons Against Glutamate-Induced Excitotoxicity by Inhibiting Ca(2+) Influx. *Cell Mol Neurobiol*

Zhang EJ, Ng KM, Luo KQ. 2007b. Extraction and purification of isoflavones from soybeans and characterization of their estrogenic activities. *J Agric Food Chem* 55: 6940-50

Zhang G, Wang Y, Zhang Y, Wan X, Li J, et al. 2012. Anti-cancer activities of tea epigallocatechin-3-gallate in breast cancer patients under radiotherapy. *Curr Mol Med* 12: 163-76

Zhang X, Jones D, Gonzalez-Lima F. 2002. Mouse model of optic neuropathy caused by mitochondrial complex I dysfunction. *Neurosci Lett* 326: 97-100

Zhang X, Rojas JC, Gonzalez-Lima F. 2006. Methylene blue prevents neurodegeneration caused by rotenone in the retina. *Neurotox Res* 9: 47-57

Zhao L, Chen Q, Diaz Brinton R. 2002. Neuroprotective and neurotrophic efficacy of phytoestrogens in cultured hippocampal neurons. *Exp Biol Med (Maywood)* 227: 509-19